A NUCLEAR MAGNETIC RESONANCE STUDY OF THE METAL-NONMETAL TRANSITION IN ARSENIC-DOPED GERMANIUM

V. G. I. Deshmukh

A Thesis Submitted for the Degree of PhD
at the
University of St Andrews

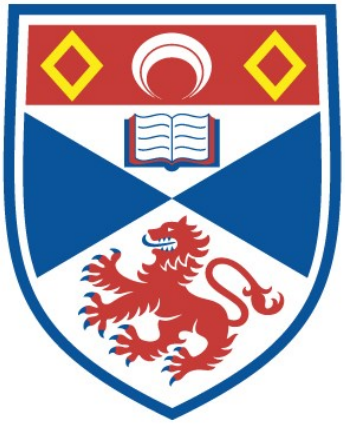

1977

A NUCLEAR MAGNETIC RESONANCE STUDY OF THE METAL-NONMETAL TRANSITION IN ARSENIC-DOPED GERMANIUM

A Thesis

presented by

V. G. I. Deshmukh B.Tech.

to the

University of St. Andrews

in application for the Degree of

Doctor of Philosophy

ProQuest LLC.
789 East Eisenhower Parkway
P.O. Box 1346
Ann Arbor, MI 48106 – 1346

For Claire

There is no death! What seems so is transition

Longfellow

ABSTRACT

An investigation of the metal-nonmetal transition in arsenic-doped germanium (Ge:As) has been performed using the technique of nuclear magnetic resonance. The host Ge^{73} resonance has been observed in twelve, single crystal, uncompensated specimens with room-temperature carrier concentrations from 7.10^{16} - $1.75.10^{19} cm^{-3}$. Measurements of the nuclear spin-lattice relaxation time T_1, Knight shift K and the nuclear linewidth ΔB for Ge^{73} are reported. Specifically, T_1 data are given at and below liquid helium temperatures for an applied magnetic field of 1.44 T and at 4.2 K alone at a field of 5 T. The Knight shifts have been measured at 4.2 K at 5 T and values of ΔB are given for both fields at 4.2 K. The T_1 measurements at low field (1.44 T) and Knight shift results show donor density dependences of free-electron type. A strong field dependence of T_1 has however been observed which is inexplicable by free-electron theory. The resonance linewidths are greater than the nuclear dipolar value, even for nonmetallic samples, and increase with doping density and magnetic field. At the critical concentration for transition to metallic behaviour K shows an abrupt change from zero to a finite value. The low-field T_1's are in contrast continuous across the transition but the high-field T_1's do show a sharp increase below the critical doping density. A calculation shows spin diffusion to be unimportant for the samples and other mechanisms which can generate a field-dependent relaxation time are discussed. Firstly, assuming that the electrons form a homogeneous system and are confined to a narrow impurity band parameterised by an appropriate Bohr radius

leads to a field dependence of T_1 in order of magnitude agreement with the data. A second qualitative model in line with recent ideas on the origin of negative magnetoresistance in doped semiconductors invokes the presence of nearly-free moments or Kondo centres in addition to the itinerant electron system. The fluctuation of the moments can furnish a relaxation process in addition to that due to Fermi contact between band electrons and nuclei. An increase in magnetic field inhibits the moment fluctuation rate and thus T_1 increases with field. Moreover the presence of moments will lead to resonance line broadening as we have observed. Finally, the magnetic properties of an Anderson transition are discussed and the abrupt appearance of K is shown to be consistent with Mott's interpretation of an Anderson transition. An important overall result is that the electron-electron effects observed in Si:P are absent in the Ge:As system. Simple estimates show that the intraatomic correlation energy is smaller in n-Ge than n-Si and it is concluded that the metal-nonmetal transition in Ge:As is of Anderson-type and that correlation plays no essential role. This proposal is shown to be in agreement with the results of other experiments in heavily-doped Ge.

ACKNOWLEDGEMENTS

The author wishes to express his sincere gratitude to Dr. D. P. Tunstall for his patient guidance and encouragement throughout this research and for his many stimulating discussions which greatly enhanced the author's understanding. He is also grateful to Tom Marshall for his great cooperation in supplying copious quantities of liquid helium and liquid nitrogen. The author is indebted to the University of St. Andrews and the Physics Trust for some personal funding which allowed the research work to be completed. He also wishes to thank Dr. D. M. Finlayson for considerable help in the performance of the low-temperature transport property experiments and for the loan of equipment for such measurements. He too is thankful to Bill Ramage for the use of his Fourier Transform computer program with which the Knight shifts were calculated. Thanks are due also to Vanita Deshmukh for her rapid and accurate typing of the manuscript.

CAREER

I entered the University of Bradford in October, 1968 and studied Mathematics, Electronics and Physics. I graduated in July, 1972 with upper second class honours in Applied Physics. In October, 1972, following the award of an S.R.C. Research Studentship at the University of St. Andrews, I was enrolled there as a research student reading for the degree of Ph. D. under the Resolution of the University Court, 1967, No. 1.

DECLARATION

I hereby certify that this thesis has been composed by me, and is a record of work done by me, and has not previously been presented for a Higher Degree.

This research was carried out in the Physical Sciences Laboratory of St. Salvator's College, in the University of St. Andrews, under the supervision of Dr. D. P. Tunstall.

CERTIFICATE

I certify that Vasant Gopal Ian Deshmukh, B.Tech., has spent nine terms at research work in the laboratories of the School of Physical Sciences, University of St. Andrews, under my direction, that he has fulfilled the conditions of the Resolution of the University Court, 1967, No. 1 and that he is qualified to submit the accompanying thesis in application for the Degree of Doctor of Philosophy.

Research Supervisor

CONTENTS

CONTENTS (Continued)

CONTENTS (Continued)

Chapter 1

INTRODUCTION

Much effort has been invested by the physics community in attempting to understand the metal-nonmetal transition[1]. The latter has been well known to be manifested as a change in, for example, the conductivity from insulating or semiconducting to metallic behaviour when some agency such as impurity concentration, pressure or magnetic field is varied. The metal-nonmetal transition has been observed in a wide variety of materials, crystalline and amorphous and one-, two- and three-dimensional. This report is restricted to a study of semiconductors and, in particular, crystalline germanium in which a transition to metallic behaviour is induced by doping the material heavily with the group V impurity arsenic. Every As impurity enters the Ge lattice substitutionally and forms a shallow, hydrogenic, donor state with a large Bohr radius a_H. For light doping ($\lesssim 10^{16} cm^{-3}$) the material is an extrinsic semiconductor and the resistivity is strongly dependent on temperature. As the doping density is increased, the donor wave functions overlap and the donor levels become broadened into an energy continuum termed an impurity band. Several mechanisms of charge transport are possible in an impurity-banded semiconductor and we discuss these in relation to plots of resistivity against temperature in later chapters. As the doping density is increased, a critical concentration N_c is attained at which the electrons behave as a degenerate gas and the semiconductor assumes a metallic character. The onset of metallic behaviour is signalled by a temperature independence of the resistivity and Hall coefficient. An important feature of the metal-nonmetal transition is that the transition occurs within an impurity band which is separate from the conduction

band - a doping density N_{cb} must be reached before the Fermi level enters the conduction band. For Ge:As,

$$N_C \sim 3.10^{17}\ \text{cm}^{-3} \quad \text{and} \quad N_{cb} \sim 2.10^{18}\ \text{cm}^{-3}$$

Whilst the concept of an impurity band is not new, the details of such a band remain poorly understood. Characteristics of the impurity band both predicted by theory and gleaned from experiment are given in following chapters. Throughout this report, we do not restrict ourselves exclusively to Ge:As with which our experiments were performed as we wish to compare and contrast our results with those in the well-studied phosphorus-doped silicon (Si:P) system.

Historically, the possibility of the existence of a metal-nonmetal transition was recognised to be a consequence of the Coulomb repulsion between electrons. By consideration of a screened Coulomb potential, Mott derived a relation between the critical concentration and the hydrogen radius as

$$N_C^{-\frac{1}{3}} \sim 2a_H \qquad (1.1)$$

This expression is well borne out by experiment though, as we note later, the agreement is in part fortuitous. A quantitative theory that predicted a metallic transition was later developed by Hubbard (chapter 3) who treated correlation only between electrons situated on the same atomic site. The transition occurs when the intraatomic correlation term U is of the order of the tight-binding bandwidth. Later work by Brinkman and Rice (chapter 3) has shown that the electron gas is highly correlated in a material just on the metallic side of the transition and there is a consequent enhancement of the spin susceptibility and electronic specific heat. Such behaviour

has been observed in Si:P and has been taken by some workers (though not all, as we describe in chapter 4) to be strong evidence for the metal-nonmetal transition in Si:P being due to electron correlation.

An important feature of doped semiconductors is that they are examples of disordered materials. The disorder arises both because of the haphazard siting of the donor atoms and from the random crystal potential created by the presence of the donors, acceptors and crystal imperfections. The idea that disorder can also lead to a metal-nonmetal transition follows from the work of Anderson (chapter 3). His model, in which the electrons are taken to be non-interacting, is to add a random potential fluctuating between the limits $\pm V_o$ to the periodic lattice potential and observe the effect on the conductivity of allowing V_o to increase. At absolute zero, carrier diffusion vanishes when V_o becomes of the order of the bandwidth. For doped semiconductors the relative importance of electron interaction with respect to disorder provides one of the most fascinating, though as yet unresolved, aspects of the metal-nonmetal transition.

The experimental methods that have been employed to investigate the transition are manifold and we have used the powerful one of nuclear magnetic resonance (NMR). In this technique, the atomic nucleus is used as a sensitive probe to gain information on the electronic environment surrounding the nucleus. If the substance studied is metallic in character then the paramagnetism of the electrons induces a shift in the nuclear resonance field from that observed when the nucleus is embedded in an insulating medium. This well-known

phenomenon is termed the Knight shift after its discoverer and clearly provides a delicate test of whether a semiconductor is metallic or not. The fact that the Knight shift should be zero for the semiconducting state and finite for the metallic state immediately poses the question as to the sharpness of the change of the Knight shift at the metal-nonmetal transition. We have measured the Knight shift K of the Ge^{73} nuclei in Ge:As at a magnetic field of 5T , and determined the dependence of K on the carrier concentration N_D.

We have also measured the characteristic time in which the Ge^{73} nuclei reach thermal equilibrium with their surroundings, the so-called spin-lattice relaxation time T_1. The variations of T_1 on N_D and temperature T yield further information on the properties of the electrons in a heavily-doped semiconductor. Our data for T_1 have been taken at and below helium temperatures at a field of 1.44 T and at 4.2 K only at a magnetic field of 5T. Finally, measurements taken of the characteristic time in which the nuclei thermally self-equilibriate, the so-called spin-spin relaxation time T_2 have been used to deduce the nuclear resonance linewidth ΔB. This provides a measure of the spread in local magnetic field experienced by the Ge^{73} nuclei.

Simple expressions are available, based on a free-electron model, for the dependence of T_1 and K on N_D and T. Deviations from such behaviour occur if electron-electron interactions are important or if there is disorder in the electron system. For example, if the electron gas in a strongly-doped semiconductor is correlated, then enhancement of the relaxation rate and Knight shift are expected.

Detailed magnetic resonance studies of Si:P have been made in recent times by Sasaki, Ikehata and Kobayashi[2-5] and by Brown and Holcomb[6]. Sasaki et al. show that deviations from free-electron behaviour occur in Si:P close to the transition and ascribe these to electron-electron interactions. A non-interacting theory is also inadequate to explain the experimental data on the electron spin susceptibility measured using electron spin resonance (ESR) techniques. Since the metal-nonmetal transition occurs at an order of magnitude lower doping density in n-Ge than in n-Si, a metallic specimen of n-Ge should constitute an example of a low-density electron gas. The density of the gas is important because, as we state in chapter 5, the spin susceptibility may be enhanced over the free-electron value by an amount which depends on the density of the electron system. In chapter 5 also, we describe an approach for narrow-band materials which yields a susceptibility enhancement factor containing an intra-atomic Coulomb repulsion, essentially the Hubbard U . The comparison between the NMR results for Ge:As and Si:P affords the opportunity of observing whether electron exchange and correlation are important for both materials. The presence or absence of electron-electron interactions provides details of the form of the impurity band and also suggests whether correlation or disorder is of greater importance as regards the occurrence of a metal-nonmetal transition.

The primary motivation for our study was to determine whether the electron interaction effects observed in Si:P could also be seen in Ge:As. Secondly, there exists some disagreement in the literature

on the sharpness of the appearance of the Knight shift in Si:P at the metal-nonmetal transition. Sasaki et al.[2] have observed an abrupt change whereas earlier results of Sundfors and Holcomb[7] show the Knight shift to appear and then gradually increase with doping density. We wished to investigate the behaviour of Ge:As in the equivalent doping regime for comparison with the conflicting data in Si:P. A third reason for our work was to enquire as to the correct way of describing the electron system in a metallic semiconductor. It is accepted that on the nonmetallic side of the transition that the electrons are localised about the donor atoms. In the metallic regime some workers take the electron gas (possibly interacting) to be a one-phase system. To the contrary, other investigators imagine the metallic region to be a two-phase electron system, i.e. localised states coexist with extended states. Experiment has so far provided balanced evidence for both descriptions. For example, Sasaki et al.[2] are able to explain their NMR data in Si:P using a two-phase model whilst Brown and Holcomb[6], obtaining essentially the same data, obtain agreement with theory within the confines of a single-phase electron system.

Having briefly outlined our motives for attempting a study of Ge:As using NMR we now describe the layout of this report of our findings. In chapter 2, we give the basic principles of nuclear interaction and relaxation and discuss deviations from free-electron formulae for T_1 and K due to electron-electron interaction and disorder. Chapter 3 is a description of some of the physical ideas peculiar to the metal-nonmetal transition in which we have drawn

heavily on the extensive writings of Mott[1]. A review of experimental investigations of the transition is given in chapter 4 and therefrom some interesting inferences may be drawn. Firstly, from the many experiments described, it is apparent that no single experiment can provide definitive evidence as to the nature of the metal-nonmetal transition. Secondly, no existing theory seems capable of explaining every experiment that has been performed, at least within a particular class of materials. By this we mean that the application of a theory to, for example, all metallic semiconductors may not be meaningful if those semiconductors show different behaviour when subjected to the same experimental conditions. If the latter holds, then it would appear more appropriate to consider each strongly-doped semiconductor as an individual material in which either correlation or disorder may play the more important role at the metal-nonmetal transition. In chapter 4, we stress that n-Ge and n-Si do not always behave identically when exposed to similar experimental investigation. Our own experimental data is summarised in chapter 5 and collated with the theories described in earlier pages. We give a synopsis of our conclusions in chapter 6 and juxtapose our results with those taken in Si:P for comparison and contrast. The differences between the NMR measurements for the two semiconductors are shown to follow those noted in chapter 4 and arguments are given to suggest that correlation is less important for Ge:As than Si:P.

Finally, we have chosen to place details of the experimental method and the characteristics of the samples in two appendices in order not to interrupt the flow of the argument of the preceding chapters.

The second appendix contains results of Hall effect and resistivity measurements on our samples at 4.2 and 300 K. Attention is drawn to the difficulty of determining the carrier concentration in n-type Ge and Si due both to practical and theoretical considerations. The former reduces to a choice of method whilst the theoretical problem concerns the variation of the proportionality constant between the carrier density and the Hall constant with temperature and doping density. The discussion also allows a proposal to be made to resolve the discrepancy existing between the Hall effect results in Si:P (cf. chapter 4) and the theories of chapter 3.

It follows that the positioning of the sample details in an appendix should not be viewed as a relegation of their importance. The fact that we had confidence in the characterisation of our samples was of great consequence to this work.

Chapter 2

THEORY OF NUCLEAR MAGNETIC RESONANCE AND RELAXATION

2.1 Introduction

This chapter is devoted to the theory of nuclear interactions and relaxations in solids. We begin by describing briefly the basic features of nuclear magnetism and define the spin-spin and spin-lattice relaxation times. A survey of nuclear-nuclear interactions is given and the electron-nuclear interaction and associated relaxation mechanisms are treated in some detail. The discussion is extended to the case of doped semiconductors and deviations from the free-electron theory due to correlation and disorder are described. Much of this chapter is taken from four comprehensive books on nuclear magnetism[8-11] but for simplicity these works are not individually referenced in the following text.

2.2 Basic Theory of Nuclear Resonance and Relaxation

The fine structure of atomic spectral lines led spectroscopists to the conclusion that a nucleus possesses an angular momentum $\underline{J}$ (in units of $\hbar$) and a magnetic moment $\underline{\mu}$. The vectors are collinear and

$$\underline{\mu} = \gamma \underline{J} = \gamma \hbar \underline{I} \tag{2.1}$$

where γ is the magnetogyric ratio of the nucleus and $\underline{I}$ is a dimensionless angular momentum operator known as the nuclear spin. If a nucleus is placed in a magnetic field $\underline{B}$, the interaction energy is describable by the Hamiltonian

$$\mathcal{H} = - \underline{\mu} . \underline{B} \tag{2.2}$$

Taking B_o to lie along the z axis

$$\mathcal{H} = - \gamma \hbar B_o I_z \tag{2.3}$$

The eigenvalues of I_z are m where m may have the (2I + 1) values between $\pm I$, so the allowed energies (Zeeman energies) are

$$E_m = -\gamma \hbar B_o m \qquad m = I, I-1, \ldots\ldots -I \qquad (2.4)$$

This equation may be written equivalently as

$$E_m = -g_n \mu_n B_o m \qquad (2.5)$$

where g_n and μ_n are the nuclear g factor and nuclear magneton respectively. Transitions between these energy levels may be induced by an oscillating magnetic field of angular frequency ω_o (the Larmor frequency) applied perpendicularly to B_o if the resonance condition

$$\hbar \omega_o = \gamma \hbar B_o \qquad (2.6)$$

is met.

In a real solid, the nuclear Hamiltonian would contain terms descriptive of the interactions of a nucleus with its neighbours, electrons and its environment. We will discuss these interactions in later sections but for the moment simply consider an isolated assembly of spins in a field B_o. Providing some nuclear-nuclear interaction exists then the spins will be in thermal equilibrium and will distribute themselves over the available energy levels in a Boltzmann distribution. The distribution is characterised by a spin temperature T_S so that, at equilibrium, the populations of two adjacent energy levels are in the ratio

$$\frac{N_{m+1}}{N_m} = \exp\left(\frac{\gamma \hbar B_o}{k T_S}\right) \qquad (2.7)$$

If the equilibrium is disturbed then nuclear-nuclear interactions will restore the system to a common spin temperature with a characteristic relaxation time T_2 called the spin-spin relaxation time.

We now drop the requirement of isolation of our spin system and consider the effect of embedding our spin assembly in a lattice at temperature T_L : at equilibrium $T_S = T_L$. If we disturb the equilibrium such that T_S is no longer equal to T_L then interactions between the spins and the lattice will tend to restore the equilibrium condition with a characteristic time constant T_1 called the spin-lattice relaxation time. For solids, $T_2 \sim \mu S$ and T_1 may be as long as several hours. Thus the spin ensemble maintains a uniform spin temperature throughout the spin lattice relaxation process.

2.3 Dipolar Interaction

We have already implied the existence of nuclear interactions and we describe here the dipolar interaction that nuclei may experience.

If a sample is placed in a magnetic field then the nuclei will be subject both to the static field and a varying local field produced by their neighbours through the dipolar interaction which leads to a broadening of the resonance line. For a system of N spins, the dipolar Hamiltonian may be written

$$\mathcal{H}_{dd} = \frac{\mu_o}{4\pi} \sum_{j<k}^{N} \frac{\underline{\mu}_j . \underline{\mu}_k}{r_{jk}^3} - \frac{3(\underline{\mu}_j . \underline{r}_{jk})(\underline{\mu}_k . \underline{r}_{jk})}{r_{jk}^5} \qquad (2.8)$$

It is convenient to rewrite this Hamiltonian in spherical polar coordinates r, ϑ , ϕ and use the raising and lowering operators I^+ and I^- . Recalling $\mu = \gamma \hbar I$, the transformed Hamiltonian reads

$$\mathcal{H}_{dd} = \frac{\mu_o}{4\pi} \sum_{j<k} \frac{\gamma_1 \gamma_2 \hbar^2}{r_{jk}^3} (A + B + C + D + E + F) \qquad (2.9)$$

where

$$A = I_{jz} I_{kz} (1 - 3\cos^2 \vartheta_{jk})$$

$$B = -\frac{1}{4}(I_j^+ I_k^- + I_j^- I_k^+)(1 - 3\cos^2 \vartheta_{jk})$$

$$C = -\frac{3}{2}(I_j^+ I_{kz} + I_{jz} I_k^+) \sin \vartheta_{jk} \cos \vartheta_{jk} \exp(-i \phi_{jk})$$

$$D = -\frac{3}{2}(I_j^- I_{kz} + I_{jz} I_k^-) \sin \vartheta_{jk} \cos \vartheta_{jk} \exp(i \phi_{jk})$$

$$E = -\frac{3}{4} I_j^+ I_k^+ \sin^2 \vartheta_{jk} \exp(-2i \phi_{jk})$$

$$F = -\frac{3}{4} I_j^- I_k^- \sin^2 \vartheta_{jk} \exp(2i \phi_{jk})$$

Terms A and B commute with the Zeeman Hamiltonian

$$\mathcal{H}_z = -\gamma \hbar B_o \sum_{i=1}^{N} I_{iz} \quad , \tag{2.10}$$

and cannot exchange energy with it. Term A represents the classical interaction between two dipoles $\underline{\mu}_j$ and $\underline{\mu}_k$ whilst term B connects states $|m_j, m_k\rangle$ to states $\langle m_j + 1, m_k - 1|$ or $\langle m_j - 1, m_k + 1|$ and can thus induce mutual spin flips between $\underline{\mu}_j$ and $\underline{\mu}_k$. This term, familiarly known as the flip-flop term, is an efficient method by which nuclear spin energy can diffuse through a spin system. The C and D terms flip one spin only such that $\Delta (m_j + m_k) = \pm 1$ and the E and F terms flip two spins in the same direction such that $\Delta (m_j + m_k) = \pm 2$. The effect of the C, D, E, F terms is to produce absorption lines at frequencies $\omega_o \pm \omega_o$ where as before ω_o is the nuclear Larmor frequency. These lines are usually so weak as to be negligible and the dipolar Hamiltonian is then truncated so as to contain only the A and B terms.

2.4 Quadrupolar Interaction [12]

The interaction energy of a nuclear charge density distribution $\rho(\underline{r})$ with an external electric potential V is

$$E = \int \rho(\underline{r})\, V(\underline{r})\, d\tau \qquad (2.11)$$

$V(\underline{r})$ may be expanded about the nuclear centre of mass as origin in a Taylor series to give an expression for E as

$$E = V_o \int \rho\, d\tau + \sum_{\alpha} V_\alpha(o) \int \alpha \rho\, d\tau + \frac{1}{2!} \sum_{\alpha\beta} V_{\alpha\beta}(o) \int \alpha\beta \rho\, d\tau + \ldots\ldots \qquad (2.12)$$

where $\alpha, \beta = x, y, z$, $V_\alpha(o) = \left.\frac{\partial V}{\partial \alpha}\right)_{r=0}$ and $V_{\alpha\beta}(o) = \left.\frac{\partial^2 V}{\partial \alpha\, \partial \beta}\right)_{r=0}$

In this expression for E, the first term represents the electrostatic energy of a point nucleus and being thus independent of nuclear size, shape or orientation is unimportant for our discussion. The second term involves the electric dipole moment of the nucleus and this term vanishes since the nuclear centre of mass and centre of charge coincide. The third term is the quadrupole term and is the largest correction to the point charge interaction. A 'principal axis' coordinate system may be chosen such that $V_{\alpha\beta} = 0$, $\alpha \neq \beta$ leaving the only non-zero components as V_{xx}, V_{yy} and V_{zz}. Moreover Laplace's equation gives

$$\sum_{\alpha} V_{\alpha\alpha} = 0 \qquad (2.13)$$

Thus for any nucleus in a cubic environment such that $V_{xx} = V_{yy} = V_{zz}$, the quadrupolar interaction vanishes. A spin $\frac{1}{2}$ (or spin zero) nucleus has no orientation dependence of its charge distribution so again the quadrupole interaction is zero. We only expect, therefore, to observe quadrupole effects for nuclei of spin $I > \frac{1}{2}$ and when they

are situated in non-cubic environments. The quadrupolar Hamiltonian in the principal axis system may be written

$$\mathcal{H}_Q = \frac{e^2qQ}{4I(2I-1)} \left[3I_z^2 - I^2 + \tfrac{1}{2}\eta (I^{+2} + I^{-2}) \right] \qquad (2.14)$$

where Q is the quadrupole moment of the nucleus, η is an asymmetry parameter and eq is the field gradient: the quantities are defined as

$$Q = \frac{1}{e}\int \rho(\underline{r})(3z^2 - r^2)d\tau \qquad \eta = \frac{V_{xx} - V_{yy}}{V_{zz}} \qquad eq = V_{zz} = \frac{\partial^2 V}{\partial z^2}$$

For axial symmetry of the field gradient, $V_{xx} = V_{yy}$ and η is zero. We note that an external charge can induce distortion in closed shell electrons surrounding the nucleus. This so-called Sternheimer anti-shielding can change V_{zz} from the bare nucleus value by up to two orders of magnitude.

If $\mathcal{H}_Q$ is small compared to the Zeeman Hamiltonian, the effect of the quadrupole interaction on a nuclear energy level may be determined by perturbation theory as

$$E_{m_j} = -\gamma\hbar B_o m_j + \frac{e^2qQ}{8I(2I-1)}(3m_j^2 - I(I+1))(3\cos^2\theta - 1) \qquad (2.15)$$

where θ is the angle between B_o and the principal z axis. In first order, the $\pm\frac{1}{2}$ levels are both shifted by the same amount and so their resonance line is unshifted. The remaining energy levels are however no longer equispaced and the result is a series of $2I - 1$ satellite lines symmetrically placed about the $+\frac{1}{2}$ to $-\frac{1}{2}$ line. The satellites may be displaced far from the central line so that the quadrupole effect is manifested only through a reduction in intensity of the central line. Finally, if $e^2qQ \sim \partial\hbar B_o$ then the $\pm\frac{1}{2}$ transition may also be shifted and a second order broadening obtains.

2.5 Electron-Nuclear Magnetic Interaction

In the absence of a magnetic field, the Hamiltonian describing the interaction between a nucleus of magnetic moment $\underline{\mu}_I$ and an electron with orbital moment $\underline{\mu}_L$ and spin moment $\underline{\mu}_S$ may be written

$$\mathcal{H}_{en} = -\frac{\mu_o}{4\pi}\left[\frac{2\underline{\mu}_I\cdot\underline{\mu}_L}{r^3} - \left\{\frac{\underline{\mu}_S\cdot\underline{\mu}_I}{r^3} - \frac{3(\underline{\mu}_I\cdot\underline{r})(\underline{\mu}_S\cdot\underline{r})}{r^5}\right\} + \frac{8\pi}{3}\,\underline{\mu}_I\cdot\underline{\mu}_S\,\delta(r)\right] \qquad (2.16)$$

The first term represents the orbital hyperfine coupling due to the field produced by the electron orbital motion. In diamagnetic materials, the nucleus is surrounded by filled electron shells having zero orbital (and spin) angular momentum and hence this term vanishes. In paramagnetic materials, the orbital angular momentum of the unbalanced spin is often quenched by the crystalline electric field and so this term is again negligible. The application of a magnetic field can lead to a slight unquenching and then the $\underline{\mu}_I\cdot\underline{\mu}_L$ interaction leads to a small shift in the nuclear resonance frequency known as a chemical shift.

The term in braces in $\mathcal{H}_{en}$ is the dipolar interaction between an electron spin and a nuclear spin. In diamagnetic substances, the lack of a resultant electron spin angular momentum leads to the vanishing of this term. In paramagnetic materials, the field at a nucleus produced by a static electron spin moment is much greater than normally attainable laboratory fields. However, the electron spin is rarely static since the presence of exchange coupling between

neighbouring electrons or fast relaxation to the lattice results in an electron spin flipping rapidly ($\sim 10^{-13}$ sec) between the two $S_z = \pm \frac{1}{2}$ states. A nucleus, then, sees the time-averaged dipolar field due to a fluctuating electron. This average field is non-zero since the populations of the states with $S_z = \pm \frac{1}{2}$ are different but the field will be very much less than that created by a stationary spin moment and so the paramagnetic nuclear resonance shift is correspondingly small. Two further properties of the dipolar term are that, firstly, it vanishes if the nucleus is in a site of cubic symmetry and secondly that the dipolar approximation is only valid for distances r greater than the nuclear radius. The latter requires us to write a so-called contact interaction valid for small r in the hyperfine Hamiltonian which is shown as term three in $\mathcal{H}_{en}$. This term assumes importance when the dipolar approximation becomes invalid, the delta function ensuring that only those electrons with finite amplitude at the nucleus (s - electrons) can contribute.

In metals, the contact interaction leads to a paramagnetic shift of the nuclear resonance of order 1%. The ratio of the shift to the applied field is known as the Knight shift K[13, 14]. Experimentally, it is found that K is nearly always positive, temperature-independent and the shift is proportional to field. An expression for K may be written

$$K = \frac{\mu_o}{4\pi} \cdot \frac{8\pi}{3} \cdot \frac{\chi_S M}{\mu_o} \langle |\psi(o)|^2 \rangle_{E_F} \qquad (2.17)$$

where M is the atomic mass, χ_S the electron spin (Pauli) susceptibility per unit mass and $\langle |\psi(o)|^2 \rangle_{E_F}$ is the s-electron

density evaluated at the nucleus, averaged over the Fermi surface and normalised in an atomic volume. Writing χ_s in the free-electron approximation yields

$$K \propto \langle|\psi(o)|^2\rangle_{E_F} \; n^{\frac{1}{3}} \qquad (2.18)$$

where n is the electron density.

In non-cubic metals or where electrons are of non-s type, then the presence of a non-zero dipolar term leads to an anisotropy in the Knight shift and resonance line broadening. The orbital term in $\mathcal{H}_{en}$ can also contribute but only in second order and only for those metals with non-s bands such as transition metals. A more significant effect for transition metals is that of core polarisation which may furnish a shift of either sign. The mechanism is, briefly, that the d valence electrons interact via exchange with s-type core electrons. These core states distort and produce a Knight shift due to their direct contact with the nucleus.

Our final consideration in this section of the electron-nuclear interaction is of the second order coupling between electron spins and nuclei. In diamagnetic materials we have noted above that the first order coupling vanishes. In second order a coupling does exist and is revealed by an indirect coupling between the nuclei which can lead to splittings of the narrow resonance lines observed in liquids. The effect of the coupling in the solid state has been considered by Bloembergen and Rowland[15] and by Ruderman and Kittel[16]. The origin of the coupling is that a nucleus of moment, say spin-up, is a favourable site for an atomic electron of parallel moment. A

neighbouring electron will prefer to be spin-down and thus its associated nucleus will tend to be spin-down. The argument shows that if either nucleus reorients its spin moment the neighbouring nucleus will also reorientate to maintain the antiparallel spin configuration. Therein lies a mechanism of indirect coupling between nuclei which is represented by the Hamiltonian

$$\mathcal{H}_{SS} = \sum_{i,j} A(\underline{r}_{ij})\, \underline{I}_i \cdot \underline{I}_j \qquad (2.19)$$

providing the electrons are of s-type and thus interact through contact with the nuclei. The form of $\mathcal{H}_{SS}$ has suggested the term of pseudoexchange coupling. This can be responsible for either a narrowing or a broadening of a resonance line subject to whether the indirect coupling is amongst like or unlike nuclei respectively. Consideration of the indirect nuclear interaction is necessary to account for the nuclear linewidths in heavy metals and in undoped III-V semiconductors.[17]

2.6 Spin Lattice Relaxation in Metals and Semiconductors

In this section we shall consider the methods by which nuclei may relax to the lattice in solid metals and doped semiconductors. Deviations from simple theory relating the Knight shift and spin-lattice relaxation time are discussed in the following section.

For metals, the dominant relaxation mechanism is often the contact term that we described in connection with the Knight shift. We may rewrite the contact term of $\mathcal{H}_{en}$ in section 2.5 as

$$\mathcal{H}_c = -\frac{\mu_o}{4\pi}\frac{8\pi}{3}\gamma_e\gamma_n\hbar^2\,\delta(r)\left[I_z S_z + \tfrac{1}{2}(I^+S^- + I^-S^+)\right] \qquad (2.20)$$

where the $I(S)^{+(-)}$ are the nuclear (electron) raising (lowering) operators. The part of $\mathcal{H}_c$ involving $I_z S_z$ was used in the first order calculation of the Knight shift. The remaining terms require simultaneous nuclear and electron spin flips analagous to the nuclear flip-flop term in the dipolar Hamiltonian. These spin flip terms imply that only those electrons within kT of E_F can take part in the relaxation process. Furthermore the time τ_c spent by an electron at an atomic site is by the Heisenberg uncertainty principle of order $\hbar/E_F \sim 10^{-16}$ sec: thus a nucleus experiences a fluctuating local field with a very short correlation time τ_c. The nuclear transition probability is then proportional to $\left|\mathcal{H}_c\right|^2_{av} \tau_c$ and the spin lattice relaxation time is then given by the approximate formula

$$\frac{1}{T_1} \sim \left|\mathcal{H}_c\right|^2_{av} \frac{\hbar}{E_F} \frac{kT}{E_F} \tag{2.21}$$

A detailed calculation gives

$$\frac{1}{T_1} = \left(\frac{\mu_o}{4\pi}\right)^2 \frac{64\pi^3}{9} \gamma_e^2 \gamma_n^2 \hbar^3 \langle|\psi(o)|^2\rangle^2_{E_F} N^+(E_F) N^-(E_F) kT \tag{2.22}$$

where $N^{+(-)}(E_F)$ are the densities of states for up(down) spins at E_F. For a degenerate free-electron gas

$$T_1 \propto n^{-\frac{2}{3}} T^{-1} \tag{2.23}$$

We thus anticipate these dependences of T_1 in simple metals and heavily doped semiconductors at low temperatures. If we combine the expressions for K and T_1 we obtain the Korringa relation[18]

$$K^2 T_1 T = \frac{\hbar}{4\pi k} \left(\frac{\gamma_e}{\gamma_n}\right)^2 \tag{2.24}$$

which is discussed in more detail below.

If the electron system is non degenerate as in, say, a doped semiconductor at high temperatures, then Maxwell-Boltzmann statistics rather than those of Fermi-Dirac apply and T_1 has been shown to scale as [160]

$$T_1 \propto n^{-1} T^{-\frac{1}{2}} \tag{2.25}$$

These temperature dependences of T_1 in materials with degenerate and nondegenerate electron gases are in contradistinction with those in substances where no conduction electrons exist: the latter usually have relaxation rates (T_1^{-1}) that decrease much faster than the first power of temperature. Another feature of relaxation by Fermi contact is the independence of T_1 on field (frequency).

2.7 Real Materials

Our conspectus of nuclear relaxation and the Knight shift in metallic materials has assumed the applicability of the free-electron theory and electron-nuclear interaction solely through the contact term. In real materials, electron-electron interactions may modify the n dependence of T_1 and K and invalidate the Korringa relation. The Korringa product S_K defined as

$$S_K = K^2 T_1 T \frac{4\pi k}{\hbar} \left(\frac{\gamma_n}{\gamma_e}\right)^2 \tag{2.26}$$

may change from its free-electron value of unity if other contributions to relaxation exist apart from the assumed s-state hyperfine coupling. We focus on these relaxation effects first, again neglecting electron-electron interactions.

The non-contact part of the electron-nuclear Hamiltonian has been stated to give no contribution to the Knight shift in cubic metals. In contrast, it is the squares of the off-diagonal elements of the Hamiltonian connecting adjacent energy levels that enter a calculation of the nuclear transition probabilities and thus determine the relaxation time. The inference is that the orbital and dipolar parts of $\mathcal{H}_{en}$ may reduce T_1 from the value computed using the contact interaction alone. Of course, in metals with s-type electrons, the contact term is always dominant but in those materials with electrons of substantial non-s character, the non-contact interaction is not negligible. As an example we quote the tight-binding calculation of Obata[19] for p- and d-band materials. The orbital interaction is found to be many times more effective than the dipolar interaction as far as relaxation is concerned. For transition metals, the contact and non-contact contributions to relaxation are of comparable magnitude. The contact term is large because the s-electron density at the nucleus is large whilst the non-contact term is of similar magnitude because the density of states of the d-electrons is great and Obata's analysis shows T_1^{-1} to be proportional to the density of states. A further contribution to relaxation important in materials with partially-filled d-bands is that due to core polarisation. Since this results from an s - d electron interaction and we have not as yet considered electron-electron effects, we shall not discuss this term further. We merely point out that, for example, Pt^{195} $(5d^9\ 6s)$ has theoretically almost equal contributions from contact, core polarisation and orbital interactions which yield a composite value of T_1T in good agreement with experiment.

The final effect we consider here, experienced only by those nuclei with $I > \frac{1}{2}$, is a quadrupole interaction between the nuclei and the field gradients created by conduction electrons. (The relaxation rate due to the interaction of nuclei with 'static' field gradients resulting from crystal distortion is negligibly small in metals.) Mitchell[20] has estimated this effect using the s- and p- parts of expanded Bloch functions and shows that the quadrupole interaction is of the order of the noncontact part of the hyperfine interaction. Kessel[21], using a similar approximation to Mitchell, has given a more general formula for the quadrupolar relaxation rate and also has shown that an indirect quadrupolar interaction between nuclei can exist similar to the Ruderman - Kittel indirect exchange term that we have described above. Finally, Haga and Maeda[22] have considered the quadrupolar coupling in metals explicitly taking the antishielding into account. In metals, field gradients are produced both by crystal fields and by conduction electrons. The induced field gradients at the nuclear sites are, as before, modified by antishielding factors but that associated with the conduction electron component is a small correction. Although the crystal field antishielding correction may be large, the fact that T_1T is a constant argues against the importance of antishielding effects in metals. Obata[23] has extended his own tightbinding calculation but finds the quadrupolar interaction to be rather ineffective in transition metals. Experimentally, the quadrupolar coupling is important for those nuclei which have a large ratio of quadrupolar to magnetic moments, e.g. Ta^{181} where the quadrupolar relaxation rate is an order of magnitude greater that the dipolar contribution.

It is important to note that the relaxation rates corresponding to contact, noncontact and quadrupole interactions are all linear in temperature. The only simple method of distinguishing between the various mechanisms is for materials which possess more than one magnetic isotope with one or more having a quadrupole moment. For two isotopes i, j the ratio of the magnetic relaxation rates is

$$\frac{T_{1_i}^{-1}\Big|_{mag}}{T_{1_j}^{-1}\Big|_{mag}} = \frac{\mu_i^2}{\mu_j^2} \tag{2.27}$$

If the equality is not satisfied then a quadrupolar contribution must be present and the equality

$$\frac{T_{1_i}^{-1}\Big|_{quad}}{T_{1_j}^{-1}\Big|_{quad}} = \frac{Q_i^2}{Q_j^2} \tag{2.28}$$

allows the separate determination of $T_{1\ mag}$ and $T_{1\ quad}$. The technique has been applied to Mo metal by Narath and Alderman[24] enabling them to make the first quantitative estimate of the quadrupole moments of Mo^{95} and Mo^{97}.

We turn now to the effects of electron-electron interaction in T_1, K and K^2T_1T. Pines[25], in an early treatment, noted that relaxation times calculated from the Korringa relation using the measured Knight shift values were shorter than those measured experimentally. Since the discrepancy could only be increased by appealing to other relaxation processes, Pines rewrote the Korringa relation to take account of the enhancement due to electron-electron interaction of the electron susceptibility (to which the Knight shift is

proportional). Relaxation times deduced from this 'interacting Korringa' relationship were then longer than measured values and thus more acceptable. Later studies by Moriya[26] and Narath[27,28] showed that the relaxation rate is enhanced as well as the Knight shift. The refined Korringa relation is then

$$K^2 T_1 T = \frac{\hbar}{4\pi k} \left(\frac{\gamma_e}{\gamma_n}\right)^2 [K(\alpha)]^{-1} \qquad (2.29)$$

where $K(\alpha)$ is a measure of the enhancements of T_1^{-1} and K and is tabulated by Narath[27]. Results show that the enhancement of T_1^{-1} is roughly five times less than that of K^2 so the overall effect, if electron-electron effects are important, is for the value of the Korringa product to rise above unity.

We now attend to some of the features of T_1 and K in heavily doped semiconductors following the analysis of Holcomb and coworkers[6,7] closely. For our purpose we first recast the expression for K in the equivalent forms

$$K = \frac{\mu_o}{4\pi} \frac{8\pi}{3} \left[\frac{N_D g \mu_B \langle S_z \rangle}{B_o}\right] P'_F$$

$$= \frac{\mu_o}{4\pi} \frac{8\pi}{3} \left[\frac{N_D g \mu_B \langle S_z \rangle}{B_o}\right] \Omega_o P_F \qquad (2.30)$$

where the term in square brackets is χ_S, P'_F is $\langle |\psi(o)|^2 \rangle_{E_F}$ normalised in a unit volume and P_F is $\langle |\psi(o)|^2 \rangle_{E_F}$ normalised in the impurity atomic volume Ω_o. The number of electrons per unit volume is N_D and g is the electronic g-value. The average value of an electron spin S_z at an atomic site is written $\langle S_z \rangle$.

Holcomb and his colleagues have called attention to the possible local variations in N, Ω_o, $\langle S_z \rangle$ and P_F and thus K that may occur in a doped semiconductor e.g. Si:P. In a first analysis, Sundfors and Holcomb[7] showed that the local variations in K could all be contained in the variations of the electron density. They reasoned that P'_F being strongly peaked at P^{31} sites (cf. chapter 4), would not depend strongly on local density fluctuations. A constant value of $\langle S_z \rangle$ was also taken since the electron spin-lattice relaxation time (10^{-8}sec) was much greater than the travelling time for a carrier between nuclear sites (10^{-14}sec). The distribution of K values was then reduced to a consideration of the fluctuation in N_D which was taken to be represented by a Poisson distribution. Their model was able to account satisfactorily for the strongly asymmetric P^{31} lineshapes (chapter 4).

Further discussion has been made by Brown and Holcomb[6]. They point out that although $N\ \Omega_o = 1$ for simple metals with all nuclear sites equivalent and one electron per atom, the equality is unlikely to hold for the P^{31} 'atoms' in doped Si since the volume used for obtaining average values of N and Ω_o may not be the same. Variations in P_F from nuclear site to nuclear site are also probable. Whilst acknowledging the complexity of interpretation of K, Brown and Holcomb are able to show that if their Knight shift distribution model is sound then two consequences emerge. Firstly, the linewidth shape should be independent of field, temperature and only slightly dependent on donor density. Further the linewidth should scale linearly with the Knight shift. The second point is that any temperature dependence of K resides in χ_S. Good agreement with experiment is found on both

counts except for a small unexpected temperature dependence of the linewidth in any given sample (cf. chapter 4).

Finally, we consider how T_1 may be modified in a doped semiconductor just on the metallic side of the metal-nonmetal transition where the electron mean free path is of the order of the interatomic distance. (We discuss this strong scattering or diffusive regime of conduction in chapter 3.) Warren[29], in his work on the so-called liquid semiconductors, gives an approximate derivation of a Korringa-type relation in this conduction regime as

$$K^2 T_1 T = \frac{\hbar}{16k} \left(\frac{\gamma_e}{\gamma_n}\right)^2 \frac{\hbar N(E_F)}{\tau_e} \qquad (2.31)$$

where τ_e is the mean free time of an electron and may be identified as the dwell time of a carrier at an atomic site. In the weak scattering limit where the mean free path is greater than the interatomic spacing then the nearly free electron theory gives

$$\tau_e \sim \hbar N(E_F) \qquad (2.32)$$

Expression 2.31 then reduces to the Korringa relation within a factor of order unity. In the diffusive regime and especially if localisation has just set in then τ_e may rise above the value $\hbar N(E_F)$. The relaxation rate will then be enhanced in line with the general fact that a localised electron (paramagnetic centre) is more efficient at relaxation than an itinerant electron. The Korringa product will then be less than unity which is in direct contrast to the behaviour of S_K when electron-electron effects are present. To illustrate this effect we quote Warren's results[29] for liquid Ga_2Te_3. The enhancement

of the magnetic relaxation rate over that deduced from the Korringa relation is

$$\eta = \frac{T_1^{-1}\ \text{mag}}{T_1^{-1}\ \text{Korr}} \qquad (2.33)$$

For Ga_2Te_3 at 1400 K, the relaxation rates for all the nuclear ingredients give $\eta \sim 2$ and $\tau_e \sim 10^{-16}$ sec. Close to the melting point of 1065 K, η rises rapidly to 150 and $\tau_e \sim 2.10^{-15}$ sec. Similar values obtain also for liquid In_2Te_3 but not for liquid Sb_2Te_3 where $\eta \sim 1$ for all temperatures above the melting point. This may be understood when notice is taken of the much higher conductivity of liquid Sb_2Te_3 over liquid In_2Te_3 and Ga_2Te_3. The inference is that Sb_2Te_3 has a more metallic character than In_2Te_3 and Ga_2Te_3 and as Warren shows, Sb_2Te_3 lies on the boundary of conductivity behaviour between those liquids describable by a nearly free electron model ($\eta = 1$) and those materials in which conduction is diffusive in nature.

2.8 Spin Diffusion

The concept of spin diffusion was first proposed by Bloembergen[30] as a means of reconciling the enormous discrepancy existing between measured and early theoretical T_1 values in a variety of materials. He showed that the presence of a few paramagnetic centres in a solid or liquid could drastically shorten the host nuclear relaxation time. Refinements to Bloembergen's ideas have been made by, for example, Khutsishvili[31] and Blumberg[32], but we do not discuss these in detail here.

The basis of the impurity-nucleus interaction is that of dipolar coupling: the scalar coupling is ineffective since the electron does not penetrate the host nuclei. The impurity is strongly coupled to its immediate neighbour nuclei since their spin energy may diffuse towards the paramagnetic centre via some spin diffusion mechanism. The rapid flipping of the electron at the paramagnetic site ensures a swift transfer of energy to the lattice. The nuclei closest to the impurity and within a sphere of radius b are relaxed fastest but because they also experience a large magnetic field due to the paramagnetic ion, their resonance frequencies are shifted considerably and they then are isolated from the bulk nuclei. For this reason b is known as the spin diffusion barrier radius, i.e. only those nuclei outside b can communicate via spin diffusion. The diffusion equation for the magnetisation M may be formally written

$$\frac{\partial M}{\partial t} = D \nabla^2 M \qquad (2.34)$$

where D is a diffusion coefficient given, for a face-centred cubic lattice of lattice constant a_o, by

$$D = \frac{a_o^2}{14 T_2} \qquad (2.35)$$

In order to discuss the various cases of spin diffusion we must first define the so-called pseudopotential radius ρ which is that distance from an impurity where a nucleus has equal probability of being relaxed directly by the impurity or spin flipping with its neighbour. The direct nuclear relaxation rate is

$$T_{dir}^{-1} = \frac{C}{r^6} \qquad (2.36)$$

where

$$C = \left(\frac{\mu_o}{4\pi}\right)^2 \frac{2}{5} (\gamma_e \gamma_n \hbar)^2 \frac{S(S+1)}{1+\omega_o^2 \tau^2}$$

and τ is the correlation time of the z-component of the spin S. Khutsishvili gives

$$\rho \sim \left(\frac{C}{D}\right)^{\frac{1}{4}} \tag{2.37}$$

The remaining characteristic dimension that we will refer to is the distance R between the paramagnetic impurities of density N_p given by the usual formula

$$\frac{4}{3}\pi R^3 N_p = 1 \tag{2.38}$$

2.8.1 Diffusion Limited Relaxation

If $b \ll \rho \ll R$ then nuclear spin energy is donated to the lattice faster than spin diffusion can transport it to the paramagnetic ion. In this case

$$T_1^{-1} \sim N_p C^{\frac{1}{4}} D^{\frac{3}{4}} \tag{2.39}$$

and since the relaxation rate is limited by the spin diffusion rate, the term diffusion limited relaxation follows. Immediately after saturation, the magnetisation does not vary exponentially with time, as shown by Blumberg[32], but eventually the recovery does show exponential dependence. We refer to such behaviour as 'short time non-exponentiality'.

2.8.2 Rapid Diffusion Relaxation

If $\rho \ll b \ll R$, the direct relaxation rate is much less than the diffusion rate. The nuclear relaxation is then independent of D but proportional to the rate of direct relaxation of the nuclei to the lattice

by the fluctuating impurity magnetic field. Then

$$T_1^{-1} \sim N_p C b^{-3} \qquad (2.40)$$

As the direct relaxation is slow, the nuclei may maintain a common spin temperature and the recovery of the magnetisation is exponential.

2.8.3 Diffusion Vanishing Relaxation

If $R \sim \rho \gg b$, the direct relaxation rate is dominant for all times after the saturation of the nuclear spin system. Then Tse and Lowe[33] give

$$T_1^{-1} \sim N_p^{\frac{1}{3}} B^{-1} \tau^{-\frac{1}{2}} D^{\frac{1}{2}} \qquad (2.41)$$

and the magnetisation recovers exponentially with time. If ρ is also small, then Tse and Hartmann[34] show that the nuclear magnetisation is non-exponential for all times after saturation of the nuclear spins.

2.8.4 Field and Temperature Dependence of the Spin-Lattice Relaxation Time

The expressions for rapid diffusion and diffusion limited relaxation contain the factor C which will show a field dependence when $\omega_o \tau$ becomes of the order of unity. We can expect an increase in T_1 with field but the actual functional dependence is difficult to determine since b and τ are also field dependent. The temperature dependence of T_1 enters through τ which generally decreases with increasing temperature. Then $T_1 T$ plots usually show a minimum at $\omega_o \tau \sim 1$ as seen by, for example, Rogerson and Tunstall[35] in GaP:Te.

An extension of the ideas of spin diffusion has been made by Jerome et al.[36] in their study of Si:P. They imagine the impurity banded regime to be a network of metallic tunnels embedded in an insulating matrix. The nuclei in metallic regions are strongly relaxed

by the conduction electrons whilst those outside can communicate through a spin diffusion process. A barrier radius analogous to that described above emerges from the theory where, in this case, those nuclei in metallic regions have their resonance frequencies shifted by the magnetic polarisation of the electrons, i.e. the Knight shift. If neighbouring nuclei have Knight shifts larger than the dipole interaction then the spin flip process is suppressed. Since b will depend on the polarisation of the band electrons and scales as $B_o^{\frac{1}{3}}$ and T_1 is proportional to b^{-3}, a direct proportionality of T_1 on B_o will result.

2.9 NMR Linewidths

The first contribution to a resonance linewidth that we consider is that due to the nuclear dipole-dipole coupling. Abragam[8] has treated the calculation of linewidths by the method of moments in some detail so we merely quote the relevant formulae here

$$B_{dip} = \frac{2.36 M_2^{\frac{1}{2}}}{\gamma} \qquad (2.42)$$

where M_2 is the second moment of the resonance curve and is defined as

$$M_2 = \int (\omega - \omega_o)^2 f(\omega) d\omega \qquad (2.43)$$

where $f(\omega)$ is a normalised shape function which we take to be of gaussian form and ω_o is the Larmor frequency. For a monocrystalline solid containing one nuclear magnetic species of 100% abundance, Abragam gives

$$M_2 = \left(\frac{\mu_o}{4\pi}\right)^2 \frac{3}{4} \gamma^4 \hbar^2 I(I+1) \frac{(1 - 3\cos^2\theta_{jk})^2}{r_{jk}^6} \qquad (2.44)$$

where r_{jk} is the internuclear distance and θ_{jk} is the angle between B_o and r_{jk}. For a polycrystalline sample, the angular term may be averaged and the lattice sum expressed in terms of the lattice constant a_o so that M_2 becomes

$$M_2 = \left(\frac{\mu_o}{4\pi}\right)^2 \frac{3}{5} \gamma^4 \hbar^2 I(I+1)(116\, a_o^{-6}) \qquad (2.45)$$

where the coefficient of a_o^{-6} is that appropriate to the face-centred cubic lattice assumed by the atoms in Si and Ge. If the system under consideration is magnetically dilute, i.e. only a fraction f of lattice sites is occupied by magnetic nuclei, then the second moment approximates to

$M_2 f$ $\qquad f < 1\%$

M_2 $\qquad f > 10\%$

$M_2 f^{\frac{1}{2}}$ $\qquad 1 < f < 10\%$

For Si and Ge, the computed values of ΔB_{dip} are 20 μT. Such a width was observed for powdered samples of lightly doped Si:P by Sundfors and Holcomb[7] and Sasaki et al.[2]. In a single crystal, such as our Ge:As specimens, the linewidth will depend on the crystallographic orientation of the crystal with respect to the external field. We made no attempt to orientate our samples in order to investigate this effect since the available signal-to-noise ratio did not merit such a study. We merely note that our measured linewidths in lightly doped Ge are larger than those computed from nuclear dipolar coupling alone. (The contribution to ΔB from inhomogeneous applied static fields is considered in Appendix 1.)

If the nuclear spin $I > \frac{1}{2}$ then quadrupolar broadening may also be present, provided that the nuclei are in non-cubic environments. A single crystal should not exhibit a large quadrupole broadening if crystalline imperfections are kept to a minimum and no macroscopic strain exists in the prepared specimen. We can also suppose that if the electron distribution about a nucleus is not symmetric then that nucleus will be subject to an environment of lower than cubic symmetry. Since Sternheimer antishielding effects of this kind are small in metals, we gauge such an effect to be negligible. It is difficult to quantify the effects of quadrupole broadening but spin echo experiments such as that described by Solomon[37] do give the values of the quadrupole interaction. We refer to such techniques in chapter 5.

Chapter 3

THEORY OF THE METAL-NONMETAL TRANSITION

3.1 Introduction

The concept of a solid undergoing a transition from an insulating to a metallic state is due to the early work of Mott[38]. His seminal ideas have been expanded and embellished by many later workers and for a review of experimental data and current thought, the reader is referred to Mott's recent book[1].

Of the many substances that exhibit a metallic transition we shall perforce consider only doped semiconductors in this chapter. We first outline the physics of doped material and describe how an increase in impurity content leads to the phenomenon of impurity band conduction and eventually to fully metallic behaviour. The Mott transition and the Hubbard model are then discussed and an expression for the critical donor concentration N_C defining a metal-nonmetal transition is derived.

The problem of disorder is then treated leading to the concepts of Anderson localisation and the Anderson transition. Finally the ideas of Mott, Hubbard and Anderson are combined in an attempt to describe the transition in extrinsic semiconductors.

3.2 Physics of Doped Semiconductors

In the elemental, group IV semiconductors, Ge and Si, the atoms each have four valence electrons which bond covalently to nearest neighbour atoms forming a 'diamond lattice' arrangement. The substitutional incorporation of a group V impurity such as As in this lattice leads to a surfeit of one electron which forms a shallow, hydrogen-like donor state just below the conduction band.

(In the following, we consider only n-type material.) This extra electron is bound to the impurity in an orbit that can extend over hundreds of lattice sites, the 'Bohr radius' a_H being given by

$$a_H = \frac{4 \pi \varepsilon_o \kappa h^2}{m^* e^2} \qquad (3.1)$$

where κ is the background dielectric constant (16 in pure germanium) and m^* is an effective mass[39]. By way of example, for n-Ge, $a_H \sim 4$ nm and for n-Si, $a_H \sim 2$ nm, there being a slight dependence of a_H on a particular donor.

An increase in doping density leads to overlap of the donor wave functions and a concomitant broadening of the impurity level into an impurity band. The haphazard siting of the impurities and random Coulombic fields of ionised impurity centres also increase the impurity level width[40] and in turn reduce the donor ionisation energy. Within the impurity band electron transport is possible[41] since carriers may tunnel from full to empty donor sites with an activation energy ε_3 and indeed this process dominates transport property measurements at low temperatures. The presence of empty donor sites is caused by the inevitable compensation of a semiconductor by minority centres i.e. acceptors in our n-type material. These centres can accept electrons from a certain proportion of donors leaving them as empty sites. At higher temperatures, electrons are excited into the conduction band, the energy of activation being termed ε_1, which is identical to the donor ionisation energy. The electrons have high mobility in the conduction band so that, at higher

temperatures, the ϵ_1 process predominates over the ϵ_3 hopping conduction mechanism. Hopping conduction can also occur in uncompensated material as we point out in chapter 4.

If the impurity concentration is further increased, a critical concentration N_C is reached beyond which the electrons behave as a degenerate electron gas and the semiconductor exhibits a metallic character. The metallic regime is distinguished by the temperature independence of the Hall constant[42,43] and the resistivity and for Ge:As, $N_C \sim 3.10^{17}$ cm^{-3} and for Si:P, $N_C \sim 3.10^{18}$ cm^{-3}. The higher value of N_C for Si as compared to Ge is to be expected since the Bohr radius for Si is substantially smaller.

3.3 The Mott Transition

One particular form of transition to the metallic state is called the Mott transition and has the following basis. We consider a uniform array of hydrogen atoms with the interatomic distance $a \gg a_H$. Clearly the material is an insulator at normal temperatures with the ground state levels exactly filled and the first excited state, about 13 eV above the ground state, completely empty. As the lattice constant a is decreased, the two energy levels will broaden into bands thus reducing the energy of formation of excited carriers and excitons. Further the increasing production of excitons leads to a screening of the Coulomb field so that the exciton binding energy E_{ex} is lowered until $E_{ex} \sim kT$ and free carriers are created.

Mott has further argued that the number of carriers created is very large and thus the transition is sharp, in the sense that, at absolute zero, the conductivity of an insulator is zero and that of a metal is finite. The argument is based on the fact that an electron and hole attract each other with a long range Coulomb force and that a potential energy $V(r)$ of the form

$$V(r) \propto - \frac{e^2}{\kappa r} \tag{3.2}$$

always leads to the formation of bound states (excitons). Hence a small number of free carriers is impossible: their number must be great enough for the Coulomb potential to become screened as

$$V(r) \propto - \frac{e^2}{\kappa r} \exp(-\gamma r) \tag{3.3}$$

with γ, the screening length, large enough to inhibit the formation of bound states. In particular

$$\gamma a_H \sim 1.2 \tag{3.4}$$

for carrier delocalisation and, writing γ in the Thomas-Fermi approximation, an expression for N_C can be derived as

$$N_C^{\frac{1}{3}} a_H \sim 0.4 \tag{3.5}$$

This relationship is well borne out by experiment[44] though, as Martino et al.[45] have pointed out, the good agreement is in part fortuitous since the constant in equation (3.5) is sensitive to the choice of wave function, the type of screening considered and the number of conduction band minima. Calculations of the constant in equation (3.5) have been made by Martino et al.[45], Berggren[46,47] Sinha and Puri[48] and Kreiger and Nightingale[49].

The question on the sharpness of the transition is still in doubt. No discontinuity in N the number of carriers is observed in doped semiconductors due presumably to the random spatial positioning of the donors, but a discontinuity is observed in other non-crystalline systems such as Cu-Ar films. Kohn[50] has suggested that the electron gas might experience an infinite series of second order transitions leading to the transition point. Mott and Davis[51] show that this can lead to a tendency of $\varkappa$ to infinity (cf. chapter 4) at the transition and thereby a small number of free carriers is allowed thus removing the requirement of a discontinuity in N.

3.4 The Hubbard Model and the Highly Correlated Electron Gas

A theory leading to a metal-nonmetal transition was developed by Hubbard[52] in the mid-sixties. Whilst the discontinuous Mott transition was based on long range forces, the Hubbard model treats electron-electron interactions only if the carriers are both on the same atom. In considering only intraatomic interactions, the Hubbard model is just an extension of the tight-binding approximation.

The energy of a pair of electrons on the same site is given by

$$U = \iint \frac{e^2}{4\pi\varepsilon_o \varkappa r_{12}} |\psi(r_1)|^2 |\psi(r_2)|^2 d^3x_1 d^3x_2 \quad (3.6)$$

and the overlap energy integral betwen two sites i, j distance R apart is

$$I = \int \psi_i^* \mathcal{H} \psi_j \, d^3x \quad (3.7)$$

where $\mathcal{H}$ is the total Hartree-Fock Hamiltonian. Overlap causes the ground state of an isolated atom to be broadened into a band of width B_w where

$$B_w = 2z I \tag{3.8}$$

and z is the coordination number of each atom.

The energy required to take an electron from one centre and deposit it on another site is, for infinite R, equal to U. For finite values of R, both electron and hole may move in bands of width B_{w1} and B_{w2}. If we now change R by, for example, changing the donor concentration in a semiconductor, then the bandwidths also change but U remains constant. At some critical value of R such that

$$U = \tfrac{1}{2}(B_{w1} + B_{w2}) \tag{3.9}$$

a metal-nonmetal transition occurs. In qualitative language[53], we can say that, at large R, the Coulomb repulsion (proportional to U) keeps the electrons localised and prevents itinerancy within a band. If the electrons could form a band, they could reduce their energy by an amount proportional to the bandwidth. Hence, as R is decreased, a point is reached where the metallic state is energetically favoured to the localised state.

Pictorially, we can consider the transition as shown in figure (3.1). This pseudoparticle density of states diagram shows two Hubbard bands and three defined regions of behaviour. We can consider the system of singly-occupied donors to form the lower Hubbard band and that of the doubly-occupied sites as forming the upper Hubbard

FIG. 3.1

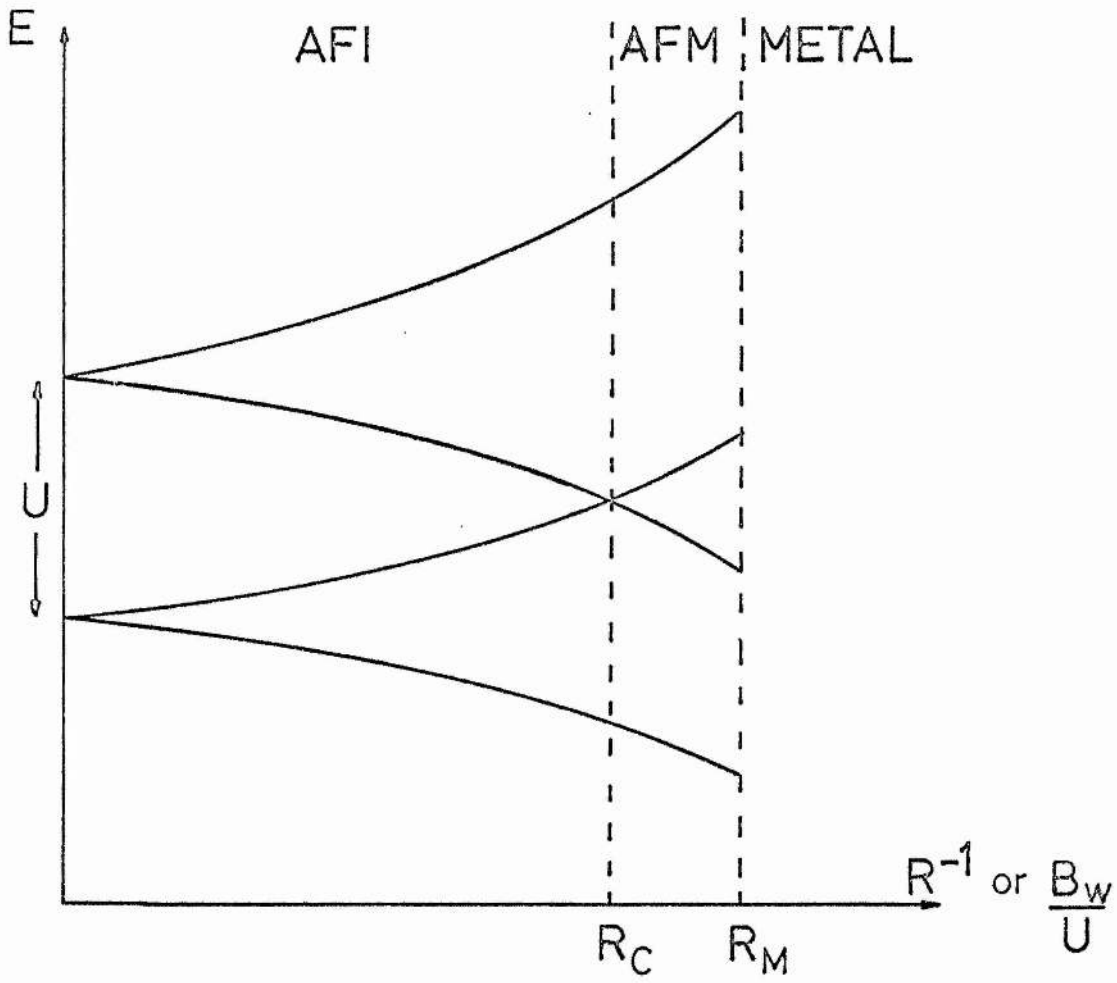

Variation in energy of the Hubbard bands with distance between centres. The transition occurs at R_C and the moments disappear at R_M. (After Mott[1]).

band or, as it is sometimes known, the D^- band. For large R, Mott[54] has shown that the material is an antiferromagnetic insulator (AFI). As R decreases, the bands overlap and metallic conduction sets in though the material remains antiferromagnetic (AFM). The AFM region is often unobservable and Mott[54, 55] conjectures that this may be due to an unstable region in a plot of free energy versus B_w / U or to a discontinuity in N though these arguments may not be valid for a doped semiconductor. Finally, a further increase in B_w / U causes the moments to disappear and the electrons form a highly correlated gas[56]. The gas is highly correlated in the sense that only a small proportion of sites are doubly-occupied or empty. These current carriers, electron-like and hole-like respectively, can move and couple with the moments on the $(1 - 2\xi)$ singly-occupied sites causing them to resonate between the two possible positions[55]. Now since the number of current-carriers is small ($\xi \sim 0.1$), the application of a field should lead to a small current flow. Now Luttinger[57] has shown that, providing long range antiferromagnetic order is absent, the shape or volume in k - space of the Fermi surface cannot be altered by electron correlation effects as contained in the Hubbard U term. Compatibility between the features of a Fermi surface enclosing one electron per atom and a small number of current carriers with a consequent small current flow can be achieved by showing that the carrier mass m_{enh} is enhanced over the band mass m_{band}. Mott shows that

$$\frac{m_{enh}}{m_{band}} = \frac{1}{2\xi} \qquad (3.10)$$

This enhanced mass leads to augmentation in the Pauli susceptibility and the electron specific heat whilst the thermopower should change sign as the number of carriers is changed[58].

We should note here that Mott[59] has discussed the highly correlated electron gas and the metallic transition by considering the carriers to be spin polarons. Since the changes in the argument are orismologic rather than physical we dwell no longer on this model.

Finally, we give a simple derivation of N_c using the Hubbard criterion. In equation (3.9) we take B_{w1} and B_{w2} to be the same as the uncorrelated tight-binding bandwidth B_w. Then the transition occurs when

$$\frac{B_w}{U} = 1 \qquad (3.11)$$

Mott[55] points out that the right hand side of this equation deduced from various treatments does not vary from unity by more than a factor of two. Assuming a coordination number of 6, then the condition (3.11) may be written

$$12 I = U \qquad (3.12)$$

Assuming hydrogenic wave functions

$$\psi = \text{const. } \exp(-\alpha R) \qquad (3.13)$$

U may be evaluated as

$$U = \frac{5}{8} \frac{e^2 \alpha}{4 \pi \varepsilon_o} \qquad (3.14)$$

In the large R limit ($\alpha R \sim 4$)

$$I \sim 10 \frac{e^2 \alpha}{4 \pi \varepsilon_o} \exp(-\alpha R) \qquad (3.15)$$

so invoking (3.12) gives

$$\propto R \sim 5 \qquad (3.16)$$

or, writing $NR^3 = 1$ and $a_H = 1$, we obtain

$$N_C^{\frac{1}{3}} a_H \sim 0.2 \qquad (3.17)$$

This is close to the Mott criterion and as Johansson[60] has observed, the different numerical estimates of the criteria are a consequence of the different ranges of potentials assumed in the two formulations.

3.5 Disorder, Anderson Localisation and the Anderson Transition

So far, we have examined the nature of a metal-nonmetal transition occurring in a regular array of atoms. A semiconductor is however, an example of a disordered material. The disorder is both 'lateral', in the sense that donor atoms are spatially distributed at random and hence overlap integrals vary, and 'vertical' in that electrons experience a random potential field caused by the presence of ionised centres, acceptors and other imperfections in the material causing on-site potentials to vary.

Anderson[61], in his difficult paper of 1958, was the first to show that, under certain conditions, the solutions of the one-electron Schrodinger equation show the electrons to be localised about a particular site. Consider the crystalline, three-dimensional array of potential wells (figure (3.2a)) in each of which resides one electron in an s-state. Overlap between neighbouring wells causes the electron levels to be broadened into a band of width $B_w = 2zI$. To every well, a random potential V fluctuating between the

FIG. 3.2a

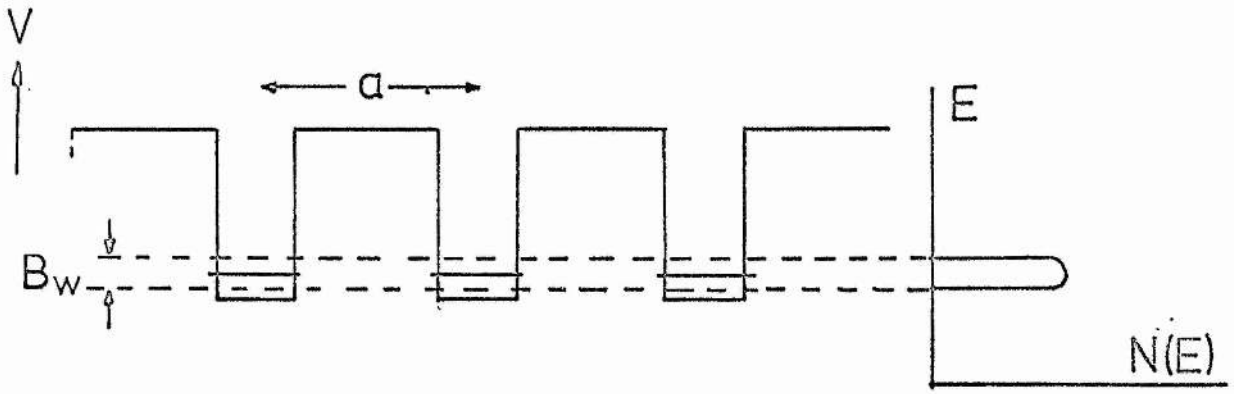

Potential wells for crystalline lattice.

FIG. 3.2b

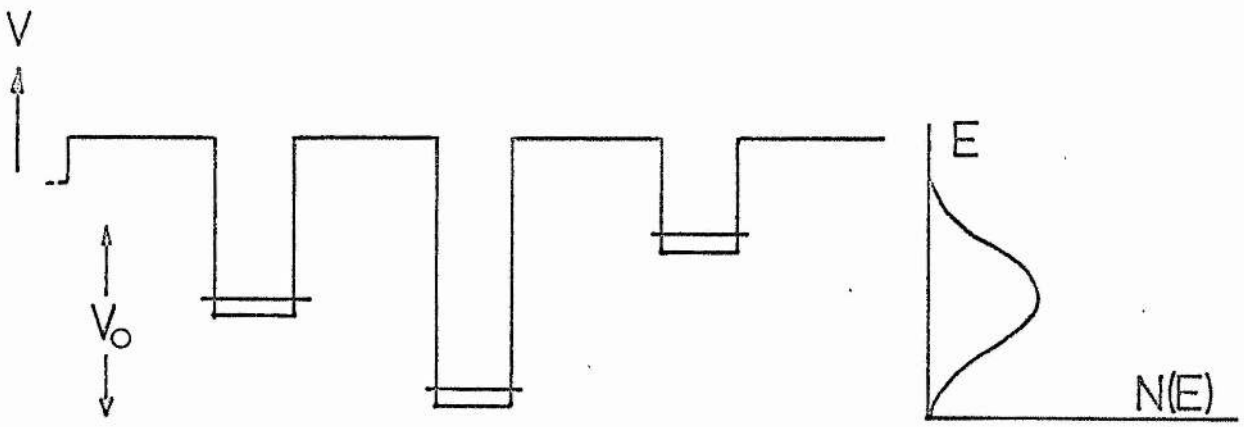

Potential wells for Anderson lattice.

FIG. 3.3a

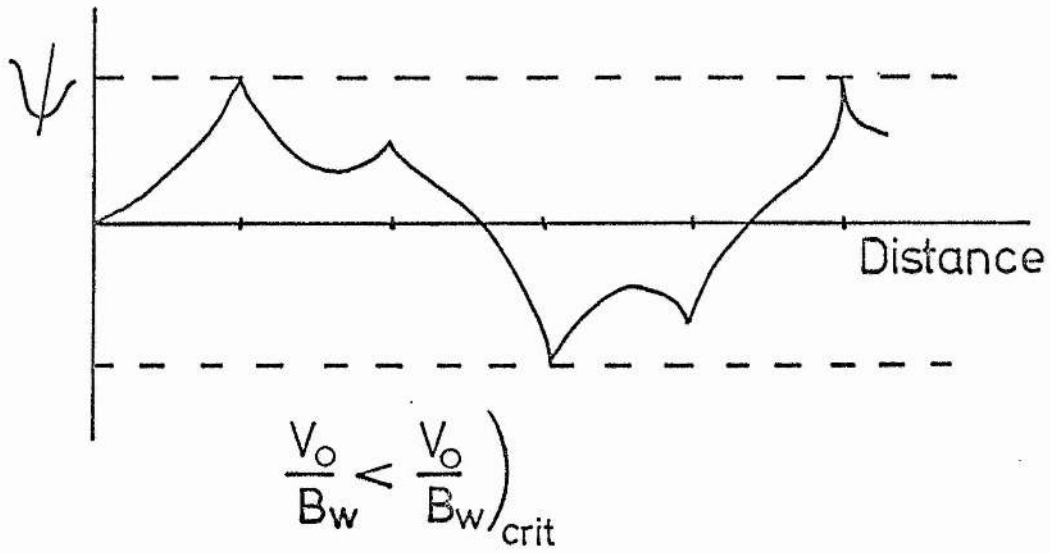

Wave Function for L~a. Extended states.

FIG. 3.3b

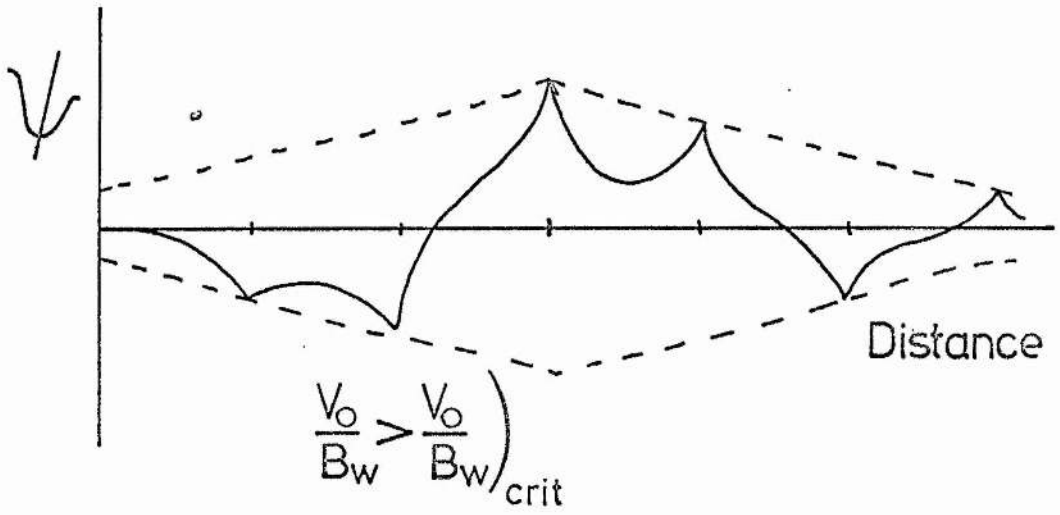

Weakly localised states.

limits $\pm V_o$ is added (figure (3.2b)). Then the Anderson theorem states that, at absolute zero, the chance that an electron will diffuse away from a particular well will tend to zero if [62]

$$\frac{V_o}{B_w} > \left(\frac{V_o}{B_w}\right)_{crit} \qquad (3.18)$$

The critical value of this ratio is difficult to calculate but is of the order of two. Wave functions for two values of V_o/B_w are shown in figures (3.3a, b). The random phase change from well to well is expected when the mean free path is of the order of the well separation as in the case of impurity conduction. Anderson[63] has observed that, at sufficiently low temperatures or excitation energies, electrons in a metal may be considered as independent entities moving in an average field: a so-called Fermi liquid. He states that a noninteracting theory is also true in the localised case and has christened the localised electron system a Fermi glass.

A consequence of Anderson localisation is that, at absolute zero, the d.c. conductivity σ is zero. Mott[1] has also pointed out that although V_o/B_w may lie below the critical value in the middle of a band, this will not be true at the extremities and thus the presence of localised states is to be expected[209]. It follows that an energy E_c must separate the energies of localised from extended states and this energy is termed the mobility edge[64] (figure (3.4)). Mott[58] expects localised tails in an Anderson band whether the disorder in the system is of vertical or lateral type. Further, if the Fermi energy at zero temperature E_{F_o} can be made to cross E_c then a metal-nonmetal transition (Anderson transition) results and the

FIG. 3.4.

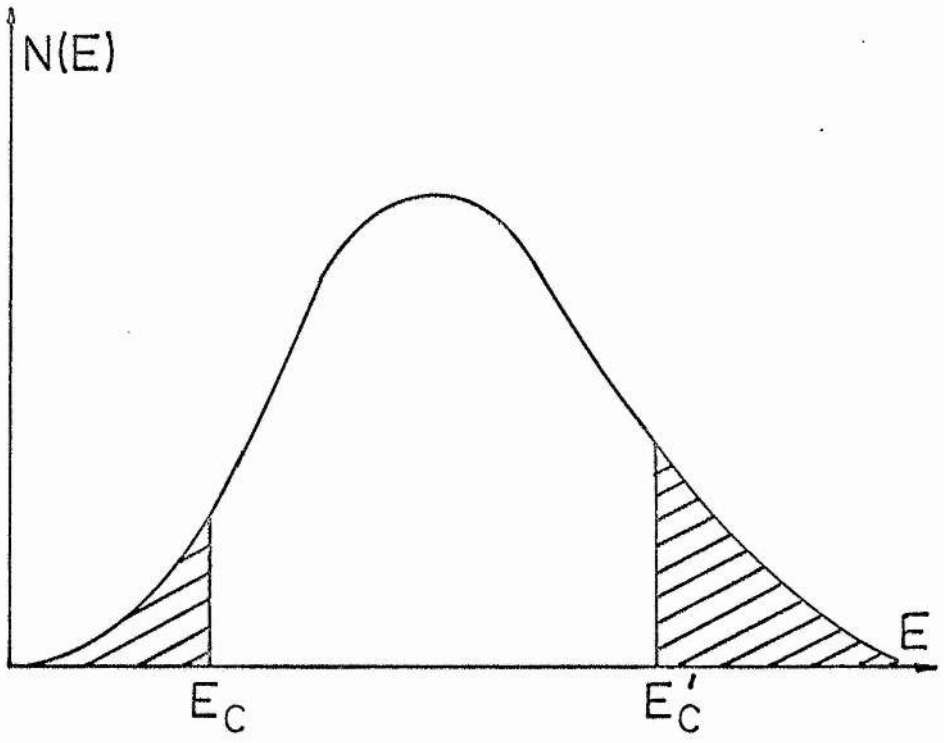

Density of states in an Anderson band with mobility edges E_C and E_C'. Localised states are shaded.

conductivity $\sigma(E)$ changes from zero ($E_{F_o} < E_c$) to a finite value σ_{min} ($E_{F_o} > E_c$). The subscript 'min' is applied because Mott has shown that, at zero Kelvin, the conductivity cannot have a non-zero value less than[65,66]

$$\sigma_{min} = \text{const.} \frac{e^2}{\hbar a} \left(\frac{V_o}{B_w} \right)^{-2}_{crit} \tag{3.19}$$

where the constant has a value dependent on a number of physical assumptions, notably the coordination number z.

On the metallic side of the transition, it is interesting to see how σ varies with V_o / B_w (figure (3.5)). For small V_o / B_w, the mean free path L is greater than the distance between atoms a and a Boltzmann formulation may be used to calculate σ. Assuming a spherical Fermi surface with surface area $S_F = 4\pi k_F^2 \sim \frac{4\pi^3}{a^2}$ where k_F is the Fermi wave vector, we have

$$\sigma = \frac{S_F e^2 L}{12\pi^3 \hbar} \sim \frac{e^2 L}{3\hbar a^2} \tag{3.20}$$

We now consider the effects of letting L tend to a. This is representative of a strong scattering regime and the Boltzmann approach is no longer valid. For $L \sim a$,

$$\sigma \sim \frac{e^2}{3\hbar a} \sim \text{const.} \frac{e^2}{\hbar a} \left(\frac{V_o}{B_w} \right)^{-2} \tag{3.21}$$

from which[58]

$$\left(\frac{V_o}{B_w} \right)_{L \sim a} \sim 0.6 \tag{3.22}$$

FIG.3.5

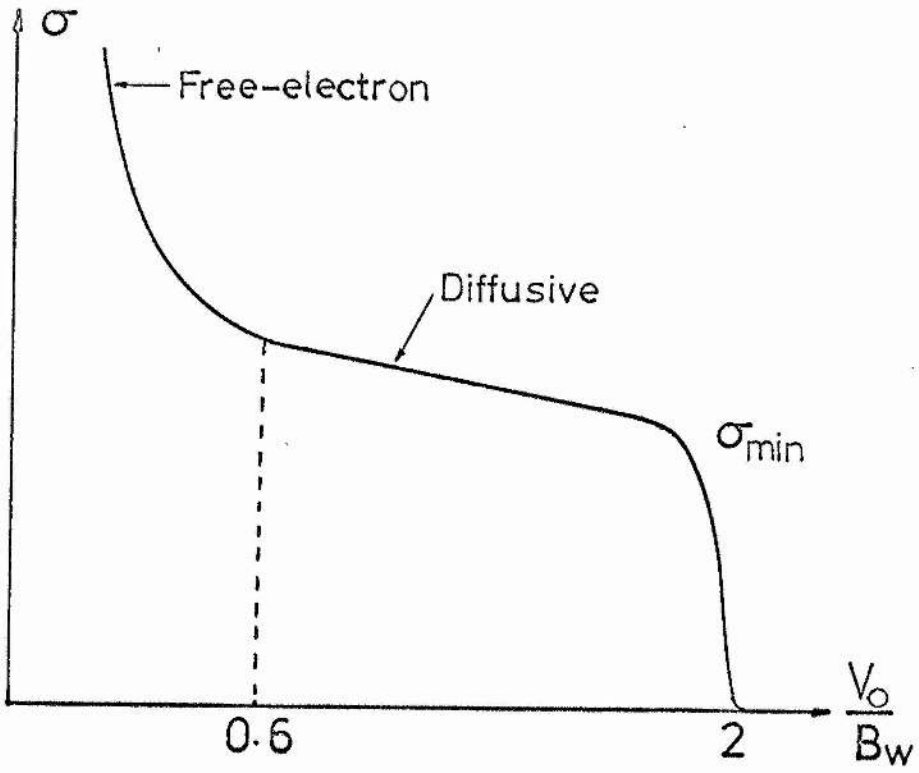

Conductivity for an Anderson band at zero temperature.

$$\left(\frac{V_0}{B_w}\right)_{L\sim a} = 0.6 \qquad \left(\frac{V_0}{B_w}\right)_{crit} = 2$$

The region defined by

$$\left(\frac{V_o}{B_w}\right)_{L\sim a} < \left(\frac{V_o}{B_w}\right) < \left(\frac{V_o}{B_w}\right)_{crit} \qquad (3.23)$$

is known as the diffusive regime and should exhibit interesting features in magnetic resonance experiments as discussed by Tunstall[67]. For doped semiconductors, the diffusive regime is approximately bracketed by the conductivity values $\sigma_{L\sim a} \sim 700\ \Omega^{-1}cm^{-1}$ and $\sigma_{min} \sim 50\ \Omega^{-1}cm^{-1}$.

Returning now to the Anderson localised states, for temperatures greater than zero and a Fermi energy $E_F < E_c$ then conduction may occur via the mechanisms of electron hopping at E_F and/or excitation of carriers to states above E_c. With regard to electron hopping, the probability will be proportional to[55, 68]

$$\exp\left(-2\alpha R - \frac{\Delta E}{kT}\right) \qquad (3.24)$$

where ΔE is the energy difference between initial and final hop states, R is the intersite distance and α is the rate of decay of the wave function on a single site. At the higher temperatures hopping to nearest neighbours occurs but as the temperature is reduced the phenomenon of variable range hopping will commence: i.e. an electron will prefer to hop a large distance if it can keep ΔE as small as possible. By minimising σ with respect to R, the temperature dependence of σ is obtained as

$$\sigma = A \exp\left\{-\left(\frac{\Omega}{kT}\right)^{\frac{1}{n+1}}\right\} \qquad (3.25)$$

where the pre-exponential factor depends on the electron-phonon coupling, Q is approximately the reciprocal of $\propto {}^{3}N(E_F)$ and n is the dimensionality of the system.

Another type of Anderson transition occurs when a conduction band and valence band, both with localised states in the tails, overlap and form a semimetal, the overlapping bands forming a 'pseudogap' in the density of states (figure (3.6)). The states at E_F will be localised if the band overlap is small or extended if the overlap is large. When extended states obtain, we have $L \sim a$ and thus, to compute the conductivity, we must have recourse to a formulation which is valid in this regime. Mott and Davis[51] calculate σ using the Kubo-Greenwood formula. Mott further points out that if the density of states at the Fermi level $N(E_F)$ is less than the free-electron value $N(E_F)_{free}$, as in a pseudogap, then an explicit dependence of σ on $N^2(E_F)$ appears in contrast to the conductivity formulae cited above. Mott[1] writes

$$\sigma = \frac{S_F e^2 a g^2}{12\pi^3 \hbar} \quad \text{. where} \quad g = \frac{N(E_F)}{N(E_F)_{free}} \tag{3.26}$$

or, with $S_F = 4\pi^3/a^2$

$$\sigma = \frac{e^2 g^2}{3\hbar a} \tag{3.27}$$

Comparing this value with σ_{min} gives the value of g at which the transition occurs. In particular

$$g \sim 0.25 \text{ to } 0.33 \tag{3.28}$$

This pseudogap model has been applied to expanded liquid mercury and liquid tellurium alloys.

FIG. 3.6

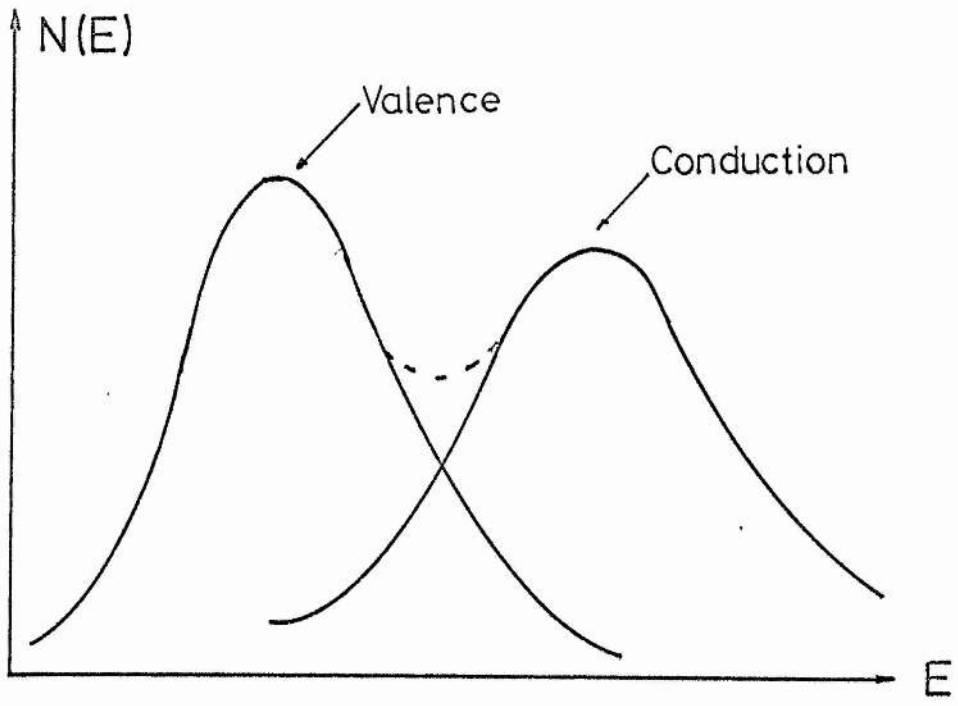

Overlapping bands forming a pseudogap.

3.6 Application of the Mott-Hubbard and Anderson Theories to Doped Semiconductors

A summary of behaviour expected for extrinsic semiconductors is perhaps best served by considering, as we started this chapter, a description of the possible conduction processes. To this effect we examine the density of states function and its expected variation with doping density.

At low densities, conduction is by thermal activation of carriers from single donor levels into the conduction band with an activation energy ε_1. If the material is compensated, then at low temperatures ($kT \sim \varepsilon_1$) some of the donor electrons will fall into acceptor levels and conduction is by hopping of electrons from full to empty donors with an activation energy ε_3. An increase in impurity concentration leads to the formation of an impurity band which may be considered to be comprised of two Hubbard bands split by the Hubbard U. Anderson localisation will obtain for the lower Hubbard band representing the hole energy spectrum and for some states in the upper Hubbard band representative of the energies of an extra electron on donor sites. The upper band will be broader than the lower one since two electrons will be less tightly bound to a donor site than a single carrier and there will be a consequent increase in the overlap and hence the bandwidth. Conductivity with an activation energy $\varepsilon_2 = E_c - E_F$ will occur at higher temperatures but at lower temperatures, conductivity may be possible with $\varepsilon_2 = E_A - E_F$ and thence hopping amongst localised states at E_A (figure (3.7)). Further increase in dopant concentration will lead to overlap of the Hubbard bands but, even though $N(E_F)$ is finite, states in the Hubbard gap

FIG.3.7

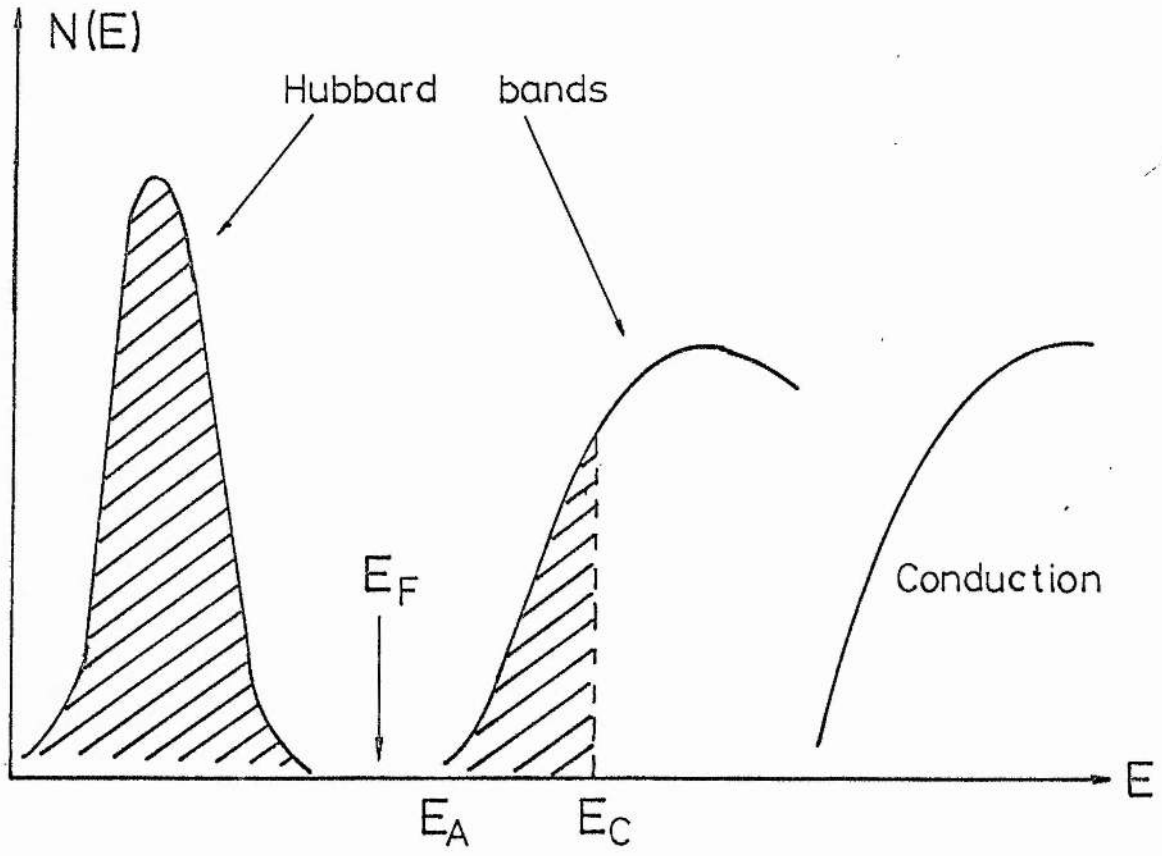

Model density of states for a doped semi-conductor. Localised states are shaded.

are still localised (figure (3.8)). At sufficiently low temperatures, $T^{\frac{1}{4}}$ hopping should be observed; at higher temperatures ϵ_2 conduction is foremost. The closing of the Hubbard gap signifies the onset of metallic behaviour and ϵ_2 goes to zero (figure (3.9)). The effect of compensation will be to broaden the band, create more localised states and lower E_F in energy, possibly again into the region of localised states (figure (3.10)).

In the absence of compensation, the disorder is of lateral type. Mott[58, 59, 70, 71] has analysed the situation by treating the donors in pairs, each donor and its nearest neighbour, distance r, apart, forming a 'molecule'. The electron energy in the ground state of the molecule will be $I \exp(-\alpha r_1)$ and since r_1 varies from pair to pair, Mott writes

$$V_o = I \exp(-\alpha r_1) \tag{3.29}$$

If the distance between molecules is r_2 then the bandwidth B_w is

$$B_w = 2 z I \exp(-\alpha r_2) \tag{3.30}$$

So, at $(V_o / B_w)_{crit}$, writing $\alpha^{-1} = a_H$ and r_1, r_2 in terms of N, we obtain

$$N_C^{\frac{1}{3}} a_H \sim 0.4 \tag{3.31}$$

Mott[70, 71] has very recently argued that localisation sets in easily in an impurity band and that this implies that the onset of insulating behaviour is determined by Anderson localisation rather than the Hubbard U producing a gap in the density of states. In this case, correlation should not play a major role at the transition. We take the view that the transition in doped semiconductors, whether

FIG. 3.8

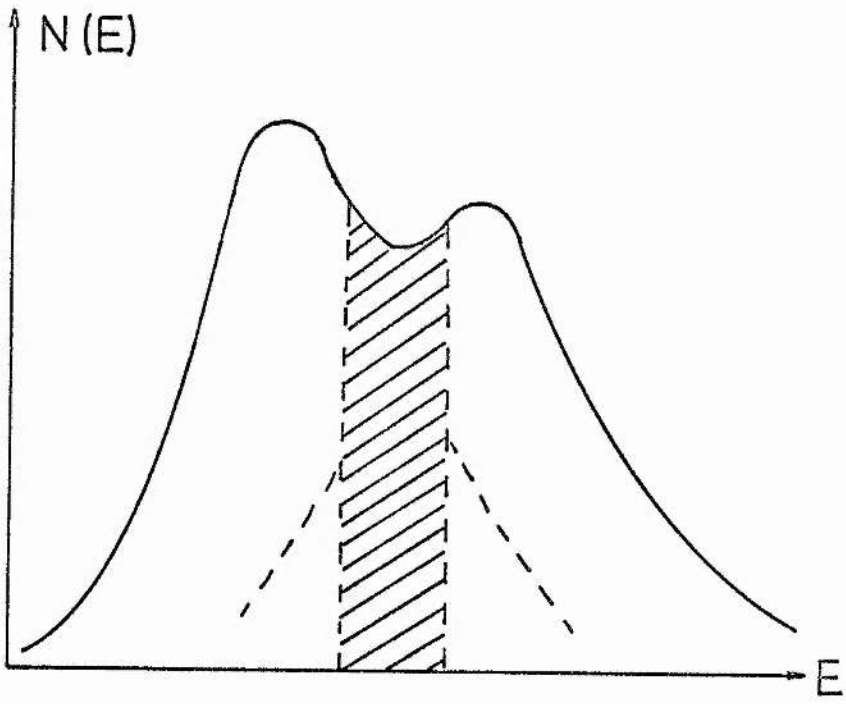

Pseudogap with Anderson-localised states.

FIG. 3.9

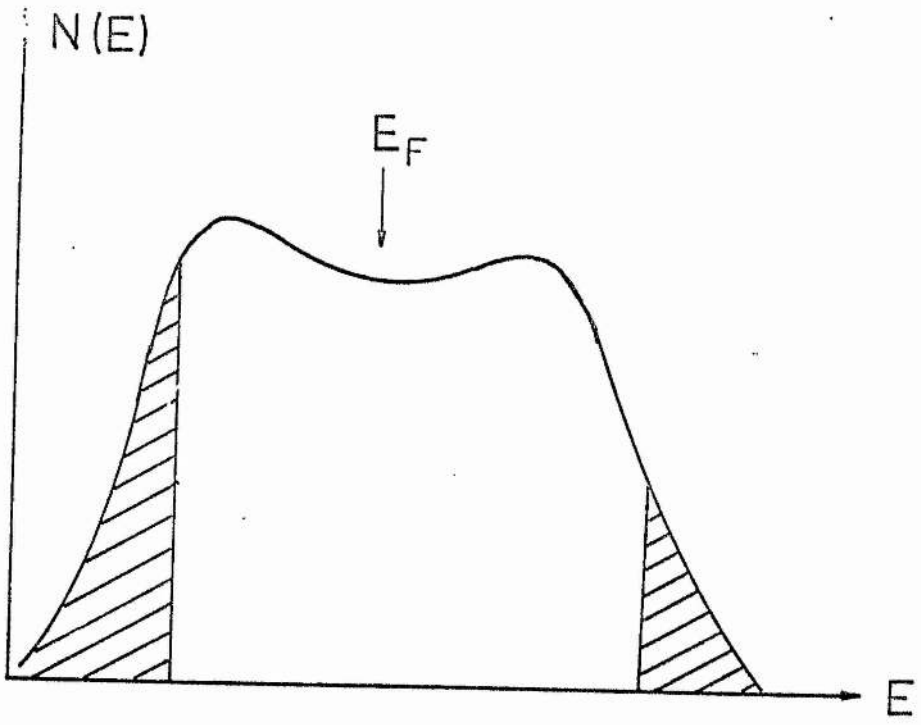

FIG. 3.10

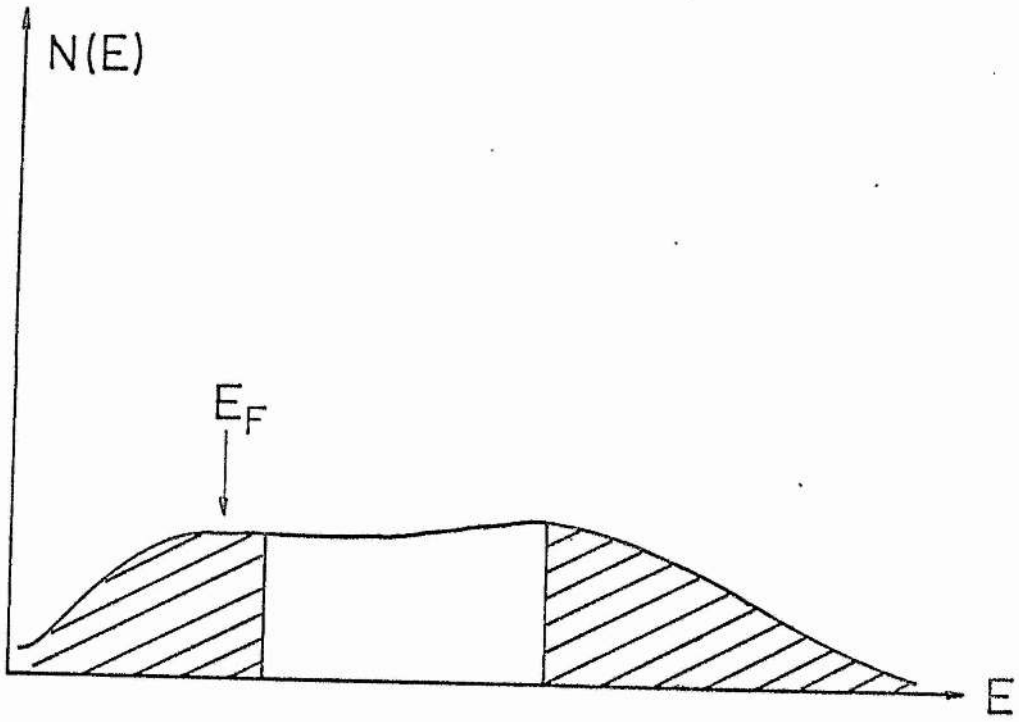

compensated or not, is of Anderson type. The importance of correlation vis-a-vis disorder must be determined by experiment.

In chapter 4, we discuss in some detail the experimental evidence of the metal-nonmetal transition and how the results relate to the ideas expressed in this chapter. Perhaps the most important point to note here is that theory is in a fluid situation and even the simplest materials exhibit properties that are not fully understood.

Chapter 4

REVIEW OF EXPERIMENTAL DATA ON THE METAL-NONMETAL TRANSITION

4.1 Introduction

In this chapter we survey the results of experiments pertaining to the metal-nonmetal transition. We begin with a resume of conduction processes illustrating the ε_i (i = 1 - 3) mechanisms outlined in chapter 3 and review the evidence for the existence of a minimum metallic conductivity. Brinkman-Rice enhancement effects are examined using the measurements of electron spin susceptibility and electronic specific heat. Other experiments pertinent to the metallic transition are also catalogued. A detailed account of nuclear magnetic resonance experiments in Si:P follows. Finally, consideration is made of the possibility of creating a metal-nonmetal transition through the use of a large magnetic field and we discuss the associated phenomenon of 'magnetic freeze out'.

4.2 Resistivity and Hall Effect

The three activation energies ε_i (i = 1 - 3) are readily visible in the work of Mott and Davis[72] on compensated Ge:Sb as shown in figure (4.1). As expected, in low density samples conductivity is via excitation to the conduction band with energy ε_1 at higher temperatures whilst at low temperatures hopping with energy ε_3 takes over. At sufficiently low temperatures variable range hopping occurs as observed by Allen and Adkins[73] and Allen, Wallis and Adkins[74]. In the intermediate region of concentration, ε_2 conduction is apparent and finally, a metal-like temperature independent resistivity is obtained for $N > N_C$ ($\sim 10^{17} cm^{-3}$ in Ge:Sb). A plot by Mott and Davis of the variation of ε_2 with interdonor

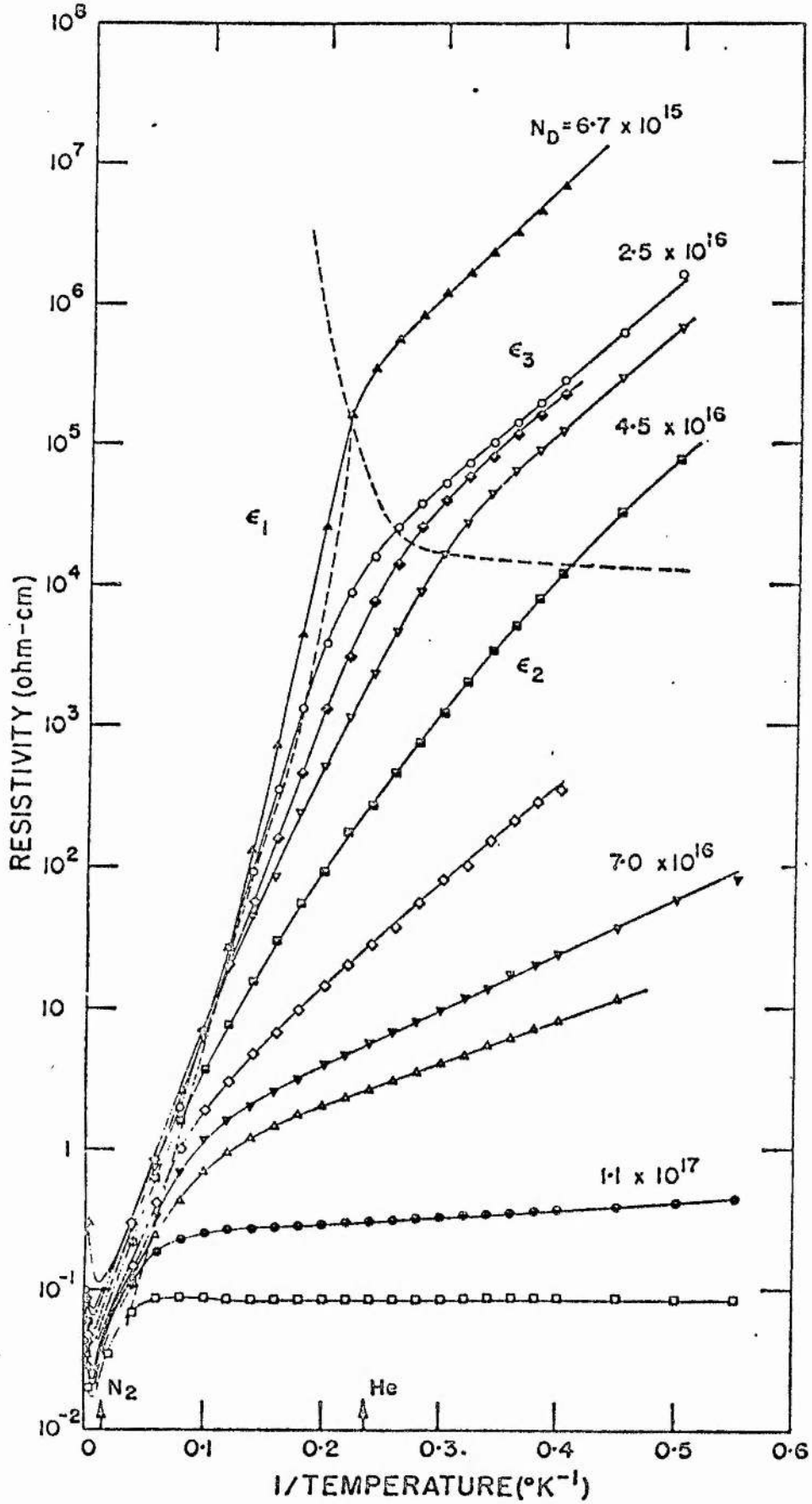

FIG. 4.1 After Mott and Davis.[72]

distance shows a deviation from linearity close to the transition. This is interpreted by Mott[55] as being due to hopping with an activation energy ε'_3. The energy ε'_3 is similar to ε_3 but it is envisaged that ε'_3 is required for electron hopping between Anderson localised states in the centre of two overlapping Hubbard bands. The ε'_3 process can thus occur in the absence of compensation and, at very low temperatures, $T^{\frac{1}{4}}$ behaviour is expected and has been observed by Wallis[75] in uncompensated Ge. Values of σ_{min} extracted from the data are in approximate agreement with the Mott formula but strong additional evidence is obtainable from experiments in conduction in two dimensional systems where hopping goes as $T^{\frac{1}{3}}$. In the latter case, σ_{min} is independent of the hop distance and may be calculated and measured accurately.

The concentration dependence of the Hall constant is more difficult to explain. Figure (4.2) shows the results of Yamanouchi et al.[76] in Si:P. (Results for n-Ge are quoted by Holcomb and Rehr[77].) If we take the transition to be of Anderson type as we have described in chapter 3, then in the low metallic region the density of states is less than the free electron value and we have $L \sim a$. Friedman[78] has calculated the Hall coefficient in this diffusive regime and obtains

$$R_H(\text{diff}) = \frac{\text{const.}}{IN(E_F)} \equiv \frac{0.7}{neg} \qquad (4.1)$$

Now we have seen that $\sigma \propto g^2$ so a logarithmic plot of $R_H(\text{free})/R_H(\text{diff})$ against σ should have a slope of 0.5.

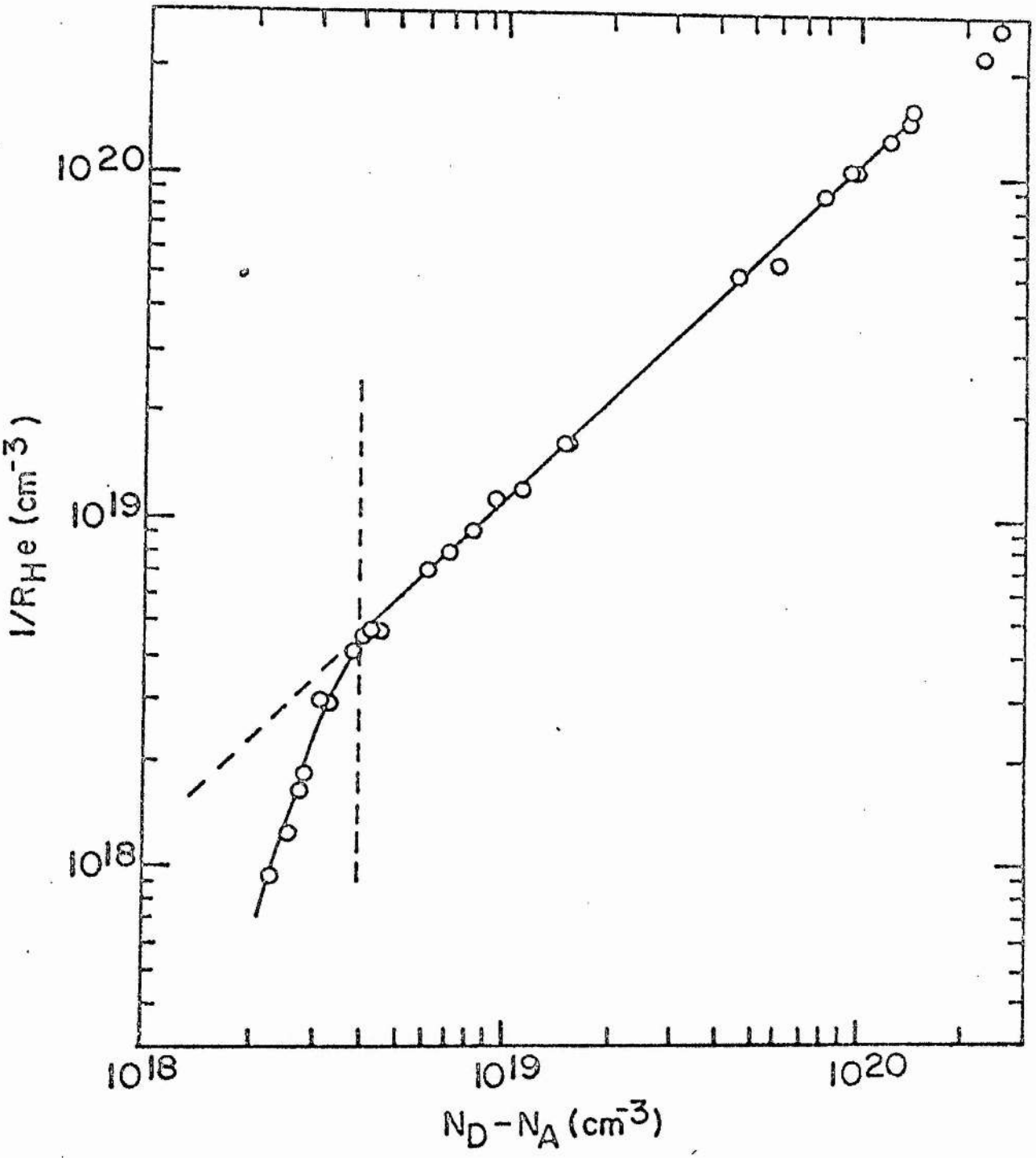

FIG. 4.2 Hall data for Si:P.

After Yamanouchi, Mizuguchi and Sasaki.[76]

Acrivos[79] has verified this behaviour in Na-NH_3 solutions and also states that a similar agreement exists for Si:P when the Yamanouchi et al.[76] data is extrapolated to zero Kelvin and N_D lies in the range $2.3 - 3.1.10^{18} cm^{-3}$, which we would take to be an activated conduction range. Mott[70] has observed that the Friedman formula does apply in Si:P at $3 - 4.10^{18} cm^{-3}$ with $g \sim 0.7$. (The vertical line in figure (4.2) was drawn by Yamanouchi et al. at $N_C = 4.10^{18} cm^{-3}$ whilst their other results and those of other workers indicate $N_C = 3.10^{18} cm^{-3}$.) It should be noted that Friedman assumed a single value of the overlap integral whereas there must be a range of I values just on the metallic side of the transition. Mott has recently speculated that the value of g may point to the fact that the density of states is not greatly reduced in going from a metallic to insulating state. The implication is that the Hubbard U is not splitting the impurity band and that it is disorder rather than correlation that is the driving mechanism for the transition in doped semiconductors. We discuss this idea in some detail in later chapters but merely point out here that the Friedman formula is perhaps only applicable if there is a real density of states reduction, i.e. as in a real pseudogap material such as mercury, but is possibly inapplicable to a Hubbard pseudogap. Even then, NMR work by El-Hanany and Warren[80] on expanded mercury casts doubt on the general suitability of the Friedman form of R_H. We discuss some further important features of the Hall effect in doped semiconductors in Appendix 2 of this report.

4.3 Electron Spin Susceptibility and Electronic Specific Heat

The electron spin susceptibility χ_S of Si:P has been measured by Quirt and Marko[81,82] and Ue and Maekawa[83] whilst results of the electronic specific heat in Si:P have been obtained by Marko, Harrison and Quirt[84]. We first consider χ_S.

It is well known that the electrons in a metal exhibit a Pauli susceptibility χ_p which is independent of temperature and may be written as

$$\chi_p = \text{const.}\ \mu_B^2\, m^*\, N_D^{\frac{1}{3}} \tag{4.2}$$

Conversely the susceptibility of a system of localised moments has a Curie-Weiss character and

$$\chi_{cw} \sim \frac{N\,\mu_B^2}{3k(T - \theta_{cw})} \tag{4.3}$$

where N is the number of atoms per unit volume. Clearly the temperature dependence of χ_S should be quite different in the cases of light and heavy doping of a semiconductor. For heavily doped Si:P, χ_S can be identified with Pauli paramagnetism since there is both temperature independence and $N_D^{\frac{1}{3}}$ dependence of the susceptibility. For metallic samples close to the transition, there is an enhancement in χ_S and the temperature dependence is that expected for a highly correlated electron gas[55]. Some workers[81-3] have sought to explain the χ_S - T variation in just-metallic Si:P by application of an 'inhomogeneity model': i.e. the assumption is made that there is a coexistence of a certain density N_{cw} of localised electrons with Curie-Weiss behaviour and a density N_p of delocalised electrons of Pauli character. An alternative approach

is that of Chao and Berggren[85,86] who have extended the Brinkman-Rice, zero temperature calculation and have obtained good qualitative agreement with the χ_s - T curves of Quirt and Marko. Further evidence against the inhomogeneity model is gained from the conduction electron spin resonance data of Pifer[87] whose linewidth results indicate that local moments do not persist above N_c.

Quirt and Marko are also able to extract the electron diamagnetic susceptibility χ_d from their data by subtracting χ_s from the static susceptibility measurements (corrected by subtraction of the core susceptibility of the Si host) χ_{stat} performed by Sasaki and Kinoshita[88]. The deviations $\Delta\chi_{LP}$ of χ_d from the Landau-Peierls diamagnetic term χ_{LP} are explained on the basis of the Kjeldaas and Kohn[89] calculation on Bloch electron diamagnetism which shows in essence that

$$\chi_d = \chi_{LP}\left(1 + \text{const.}\left[\frac{m^*}{m_o}\right]N^{\frac{2}{3}}\right) \qquad (4.4)$$

where m_o is the free-electron mass.

In contrast, measurements[90] of the carrier susceptibility $(\chi_s + \chi_d)$ in n-Ge, extracted from χ_{stat} show a functional dependence on N that is well represented by identifying χ_s with χ_p and χ_d with χ_{LP} throughout the doping range 3.10^{17} to $3.10^{19}\,cm^{-3}$. Moreover $\Delta\chi_{LP}$ is independent of impurity concentration. For donor densities less than $3.10^{17}\,cm^{-3}$, the susceptibility takes a form suggesting the diamagnetism is due to electrons in atomic states. A calculation by Saitoh et al.[91] for impurity band electrons and assuming electron correlation to be

negligible yields a concentration independent $\Delta\chi_{LP}$. It would clearly be of interest if a direct measurement of the spin susceptibility in n-Ge could be made as has been performed in n-Si.

We turn now to the electronic specific heat C_e. Results for Si:P show smaller enhancements close to the transition than predicted by the Brinkman-Rice analysis. Again there have been attempts to fit the data assuming the simultaneous existence of localised and delocalised carriers close to the metallic side of the transition[84]. The carrier division is less easy to visualize than in the case of the susceptibility but it is reasonable to assume that electrons in extended states contribute the familiar electronic term linear in temperature whilst localised carriers should contribute a Schottky term to C_e[92]. If these localised electrons exist, then the application of a magnetic field should show a large effect on C_e. This experiment has been performed by Hedgcock et al.[93] - they found no difference in C_e at 1.5 to 4.2 K for zero field and one of 2.85 T. Marko et al.[84] have criticised the Hedgcock et al. experiment, claiming that fields in excess of 10 T and temperatures below 1.5 K were needed for the effect of a magnetic field on C_e to be observable. (The field of 2.85 T was chosen by Hedgcock et al. to maximise the effect of the magnetic field.) Accordingly, Harrison and Marko[94] have performed magnetic specific heat measurements at 0.1 to 1 K in an applied field of 2.2T. They, like Hedgcock et al., found no field dependence of C_e and therefore conclude that the inhomogeneity model is untenable.

Regarding n-Ge, no such detailed studies have been made as for Si:P. However, we should note here that the early results of Bryant and Keesom[95] do not demonstrate any enhancement of C_e as expected for the Brinkman-Rice highly correlated electron gas.

4.4 Raman Spectroscopy

The Raman spectra of Ge:As and Si:P have lately been measured as a function of donor concentration by Doehler[96] and Jain et al.[97] respectively. Very briefly, the origin of the spectra is that, in indirect gap materials such as Ge and Si, with n equivalent conduction band minima, the n-fold degenerate ground state is split by a valley-orbit interaction. The Raman line originates from a transition within the valley-orbit-split ground state.

The spectra of Ge:As and Si:P both show a valley-orbit line which broadens asymmetrically as the impurity concentration approaches N_c. Simultaneously a continuous, single-particle, background appears and eventually dominates the spectra (figures (4.3),(4.4)). Doehler claims that the shift of the valley-orbit line in Ge:As to lower energies in the metallic regime is indicative of the presence of localised states on the metallic side of the transition. This follows from the fact that if only free electrons were responsible for the spectrum then theory states that the shifts should be to higher energies since the shift is proportional to the electron Fermi velocity which is in turn proportional to the carrier concentration. Against this hypothesis we note firstly that if the temperature independence of the Hall effect and resistivity at low

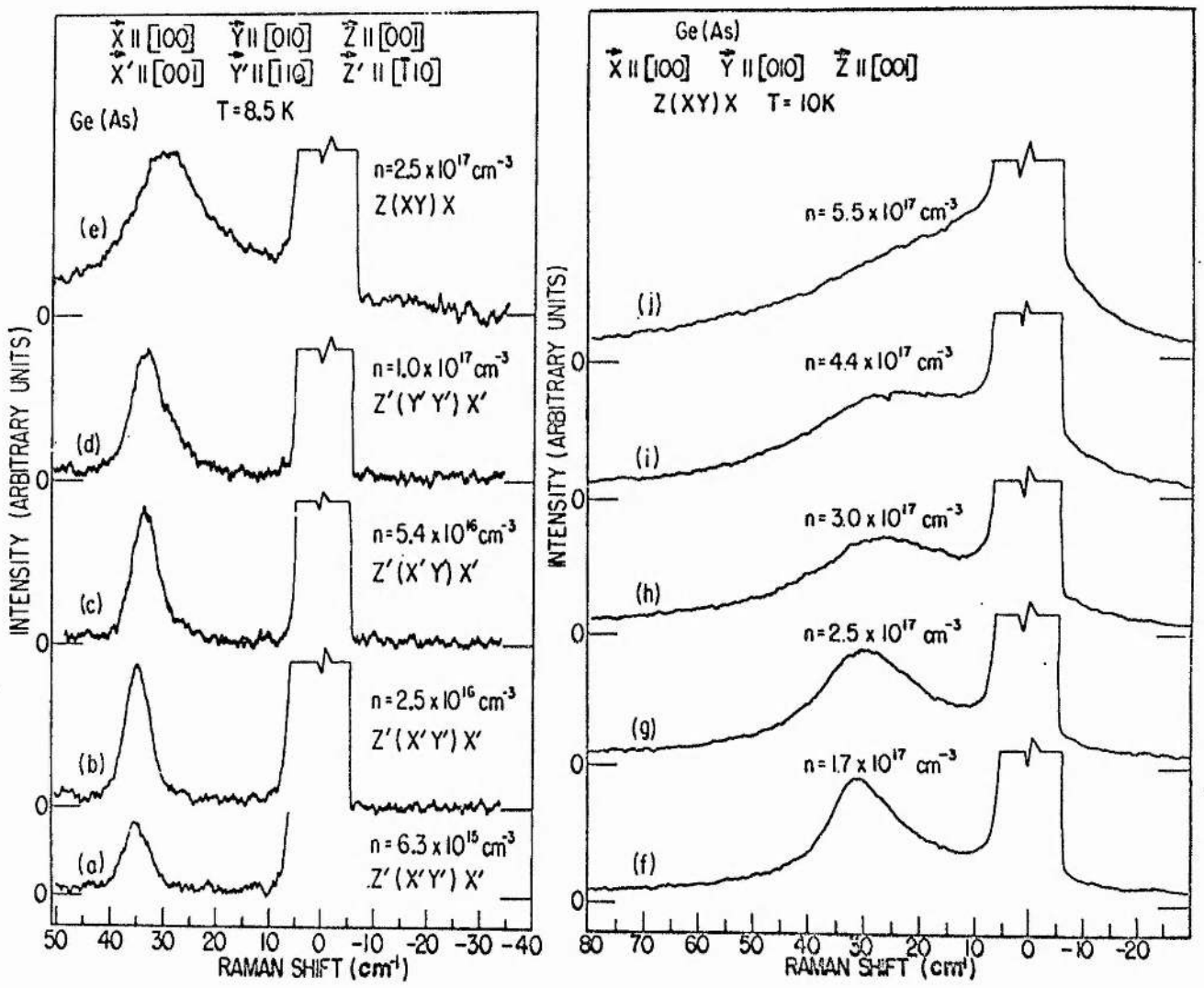

FIG. 4.3 Raman spectra for Ge:As.
After Doehler.[96]

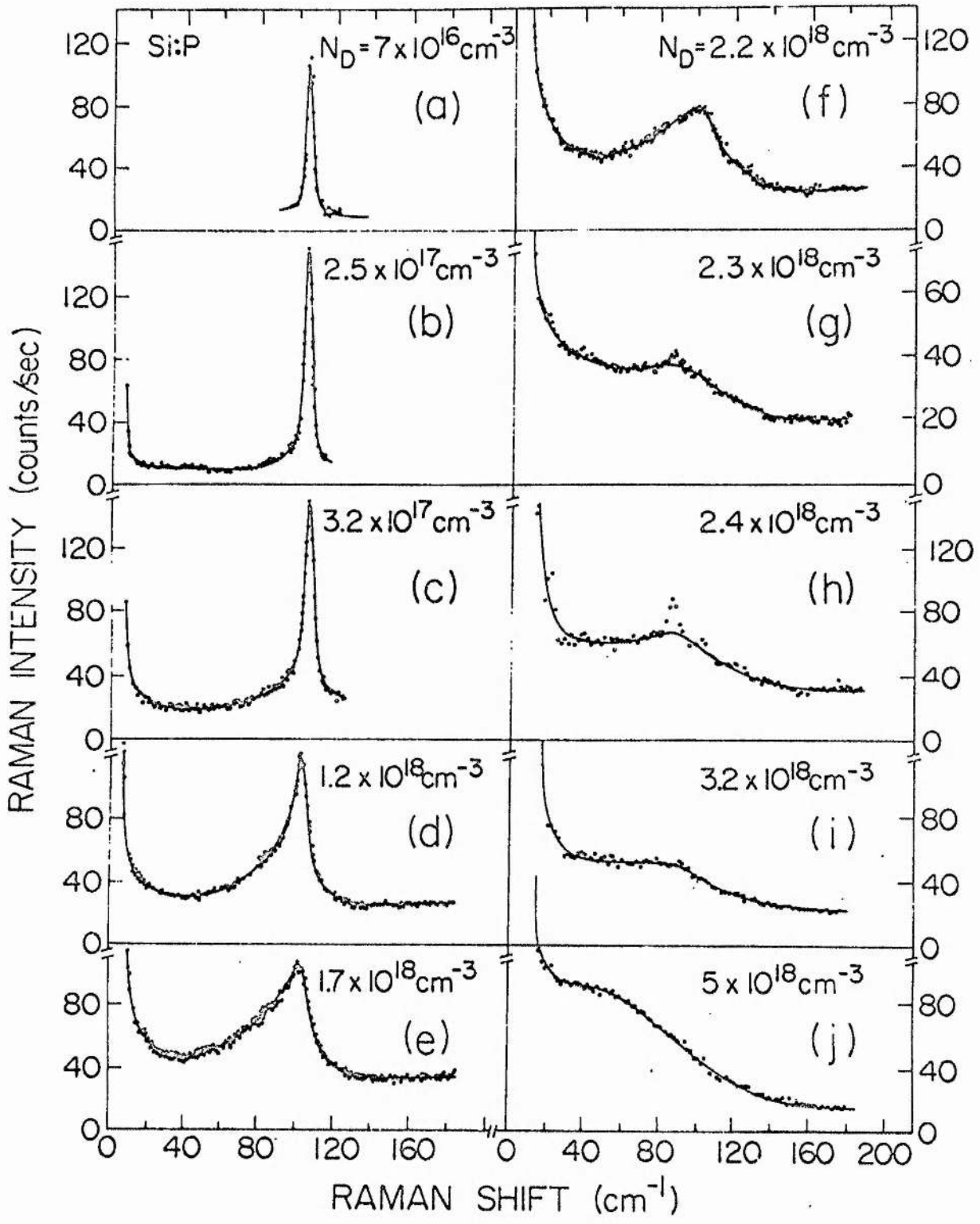

FIG. 4.4 Raman spectra for Si:P.
After Jain, Lai and Klein.[97]

temperatures is taken as the criterion for the onset of metallic behaviour, then Doehler only has one (or possibly two) samples in the metallic regime which shows a 'knee' rather than a peak in the spectrum. Secondly, the detailed analysis of the continuum line shape in Si:P by Jain et al. shows that a knee in the spectrum which they observe for N_D just greater than N_C, is explicable in terms of the shape of the continuous spectrum alone. These authors show that a maximum in the continuum spectrum is expected on quite general theoretical grounds (the fluctuation-dissipation theorem) and may be generated by a model in which the continuum is taken to arise from transitions within a partially-filled band. Thus it may not be necessary to assume that the knee observed by Doehler is due to valley-orbit transitions on isolated donors existing above the metal-nonmetal transition. Doehler[96] plots an interesting graph reproduced as figure (4.5), showing the increase of the Raman linewidth and the decrease in resistivity taken from Fritzche's[42] data on passing from semiconducting to metallic behaviour in Ge:As. Doehler does not give details of how he has chosen the resistivity values that he has plotted but inspection of the Fritzche results indicate that Doehler has extrapolated Fritzche's graphical data to 1 K to obtain the resistivities. Now the Raman measurements were taken at 8 K and for samples doped from $9.10^{16}cm^{-3}$ to $2.8.10^{17}cm^{-3}$, the change in resistivity from 1 K to 8 K is from eleven to two decades respectively. We show the change in resistivity with doping density at 8 K as the dotted line in figure (4.5): this does not, of course, change Doehler's conclusion

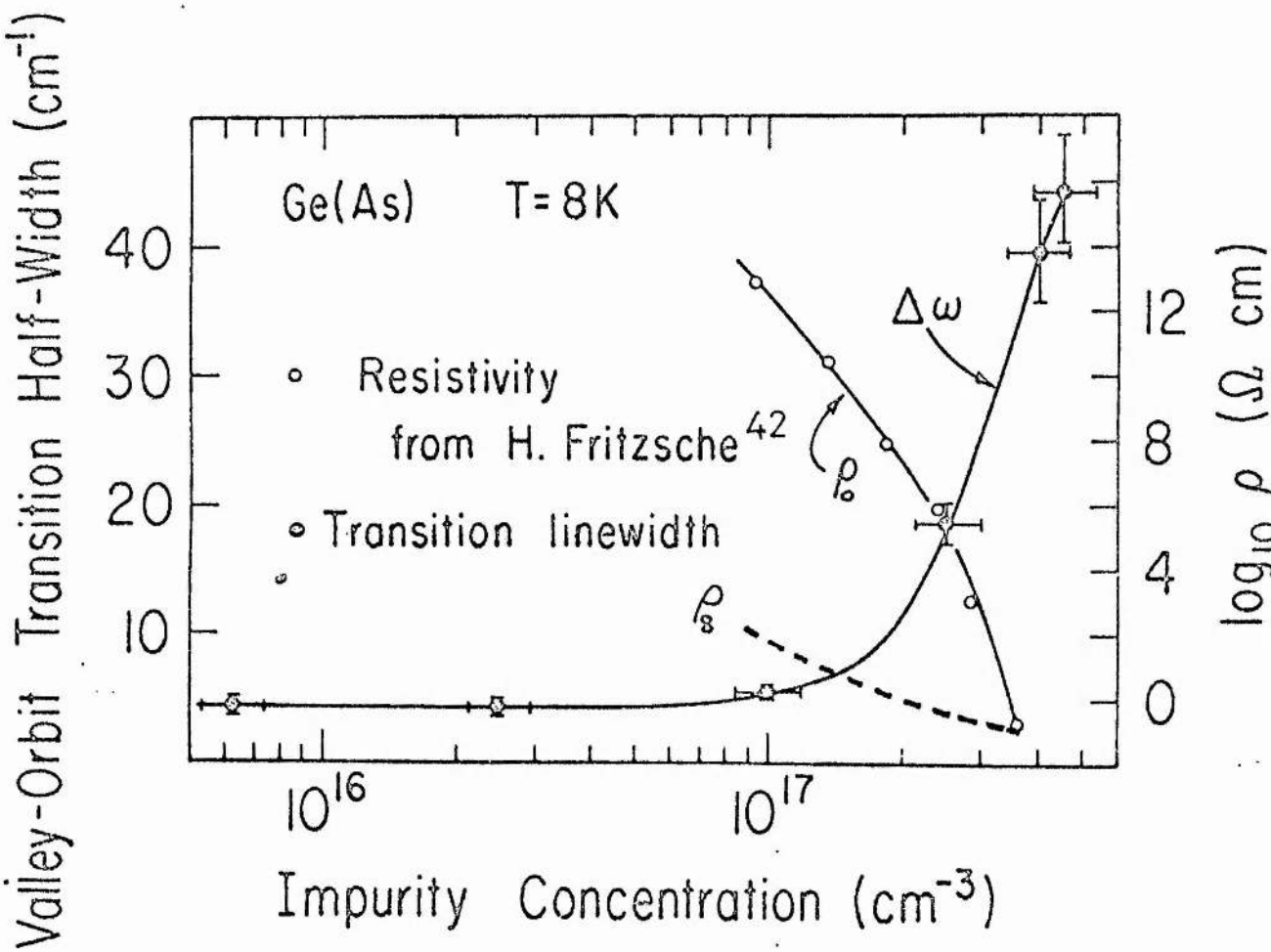

FIG. 4.5 Raman linewidth for Ge:As.

After Doehler.[96]

that localised states are present in just-metallic Ge:As. A similar plot for Si:P (figure (4.6)) is given by Jain et al.[97] using resistivity and ϵ_2 data from the work of Yamanouchi et al.[76]. In contrast to the Ge:As results, the Si:P data show the valley-orbit line to broaden beyond recognition before the metal-nonmetal transition is reached.

A direct band gap material may be studied by the spin flip Raman scattering technique (SFRS) wherein the ground state is split by a magnetic field. Romestain, Geschwind and Devlin[98] have recently performed SFRS experiments on CdS; which has a critical donor concentration of $2.4.10^{17}cm^{-3}$, and also spin Faraday rotation experiments which yield the spin susceptibility χ_S. In insulating material, the Raman linewidth is the same as that determined by electron paramagnetic resonance. In metallic samples, the motion of the electrons causes a Doppler shift of the Raman line whilst the electron scattering causes the line to be collisionally narrowed. This diffusional character is apparent in samples with $N_D \gtrsim 2.4.10^{17}cm^{-3}$. The Faraday rotation results show χ_S is Curie-Weiss-like below the transition and of Pauli-type in highly doped crystals. For material with $N_D \sim N_C$, however, there is an enhancement in χ_S at low temperatures which Romestain et al.[98] interpret as evidence for the existence of the highly correlated electron gas of Brinkman and Rice.

A further result which is crucial is that for samples with $N_D \geq N_C$, only a diffusional line is observed. If localised electrons coexisted with mobile carriers above N_C then they should contribute a superposition of a narrow, unshifted line and a diffusional line,

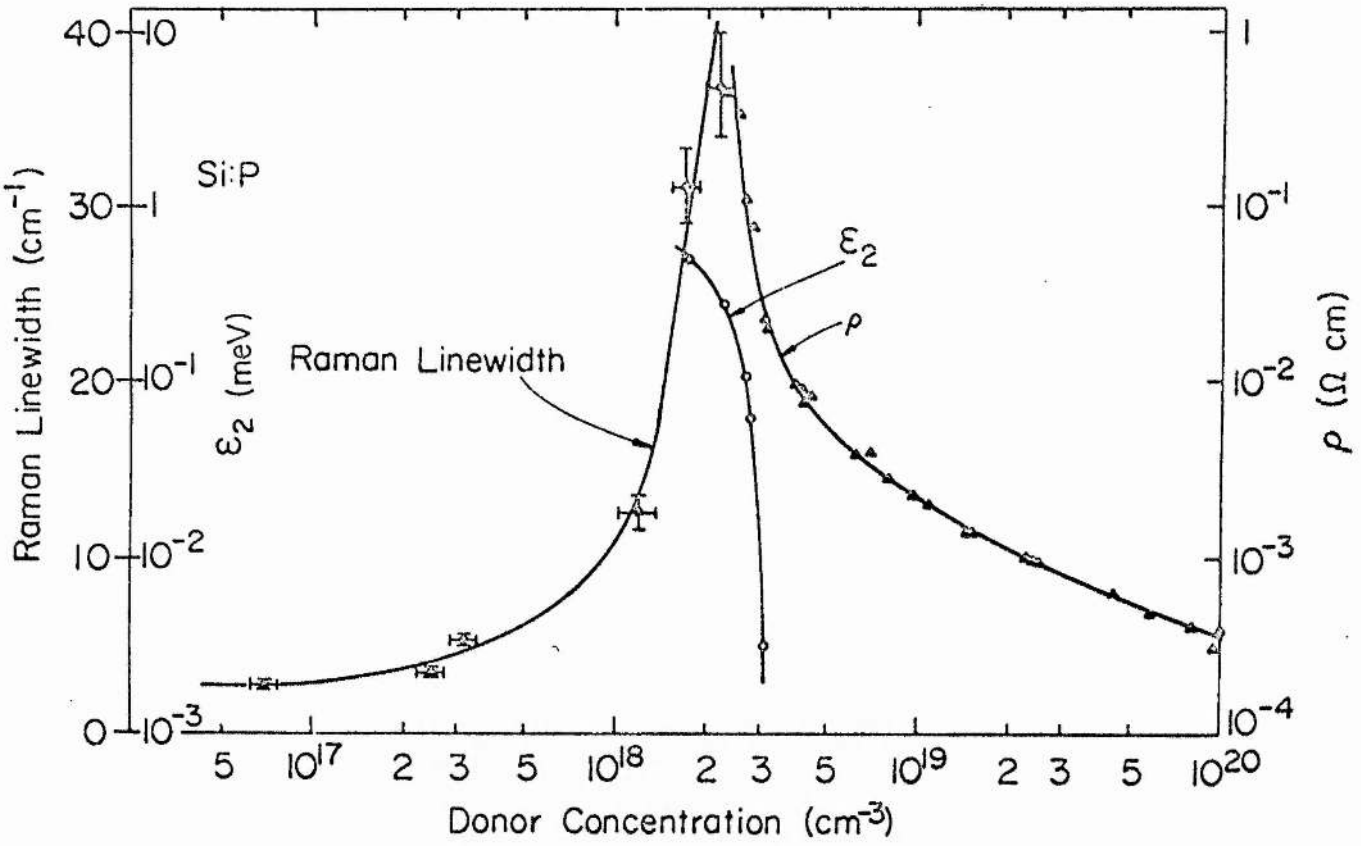

FIG. 4.6 Raman linewidths for Si:P. After Jain, Lai and Klein.[97]

respectively. The observed absence of a narrow line for samples with $N_D \geqslant N_C$ is strong evidence for considering the electrons as a single-phase system.

4.5 Magnetoresistance

As we have been discussing the possibility of existence of localised electrons above the metallic transition, it is apposite here to describe the results of magnetoresistance experiments in extrinsic semiconductors in the metallic region.

The general features[99,100] are that at low fields, the magnetoresistance is negative and, as the field is increased, the magnetoresistance passes through a minimum and then becomes positive (as B^2) for high fields. Usually, the lower the carrier concentration or temperature the lower the field at which the magnetoresistance changes sign. Explanations have been made in terms of a local moment model and a two band model which we now outline and compare with experiment.

The local moment model stems from the observation of negative magnetoresistance in Cu doped with Mn. The argument here is that the s - d exchange interaction between conduction and localised spins leads to a spin dependent scattering of the carrier. Simplistically, the effect of a magnetic field is to align the local moments and reduce the scattering and thence the resistivity.

In strongly doped semiconductors, Toyozawa[101] postulated that local moments might exist if, due to statistical fluctuations in donor density, an impurity found itself relatively isolated from

other centres. The word 'relatively' is used in the sense that a localised spin must have sufficient interaction with neighbouring mobile electrons to create a local spin polarisation. This is a necessary condition to account for the huge size of the local moment as deduced from the magnetoresistance data. Whilst the Toyozawa model explains the data qualitatively, two shortcomings are apparent. Firstly, the negative magnetoresistive component would be expected to vanish for high donor concentrations which does not occur, and secondly the predicted field dependence of the negative component is quadratic whilst a linear relationship is observed in practice.

Khosla and Fischer[100], cognizant that resistance anomalies (Kondo effect) had been describable theoretically by third order perturbation theory, have considered these higher order terms in their analysis of spin dependent scattering. They write a semi-empirical formula for the magnetoresistance

$$\frac{\Delta\rho}{\rho} = -C_1^2 \ln(1 + C_2^2 B^2) + \frac{C_3^2 B^2}{1 + C_4^2 B^2} \qquad (4.5)$$

The first term contains the negative component and the parameters C_1, C_2 are related to the exchange interaction. The second term is a 'band' term: it represents the fact that at high magnetic field, carriers can be frozen out of the conduction band into a band of lower mobility. The magnetic field can change the populations of the two bands and thereby furnish a field-dependent term in the magnetoresistance.

We now briefly survey the band model of Hedgcock and coworkers[102,103] and Lass[104]. They envisage a mobility edge separating impurity band states with zero mobility from conduction band states with high mobility. Negative magnetoresistance, linear in field, results from a magnetic field shifting the population ratio above and below the mobility edge and localised moments need not be invoked.

Comparison of the two approaches[99] with data in Si:P[105] is shown in figure (4.7). Whilst the Khosla-Fischer fit is clearly better, it is arguable that an expression involving four adjustable parameters will always give a good fit to experimental data.

Mott[1] considers the magnetoresistance phenomenon to be explicable as follows: orbit shrinking due to a large magnetic field leads to the B^2 behaviour at high fields. At low fields, the negative magnetoresistance results from Kondo moments with a low Kondo temperature T_K. These moments are thought to arise from relatively isolated donors or from donor clusters. A uniform distribution of T_K values can then lead to a negative magnetoresistance linearly proportional to field.

Finally, we note that if large local moments exist as in the Toyozawa scheme, then they should have significant effects on the NMR linewidth. The work of Brown and Holcomb[6] shows no sign of the existence of localised moments though cannot definitely rule them out.

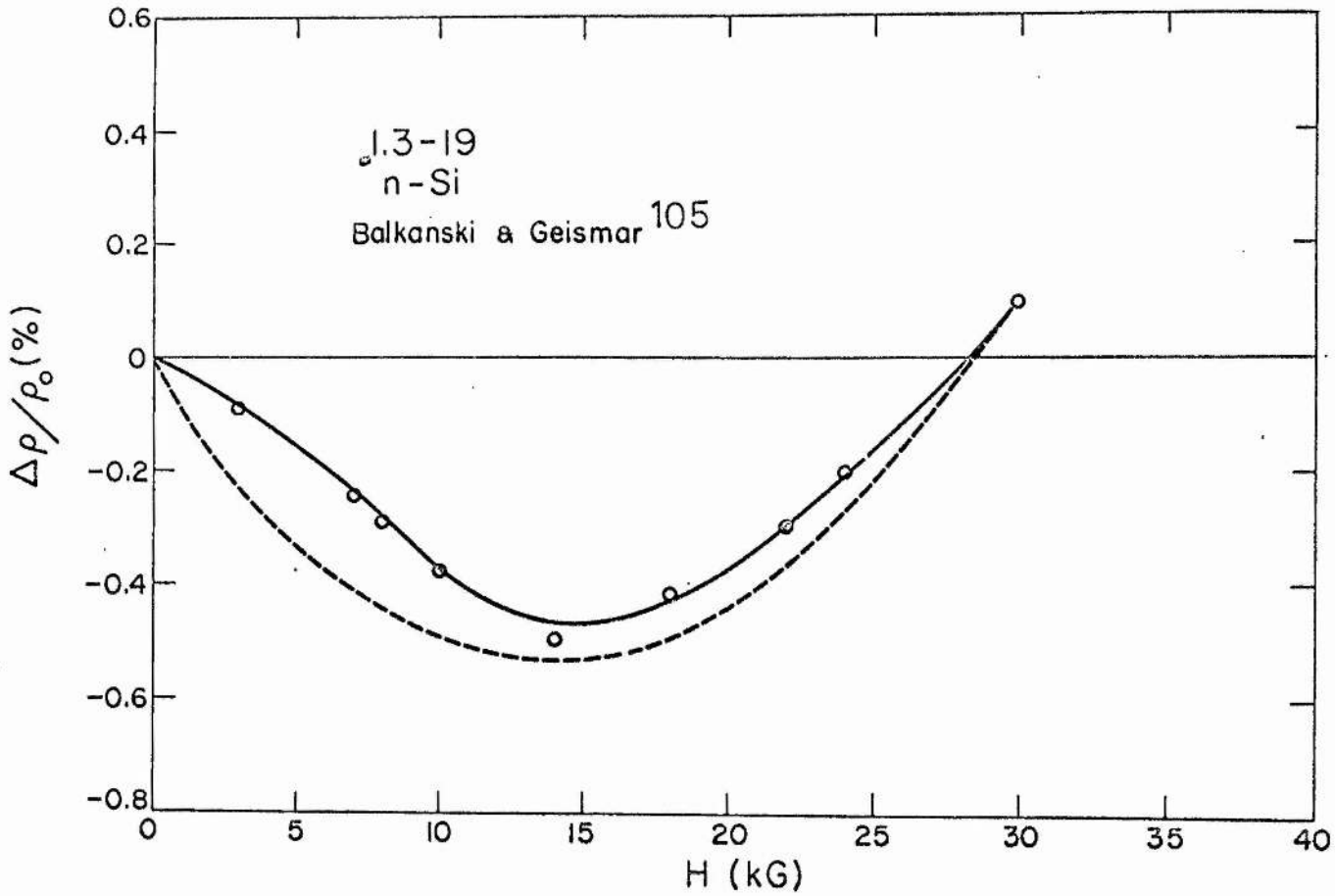

FIG. 4.7 Magnetoresistance in Si:P.
After Khosla and Fischer.[99]

4.6 Electron Spin Resonance

The electron spin resonance (ESR) of bound electrons in Si:P was first observed by Fletcher et al.[106] as two sharp, well-separated lines. In general[107] the hyperfine interaction between a donor nucleus of spin I and the donor electron yields a spectrum consisting of $2I + 1$ lines. The field separation of the lines is proportional to the square of the electronic wave function at the donor nuclei and Kohn[39] has shown that good agreement exists between the experimental and the effective mass approximation values of $|\psi(o)|^2$. The widths of the resonance lines are due to the hyperfine interaction between the donor electron and a host nucleus. Since the lines are well resolved, the donor nucleus-donor electron hyperfine interaction is clearly stronger than that between host nucleus and donor electron from which it follows that the electronic wave function is strongly peaked at the donor site.

Regarding Si:P, the ESR spectrum[108] shows a marked change as the phosphorus concentration is increased (figure (4.8)). At medium densities ($2.5.10^{17} cm^{-3}$) several satellite lines superimposed on a broad asymmetric background appear between the hyperfine-split phosphorus doublet. Following the work of Slichter[109], the satellite lines are known to arise from clusters of mainly two or three P atoms in the Si matrix. In such a cluster, antiferromagnetic exchange strongly couples the electron spins so that they respond as a single entity to an average magnetic field produced by the hyperfine coupling with the nuclei involved. The asymmetric background has a maximum whose position is dependent on

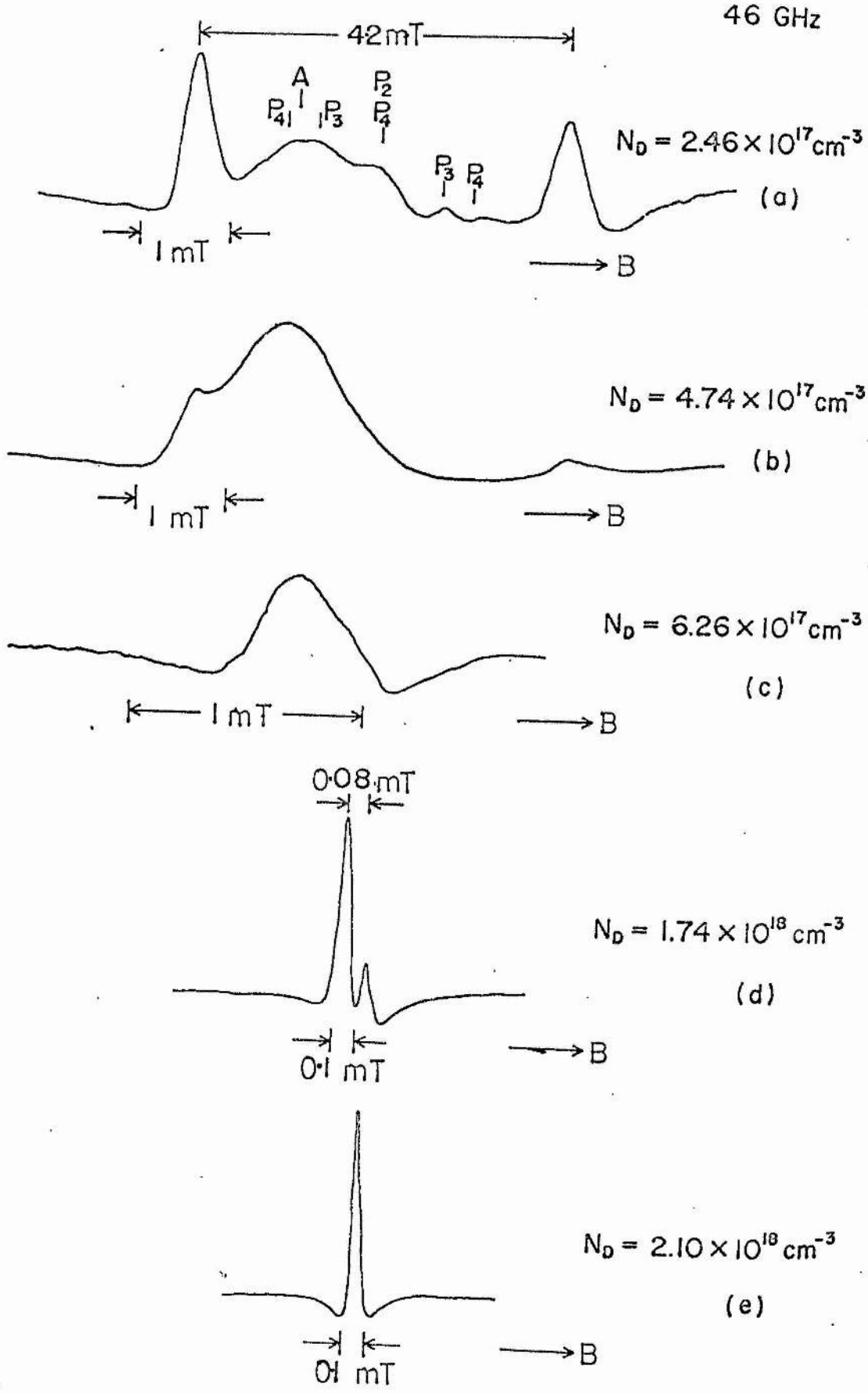

FIG.4.8 ESR spectra in Si:P.

After Morigaki and Maekawa.[108]

temperature, magnetic field and impurity concentration. This line dominates the ESR spectrum in the concentration range just less than N_C and has recently received the attention of Rosso[110].

Rosso finds that for values of the exchange coupling constant J very much greater or very much less than the hyperfine coupling constant A that the calculated spectrum is symmetric. The case $J \ll A$ corresponds to the isolated donor situation whilst the inequality $J \gg A$ is expected to hold within a strongly coupled donor cluster. The wide ranging values of J follow from its strong dependence on interdonor distance which in turn has a large spread due to the random positioning of the donors. Rosso shows that asymmetry in the spectrum may be generated if $J \sim A$. This condition corresponds to those exchange interactions existing between clusters or between a cluster and an isolated donor. Good agreement between theory and experiment is obtained for the spectrum shape[111].

A further metamorphosis in the ESR spectrum occurs when $N_D \sim N_C$: the spectrum collapses to a single, narrow line. This broadens with a further increase in N_D due to lifetime broadening[9].

Experimentally, ESR in n-Ge has proved more difficult than for n-Si though Wilson[112] has observed the resonance in lightly doped material. The ESR linewidth and electron spin-lattice relaxation time are discussed by Chazalviel[113] and references therein.

Finally, we note here that experiments have been made to measure the conductivity of an extrinsic semiconductor in the

presence of microwave radiation. 'ESR enhanced conductivity' has been observed in doped Si[114] and Ge[115]. Figure (4.9) shows the resistivity decrease in Ge:As at 1.3 K. Morigaki and Onda[115] have explained these results in terms of a model involving two electron species. They imagine the microwave energy to be absorbed by localised electrons and then transferred via an exchange mechanism to mobile electrons promoting the latter's kinetic energy and mobility. Mott[55], however, has given the interpretation that localised spins absorb the microwave energy and then transfer it to localised states near E_F so that they may hop in the variable range manner, without thermal activation. A timely publication by Kamimura and Mott[116] has re-examined the situation and affirmed the Mott proposal with the energy transfer mechanism being the combined effects of exchange and spin-orbit interaction. An important feature of the Kamimura-Mott model is their assumption of a homogeneous electron system: the idea advanced by Morigaki and Onda[115] that localised and mobile electrons coexist is thus dispensable.

4.7 Dielectric Properties

We noted in chapter 3 that at the metal-nonmetal transition, if the dielectric constant κ went to infinity, then a small number of free carriers was allowed and consequently there would be no discontinuity in N_D. A series of experiments by Castner and coworkers[117-9] have shown that κ can take large values when $N_D \sim N_C$. Figure (4.10) shows their results for As, P and Sb

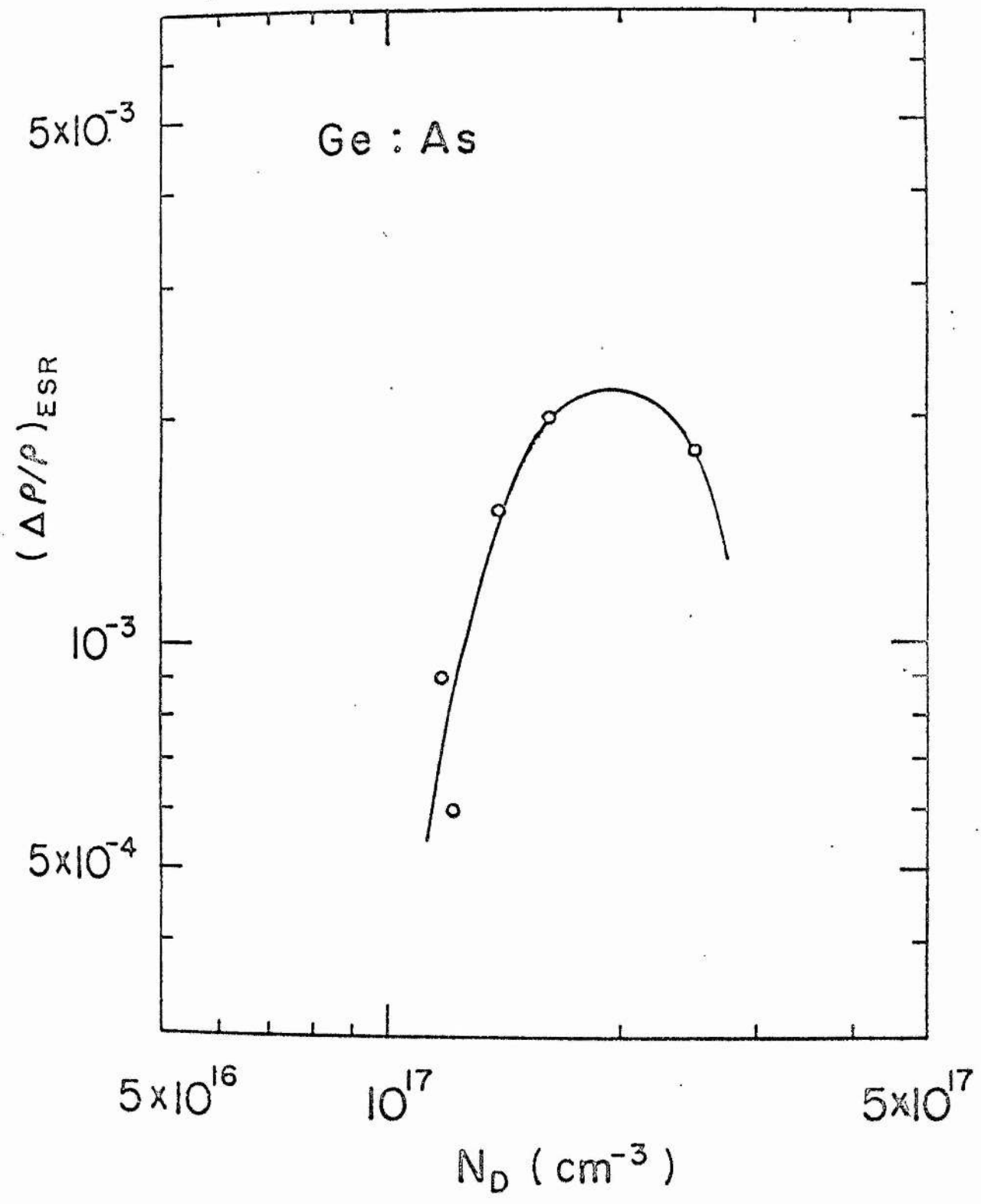

FIG. 4.9 ESR enhanced conductivity in Ge:As. After Morigaki and Onda.[115]

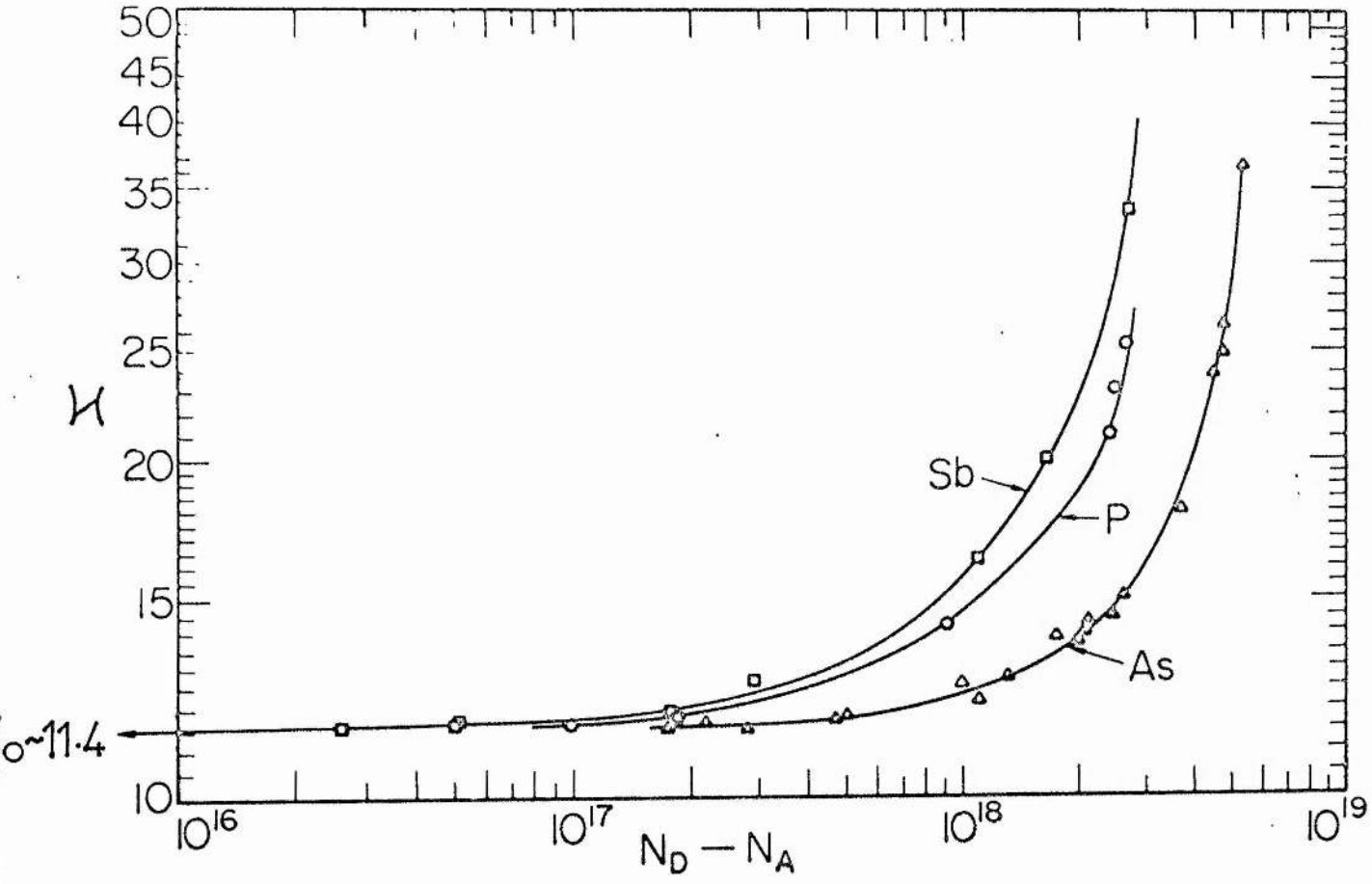

FIG. 4.10 Dielectric constant for n-Si.

After Castner, Lee, Cieloszyk and Salinger.

donors in Si. The donor dependence is due to the different ionisation energies and polarizabilities of As, P and Sb. Figure (4.11) shows the Clausius-Mosotti factor plotted against N_D. Donor polarizabilities obtained from the linear parts of the curves are in reasonable agreement with values calculated within the effective mass approximation. The deviations apparent for $N_D \sim N_C$ are taken to be due to the increased polarizabilities resulting from weakening binding energies of electrons to donors.

As regards Ge, D'Altroy and Fan[120] showed that κ increased with increasing donor concentration but the situation for Ge is clouded by the reflectivity experiments of Yoshihiro et al.[121, 122] who find a concentration-independent κ. It is appropriate here to refer again to the investigation of variable range hopping in n-Ge undertaken by Allen and Adkins[73]. They point out that κ should increase as N_D tends to N_C due to the increase in polarizability that we have discussed above. In variable range hopping, an electron hops from one site to a far site, perhaps with occupied sites in between. These filled sites ensure that the hopping electron sees a medium of different permittivity than in the pure crystal or in the nearest neighbour hopping regime. Allen and Adkins estimate values of κ from their data and show that high values (~ 90) may be reached for $N_D \sim N_C$. They point out that in determining these values of κ they have included the total contribution to the polarizability from the $(N_D - N_A)$ occupied sites. Since this will be a poor approximation for short hops where there may be no or only a few intervening sites, their calculated values of κ should represent an upper limit.

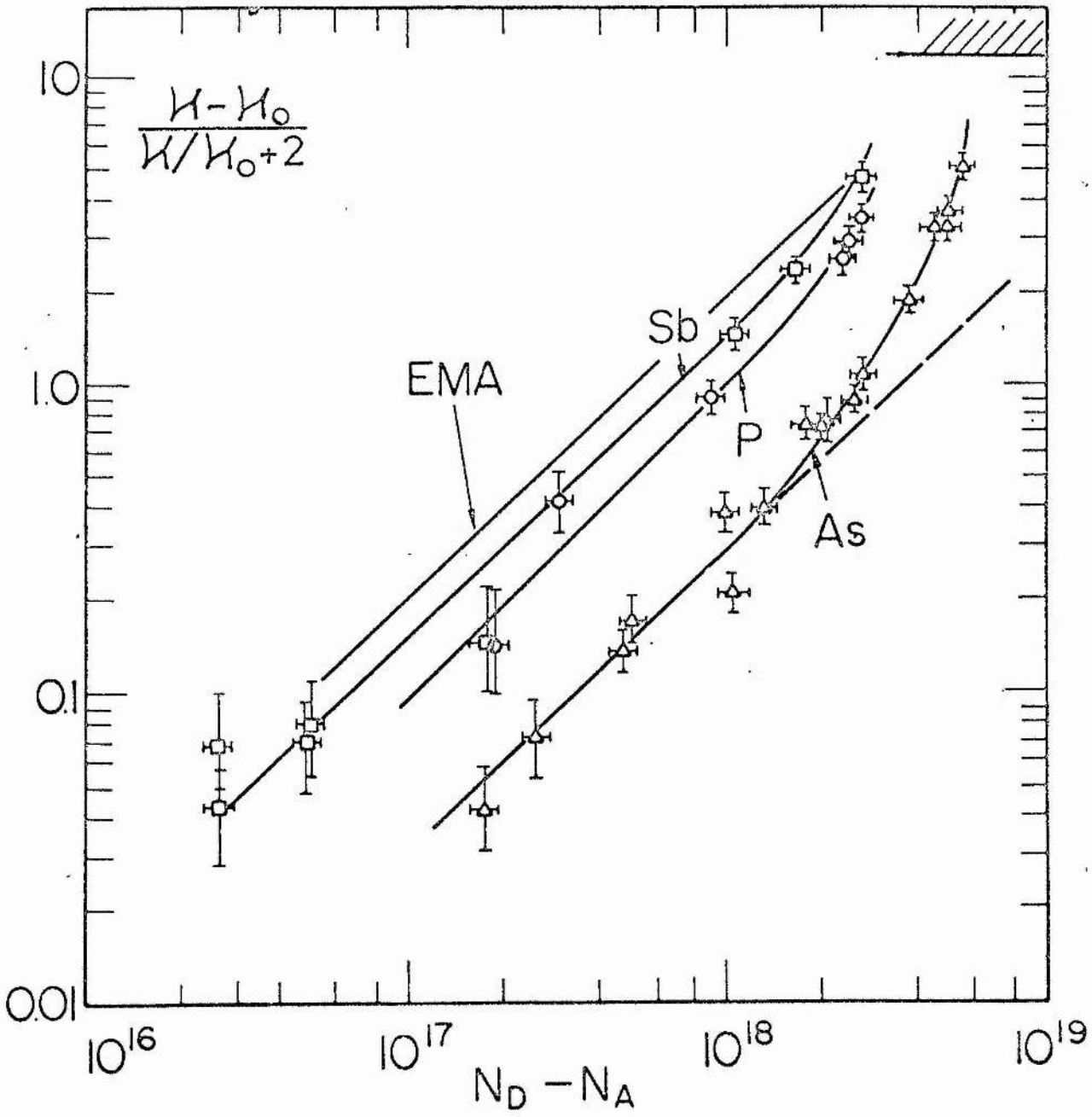

FIG.4.11 Clausius-Mosotti factor for n-Si.
After Castner et al.

The magnitudes of the observed conductivities in the variable range hopping region are then reasonably in accord with the theoretical predictions of Miller and Abrahams[68] if the dielectric constant is taken to lie somewhere in the range $16 \longrightarrow 90$. Allen and Adkins note that their data is also in accord with a percolation theory of conduction but in this case much higher values of κ are obtained ($\sim$500).

4.8 Photoconductivity

We have discussed Hubbard bands in some detail above and provided evidence of them and their characteristics using the results of transport property experiments. A more direct observation of the upper Hubbard band in Si:P,As has been provided of late by Norton[123]. His method is to monitor the change in spectral response of a photoconductive signal produced by electrons photoexcited from the upper Hubbard to the conduction band.

At low doping densities ($\sim 10^{14}$ P or As cm^{-3}) the spectral response is very similar to the photodetachment spectrum of H^- ions (when scaled by the appropriate effective mass approximation quantities m^* and κ). At a particular value of N_D, the spectral response shifts to higher energies indicating the formation of a band. Now as we mentioned in chapter 3, the binding energy of two electrons on a single site is less than a single electron at a single site. Hence we expect overlap of doubly occupied sites to occur at a lower doping density than for singly-occupied sites. Norton finds

$$N_D \text{ (upper Hubbard)} \sim 3.10^{15} \text{ donors } cm^{-3}$$

whilst from hopping experiments

$$N_D \text{ (lower Hubbard)} \sim 10^{17} \text{ donors cm}^{-3}$$

in agreement with our expectation.

We should note that during the formation of the upper Hubbard band, an extra electron moving over groups of donors has its binding energy increased[124]. Thus the photoconductive response should go to higher energies as N_D increases, as Norton observes.

Proof of the existence of a band of the Hubbard type with Anderson localised states in the tail is provided by Norton's analysis of the temperature dependence of the spectral response. For a sample of $8.5.10^{15}$ P cm^{-3}, the low energy response falls markedly for temperatures just greater than 2 K owing to weakly bound states being thermally stripped. At higher temperatures (to 6.5 K) the spectrum acquires a stable shape with only a decreasing intensity variation with temperature. This behaviour is consistent with a band of localised states existing in the upper Hubbard band. Norton shows them to be $\sim$ 8 meV below the bottom of the conduction band.

Taniguchi and Narita[125] have also studied the D^- state in Si:P and obtain a value of

$$N_D \text{ (upper Hubbard)} \sim 4.10^{16} \text{ donors cm}^{-3}$$

They also show that stressing a sample to force all the electrons into two valleys makes the D^- state unstable. Taniguchi and coworkers[126,127] have performed similar measurements in n-Ge. They find

$$N_D \text{ (upper Hubbard)} \sim 1.1 - 3.7.10^{16} \text{ cm}^{-3}$$

in agreement with the estimate of 3.10^{16} cm^{-3} of Yoshihiro et al.[122].

4.9 Nuclear Magnetic Resonance

In this section, we discuss results obtained from NMR experiments conducted in the Si:P system of which the earliest study was by Shulman and Wyluda[128]. (Other materials studied are SiC:N by Alexander[129], n-CdO by Benedict and Look[130] and CdS:Cl by Adams et al[131].) The measured quantities of interest are the spin-lattice relaxation time T_1, the spin-spin relaxation time T_2, the resonance linewidth ΔB and the Knight shift K.

The metal-nonmetal transition in Si:P was first studied by Sundfors and Holcomb[7] and has subsequently been the subject of a number of papers by Sasaki et al.[2-5] and Brown and Holcomb[6]. Sundfors and Holcomb found, for $N_D \geqslant 3.10^{18} cm^{-3}$ that T_1 (Si^{29}) was proportional to the inverse of temperature (figure (4.12)) implying that relaxation of the nuclei is via the Fermi contact interaction with mobile electrons. Above $N_D = 3.10^{19} cm^{-3}$, the concentration dependence of T_1 (Si^{29}) at 1.6 K scales as $N_D^{-\frac{2}{3}}$ again indicative of relaxation by a degenerate electron system (figure (4.13)). K (Si^{29}) shows an $N_D^{\frac{1}{3}}$ dependence at high values of N_D but falls away for $N_D \lesssim 5.10^{19} cm^{-3}$ (figure (4.14) : this is a corrected plot of the Sundfors-Holcomb data given by Alexander and Holcomb[44]). The Korringa relation holds for $N_D \geqslant 5.10^{19} cm^{-3}$. Linewidth data indicates $\Delta B(Si^{29}) \sim 20$ μT is ascribable to nuclear dipole-dipole interaction in the semiconducting range while the increase in $\Delta B(Si^{29})$ to 100 μT in the transition and metallic regimes is explained on the basis of the Knight shift distribution model described in chapter 2.

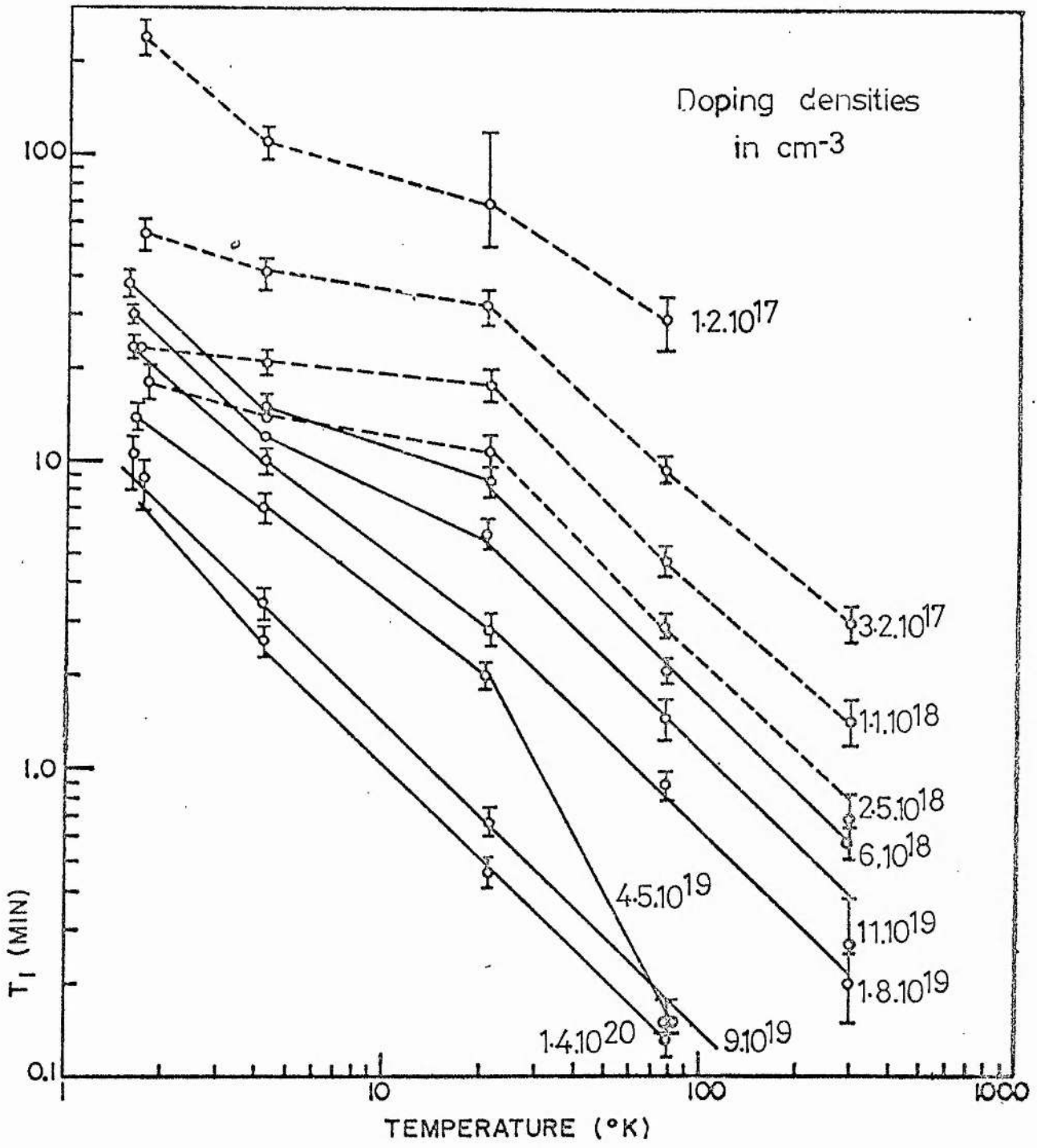

FIG.4.12 $T_1(Si^{29})$ in Si:P.

After Sundfors and Holcomb.[7]

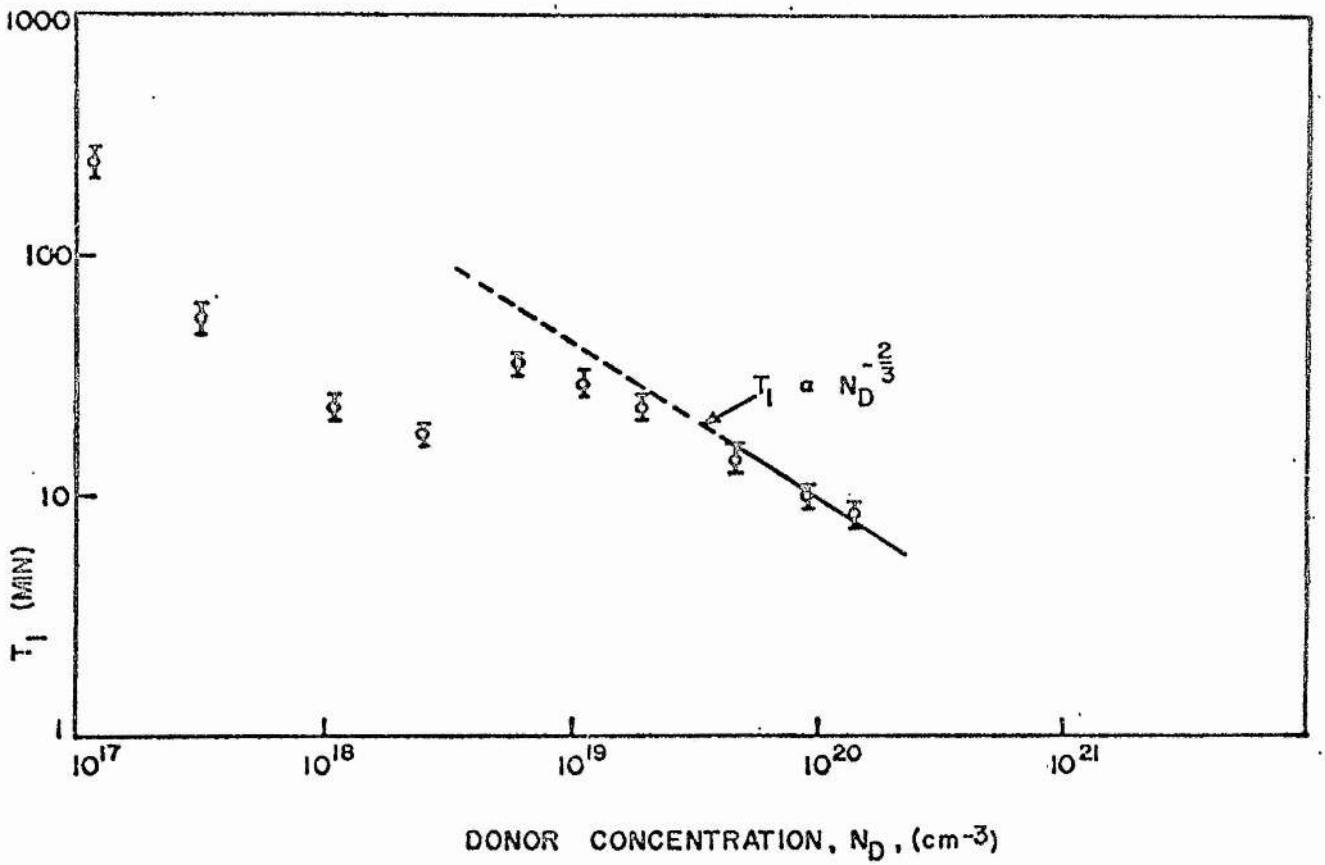

FIG.4.13 $T_1(Si^{29})$ in Si:P.

After Sundfors and Holcomb[7]

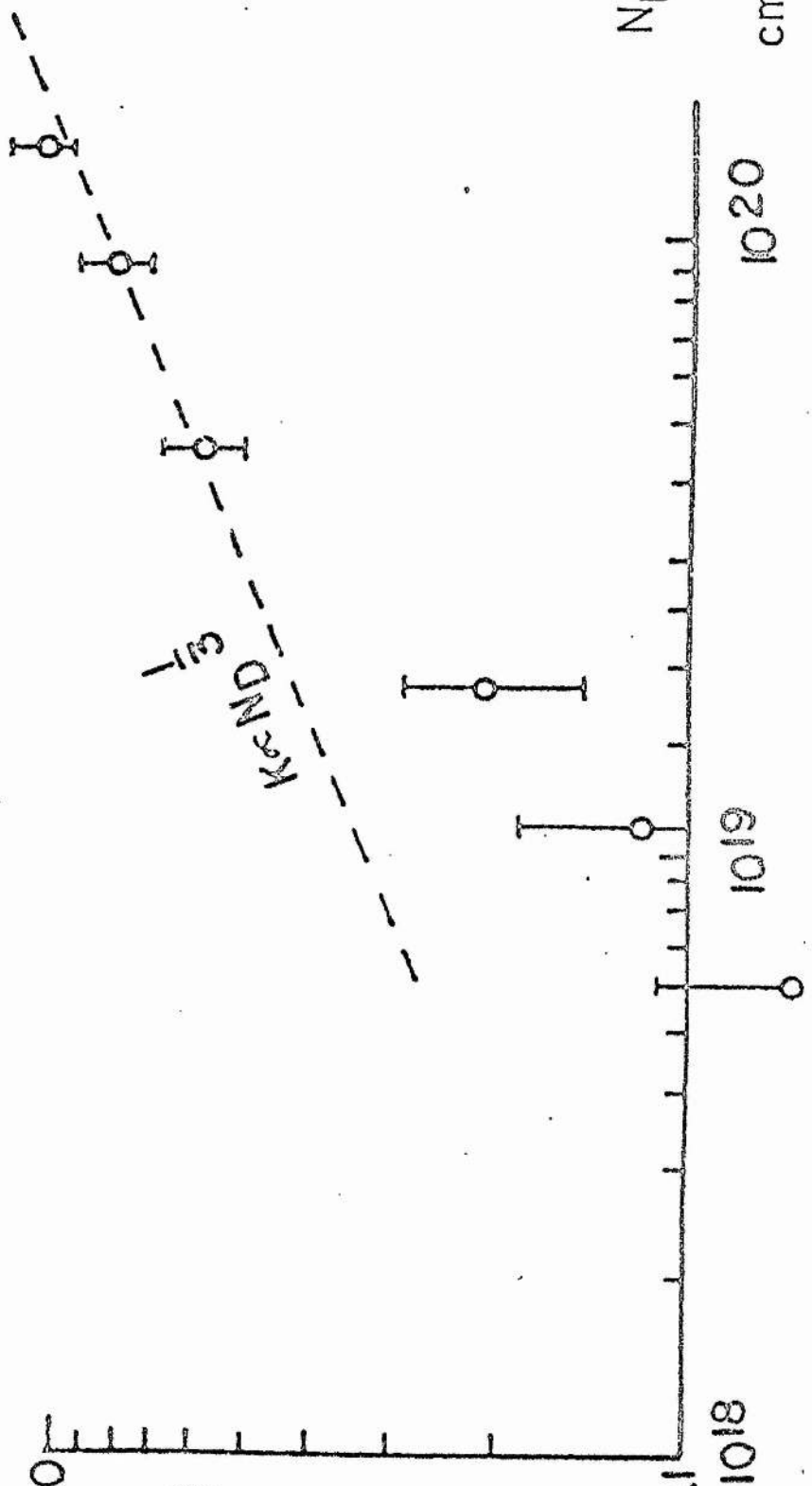

FIG. 4.14 $K(Si^{29})$ in Si:P.

After Alexander and Holcomb.[44]

Sundfors and Holcomb also observed the P^{31} resonance in Si:P for $N_D \geq 9.10^{19} cm^{-3}$. The P^{31} resonance line is asymmetric, of width ~ 100 times the dipolar width and shows a much larger Knight shift than Si^{29}. The size of $K(P^{31})$ is expected since the probability amplitude of the electron wave function is much greater at P^{31} sites than at Si^{29} atoms. A detailed examination of the P^{31} resonance in Si:P has been performed by Brown and Holcomb[6] following the earlier work of Carver, Holcomb and Kaeck[132]. Brown and Holcomb find that the temperature dependences of ΔB and K follow that of the spin susceptibility χ_S which we have considered above. They do not however favour the 'inhomogeneity model' of Quirt and Marko: their reasoning is twofold[133]. Firstly, they find that their results are reasonably well explained on the basis of the Knight shift distribution model in which all donor electrons are taken to be delocalised. Secondly, if a two-phase electron system were to exist, then local moments must be present in the metallic samples. Now it is well known that an electron gas is exchange coupled via the RKKY interaction to a local moment, leading to spin density oscillations of the form

$$\frac{\cos 2k_F r}{r^3} \qquad (4.6)$$

where k_F is the Fermi wave vector and we have taken the origin to be at the magnetic impurity site. Since the conduction electrons couple to the nuclei via the hyperfine interaction we expect the local field at nuclear sites to vary in a similar manner to equation (4.6). The nett result in a magnetic resonance experiment

should be a broadening of the host resonance line and this has been observed in dilute Cu:Mn alloys where the Cu^{63} line broadens substantially for the addition of less than 0.1 atomic per cent of manganese. Moreover, since the electronic spin-lattice relaxation time, i.e. $T_{1e}(Mn)$ is much less than the nuclear spin-spin relaxation time (T_2 (Cu)) the Cu^{63} nuclei experience a time-averaged magnetic moment of the paramagnetic centres $\langle \mu(Mn) \rangle$ which will thus be aligned with the external magnetic field B. Now Bloembergen's analysis gives[134]

$$\langle \mu(Mn) \rangle \propto \frac{B}{T} \qquad (4.7)$$

so $\Delta B(Cu^{63})$ should be proportional to field and the inverse of temperature which is precisely the observed behaviour.

With regard to the Si:P system, we should identify local moments as isolated P donors which couple, through the RKKY interaction and then the hyperfine interaction to P^{31} nuclei at ionised donor sites. The inequality $T_{1e}(P^{31}) \ll T_2(P^{31})$ holds. Thus $\Delta B(P^{31})$ should be proportional to B/T and this is indeed what Brown and Holcomb find. There are two facts, however, which strongly conflict with the idea of local moments existing in metallic Si:P.

Firstly, both theory and experiment[136, 137] show that the host Knight shift is affected negligibly by the RKKY interaction which is clearly at variance with the Brown-Holcomb data. Secondly, both experiment and theory[136-8] show the Lorentzian form of the nuclear line shape whilst Brown and Holcomb and also Ikehata et al.[3] observe

strong asymmetry in the P^{31} line shape. It is important to note that none of the arguments on the local moment question presented above are altered by the aperiodicity of the P^{31} atomic arrangement. Heeger et al.[139] have shown that the presence of non-scattering centres leads to a damping of the RKKY oscillations so that the spin density oscillations have a form

$$\frac{\cos 2k_F r}{r^3} \; e^{-r/\lambda} \qquad (4.8)$$

with λ a mean free path of the damping. For $Cu_{1-x}Al_x$:Mn, Heeger et al.[139] find $\lambda \sim 40$ lattice spacings with $x = 0.01$. Again theory and experiment[137-9] are in good agreement on the Lorentzian shape of the resonance.

With respect to electron correlation effects, Brown and Holcomb find a Korringa product which increases above unity as N_D approaches N_C from the metallic side of the transition. Their conclusion is that $K(P^{31})$ may be enhanced by electron correlation in the manner we have outlined in chapter 2. The uncertainty in this conclusion is generated by the difficulty in measuring $T_1(P^{31})$ for a small number of impurity spins to the required degree of precision. To the contrary, the chief difficulty for Si^{29} is an accurate measurement of the small Knight shift. Brown and Holcomb hypothesise that the decrease in the Korringa product for Si^{29} in the transition region may be due to incipient localisation leading to a Warren-type increase in relaxation rate such as we have described in chapter 2.

We now examine the Japanese data on the Si:P system and note the qualitative and quantitative differences between these results and those of the Holcomb group. Figures (4.15), (4.16) depict the $K(Si^{29})$ and $T_1(Si^{29})$ variation with N_D. The relaxation time varies as $(TN_D)^{-1}$ for $N_D > 7.10^{18}\ cm^{-3}$ whilst K holds to the $N_D^{\frac{1}{3}}$ dependence until $N_D = N_C$ at which there is abrupt fall of K to zero. The absorption line shows three regions of behaviour. For light doping ($N_D < 10^{18} cm^{-3}$), ΔB is of the order of the dipolar linewidth for Si^{29} nuclei and is temperature independent from 4.2 to 0.4 K. In the intermediate region ($10^{18}\ cm^{-3} < N_D < 4.10^{18} cm^{-3}$), the line is symmetric and of the order of the dipolar width at 4.2 K but ΔB increases and the line becomes asymmetric with a low field tail as the temperature is reduced below 1 K. In the metallic region, the line is asymmetric at 4.2 K and ΔB increases with N_D. For $4.10^{18} cm^{-3} < N_D < 2.5.10^{19} cm^{-3}$, ΔB increases with decreasing temperature but this dependence weakens as N_D increases and vanishes when N_D exceeds $5.3.10^{19} cm^{-3}$.

The explanation of $\Delta B(Si^{29})$ due to Sasaki et al.[2] is the following. Considering first the donor dependence, at low concentrations the line width is in accord with the dipole interaction between Si^{29} nuclei as Sundfors and Holcomb also concluded. At high concentrations, the asymmetry of the absorption line is a consequence of the inhomogeneous contact field between electrons and Si^{29} nuclei. The contact field is proportional to the probability amplitude $\langle|\psi(o)|^2\rangle_{E_F}$ of electrons at the Fermi surface and

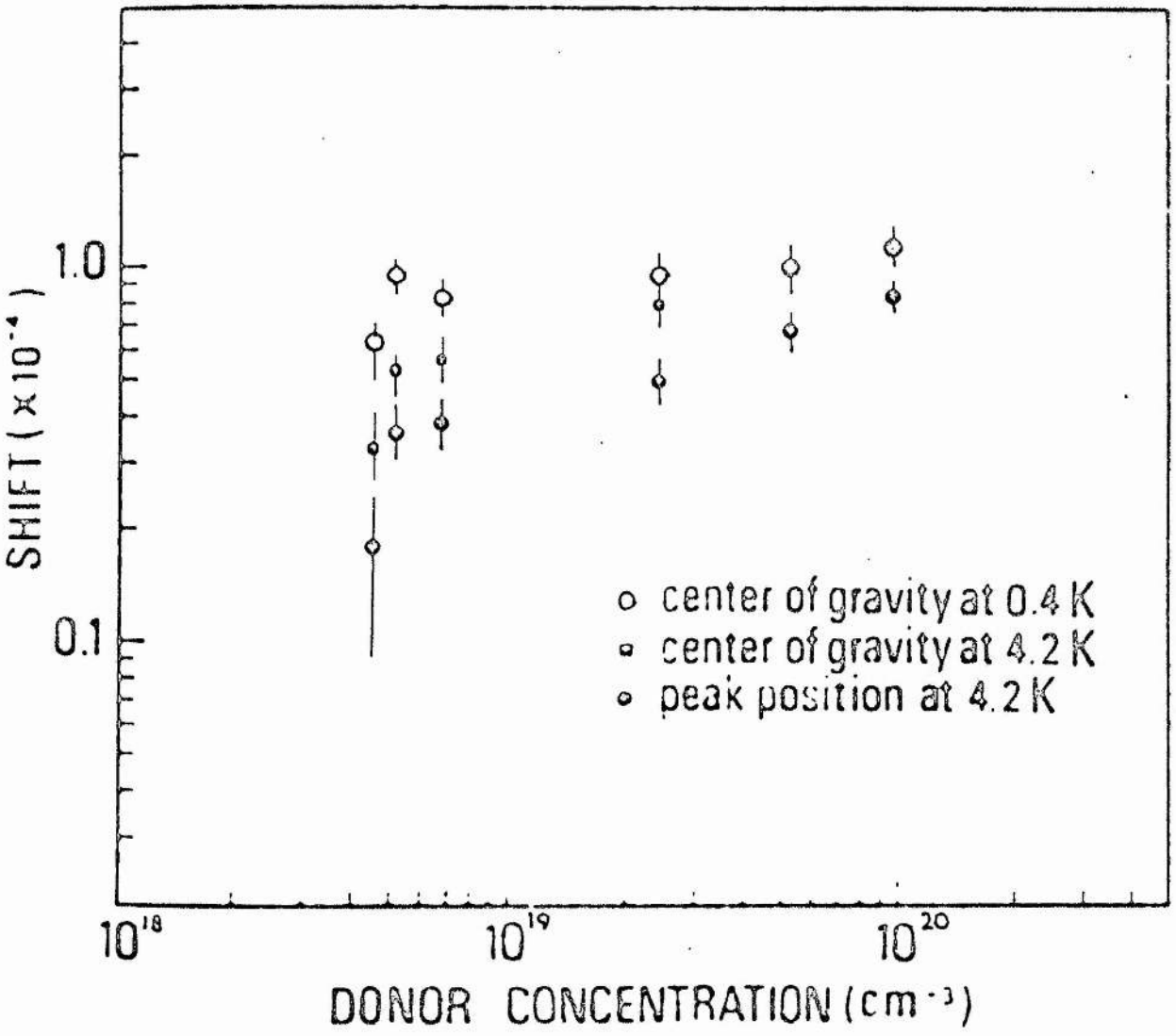

FIG.4.15 $K(Si^{29})$ in Si:P.

After Sasaki, Ikehata and Kobayashi.[2]

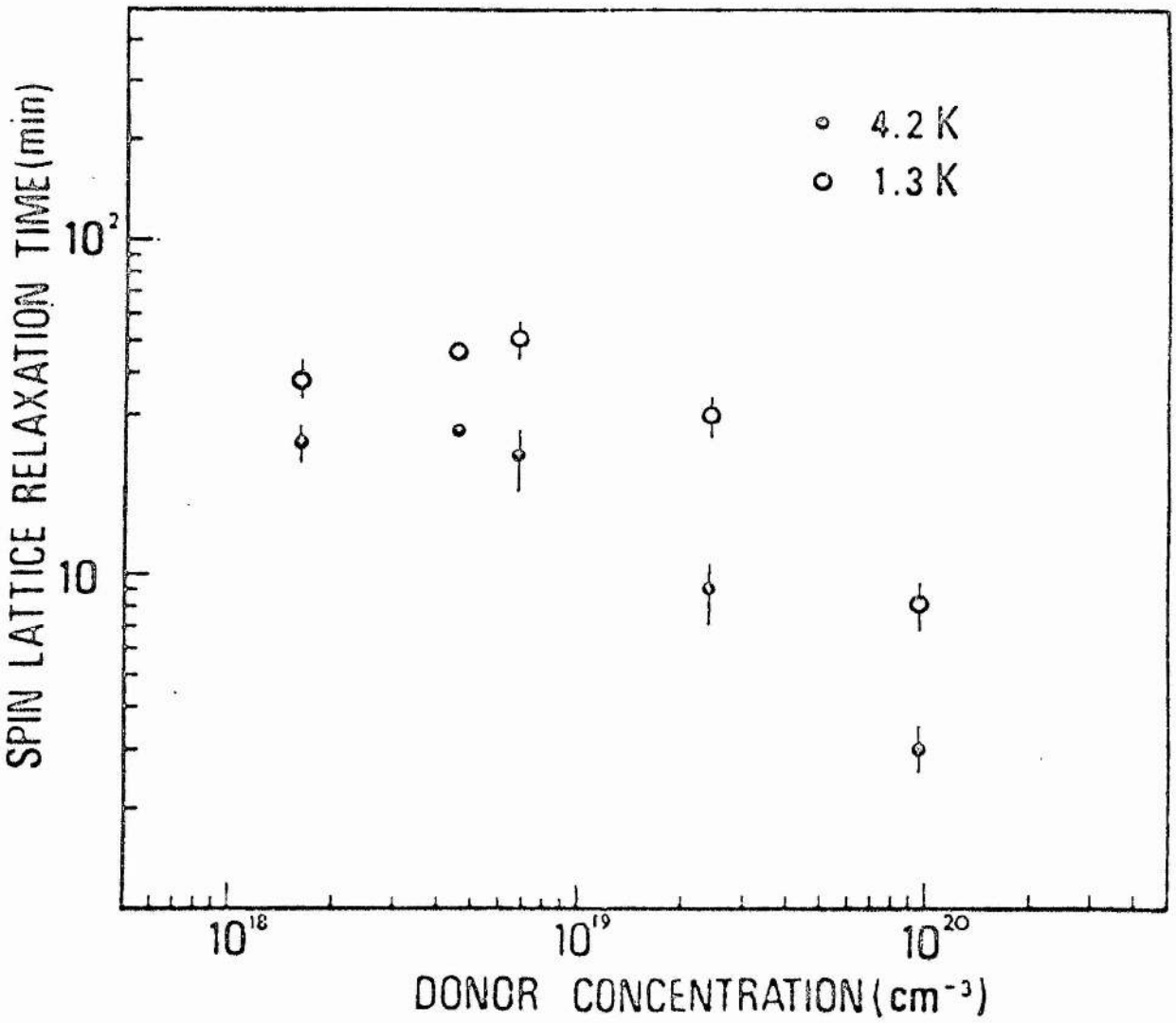

FIG.4.16 $T_1(Si^{29})$ in Si:P.

After Sasaki et al.[2]

assuming a hydrogenic form for $\psi \sim \exp(-r/a_H)$ it follows that the number of Si^{29} nuclei experiencing a given contact field will have some inverse dependence on the magnitude of $\langle|\psi(o)|^2\rangle_{E_F}$. Hence the absorption line should show a low-field tail and a rather sharp cut-off at high fields precisely as Sasaki et al. find.

To explain the temperature dependence of $\Delta B(Si^{29})$, we first adumbrate the metal-nonmetal transition as then viewed by Sasaki et al.. They imagine the transition to occur locally rather than over the entire crystal and also that low density samples $N_D \lesssim N_C$ consist of metallic islands separated by insulating regions. The metallic clusters can contain either an even or an odd number of electrons. Clusters containing an even number of carriers lose their magnetic susceptibility and yield a sharp line at the zero Knight shift position but odd-number clusters have a Curie susceptibility and contribute a broad line with a temperature dependent width and position. For $N_D > N_C$, Sasaki et al. claim that metallic channels exist across the sample giving conductivity of a metallic nature as well as isolated pockets of metallic condensate. The electrons in metallic channels are thought to provide a Knight-shifted line with metallic islands contributing an asymmetry as before. Furthermore, the sudden appearance of the Knight shift is taken to be the result of percolation of the metallic condensate rather than the result of an Anderson transition. When the $K(Si^{29})$ values are combined with $T_1(Si^{29})$ data, the Korringa product is found to be greater than unity. This is taken to be a sign of Knight shift enhancement resulting from electron correlation effects.

Comparing the Sundfors-Holcomb and Sasaki et al. articles we note three main differences. Firstly, Sundfors and Holcomb (and also Brown-Holcomb) advocate a one-phase electron system. Secondly, the magnitudes and concentration dependence of their Knight shifts are quite different from those of Sasaki et al.. Thirdly, the decrease in Korringa product rules out the correlation effects which are necessarily adhered to by Sasaki and coworkers. The latter workers have suggested that the discrepancies that exist in the two sets of $K(Si^{29})$ data are due primarily to the different methods used to determine N_D in the different laboratories. We discuss sample characterisation in some depth in Appendix 2.

Before giving details of additional experimental data recently compiled by Sasaki et al. we wish to point out that alternative explanations exist for the observed line shape and donor density dependence of the Knight shift which do not assume a two-phase electron system nor the application of a percolation model. Firstly Kamimura[140] has obtained a theoretical, asymmetrical line shape whose width is determined by the spatial inhomogeneity of the tight binding wave function over the Si^{29} nuclei. The different donor dependences of the peak and centre-of-gravity Knight shift are brought out, in agreement with the results of Sasaki et al.. The N_D dependence comes partially from that of χ_S which was calculated previously assuming correlated electrons and the applicability of the Hubbard approximation. Good fits to the experimental data are obtained taking $a_H = 2.3$ nm which compares to the isolated donor Bohr radius of 1.7 nm[142],

and $|\psi(o)|^2 = 3$ which is much less than other estimates[128,143] though these themselves differ widely.

On the subject of the sudden appearance of the Knight shift, Mott[144] has suggested that this is consistent with an Anderson form of metal-nonmetal transition. For extended states, application of a magnetic field ~~with~~ will spin flip electrons whose number is proportional to $\mu_B N(E_F)$. These extend throughout the crystal leading to a Knight shift. If states are localised within a sphere of α^{-1} ($\psi \sim \exp(-\alpha r)$) then a magnetic field removes a few spin-down electrons from states just below E_F to a few spin-up states just above E_F and the majority of host nuclei do not experience an extra field that can produce a Knight shift of their resonance. It is important to note here that since the Knight shift is proportional to χ_S we have tacitly assumed that χ_S does not change discontinuously at the transition. That this is true results from the recognition that χ_S is proportional to the density of states at the Fermi level $N(E_F)$ and $N(E_F)$ does not change at the transition. We therefore expect χ_S to be continuous through the transition and this is observed by, for example, Ue and Maekawa[83] in Si:P. Mott's model also implies that the NMR line should exhibit structure, i.e. that resonance lines corresponding to spin-up or down, singly occupied sites and unshifted, doubly occupied sites. Such structure might be unresolved but would then lead to some overall broadening.

The P^{31} resonance in Si:P has been studied by Ikehata, Sasaki and Kobayashi[3]. Their results are in accord with those of Brown

and Holcomb[6]; viz an abrupt appearance of a Knight shift at $N_D = N_C$ with a magnitude much greater than the Si^{29} shift and thereafter decreasing with increasing N_D and an asymmetric line again greater than $\Delta B(Si^{29})$ which broadens as N_D decreases and shows a slight temperature dependence for N_D values less than N_C. Brown and Holcomb use the Knight shift distribution model to explain their results and obtain reasonable agreement with experiment although they are unable to explain the temperature dependence of $\Delta B(P^{31})$ on this model. Ikehata et al. discuss their data in terms of the two-phase electron system we have described above.

Both sets of workers find the Korringa product to be greater than unity close to the transition and Ikehata et al. attribute this to a definite enhancement of $K(P^{31})$ through electron correlation effects with enhancement factors identical to those determined for Si^{29} at equivalent N_D values. An additional property of $T_1(P^{31})$ is observed by Ikehata et al. at low temperatures with N_D in the metallic range (figure (4.17)). The temperature dependence of $(T_1T)^{-1}$ is as $(T - T_N)^{-\frac{1}{2}}$ which is the dependence predicted by Moriya and Ueda[145, 146] in their theory of the relaxation rate in antiferromagnetic metals. The deduced Neel temperature T_N is 0.1 K. A similar behaviour of $(T_1T)^{-1}$ for Si^{29} is observed by Ikehata et al.[4] at low temperatures and at N_D values close to the transition (figure (4.18)). In addition $T_1(Si^{29})$ increases with field for metallic specimens at 0.6 K though this dependence is quenched in strongly metallic samples.

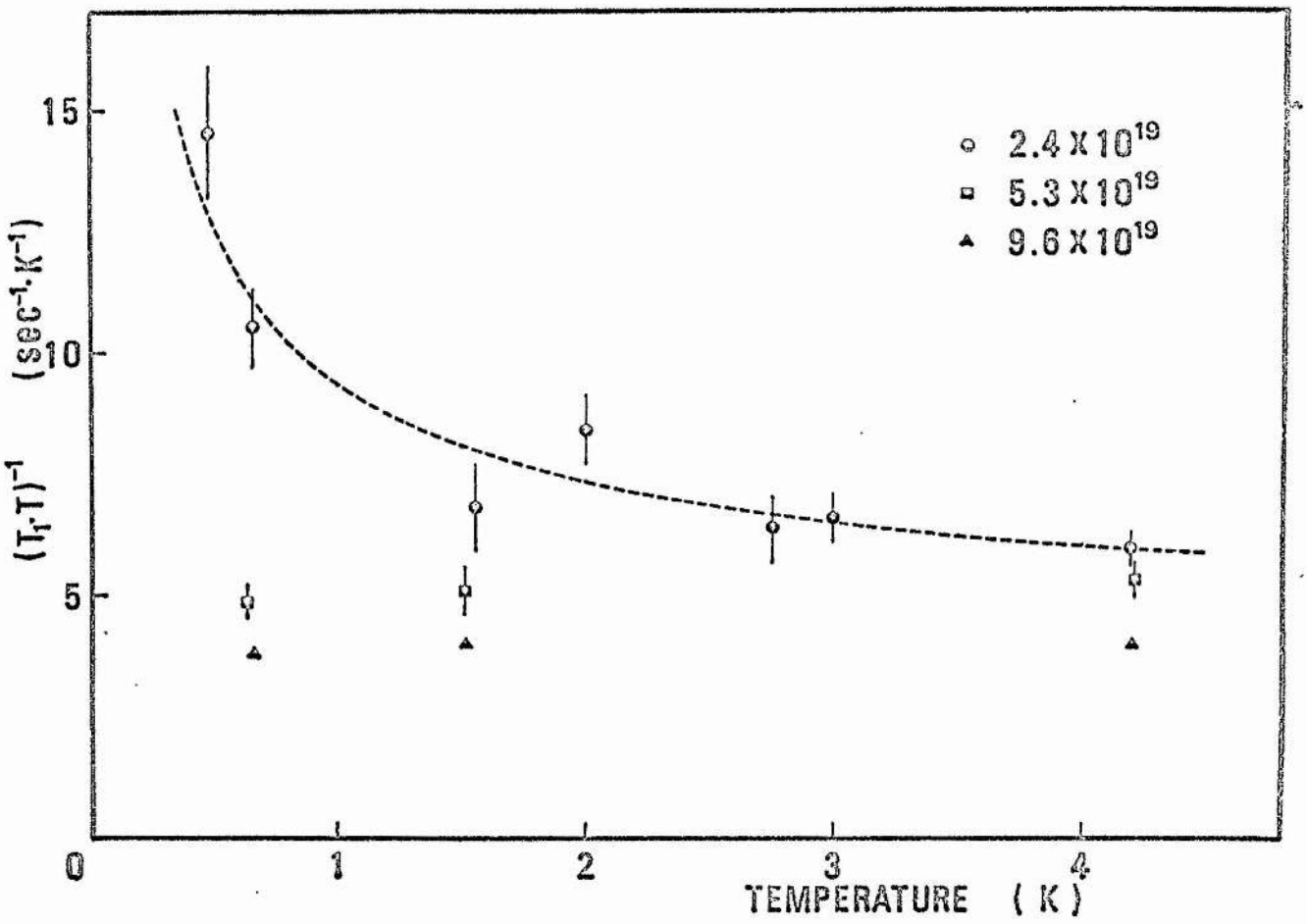

FIG.4.17 $(T_1(P^{31}).T)^{-1}$ in Si:P.

After Ikehata, Sasaki and Kobayashi.[3]

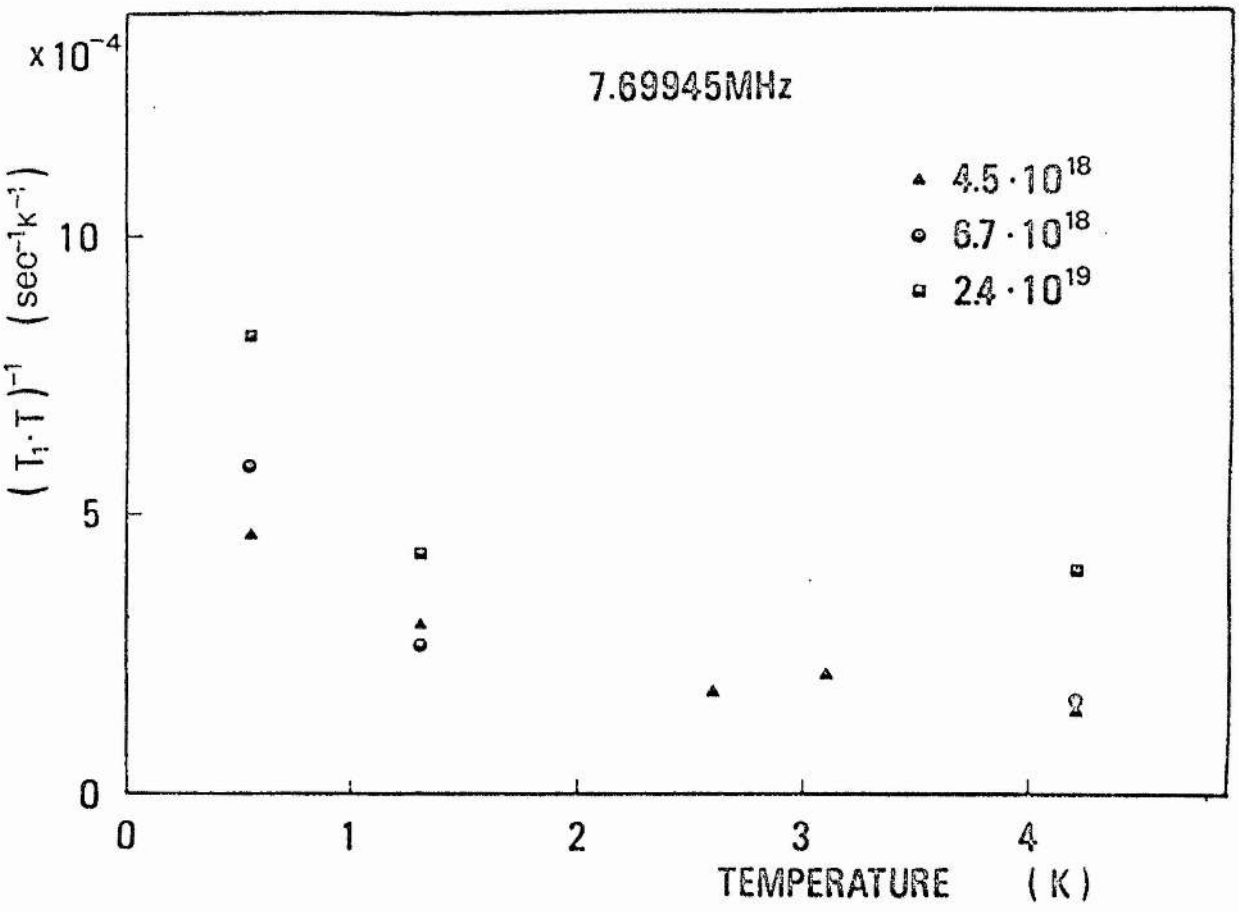

FIG.4.18 $(T_1(Si^{29}).T)^{-1}$ in Si:P.

After Ikehata, Sasaki and Kobayashi.[4]

Sasaki takes the view that the donor electrons have antiferromagnetic order below T_N but for slightly higher temperatures, T_1 is shortened by spin fluctuations. The increase of T_1 with field is then due to suppression of the spin fluctuations by the field.

4.10 Magnetic Freeze-Out

The effect of a strong magnetic field on a localised electron is to shrink the electron orbit towards the origin of the localising potential. Yafet, Keyes and Adams[147] first considered the problem by calculating the effect of a magnetic field on the ionisation energy of the hydrogen atom and found that the energy would increase when

$$\gamma = \frac{\hbar \omega_c}{2\ Ry} \geqslant 1 \qquad (4.9)$$

where ω_c is the cyclotron frequency and Ry the Rydberg constant. The field value for $\gamma = 1$ was the enormous one of 0.2 MT. If, however, we write out the expressions for ω_c and Ry

$$\omega_c^* = \frac{eB}{m^*} \qquad Ry^* = \frac{m^* e^4}{(4\pi\varepsilon_o)^2 \varkappa^2 2h^2}$$

(where we have added asterisks to indicate that we are using effective masses in the definitions) then the field $B\ (\gamma = 1)$ may be written

$$B(\gamma = 1) = \text{const.}\ \frac{m^{*2}}{\varkappa} \qquad (4.10)$$

Thus, for hydrogenic centres in a semiconductor with low effective mass and high dielectric constant the value of $B(\gamma = 1)$ may be

reduced to attainable values. The best example[148] is InSb which has $m^* = 0.01\ m_o$, $\varkappa = 16$ and $B(\gamma = 1) = 0.15$ T. Germanium has an anisotropic effective mass but taking the transverse value $m_t^* = 0.08\ m_o$ and $\varkappa = 16$ yields $B(\gamma = 1) = 6$ T. Now we have already seen that a large number of electrons can screen a positive ion potential such that no bound states for electrons exist. If a magnetic field is applied to a degenerate semiconductor at zero Kelvin the shrinkage of the wave functions can lead to the formation of bound states at a certain field value. As bound states form, the electron screening is reduced hence allowing more electrons to become localised at impurity ion sites. This regenerative process means that a discontinuous change in the number of current carriers occurs at absolute zero and we have a magnetic-field-induced Mott transition[149]. At higher temperatures there will be no discontinuity in N_D but the carrier density will change very rapidly.

Bound states will form when the volume of a bound state is less than the average volume of an impurity. The bound state volume is a cigar-shaped region of length a_H and radius $\lambda = (h/eB)^{\frac{1}{2}}$ and the average impurity volume is N^{-1} so that the criterion for the formation of localised states is $N\pi\lambda^2 a_H < 1$.

Experimentally, the effect has been observed by Keyes and Sladek[150] in InSb but the activation energy and its variation with field were less than that calculated by the Yafet et al.[147] theory. To account for the disaccord, Fenton and Haering[149] have

considered the influence of electron-electron effects whilst Dyakonov, Efros and Mitchell[151] have explicitly taken the disorder of the system into consideration. Recently, Serre, Ghazali and Leroux Hugon[152] have shown that both correlation and disorder must be included in a calculation of the critical field and impurity concentration for the onset of an activated conduction regime.

Galvanomagnetic investigations have been made in Si:As by Straub et al.[153], Ge:As by Matveev et al.[154] and Ge:Sb by Sadasiv[155] and Yamanouchi[156]. The Si:As results show changes with field in the Hall coefficient and magnetoresistance of hundreds of percent for N_D values close to N_C decreasing to a few percent for more heavily doped samples. The effects are also highly temperature dependent being greatest at the lowest temperature studied of 1.3 K. Straub et al.[153] and Friedman and Mott[157] have interpreted the data as indicative of a modification of the density of states by the magnetic field, i.e. the pseudogap is lowered and the Friedman formula for R_H applies to the (still metallic) samples. Mott[1] has subsequently argued that since a Hall anomaly is observed and the Friedman formula seems unapplicable to metallic semiconductors then the effect of the magnetic field must be to transform the specimens to semiconducting behaviour.

4.11 Summary

We have reviewed a variety of experimental studies of the metal-nonmetal transition in this chapter, many of them performed very recently. Although it would be gratifying to be able to describe some definite organising principle for the data, this is too ambitious a task here. We have seen that results may be explained by different, often antithetical models. Two facts emerge from this survey, however. Firstly, there is a duel between the relative importance of correlation and disorder in determining the driving mechanism for a metal-nonmetal transition. Secondly, whilst it might have been expected that the experimental behaviour of Ge and Si would have been similar, (apart from the scaling of such quantities as m^* and $\varkappa$), this is not true in practice.

Chapter 5

RESULTS AND DISCUSSION

5.1 Introduction

The purpose of this chapter is to list the results of our NMR experiments on the Ge:As system and to attempt to interpret the data in terms of the current ideas advanced on the metal-nonmetal transition that we have outlined in chapter 3. We also discuss the validity of our interpretation with respect to other experimental results such as we have reviewed in chapter 4.

5.2 Results

Initially, measurements of the nuclear spin-lattice relaxation time T_1 of the Ge^{73} nucleus in twelve samples of Ge:As were performed at 2.14 MHz, corresponding to a resonance field of 1.44 T, at temperatures at and below 4.2 K. The purchase of a superconducting magnet system allowed measurements of T_1 and the Knight shift K to be made at the higher frequency of 7.4 MHz (5T) at 4.2 K. Linewidth data at both fields are also available. Details of the experimental techniques and some of the difficulties encountered are given in Appendix 1.

Figure (5.1) shows the variation at 4.2 K of the spin-lattice relaxation time at 2.14 MHz, which we hereafter write $T_1(2)$, with doping density N_D. In this and later diagrams, N_D is the room temperature carrier concentration as determined from Hall effect and resistivity measurements. Our reasons for choosing a high temperature N_D value are twofold. Firstly, those researchers who have studied the Si:P system plot their data with respect to a room temperature carrier concentration and so our adoption of a

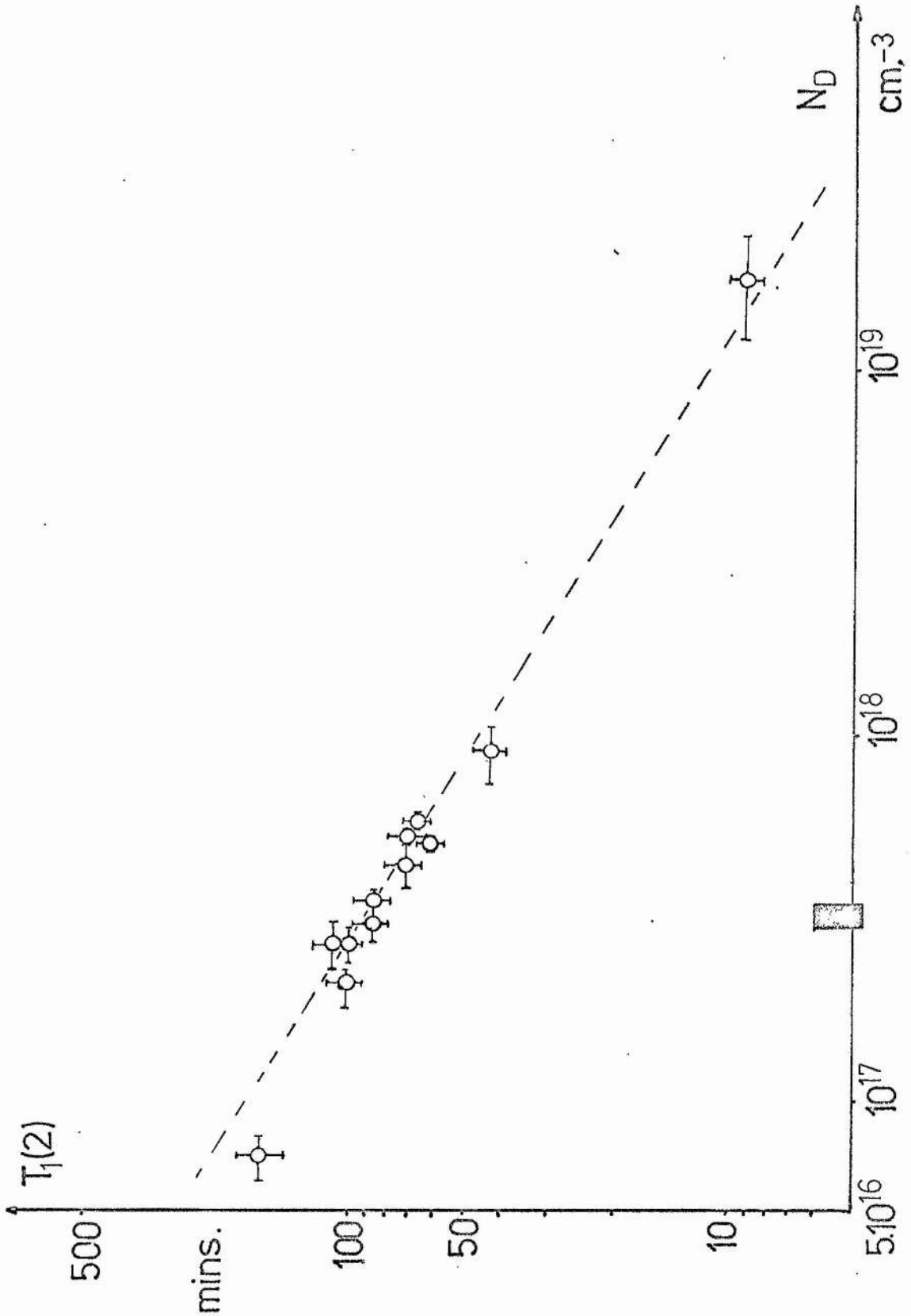

FIG.5.1 Spin-lattice relaxation time at 2·14 Mhz and 4·2 K.

similar practice permits ready comparison between the two materials. Secondly, metallic behaviour is, as we have noted in chapters 3 and 4, evidenced by a Hall effect which has but a slight temperature dependence from liquid helium to room temperatures. Hence, for the majority of our samples, $N_D(300\,K) \equiv N_D(4.2\,K)$. A full description of the characterisation of our samples from transport property measurements is given in Appendix 2.

The dotted line in figure (5.1) has a slope of $-\frac{2}{3}$ and the solid bar on the abscissa indicates the position of the metal-nonmetal transition as determined by the aforementioned d.c. electrical techniques.

Figure (5.2, a to j) show the dependence of $T_1(2)$ on temperature for various samples. The restriction to temperatures $< 4.2\,K$ is a consequence of practical and physical requirements. Experimentally, the greatest signal-to-noise ratio is achieved at low temperatures whilst physically we wished to study the behaviour of a degenerate electron gas via nuclear resonance. A free-electron expression for the degeneracy or Fermi temperature T_F of an electron gas is

$$T_F = \frac{E_F}{k} = \frac{\hbar^2}{2mk}(3\pi^2)^{\frac{2}{3}} N_D^{\frac{2}{3}} \qquad (5.1)$$

from which

$$T_F \sim 200\,K \text{ at } N_D = 10^{19}\,cm^{-3}$$
$$T_F \sim 45\,K \text{ at } N_D = 10^{18}\,cm^{-3}$$
$$T_F \sim 9\,K \text{ at } N_D = 10^{17}\,cm^{-3}$$

Thus, for our range of arsenic concentration we must operate at a temperature lower than $\sim 9\,K$.

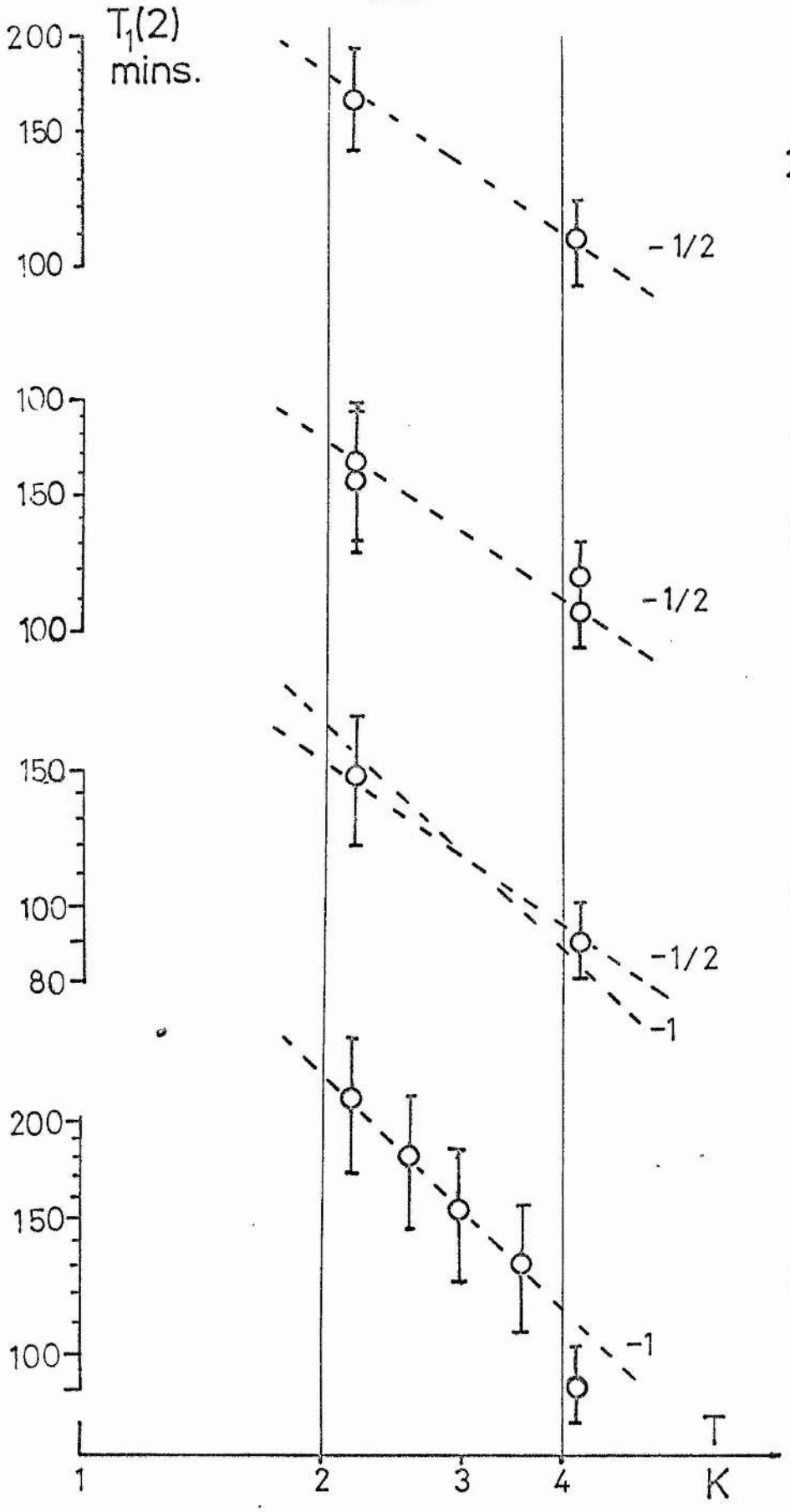

FIG. 5.2 (a)→(d). $T_1(2)$ against temperature.

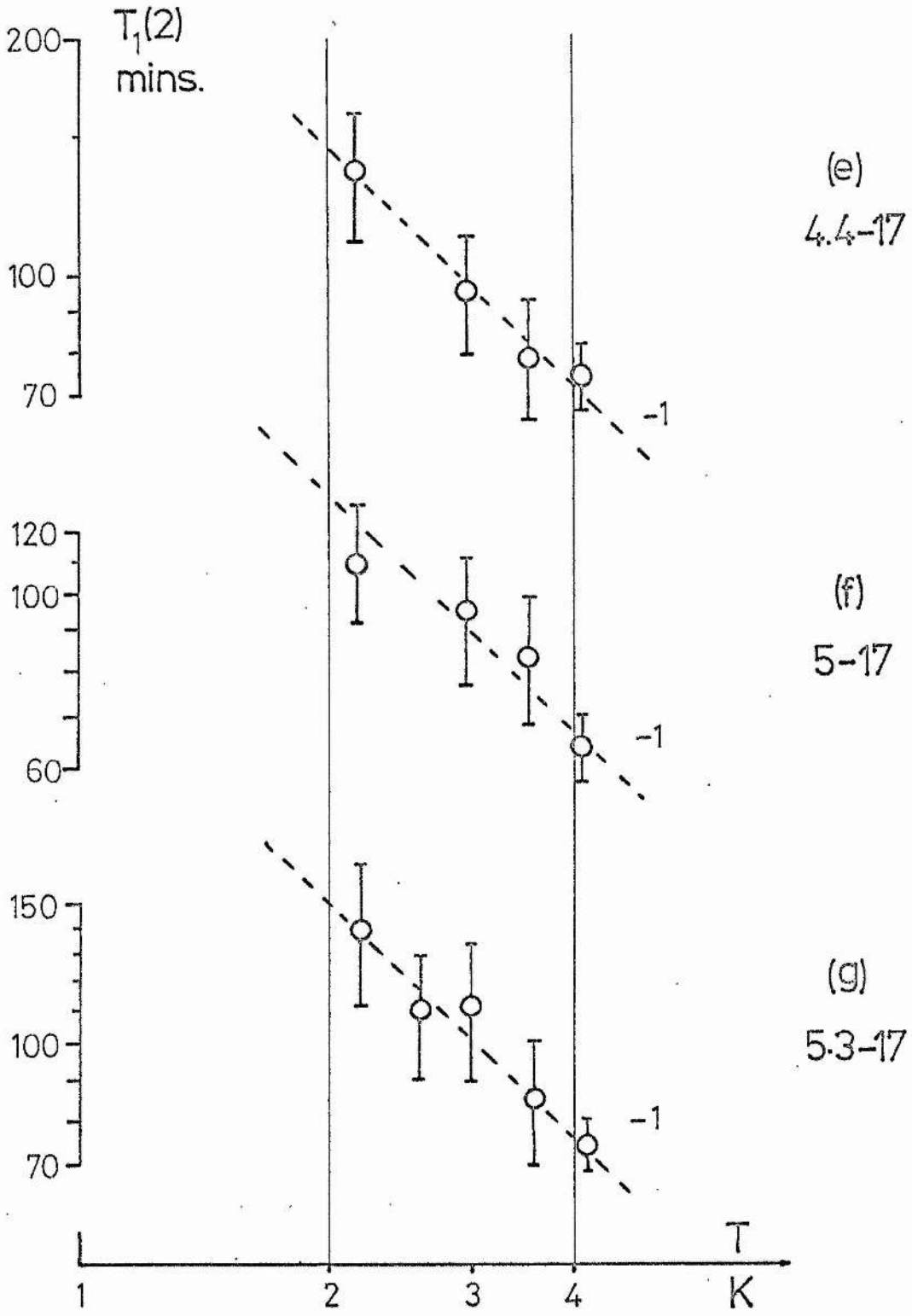

FIG. 5.2 (e)-(g). $T_1(2)$ against temperature.

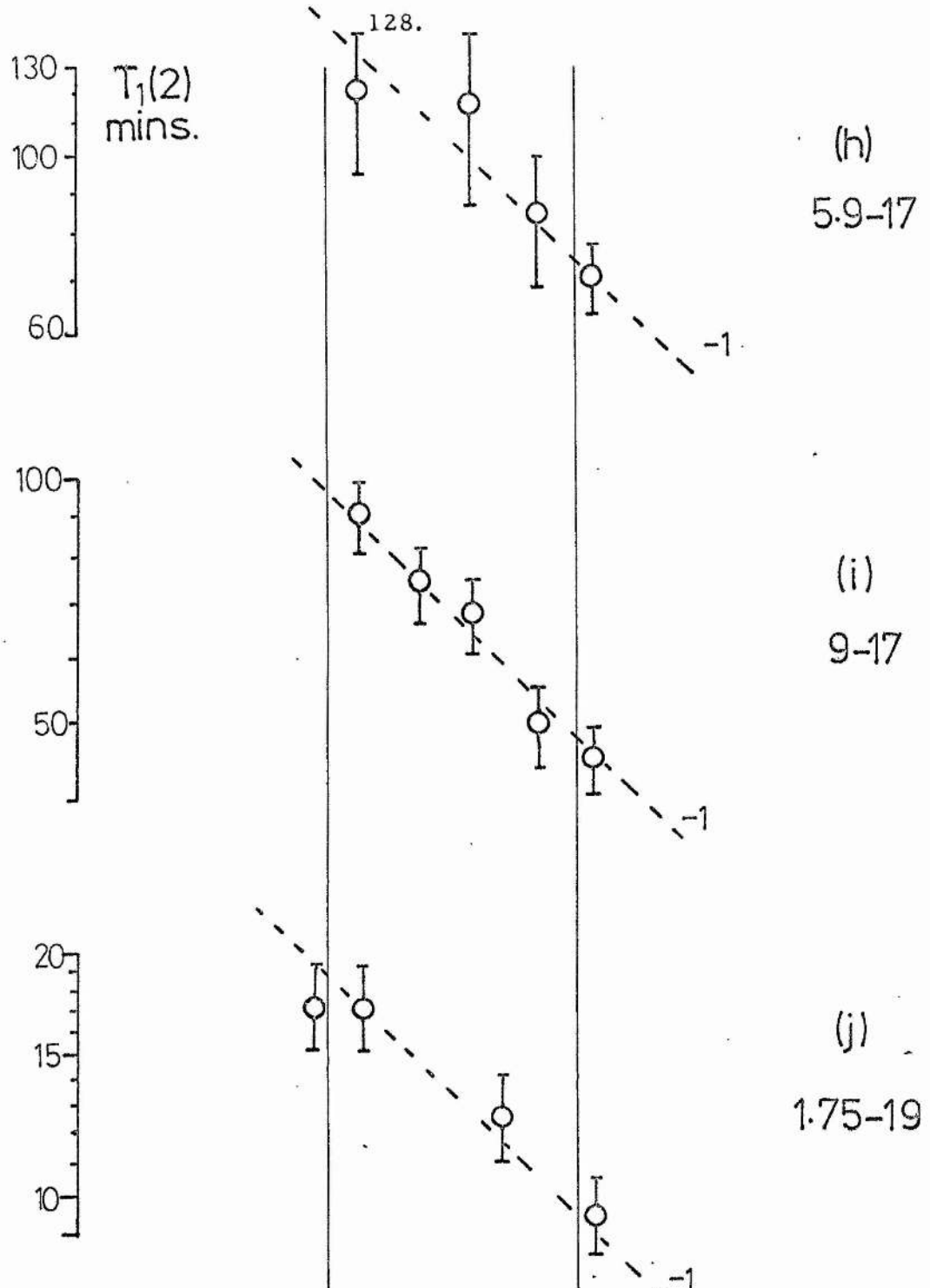

FIG. 5.2 (h)→(j). $T_1(2)$ against temperature.

The (peak) Knight shift measurements, taken at 7.4 MHz are displayed as a function of N_D in figure (5.3); the solid bar on the horizontal axis again represents the concentration N_C at which the metal-nonmetal transition occurs. The absence of data points for $N_D < N_C$ indicates that K is zero in the concentration range. As we have mentioned above, the Knight shift and spin-lattice relaxation time are related though the Korringa relation

$$K^2 T_1 T = \frac{\hbar}{4\pi k} \left(\frac{\gamma_e}{\gamma_n}\right)^2 \qquad (5.2)$$

for systems in which contact between the nuclei and electrons is the dominant interaction and the electrons are non-interacting. Figure (5.4) is a plot of $K^2 T_1(2) T$ versus N_D where the dashed horizontal line is the value appropriate to Ge of the constant appearing on the right hand side of the Korringa relation. We emphasize that in this diagram the ordinate is a hybrid of high field K and low field T_1 measurements.

From an experimental viewpoint, the fact that our T_1 measurements are greater than those in Si:P by a factor of roughly four to five might indicate that the value of K(Ge) calculated from the Korringa relation would be much less than K(Si) and possibly unobservable. Fortunately, the ratio of $\frac{\gamma_e}{\gamma_n}$ is larger for Ge than for Si so we have

$$\frac{K^2(Ge)}{K^2(Si)} = \left(\frac{\gamma_e}{\gamma(Ge)}\right)^2 \left(\frac{\gamma(Si)}{\gamma_e}\right)^2 \frac{T_1(Si)}{T_1(Ge)} \qquad (5.3)$$

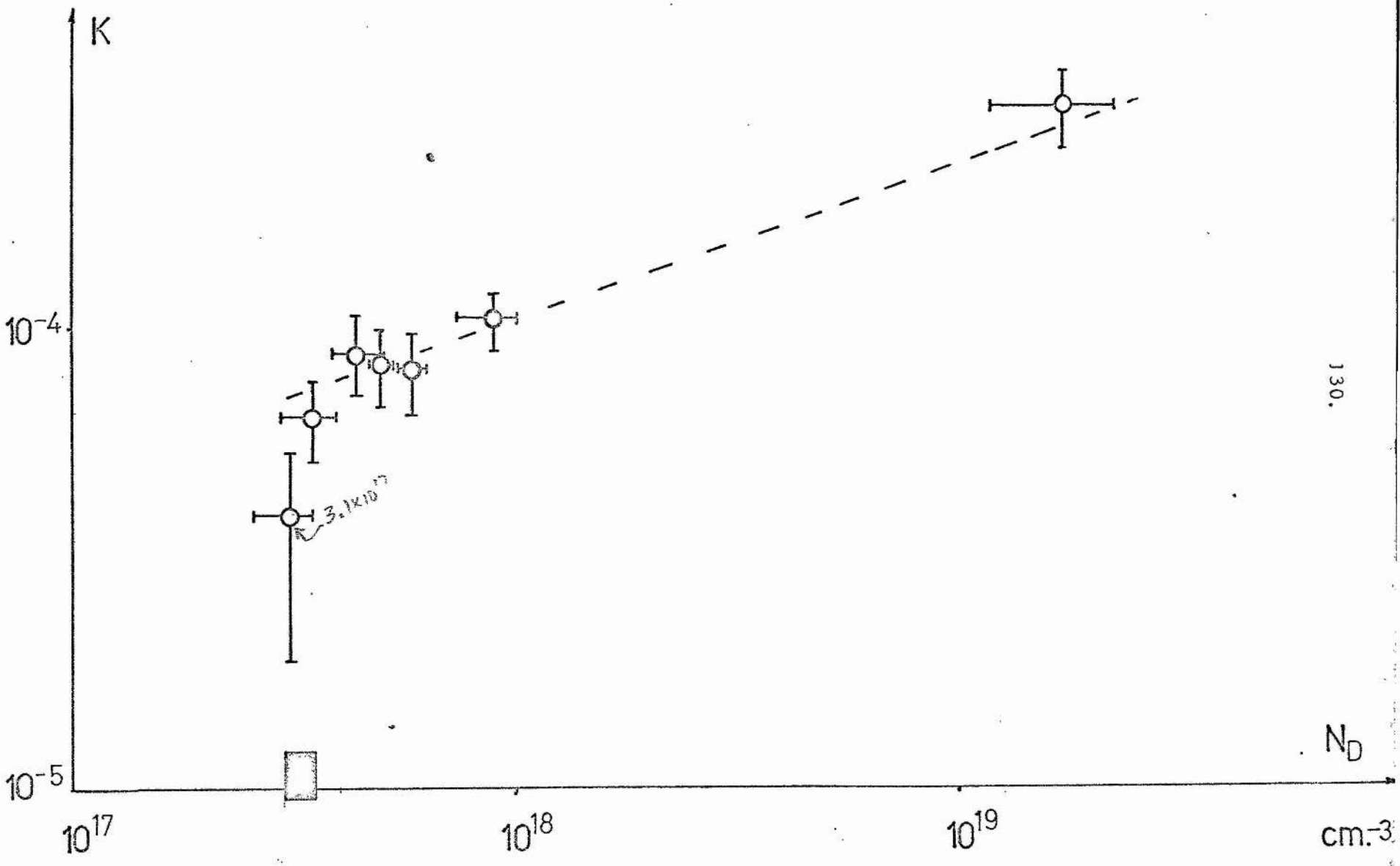

FIG.5.3 Variation of Knight shift with doping density.

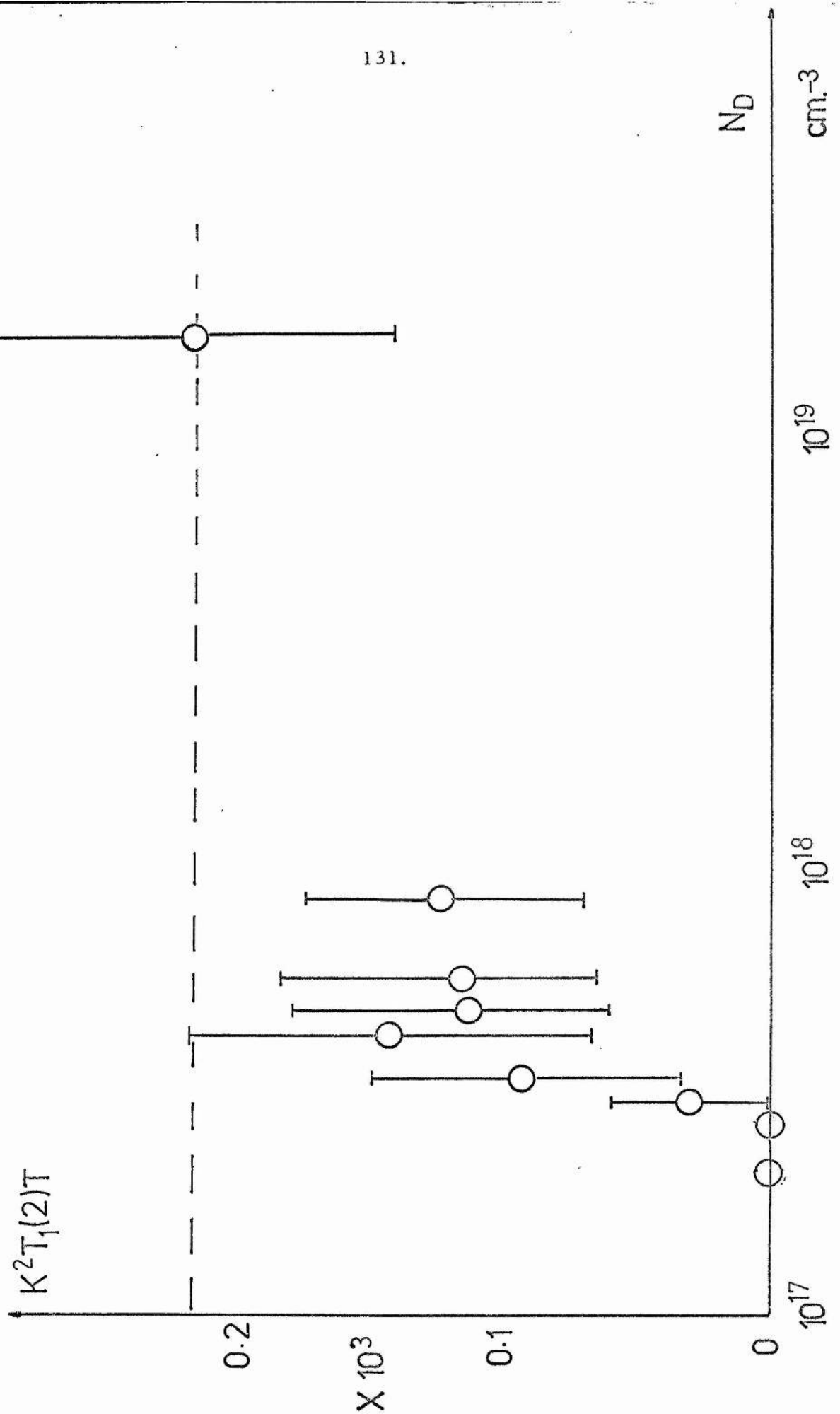

FIG.5.4 Low field Korringa product.

Using the values $\gamma_e = 1.76.10^{11} T^{-1}s^{-1}$ and γ (Ge), γ (Si) from table (5.3), then $\frac{K(Ge)}{K(Si)} \sim 2.5$ which is borne out by our results and those of Sasaki et al.. This does not mean however that K(Ge) is a more easily measured quantity than K(Si) since the long T_1 values in Ge:As prohibit the use of signal averaging techniques to improve the signal-to-noise ratio and also, the wider resonance lines that we observed make the shift more difficult to ascertain.

Spin-lattice relaxation times at 7.4 MHz, designated by the symbol $T_1(7)$ were measured only at 4.2K and these are shown in figure (5.5) as a function of N_D. The inordinate lengths of $T_1(7)$ precluded an investigation of the temperature dependence of this quantity. The variation with N_D of the Korringa relation, with K and $T_1(7)$ taken at the same magnetic field, is shown in figure (5.6). Figures (5.5) and (5.6) include data points for 2.14 MHz to display the field dependences of the ordinate variables. Values of $T_1(7)$ and $T_1(2)$ at various temperatures are listed in table (5.1).

Finally linewidths ΔB at both low and high fields are tabulated in table (5.2). The linewidths for $N_D < N_C$ are greater than the dipolar width computed in chapter 2 and this is in contrast to the behaviour in Si:P in the analogous doping regime where

$$\Delta B(Si) \equiv \Delta B_{dip}.$$

The main features of our results which must be explained with due regard to the physics of the metal-nonmetal transition are conveniently summarised as follows (N_C is taken as $3.1.10^{17} cm^{-3}$):

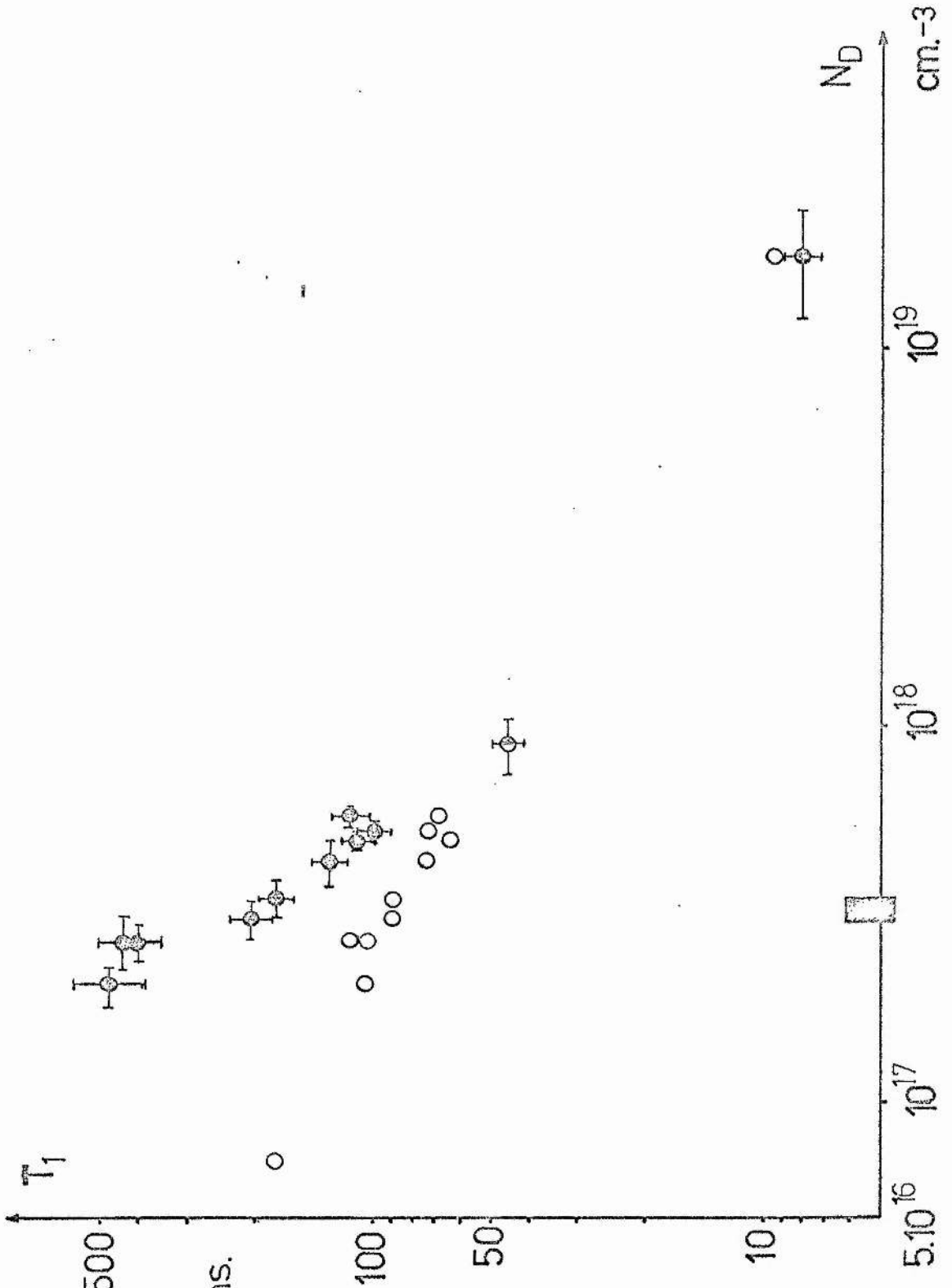

FIG.5.5 Spin-lattice relaxation times at 4.2K. ○ $T_1(2)$; ● $T_1(7)$.

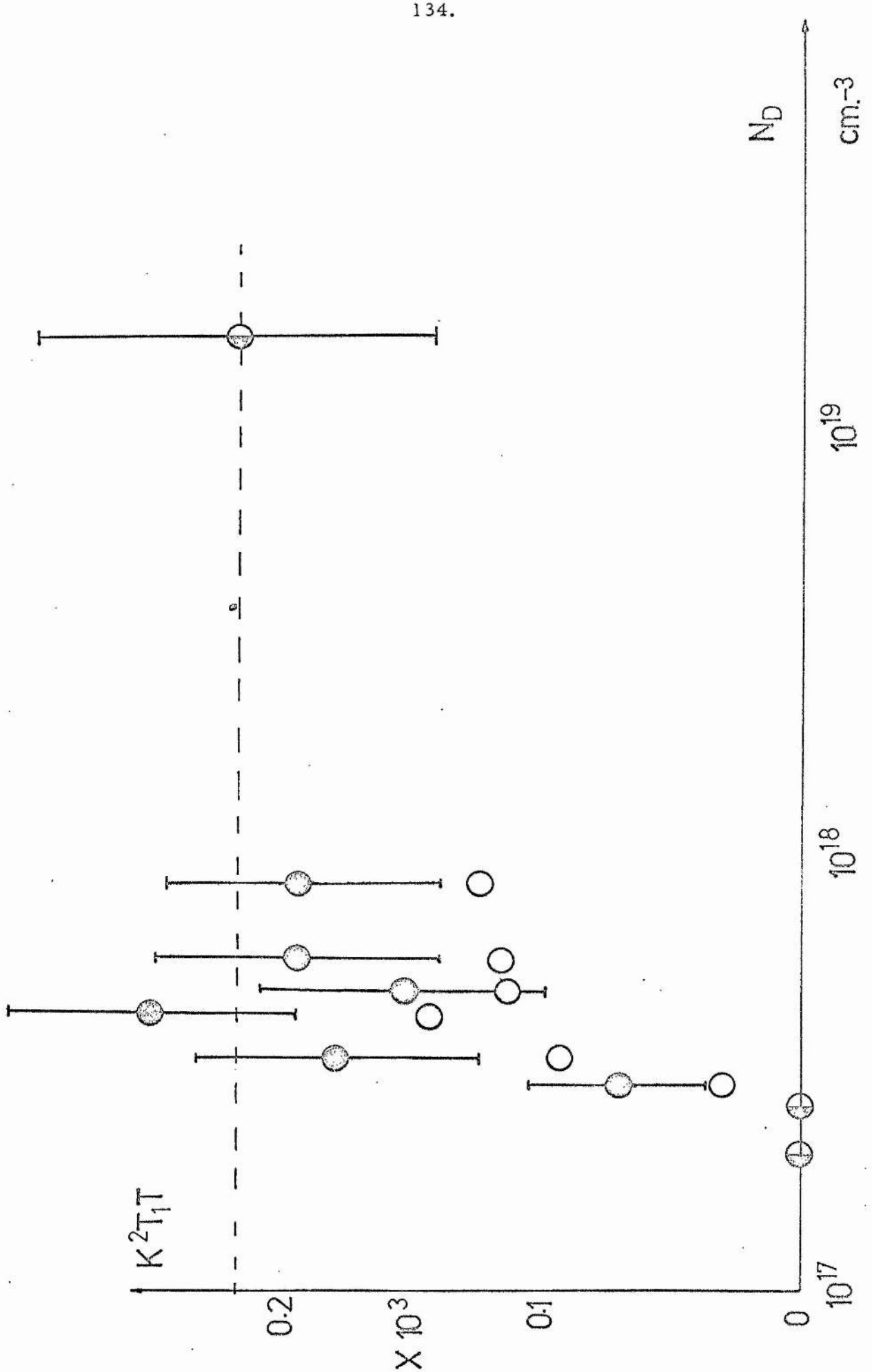

FIG. 5.6 Low and high field Korringa products. O $T_1(2)$; O $T_1(7)$.

TABLE 5.1

Spin-Lattice Relaxation Times for Ge:As
i) 2.14 MHz

Sample	Temperature K	Spin-Lattice Relaxation Time (mins)
7-16	4.2	178
2.1-17	4.2	106
2.1-17	2.2	163
2.7-17	4.2	116
2.7-17	2.2	158
2.7-17	4.2	104
2.7-17	2.2	166
3.1-17	4.2	90
3.1-17	2.2	146
3.5-17	4.2	91
3.5-17	3.6	130
3.5-17	3.0	153
3.5-17	2.6	181
3.5-17	2.2	213
4.4-17	4.2	74
4.4-17	3.6	78
4.4-17	3.0	95
4.4-17	2.6	135
5.0-17	4.2	64
5.0-17	3.6	83
5.0-17	3.0	95
5.0-17	2.2	108
5.3-17	4.2	74
5.3-17	3.6	85
5.3-17	3.0	112
5.3-17	2.6	100
5.3-17	2.2	140

TABLE 5.1
(continued)

Spin-Lattice Relaxation Times for Ge:As
i) 2.14 MHz

Sample	Temperature K	Spin-Lattice Relaxation Time (mins)
5.9-17	4.2	70
5.9-17	3.6	84
5.9-17	3.0	114
5.9-17	2.2	119
9-17	4.2	45
9-17	3.6	50
9-17	3.0	68
9-17	2.6	74
9-17	2.2	89
1.75-19	4.2	9.5
1.75-19	3.3	12.5
1.75-19	2.7	13
1.75-19	2.2	17
1.75-19	1.9	17

ii) 7.4 MHz and 4.2 K

Sample	Spin-Lattice Relaxation Time (mins)
2.1-17	480
2.7-17	404
2.7-17	440
3.1-17	205
3.5-17	177
4.4-17	130
5.0-17	109
5.3-17	99
5.9-17	117
9-17	46
1.75-19	8

TABLE 5.2

Linewidth Data at 2.14 and 7.4 MHz

Sample	$\Delta B(2)$ (mT)		$\Delta B(7)$ (mT)		$\Delta B'(7)$ (mT)
7-16	0.18		0.32		0.33
2.1-17	0.22		0.44		0.46
2.7-17	0.32		0.44		0.46
2.7-17	0.32		0.44		0.48
3.1-17	0.34	0.26	0.44	.26	0.54
3.5-17	0.40	0.30	0.48	.24	0.64
4.4-17	0.48		0.62		0.79
5.0-17	0.54	0.42	0.62	.42	0.87
5.3-17	0.56		0.62		0.87
5.9-17	0.62		0.72		0.90
9-17	0.64	0.48	0.98	.55	1.12
1.75-19	0.64	0.48	1.42	1.40	1.7

Note 1) $\Delta B(2)$ is the linewidth at 2.14 MHz deduced from the expression

$$\Delta B(2) = \frac{2}{\gamma T_2^*}$$

where T_2^* is taken from the recorded free-induction decay

2) $\Delta B(7)$ in column 3 is similarly calculated

3) $\Delta B'(7)$ is the value measured from the Fourier Transform plots

4) The linewidths are not corrected for magnetic field inhomogeneities. These corrections are less than the error in ΔB which is of order $\pm$ 0.1 mT

1) $T_1(2)$ is closely proportional to $N_D^{-\frac{2}{3}}$ over more than two decades of impurity concentration

2) $T_1(2) \propto T^{-1}$ for $N_D > N_C$

   $T_1(2) \propto T^{-n}$ for $N_D < N_C$ with $n < 1$

3) $T_1(2)$ is continuous through the transition

4) $K \propto N_D^{\frac{1}{3}}$ for $N_D > N_C$

   $= 0$ otherwise

5) K shows a sharp change from zero to a finite value at N_C

6) $K^2T_1(2)T$ is close to the Korringa value at high doping density but falls below this value as N_C is approached from above

7) $K^2T_1(7)T$ is close to the Korringa value for $N_D > N_C$

8) $T_1(7) = T_1(2)$ for $N_D > 9.10^{17}\,cm^{-3}$

9) $T_1(7) \propto N_D^{-m}$ with $m \sim 1.25$ for $N_C < N_D < 9.10^{17}\,cm^{-3}$

10) ΔB increases with N_D from $\sim$ 0.2 - 0.6 mT at 2.14 MHz and $\sim$ 0.3 - 1.7 mT at 7.4 MHz over the range $7.10^{16} \rightarrow 1.7.10^{19}\,cm^{-3}$. $\Delta B(7) > \Delta B(2)$ by a factor of 1.5 - 2 over this range of doping density.

These features are numbered roughly in the chronological order in which the experiments were performed. In the ensuing discussion, it will be convenient to retain this order, at least in the first part of our analysis. Points (1) to (6) above (essentially the low field data) have been published as an interim report by us in the literature[158]. A fuller analysis is in preparation.

5.3 Discussion

Before examining our data we first list the properties of the Ge^{73} and Si^{29} nuclei which are important from a magnetic resonance viewpoint and then briefly describe an early NMR experiment in Ge.

TABLE 5.3

NMR Parameters of Ge and Si

Isotope	γ $(10^6 T^{-1}s^{-1})$	Natural Abundance (%)	Magnetic Moment (μ_n)	Spin I	Quadrupole Moment $(10^{-28}m^2)$
Ge^{73}	9.331	7.6	- 0.88	9/2	- 0.2
Si^{29}	53.16	4.7	- 0.55	1/2	0

An attempt by Jeffries [159] to observe the Ge^{73} resonance in the pure powdered element using continuous wave NMR was unsuccessful which, as Bloembergen[160] noted, was to be expected since his analysis indicated that the T_1 should be very long. The first reported NMR experiment in doped germanium was that of Wyluda[161] who measured T_1 from 20 to 300K for five samples of n-type Ge (dopant unspecified) with electron concentrations in the range 4.10^{14} cm^{-3} to 4.10^{17} cm^{-3} at a working frequency of 2 MHz. His main result is that relaxation in pure Ge is dominated by the interaction of the nuclear quadrupole moment with electric field gradients resulting from thermal vibrations of the lattice. Table (5.4) gives his results for the two most heavily doped specimens.

TABLE 5.4

T_1 Data of Wyluda[161] for Ge:As

Sample	N_D (cm^{-3})	T_1 (mins) at 77 K	T_1 (mins) at 20 K
GE ZL 1123 AR	$5 - 7 \times 10^{16}$	4	166
GE FP 164 M	$3.5 - 4.3 \times 10^{17}$	3	21

Although $N_D > N_C$ for the second sample in table (5.3), the constancy of the product T_1T, which is expected when nuclear relaxation is by means of a degenerate electron gas, cannot be tested since the T_1 measurements were taken at temperatures greater than the Fermi temperature appropriate to N_D. However these T_1 results were of importance to us in that we could obtain order of magnitude estimates for T_1 at our working temperature and concentration ranges. In particular, if we assume T_1T is constant from 20 to 4.2 K and further that $T_1 \propto N_D^{-\frac{2}{3}}$ for $N_D > N_C$, then using $T_1(4 - 17, 20\,K) = 21$ mins,

$$T_1(4 - 17, 4.2\,K) \sim 100 \text{ mins}$$

$$T_1(1 - 19, 4.2\,K) \sim 11 \text{ mins}$$

These estimates were of assistance in our initial search for the Ge^{73} resonance. By way of comparison we found

$$T_1(4.4 - 17, 4.2\,K) \sim 74 \text{ mins}$$

$$T_1(1.75 - 19, 4.2\,K) \sim 9.5 \text{ mins}$$

We have already alluded to possible relaxation mechanisms in our samples so it is useful to list the expected parametric dependences of T_1, K and S_K.

$T_1 \propto N_D^{\frac{2}{3}} T^{-1}$	Degenerate electron gas, $N_D > N_C$, $T < T_F$, field independent
$T_1 \propto N_D^{-1} T^{-\frac{1}{2}}$	Non degenerate electron gas, field independent
$K \propto N_D^{\frac{1}{3}}$	Free-electron behaviour
$S_K = 1$	Free-electron behaviour
$S_K > 1$	Electron-electron interaction enhancing K and T_1^{-1}
$S_K < 1$	Additional relaxation paths for nuclei or enhancement of single relaxation rate

5.3.1 T_1 and $K^2 T_1 T$ at Low Field

The data of figure (5.1) are clearly not inconsistent with the expected dependence of T_1 on N_D when the relaxation of the Ge^{73} nuclei is through the contact interaction between the nuclei and a degenerate electron gas. This behaviour is further borne out by the temperature dependence of T_1 shown in figures (5.2, a - j). The contrast between these results and those in the Si:P system which show a marked reduction in T_1 in the transition region is noteworthy. Our results show that electron correlation, which is cited to be of importance in enhancing T_1^{-1}, K and S_K in the Si:P system, seems not to play such an essential role in Ge. Indeed the values of $K^2 T_1 T$ computed using K evaluated at high field, fall

below the Korringa constant (figure (5.4)) as N_D approaches N_C which is at distinct variance with the results of Si:P where S_K rises above unity. We note that in the calculation of the Korringa product, the use of K and T_1 measured in different magnetic fields is acceptable providing that neither quantity is field dependent as we expect from the theory of relaxation and the Knight shift owing to the interaction of nuclei and free electrons. The plot of K^2T_1T in figure (5.4) is strongly suggestive of the presence of relaxation paths for the nuclei in addition to that due to Fermi contact. Our discourse in chapter 2 stated that electrons may interact with nuclei through not only a contact term but also a non-contact (dipolar and orbital) and, for $I > \frac{1}{2}$, a dynamic quadrupolar term. Moreover these additional contributions to the relaxation rate have a similar temperature dependence (T^{-1}) and the field independence displayed by the contact electron-nuclear interaction and would not thus be distinguishable in a $T_1 - T$ plot. Now Obata[19,23] has calculated the relaxation rates due to the non-contact and quadrupolar interactions for a tight-binding p-band as

$$\frac{1}{T_1}_{Dip+Orb} = \left(\frac{\mu_o}{4\pi}\right)^2 \frac{13\pi}{45}(\gamma_e\gamma_n)^2\hbar^3 kT N^2(E_F)\langle r^{-3}\rangle^2 \qquad (5.4)$$

$$\frac{1}{T_1}_{Q} = \frac{12\pi}{5\hbar}\left(\frac{e^2Q}{4\pi\varepsilon_o I}\right)^2 \frac{3(2I+3)}{10(2I-1)}\, kT N^2(E_F)\langle r^{-3}\rangle^2 \qquad (5.5)$$

Here $\langle r^{-3}\rangle^2$ is the square of the average value of the radial part of the p-wave function and we have written the density of states factor as $N^2(E_F)$ in place of the product of the densities of states

for up and down spins $N^{-}(E_F)$ $N^{+}(E_F)$. Values of $\langle r^{-3} \rangle$ may be computed using results of optical hyperfine splitting experiments and standard formulae quoted by Kopfermann[162]. The value of $\langle r^{-3} \rangle$ measured by Childs and Goodman[163] is $4.5.10^{31} m^{-3}$. The density of states may be calculated from the free electron expression for the specific heat and the appropriate measurements of Bryant and Keesom[95], viz.

$$\gamma = \tfrac{2}{3} \pi^2 k^2 N(E_F) \qquad (5.6)$$

and $\gamma = 0.0215$ mJ mole^{-1}deg^{-2} for Ge doped with $4.7.10^{18}$ As cm^{-3}. Thus we obtain $N(E_F) \sim (1 - 3).10^{16}$ J^{-1} atom^{-1} for Ge:As in the transition region of impurity concentration. If these values of $N(E_F)$ and $\langle r^{-3} \rangle$ are inserted in equations (5.4) and (5.5) the calculated values of $T_{1_{Dip+Orb}}$ and T_{1_Q} are much longer ($T_{1_{Dip+Orb}} \sim 200$ hrs, $T_{1_Q} \sim 400$ hrs) than our observed T_1's as too are the estimates of T_{1_Q} using the Mitchell and Kessel formulation. We have inevitably to conclude that such relaxation processes are negligible in our samples. However, other relaxation mechanisms may be present which are not describable by the theories we have given as being applicable to real metals. These additional paths of nuclear relaxation may be due to the dynamics of the electron system in a heavily doped semiconductor but we defer speculation on the nature of such electron dynamics until our description of the relaxation data at 5 T.

Referring again to figure (5.4) it is clear that for the most heavily doped Ge specimen, the Korringa relation holds well. Now

we have seen that in chapter 2 that, for relaxation by degenerate electrons,

$$T_1^{-1} \propto \langle |\psi(o)|^2 \rangle_{E_F}^2 = P_F^2 \qquad (5.7)$$

and thus our relaxation time measurement can give us a value of P_F which we may then compare to the electron probability density in a free Ge atom $|\psi(o)|_A^2 = P_A$. We estimated P_A in the following way. Kopferman[162] writes the hyperfine splitting factor for an s valency electron as a corrected form of Goudsmit's formula

$$a_s = \frac{8}{3} R_\infty \alpha^2 \frac{Z_i Z_a^2}{n_a^3} g_I' \left\{ \left(1 - \frac{d\sigma}{dn}\right) F_r(j, Z_i)(1-\delta)(1-\varepsilon) \right\} \qquad (5.8)$$

and

$$P_A = \frac{1}{\pi a_{HO}^3} \frac{Z_i Z_a^2}{n_a^3} \{ \ldots \} \qquad (5.9)$$

In these equations, R_∞ is the Rydberg constant, α the fine structure constant, a_{HO} the first Bohr radius and g_I' the effective g_I value defined as

$$g_I' = \frac{\mu_I}{\mu_B I} \qquad (5.10)$$

where μ_I is the nuclear moment in nuclear magnetons. The symbols Z_i, Z_a represent effective inner and outer atomic numbers respectively: i.e. allowance is made for the different forces experienced by an electron when inside the atomic core (eZ_i) and outside (eZ_a). Empirically, it is found that $Z_i = Z$ (the atomic number) for s electrons and $Z - 4$ for p electrons. These values

of Z_i are confirmed by a graphical method due to Barnes and Smith[164]. The effective outer atomic number Z_a is unity for singly-ionised atoms, two for doubly-ionised atoms, etc.. The effective quantum number n_a is given by

$$n_a = n - \sigma \tag{5.11}$$

where n is the true principal quantum number and σ the Rydberg correction (a function of n). $F_r(j, Z_i)$, where j is the total angular momentum quantum number, is a relativistic correction factor tabulated by Kopferman[162]. The terms $(1 - \delta)$, $(1 - \varepsilon)$ are, respectively, corrections to allow for the fact that the nuclear charge and nuclear moment are not point entities but distributed over a finite nuclear surface area and volume. All the terms in braces are of order unity and whilst we included them in our calculation they will not be discussed further here. To obtain n_a, we use the formula

$$n_a^2 = \frac{R_\infty Z_a^2}{T_v} \tag{5.12}$$

where T_v is the absolute term value for the state under consideration $(5s^2 S_{\frac{1}{2}})$. We follow Knight[13] and assume Ge atoms to be triply ionised in the solid state (hereafter designated GeIV) and then $Z_a = 3$. We can obtain T_v from the compilation of term values for GeIV of Bacher and Goudsmit[165]. Since the quoted values are not absolute we work back from the ionisation energy for GeIV of 45.5 eV to obtain an absolute value for $T_v(5s^2 S_{\frac{1}{2}})$.

Insertion of the appropriate numbers in equations (5.8) and (5.9) gives

$$P_A \sim 3.4.10^{31} m^{-3} \qquad a_s = 2.5\ m^{-1}$$

The value of a_s compares well to that quoted by Knight[13] of $2.6\ m^{-1}$. His calculation differs from ours in that he determines a_s for neutral germanium and then scales his results by an empirical factor to obtain a_s for GeIV. We may also, within the same approximation, determine the value of $\langle r^{-3} \rangle$ from the formula

$$\langle r^{-3} \rangle = \frac{4\pi}{\mu_o} \frac{h c}{2 \mu_B^2} \frac{(\delta\omega^o)}{(1 + \frac{1}{2})} Z_i H_r (1, Z_i) \qquad (5.13)$$

where $\delta\omega^o$ is the doublet splitting between the $5p^2P_{3/2}$ and $5p^2P_{1/2}$ levels and $H_r(1, Z_i)$ is another relativistic correction tabulated by Kopferman. We obtain

$$\langle r^{-3} \rangle = 2.5.10^{31} m^{-3} \qquad (5.14)$$

which is in agreement with the experimentally determined value of $4.5.10^{31}\ m^{-3}$ by Childs and Goodman and the calculations of Bessis et al.[166] of $3.2.10^{31}\ m^{-3}$ using Hartree-Fock wave functions.

The value of P_F obtained from T_1 for sample 1.75 - 19 is

$$P_F \sim 3.10^{31} m^{-3} \qquad (5.15)$$

and so

$$\xi = \frac{P_F}{P_A} = 0.9 \qquad (5.16)$$

which is in the range typical for many metals. That $\xi < 1$ indicates that the wave function in the solid is expanded in comparison to the

wave function in the free atom. This expansion is due to the closeness between the positive ions in a solid material. Our value of ξ compares with those determined for other heavily doped semiconductors, i.e.

ξ (Si:P) $\sim$ 0.8 ξ (CdO) $\sim$ 0.9

Benedict and Look[130] have argued that the closeness of ξ to unity implies that the electrons are not localised around impurity centres but extended so as they may interact with all the bulk nuclei. Thus, in the view of Benedict and Look the electrons are characteristic of the host conduction band and the Fermi level must be in the conduction band. It is not however obvious that ξ should fall well below unity for an impurity banded semiconductor so that, by itself, the value of ξ does not seem to us to show whether the electrons are in a separate impurity band or in the conduction band.

Alexander and Holcomb[44] have reviewed experimental evidence which suggests that the Fermi level enters the conduction band in Ge:As at a concentration of donors $N_{cb} \sim 10^{18} cm^{-3}$. For $N_D < 10^{18} cm^{-3}$ the low temperature bulk susceptibility data fall below a free-electron $N_D^{\frac{1}{3}}$ dependence and for $N_D \gtrsim 10^{18} cm^{-3}$, the Hall mobility shows the simple N_D^{-1} dependence expected of conduction band electrons. The calculation of Matsubara and Toyozawa[167] gives $N_{cb} \sim 2.10^{18} cm^{-3}$ using a Bohr radius of order 30.10^{-10}m. Thus sample 1.75 - 19 is well into the heavily metallic region and our value of ξ is at least consistent with this.

5.3.2 Knight Shift Measurements

Figure (5.3) shows the variation of K with N_D for our samples at 7.4 MHz and 4.2K. We recall that a free-electron picture gives $K \propto N_D^{\frac{1}{3}}$ and this dependence is shown as the dotted line in the diagram. The data show that K falls abruptly to zero at the metal-nonmetal transition (indicated by the solid block on the abscissa of figure (5.3)), and throughout the high density region is, within experimental error, well represented by a $N_D^{\frac{1}{3}}$ dependence. No dependence of K on crystal orientation with respect to the external field was observable within our experimental limits. These are important results in the context of comparison with the behaviour witnessed by other workers in alternative semiconductor systems. These may be listed as:

Si:P Gradual rise in $K(Si^{29})$ with N_D for $N_D > N_C$ until $N_D > 2.10^{19} cm^{-3}$ when $K \propto N_D^{\frac{1}{3}}$ (Sundfors and Holcomb[7], Alexander and Holcomb[44]).

Si:P Abrupt rise in $K(Si^{29})$ from zero to finite value at $N_D = N_C$. $K \propto N_D^{\frac{1}{3}}$ for $N_D > N_C$. Some enhancement of K for N_D just greater than N_C (Sasaki, Ikehata and Kobayashi[2]). Abrupt appearance of $K(P^{31})$ at $N_D = N_C$. $K \propto N_D^{-\frac{1}{3}}$ for $N_D > N_C$ (Ikehata, Sasaki and Kobayashi[3]). Similar behaviour for $K(P^{31})$ observed by Brown Holcomb[6].

SiC:N $K(C^{13}) \propto N_D^{\frac{1}{3}}$ in metallic region. No data available for $N_D \sim N_C$ (Alexander[129]).

n-CdO Gradual rise in $K(Cd^{113})$ with N_D for $N_D > N_C$ until $N_D > 2.10^{19} cm^{-3}$ when $K \propto N_D^{\frac{1}{3}}$ (Benedict and Look[130]).

CdS:Cl Gradual rise in $K(Cd^{113})$ with N_D for $N_D > N_C$ until $N_D > 2.10^{18} cm^{-3}$ when $K \propto N_D^{\frac{1}{3}}$ (Adams, Look, Brown and Locker[131]).

Our data, then, can be seen to be closest in type to the most recent work in Si:P and does provide support for the Sasaki et al.[2] results over the earlier investigation of Si:P performed by Sundfors and Holcomb[7]. However, it is noteworthy that the enhancement of K observed by Sasaki et al. in Si:P is absent in our material. This feature, combined with the lack of enhancement in $T_1(2)^{-1}$ to which we have referred above is strong evidence for the unimportance of electron-electron correlation in the doped germanium system.

The sudden appearance of the Knight shift at N_C is in accord with Mott's theoretical prediction concerning the behaviour of K when the metal-nonmetal transition is of Anderson type (cf. chapter 3). It is interesting to notice that the precipitous change in K at N_C is not mirrored in the $T_1(2)$ measurements which appear to be continuous through the transition.

We can attempt to obtain an approximate value for the spin susceptibility from our K and P_F data. We first write

$$K = \frac{\mu_o}{4\pi} \frac{8\pi}{3} \frac{\chi_S M}{\mu_o} P_F \Omega_o \qquad (5.17)$$

Here Ω_o is the atomic volume, M the atomic mass and χ_S is expressed in mks mass units. For sample 1.75 - 19, we obtain

$\chi_S \sim 2.7.10^{-11}$ mks kg^{-1}. Now Bowers has measured the static electron susceptibility which consists of an orbital and a spin component, χ_O and χ_S respectively and obtains $\chi \sim 10^{-9}$ mks kg^{-1}. Thus the ratio of spin to orbital contributions to the electron susceptibility is

$$\frac{\chi_S}{\chi_O} \sim 2.5\% \qquad (5.18)$$

Bowers quotes a value of 6% for this ratio so the agreement is passable considering the limits of accuracy of the data. The reason that the diamagnetic part of the susceptibility dominates can be deduced from inspection of the usual expressions for χ_O and χ_S

$$\chi_S \propto m^* \qquad \chi_O^{-1} \propto m^*$$

For a free-electron gas, $m^* \rightarrow m_o$ and $\chi_O = -\frac{1}{3}\ \chi_S$. However, the effective mass in Ge is small ($m_t^* \sim 0.08\ m_o$) so we can expect the orbital contribution to a static susceptibility measurement to predominate over the spin paramagnetic part.

5.3.3 T_1 and K^2T_1T at High Field

The measurements of $T_1(7)$ of 4.2 K for our Ge:As specimens are shown in figure (5.5). $T_1(2)$ results are also shown for comparison.

Our analysis so far has been consistent with the notion that relaxation in our samples is primarily that due to contact between the nuclei and a degenerate electron gas. Moreover the donor concentration dependences of $T_1(2)$ and K suggest that the electrons behave in a free-electron manner. It is, however, a feature of nuclear relaxation via Fermi contact that the measured relaxation

times are independent of the applied magnetic field. Whilst this fact holds for our two most heavily doped samples, there is a clear inconsistency between this assumption and our data for samples in the transition region where a remarkable field dependence of T_1 is apparent. Worthy of note also is the rather sudden increase in $T_1(7)$ for doping densities just below the transition: clearly the continuous nature of $T_1(2)$ through the transition is not preserved at high field.

The values of K^2T_1T obtained using $T_1(7)$ are shown in figure (5.6). They lie close to the value computed from the Korringa relation, which we recall as being applicable to an assembly of non-interacting electrons, throughout the impurity concentration range $N_D > N_C$. An equivalent statement is that the Korringa product at 5 T is unity for $N_D > N_C$ indicating that neither electron correlation nor an enhancement of the relaxation rate due to, for example, the Warren mechanism, are of significance for our samples. It must be stated, however, that any conclusions drawn thus far from our data must be viewed with a certain degree of caution. We have seen that <u>either</u> the low field T_1 data or the high field K and T_1 data are readily explainable by simple theory based on a non-interacting electron system which we have outlined in chapter 2. There is, though, a discrepancy between such a naive picture and our results when the latter are taken in toto. This is perhaps not surprising when it is remembered that the impurity band is essentially a poorly understood phenomenon as we have attempted to demonstrate in our review in chapter 4. We pointed out there

also that Si and Ge sometimes exhibit different behaviour when subjected to similar experimental probing. It is thus interesting to note that very recently published data for the Si:P system by Sasaki et al.[3] show that both $T_1(Si^{29})$ and $T_1(P^{31})$ are field dependent in the phosphorus doping range analogous to our arsenic impurity range. The percentage increase in the host T_1 with magnetic field for 'equivalent' doping densities in both systems is roughly the same and the field independent T_1 that we observed in highly doped Ge is also apparent in heavily phosphorus doped silicon. The Japanese workers have performed their experiments at much lower temperatures than ours (0.6K compared to 4.2K) and also at less intense applied fields (0 to 0.9 T compared to 1.44 T and 5 T).

The succeeding paragraphs of this chapter are devoted to attempts to explain our NMR measurements via various physical models. We are mindful that such models must be compatible with other experiments such as we have listed in chapter 4.

5.4 Spin Diffusion

We have recounted in chapter 2 the phenomenon of spin diffusion and stated that if nuclear relaxation is dominated by this mechanism of spin energy transport then theory shows that a field dependent T_1 may result. To determine whether spin diffusion is important we must consider the local magnetic fields experienced by the nuclei in our samples. The host nuclei in a lightly doped sample may be considered to be in two categories: those in the body of the

sample in which the local field is created by the nuclear dipole-dipole interaction and those that are nearer to an impurity site whose local fields are generated by the fluctuating electron moment on the foreign atom. In this case, nuclear relaxation is usually governed by the diffusion rate of spin energy through the nuclear spin assembly to the paramagnetic impurities which can rapidly give up energy to the lattice. The problem then is to calculate at what doping density there is a small fraction of the crystal volume in which the local magnetic fields due to an impurity are larger than the dipolar fields - this is the condition where spin diffusion may be expected to be important.

In our samples, the local field at the nucleus due to an impurity is a consequence of the Fermi contact interaction which is written

$$B_{con} = \frac{\mu_o}{4\pi} \frac{8\pi}{3} \gamma_e \hbar \langle S_z \rangle |\psi(o)|^2 \qquad (5.19)$$

We take B_{con} as representing the local field since our linewidth measurements indicate that the nuclei experience local fields that are greater than those expected for nuclear dipole interaction. Estimation of the magnitude of this field involves a knowledge of $|\psi(o)|^2$ which is available from the effective mass theory of Luttinger and Kohn[143].

In the simplest approximation, the wave function ψ is written as the product of a hydrogenic envelope function $F(\underline{r})$ and a Bloch function $\psi(\underline{k}, \underline{r})$

$$\psi = F(\underline{r})\, \psi(\underline{k}, \underline{r}) \qquad (5.20)$$

where the $F(\underline{r})$ satisfy the so-called effective mass equation.

Since there are N equivalent minima in the conduction bands of Ge and Si (N = 4 or 6 respectively), the normalised ground state wave function is

$$\psi = N^{-\frac{1}{2}} \sum_{i=1}^{N} F^{N}(\underline{r}) \; \psi \; (\underline{k}^{N}, r) \tag{5.21}$$

Thus

$$|\psi(o)|^2 = N |F'(o)|^2 \; |\psi(k', o)|^2 \tag{5.22}$$

In this first approximation, values of $|\psi(o)|^2$ computed from equation (5.22) are an order of magnitude smaller than those determined by, for example, the hyperfine splitting of donor electron spin resonance lines. Kohn and Luttinger[143] show how corrections to the effective mass formulation can bring good agreement with experiment but, for brevity, we ignore this discussion here and merely insert a factor 10 in our later expression for $|\psi(o)|^2$. Now the envelope function is anisotropic and written by Kohn and Luttinger as

$$F' = \left(\frac{a^2 b}{\pi}\right)^{\frac{1}{2}} \exp \left\{ - (a^2(y^2 + z^2) + b^2 x^2)^{\frac{1}{2}} \right\} \tag{5.23}$$

However, we neglect the anisotropy and write

$$F' = \left(\frac{1}{\pi a_H^3}\right)^{\frac{1}{2}} \exp \left\{ - \frac{r}{a_H} \right\} \tag{5.24}$$

where we have taken $a^{-1} = b^{-1} = a_H$. This should not be too bad an approximation since Kohn[39] has pointed out that the wave function is not far from spherical even with an effective mass anisotropy of 20 such as the case in Ge. Thus we obtain

$$|\psi(o)|^2 = \frac{10N}{\pi a_H^3} |\psi(k', o)|^2 \exp\left\{-\frac{2r}{a_H}\right\} \qquad (5.25)$$

To be specific, we take the case of Si:P first. Here $N = 6$, $a_H \sim 15.10^{-10}$ m and from the paper by Kohn and Luttinger, $\psi(k', o)^2 \sim 300 \pm 50\ m^{-3}$ (normalised in an atomic volume).

The remaining unknown quantity is our expression for the contact field in which is $\langle S_Z \rangle$ which we may write

$$\langle S_Z \rangle = \frac{\frac{1}{2}\left\{1 - \exp -\left[\frac{\mu_B B}{kT}\right]\right\}}{1 + \exp -\left[\frac{\mu_B B}{kT}\right]} \sim \frac{\mu_B B}{4kT} \qquad (5.26)$$

at a field B of 1 T, we calculate B_{con} as

$$B_{con} \sim 0.1 \exp\left\{-\frac{2r}{a_H}\right\} \qquad (5.27)$$

Now the nuclear dipole field is 20 μT and so, by equating this value with B_{con} we obtain a value for r and thus a critical doping density N_D from $\frac{4}{3}\pi (2r)^3 N_{D_{spin}} = 1$. For Si:P, we find $N_{D_{spin}} \sim 5.10^{17} cm^{-3}$. Thus for doping densities less than $N_{D_{spin}}$ we expect spin diffusion to play a significant role in nuclear relaxation. This value of $N_{D_{spin}}$ is identical to that quoted by Sundfors and Holcomb[7] though they supply no details whatever of their calculation of that quantity.

A similar computation for Ge at 5 T yields

$$N_{D_{spin}} \sim 10^{16} cm^{-3} \text{ for } a_H = 30.10^{-10} m$$
$$N_{D_{spin}} \sim 4.10^{16} cm^{-3} \text{ for } a_H = 20.10^{-10} m \qquad (5.28)$$

The quantity a_H is often taken in the literature to be $\sim 30.10^{-10}$m but we include the second estimate of $N_{D_{spin}}$ for an a_H of 20.10^{-10}m because the magnetic freeze-out experiments that we described in chapter 4 indicated that appreciable shrinkage of the wave function can occur in high external fields.

The overall conclusion from this simple calculation is that spin diffusion should not play a dominant part in the nuclear relaxation process in our samples since the doping density range of interest is greater than our estimates of $N_{D_{spin}}$. We must therefore seek alternative methods of explanation of the field dependence of our relaxation time measurements.

5.5 The Effects of a Narrow Impurity Band

We have stated in chapter 2 that the relaxation rate for nuclei in a metallic environment has the proportionality

$$T_1^{-1} \propto N^+(E_F)N^-(E_F)$$

where the right hand side is the product of the densities of states for up and down spins and is usually approximated $N^2(E_F)$. This approximation is valid for those materials with wide densities of states but may not be applicable in a narrow impurity band, where N^+ is not necessarily the same as N^-. Furthermore the application of a magnetic field will result in the product N^+N^- having a different value from that in zero field. In an attempt to quantify the situation, we imagine the density of states to have the parabolic form shown in figure (5.7a).

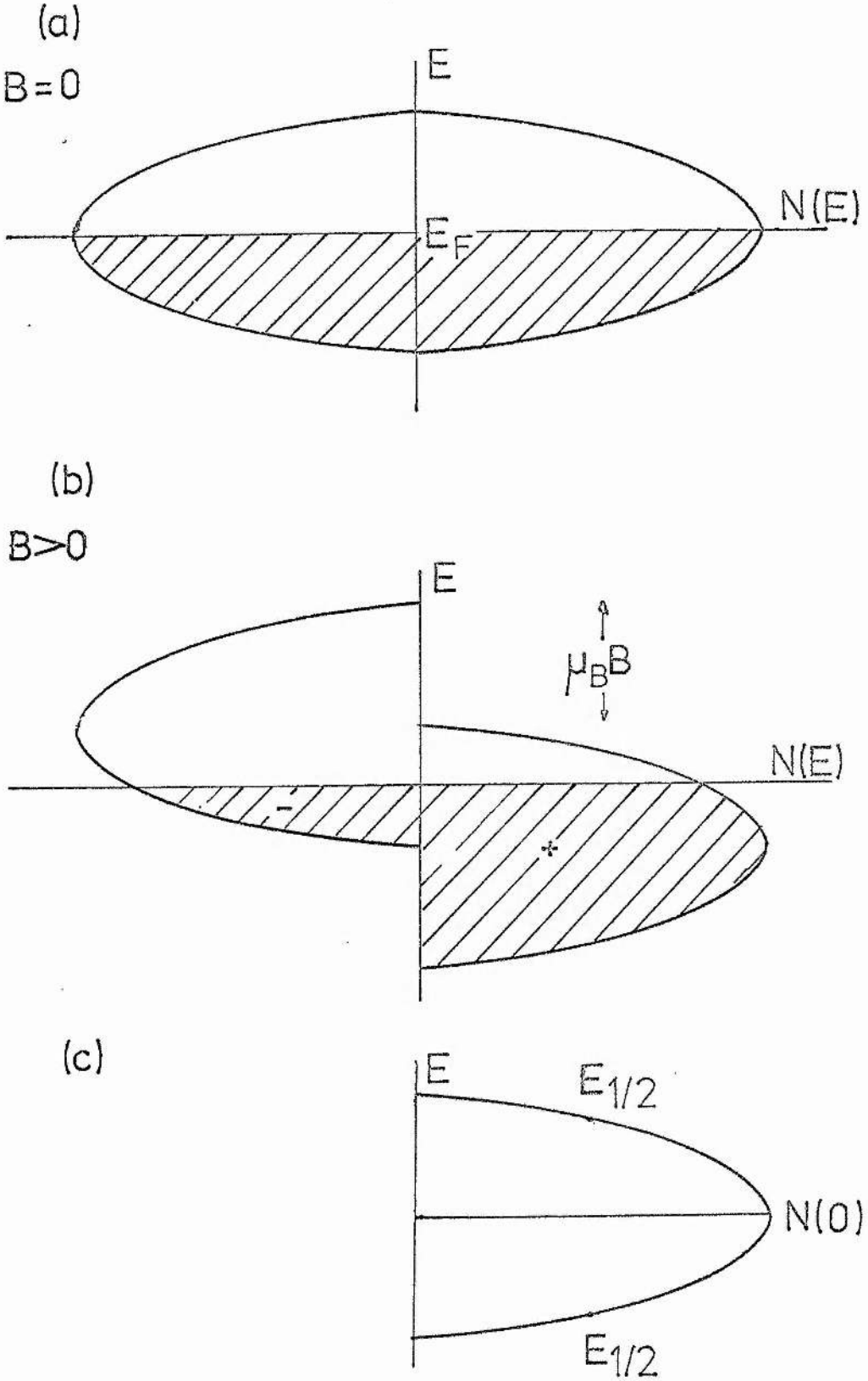

FIG. 5.7 Density of states for a narrow impurity band.

Application of a field will shift the densities of states for the up and down spins as depicted in figure (5.7b). From the diagram

$$N^+N^-\big|_{B>0} < N^+N^-\big|_{B=0} \tag{5.29}$$

and hence we may expect an increase in T_1 with the external magnetic field.

We write, with C as a constant

$$N(E_F) = N(E_F, B=0) - CE^2 \tag{5.30}$$

or $$N(E_F) = N(0) - C(\mu_B B)^2 \tag{5.31}$$

Now

$$N(E_{\frac{1}{2}}) = \frac{N(0)}{2} \tag{5.32}$$

where the energies $E_{\frac{1}{2}}$ are shown in figure (5.7c). Hence

$$C = \frac{N(0)}{2E_{\frac{1}{2}}^2} \tag{5.33}$$

We take the bandwidth $B_w = 2E_{\frac{1}{2}}$ and recalling that in the tight binding approximation

$$B_w = 2zI \tag{5.34}$$

where I is the overlap energy integral and z the coordination number which we assume is six, then the product N^+N^- may be written

$$N^+N^- = N(0)^2 - \frac{N(0)^2}{36}\left[\frac{\mu_B B}{I}\right]^2 + \ldots. \tag{5.35}$$

N(0) may be determined as before from specific heat data: we take

$$N(0) = 1.33.10^{16}\ J^{-1}atom^{-1} \tag{5.36}$$

This is, incidentally, identical to the value obtainable from the specific heat data of Marko, Harrison and Quirt[84] for the Si:P system for the sample of analogous phosphorus doping ($3.10^{18}cm^{-3}$) at 4.2 K.

The overlap energy I may be evaluated using, for example, the formula cited by Berggren[168]

$$I = \frac{e^2}{4\pi\epsilon_o \varkappa N^{\frac{1}{2}} a_H} \left\{ \left\{ -\frac{1}{2}\left(1 + \frac{R}{a_H} + \frac{1}{3}\left(\frac{R}{a_H}\right)^2\right)\right\} \exp\left(-\frac{R}{a_H}\right) - \left\{1 + \frac{R}{a_H}\right\} \exp\left(-\frac{R}{a_H}\right)\right\} \qquad (5.37)$$

Each impurity may be thought of as having a 'sphere of influence' of radius R. The impurities are at a distance R' apart where $\frac{4}{3}\pi R'^3 N_D = 1$ and then $R = 2R'$. Now, owing to the exponential term, the value of I is extremely sensitive to the quotient (R/a_H) and we must therefore choose a_H with care. It transpires that the choice of a_H is not a trivial problem. The simple hydrogenic expression

$$a_H = \frac{4\pi\epsilon_o \varkappa h^2}{m^* e^2} \sim 40.10^{-10} \text{ m} \quad \text{for Ge:As} \qquad (5.38)$$

is certainly an overestimate. We might expect that a value of a_H taken from a Mott-type expression for the metal-nonmetal transition

$$N_C^{\frac{1}{3}} \cdot a_H = \text{constant} \qquad (5.39)$$

would be the most appropriate but here the constant on the right hand side of the Mott formula turns out to be a sensitive function of the type of screening potential assumed in the derivation of the formula. An alternative procedure is to calculate a_H from the donor ionisation energies computed using the effective mass approximation or determined from optical experiments. The accompanying table (5.5) gives values for a_H for Ge:As and Si:P

TABLE 5.5

Bohr Radii for Ge:As and Si:P

				a_H (nm) Ge:As	a_H (nm) Si:P
1. Mott[1]	$N_C^{\frac{1}{3}} a_H$	0.2	(Thomas-Fermi)	2.96	1.4
		0.4	(Hulthen)	5.9	2.8
2. Berggren[46]	$N_C^{\frac{1}{3}} a_H$	0.2	(a_H defined in terms of the ionisation energy)	3.5	1.35
3. Kreiger and Nightingale[49]	$N_C^{\frac{1}{3}} a_H$	0.1	(4-valley, Thomas-Fermi)	1.5	-
		0.05	(6-valley, Thomas-Fermi)	-	5.5
		0.23	(Lindhard)	3.4	1.6
4. Martino et al.[45]	$N_C^{\frac{1}{3}} a_H$	0.305	(4-valley, Hubbard-Sham)	4.2	-
		0.295	(6-valley, Hubbard-Sham)	-	2.1
5. Sinha and Puri[48]	$N_C^{\frac{1}{3}} N^{\frac{2}{3}} a_H$	0.36	(screened Coulomb)	2.1	0.75
		0.422	(Hulthen)	2.5	0.9
		0.477	(experimental using a_H defined in (10))	2.7	1.0
6. Alexander and Holcomb[44]	$N_C^{\frac{1}{3}} a_H$	0.23	(experimental)	3.4	1.45
7. Uncorrected effective mass theory[39]	$a_{H_{ema}} = \frac{e^2}{2\kappa(4\pi\varepsilon_o)E_o}$			4.9	2.1
8. Uncorrected effective mass theory using E_o, expt.[39]				3.2	1.3
9. Corrected effective mass theory[39]	$a_{H_{corr}} = a_{H_{ema}} \left(\frac{E_o}{E_{o,\,expt}}\right)^{\frac{1}{2}}$			3.9	1.65
10. Sinha-Puri definition of a_H[48]	$a_H = \frac{E_c}{E_g^2} \frac{e^2}{2\kappa(4\pi\varepsilon_o)}$			2.2	0.96

Notes

1) The type of screening assumed is given in parentheses

2) The assumption is made that

N_C (Ge:As) $= 3.10^{17}\text{cm}^{-3}$ $\quad$ N_C (Si:P) $= 3.10^{18}\text{cm}^{-3}$

κ (Ge) $= 16$ $\quad$ κ (Si) $= 12$

3) N is the number of valleys

4) $E_{c,g}$ defined in figure (5.8)

obtained using the results of several workers; the wide variation in a_H is evident.

We feel that the most satisfactory method of calculating a_H is from the ionisation energy in keeping with the most recent derivation of the Mott formula by Sinha and Puri[48]. These workers have attempted to take into consideration the deviation between the effective mass theory and experiment in their definition of a_H. For instance, it is known that the impurity wave function has a pronounced bunching at the impurity site which leads to the inclusion of a so-called central-cell correction in the effective mass theory. This correction was briefly alluded to in the preceding section in our calculation of the wave function probability density. Kohn[39] has pointed out that the larger Bohr orbits present in doped germanium should lead to a less intrusive effect of the central cell than in doped silicon and, at the time of Kohn's review, better agreement between theory and experiment was obtained for Ge over Si. The ESR data of Wilson[112], however, showed that the wave function pile-up was an order of magnitude greater at impurities in Ge than in Si so that it would be expected that the central cell correction would be as important in Ge as in Si. Later optical determinations[169] of ground state energies have shown that the values by earlier experimenters and quoted by Kohn to be sufficiently in error that we must accept that the central cell correction is as important in Ge as for Si.

In the effective mass approximation an N-valley semiconductor has an N-fold degenerate ground state at $-E_o$ (figure 5.8)). The

(excited states)

effective mass theory correction to effective mass theory

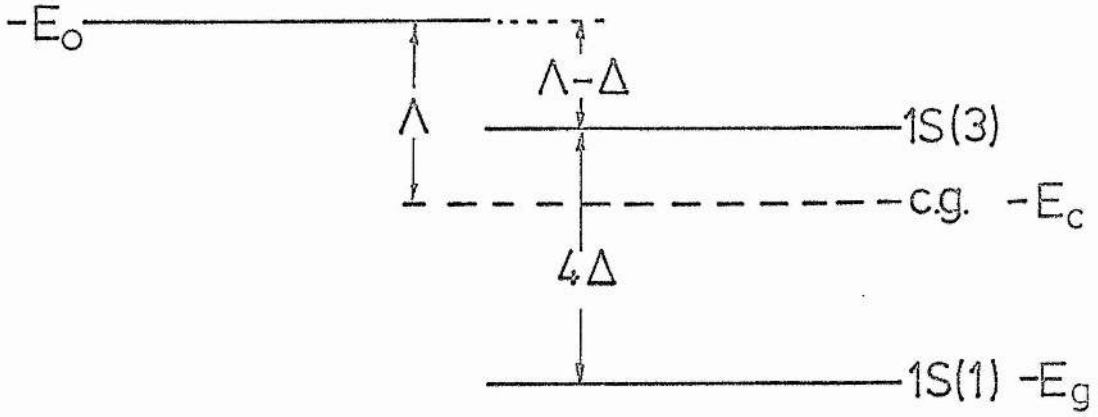

FIG.5.8 Energy level scheme for a group V impurity in germanium.

For arsenic,

$-E_o$= 9.2 meV. (Kohn[39])

$-E_g$=14.2 meV. (Reuszer and Fisher[169]

$-E_c$=10 meV. and Faulkener.[170])

crystal field splits the ground state into a singlet 1s level and a triply degenerate 1s level and also shifts the centre of gravity (c. g.) of the original level. The corrections, labelled in the accepted notation, are shown in figure (5.8) which also defines the energies E_c and E_g appearing in the Sinha-Puri definition of the hydrogen radius. In practice, the depression of the ground state energy in the corrected, as opposed to the uncorrected, effective mass approximation is greatest in germanium when doped with arsenic.

We now wish to consider the effect of a magnetic field. Our description of magnetic freeze-out in chapter 4 leads immediately to the idea of wave function shrinkage in a magnetic field. Czavinsky[170] and Miller and Abrahams[68] considered the effect of a magnetic field on a lightly doped semiconductor and found that the decrease in a_H was only a few per cent. Sadasiv[155], in his magnetoresistance measurements in Ge:As found that the Miller expression seriously underestimated the effect of the field on a_H. This is perhaps not surprising since the Miller formula applies in the dilute donor case whilst Sadasiv's samples had reasonably high doping levels.

Accepting that wave function shrinkage occurs in a magnetic field it might be imagined that the central cell correction will thereby necessarily increase. However the binding energy calculated in the effective mass approximation also increases with field so that it is not obvious how the central cell correction varies with field, if at all. Experimentally, it appears that the central cell correction increases as a function of field: Larsen[171] finds the functional dependence as $B^{3/2}$. The quantities Δ and Λ are also likely

to be field dependent. The effect of an increase of Λ with field is to lower all the ground state energies and an increase in Δ increases the separation of the 1s states[172]. These effects are likely to be of importance in high fields for As donors in Ge where the Δ , Λ corrections are large. A comprehensive review of electronic impurity levels in semiconductors containing discussion of some of these effects is that of Bassani, Iadonisi and Preziosi[173].

The overall conclusion is that the impurity wave function varying as $\exp(-r/a_H)$ has a greater decay constant (a_H^{-1}) in a large magnetic field than in the field-free case. The overlap energy is, in consequence, reduced which implies that the impurity band may be quite narrow. We have calculated I, B_w and the ratio of the relaxation times in a field of 5 T to that in low field, $T_1(B)/T_1(0)_{th}$ taking the value of a_H to be 20.10^{-10}m. The experimental values of T_1 enhancement in high field, $T_1(B)/T_1(0)_{ex}$ are taken from smooth curves through the data points rather than using individual data values. The results are shown in table (5.6). It is clear that experiment shows $T_1(B)/T_1(0)$ to be greater than unity in the transition region whilst our simple calculation gives $T_1(B) \sim T_1(0)$ in this region of impurity concentration. However, the generation of relaxation time enhancements of the right order of magnitude for samples close to N_C is encouraging given the simplicity of the model and our ignorance of the true shape of the impurity band. Our approach also implies that at a particular field, one spin sub-band would be completely full and the other totally empty. At this stage, the susceptibility would saturate and show

TABLE 5.6

Bandwidths and Field-Dependent Relaxation Times for Ge:As

Sample	3.1-17	3.5-17	4.4-17	5-17	5.3-17	5.9-17	9-17	1.75-19
$I(\overset{m}{M}eV)$	0.061	0.094	0.15	0.22	0.23	0.3	0.8	12.4
I(K)	0.7	1.1	1.8	2.5	2.7	3.5	9	144
$B_w(K)$	8.4	13.2	21.5	30	32.5	42	108	1728
$T_1(B)/T_1(o)_{th}$	2.6	1.4	1.1	1.1	1.1	1.0	1.0	1.0
$T_1(B)/T_1(o)_{ex}$	2	1.8	1.7	1.5	1.4	1.3	1.0	1.0

no further increase with field but even for our narrowest band the field required for such behaviour is rather larger than normally attainable laboratory fields ($\sim 14\,T$). We note also that an exchange mechanism existing between up and down spins would augment the band shifting in a magnetic field and possibly produce better agreement with experiment but our model is too crude to warrant consideration of this in any quantitative form.

The concept of a narrow impurity band has been advocated by Jerome et al.[36] for the case of Si:P. From the elementary properties of Fermi integrals they write the temperature dependence of the electron spin susceptibility as

$$\chi_S(T) = \chi_S(o) \left(1 + \frac{\pi^2}{6} (kT)^2 \frac{N''(E_F)}{N(E_F)} \right) \qquad (5.40$$

From their low temperature susceptibility measurements they obtain a bandwidth for a Si:P sample doped with $2.5.10^{18}$ carriers cm^{-3} of $\sim 19\,K$, which is comparable to our bandwidth for sample 3.1-17 of $\sim 9\,K$.

Allen and Adkins[73], in their study of hopping conduction in compensated Ge:Sb, quote an estimate of the bandwidth at $4.7.10^{17}$ carriers cm^{-3} of 60 K. Since the metal-nonmetal transition occurs at a lower impurity density in Ge:Sb than Ge:As, it is reasonable that the bandwidth for As donors is less than that for Sb donors in germanium at the same doping levels. These numerical comparisons are important since values of B_w and I greater than we give in table (5.5) lead to the fact that the field will have a negligible effect on T_1 and our proposed model would fall to the ground.

Interestingly, equation (5.40) implies that the susceptibility can be reduced in a narrow band situation or, more precisely, if there is strong negative curvature at the Fermi level such that the second term in equation (5.40) takes a large negative value. It follows that the Knight shift will be correspondingly reduced and also that a hybrid Korringa product K^2T_1T, where K is taken at high field and T_1 at low field, will fall below the normal Korringa value with the discrepancy increasing as N_D approaches N_C from the metallic side. This is precisely the behaviour represented by the plot of $K^2T_1(2)T$ against N_D in figure (5.4) although within our rather wide experimental limits, there does not appear to be any deviation of K from $N^{\frac{1}{3}}$ behaviour shown in figure (5.3).

Theoretical calculations of the density of states in Si:P have recently been made by Aoki and Kamimura[174], using the Hubbard model, without and with[175] the added complication of disorder. In their first paper, they show that for unequal numbers of up and down spins, corresponding to the application of a magnetic field to a semiconductor, there is an exchange splitting of the spin-up and spin-down bands. In the Hartree-Fock approximation, the sub-bands are rigid and undergo a rigid splitting in the magnetic field, but in the Hubbard model the bands split and also distort under the action of the field. The inclusion of disorder shows that the densities of states for up and down spins are unlike and very different from their form in the field-free case. The bands are then not necessarily narrow: the application of a field deforms the bands

such that the peaks of the density of states are shifted away from the zero field position at E_F. The product $N^+N^-\big|_{B>0}$ can then be much less than $N^+N^-\big|_{B=0}$ indicating that T_1 may be expected to increase with field.

By utilising the Hubbard model, Aoki and Kamimura are assuming that the Hubbard U, i.e. correlation, is playing a prominent part in the dynamics of the electrons. This is in accord with the conclusions reached by for example, Sasaki et al.[2], from the NMR data which shows correlation to be the prepotent effect in Si:P. As we have stated earlier in this chapter, the same electron-electron interaction is not registered in our data for Ge:As. We must therefore take our impurity band to be not of the upper Hubbard type. Alexander and Holcomb[44] list a variety of experimental results which support the idea that the impurity band is separate from the conduction band in our concentration region. A very clear indicator of this is provided by a plot of the Hall coefficient versus inverse temperature. At a certain temperature, conduction is both by high mobility electrons thermally excited into the conduction band and by lower mobility electrons moving within the impurity band. The critical temperature is evidenced by a hump in the Hall coefficient and has been widely seen. The Hall effect data of Le Hir[43] in Ge:As samples which we believe are closely akin to our specimens (cf. Appendix 2) show no characteristic maxima in the Hall coefficient. Since Le Hir's and our samples were uncompensated, the shape of the Hall curve is taken to be composed of ε_1 conduction at high temperature with a gradual change to ε_2 conduction as the temperature

decreases. The metal-nonmetal transition still, of course, occurs wholly in an impurity band separate from the conduction band.

The calculation of U in the same approximation as we have used for the determination of I and B_w provides an interesting result.

$$U = \frac{5}{8} \frac{e^2}{4\pi\varepsilon_o \varkappa a_H} \sim 10 B_w \quad \text{for } a_H = 20.10^{-10} \text{m} \qquad (5.41)$$

Such a large value of U is untenable and indicates that some screening must be taking place so that $U_{scr} \ll U$. Mott[1] has pointed out that an electron in a narrow band can lower its energy by distorting its surroundings and other workers[176] have developed the concept of an electronic polaron. We may then imagine it to be reduced to a value $U_{scr} \sim B_w$.

A final piece of experimental evidence that we wish to view is the ESR measurements of the electron spin susceptibility in Si:P undertaken by Quirt and Marko[82]. A narrow band approach predicts the slope of the χ_S^{-1} versus T curve to be an increasing function of temperature at low temperatures. This is opposite to the observed dependence which shows the slope of χ_S^{-1} versus T to be a decreasing function of temperature.

To summarise this section we may say that our simplistic model of a narrow impurity band can yield increase of T_1 with magnetic field. On the debit side, rough agreement of the T_1 data is only achieved by assuming rather smaller bandwidths than we would normally envisage. It is however true that assuming the band is situated ~ 14 meV below the conduction band edge, which corresponds

to the ground state energy of an As donor at infinite dilution, then our band will overlap the conduction band for N_D just greater than $\sim 10^{18} cm^{-3}$. This is in agreement with the value deduced by Alexander and Holcomb[44] of $\sim 2.10^{18}$ As cm^{-3}. The work of Aoki and Kamimura[174,175] shows that the distortion of the bands in a magnetic field may be more important than the rigid band shifting that we have assumed. Finally, we have noted that there is some experimental data which argues against the existence of a narrow impurity band in Si:P. This may or may not be of import to the case of germanium since we have seen that the two semiconductors can behave differently under the same experimental conditions.

In the following sections we attempt to describe our data in terms of some of the modern ideas on the metal-nonmetal transition that have been advanced, notably in the book by Mott[1]. Detailed theories are at present unavailable as are experiments to confirm such thinking. Our descriptions then are necessarily qualitative and also tentative.

5.6 Kondo Centres, Local Moments and Antiferromagnetic Metals

Our synopsis of the phenomenon of negative magnetoresistance in extrinsic semiconductors (chapter 4) introduced the Toyazawa theory of the existence of localised moments in such materials. The spatial randomness of the dopant was assumed to be a sufficient condition for such isolated moments to be extant. Mott has argued that free moments cannot exist in a metal but that Toyazawa's ideas are tenable if the free moments are replaced by nearly-free moments,

i.e. those with a low Kondo temperature T_K. The Kondo effect is well known to be manifested as a minimum in the resistivity-temperature plots of dilute alloys when the solute is magnetic[177,178]. The extrapolation of Kondo behaviour to doped semiconductors is qualitatively feasible but difficult to quantify.

The work of Friedel showed that transition metal atoms embedded in a metallic host can lead to the formation of a virtual bound state or resonance of width Δ. Two electrons may occupy this state so that it follows that the criterion for the occurrence of singly occupied centres or moments is just

$$\frac{U}{\Delta} > 1 \qquad (5.42)$$

The moments may interact with each other via an exchange or RKKY mechanism where the latter may be damped if non-magnetic as well as magnetic impurities are present. If the moment-moment interaction is negligible this does not mean that the moments are free: the moments interact with conduction electrons and can then spin flip at the Kondo frequency ω_K. We may compute T_K and ω_K from the formula[1]

$$T_K = \frac{\hbar\omega_K}{k} = \frac{\Delta}{K} \exp\left\{-\frac{\Delta}{J}\right\} \qquad (5.43)$$

where J is the conduction electron-moment exchange energy. The value of Δ is estimated for the Ge:As system by scaling the value appropriate to dilute metal alloys (~ 0.5 eV) with respect to the electron bandwidths for the doped semiconductor and metal systems: we take $\Delta \sim 0.5$ meV. The exchange constant, available from

magnetoresistance data[179] is $\sim 1 \rightarrow 2$ meV. Thus $T_K \sim 4K$ and $\omega_K \sim 5.10^{11} sec^{-1}$.

In view of the approximations involved this value of T_K should be taken only as indicative of its probable order of magnitude. At low temperatures we expect a large negative magnetoresistance to be observed and this is borne out by Sasaki's experiments[179]. The negative magnetoresistance saturates at absolute zero at a field B_{sat} given by

$$\mu_B B_{sat} = kT_K \qquad (5.44)$$

At finite temperatures, B_{sat} is reduced, being roughly proportional to T^{-1}. Thus, at helium temperature we expect the negative component of the resistivity to saturate at 1.5 T. This is in surprisingly good agreement with experiment (1.7 T) and must be in part fortuitous. We have tacitly assumed that a single value of T_K exists for our system but, in reality, a range of values must exist due to the randomness of a doped semiconductor. For example, the work of Saint-Paul et al.[180] shows that T_K is reduced if impurity atoms are clustered rather than isolated. Evidence for impurity clustering in doped Ge is obtainable from the ESR lineshapes reported by Gershenzon et al.[181, 182]. Mott[1] assumes that a uniform distribution of T_K values exists to explain the negative magnetoresistance linear in field.

As regards nuclear relaxation, we may expect that the spin fluctuations of the Kondo centres provide a relaxation mechanism in addition to that due to conduction electrons. Evidence for this may

be seen in, for example, the work of Alloul and Bernier[183, 184]. They show that the addition of as little as 100 ppm of Mn to Cu gives an alloy whose relaxation time is roughly half that of the pure noble metal host. The relaxation of the dilute alloy at $T > T_K$ is proportional to B/T and the concentration of impurities and is shown to be the result of the coupling of the nuclei with the transverse fluctuations of the impurity moments through the RKKY interaction. Other relaxation processes due to the presence of moments are possible but the mechanism cited predominates in Cu:Mn when account is taken of the mechanics of diffusion of the nuclear spin energy. Good agreement of the observed field and temperature dependences of T_1 are obtained by applying the spin diffusion theory that is normally used for diamagnetic materials doped with paramagnetic centres to which we briefly referred in chapter 2. Moreover, the nuclear magnetisation recoveries show short-time non-exponentialities which become more pronounced as the Mn concentration increases. At $\sim$ 1500 ppm Mn, the nuclear recovery is not exponential even at long times following the saturating pulse. These characteristics of the nuclear magnetisation are hallmarks of various spin diffusion regimes. We do not believe spin diffusion to be of importance in Ge:As so that the other relaxation mechanisms due to moments which are described in detail in the publications by Alloul and Bernier may be prominent. These relaxation rates are proportional to temperature and to a function of the impurity fluctuation time and can thus be expected to decrease with increasing magnetic field.

Thus our high field results are explicable on the basis that spin flip of Kondo moments is almost totally inhibited ($\mu_B B \sim kT_K$) and nuclear relaxation and the Knight shift are a consequence of the contact interaction between the nuclei and conduction electrons and are describable by expressions of the free-electron type The N_D dependence of T_1 ($T_1 \propto N_D^{-1.25}$ for $3.1.10^{17} < N_D < 5.9.10^{17} cm^{-3}$) is not that of a degencrate free electron gas, but as we have seen, the magnetic field may have important effects on the dynamics of the electron system. At low field values the total relaxation rate is the sum of conduction electron and Kondo moment contributions. The free-electron-like dependence of T_1 on N_D must then be taken as fortuitous. (In fact $T_1 \propto N_D^{-n}$ with n closer to 0.6 than the free-electron value of 2/3 but the error bars do not allow us to determine n to better than $\pm$ 0.1.)

If relaxation by moments is of substantial importance at low field, then, the T_1 data would not be expected to exhibit any sharp changes at the metal-nonmetal transition. At high field, where relaxation by the conduction electron system is dominant, a sudden change in relaxation at N_C is forecast since we know from the Knight shift data that there is an unequivocal alteration in the behaviour of the electron system at N_C. These predictions are in agreement with the observed data. The existence of moments should also lead to broadening of the NMR lines at the lower doping densities where the linewidth should be dipolar in origin. At higher densities, the distribution of Knight shifts is an alternative contributor to the resonance linewidth. Our measured linewidths are broader than

the dipolar linewidth and increase with field. This is in contrast to Si:P where the Si^{29} linewidths are clearly of nuclear dipolar type at the lower impurity concentrations. We may briefly digress here to consider the linewidth data in more detail.

Since Ge has a spin $> \frac{1}{2}$, the possibility exists for a possible contribution of ΔB of quadrupolar origin. This would not be operative in the case of Si:P where both nuclei are of spin $\frac{1}{2}$. Now we have noted in chapter 2 that the quadrupole interaction vanishes if an atom is situated in a site of cubic symmetry. In a doped, perfect crystal semiconductor the only nuclei that will experience non vanishing field gradients are those in the immediate vicinity of a particular atom. Since the field gradient at a distance r from a foreign atom falls off as r^{-3} (and the second order frequency shift will then vary as r^{-6}) then we may imagine that the quadrupole effect may be rather ineffective in broadening the resonance lines if the concentration of impurities is small. Now we have worked with single crystal samples of Ge:As so that, providing the specimens do not contain a high concentration of crystalline imperfections such as dislocations, etc., and the samples are not subject to a permanent strain due to the fabrication process, then we would believe the quadrupolar contribution to ΔB to be small. We are without experimental information on the degree of crystalline perfection in our samples though we see no reason why our samples should be severly strained or containing a multiplicity of crystalline imperfections. Moreover if quadrupole effects are present then we should be able to use the spin-echo technique to view such effects as Solomon[37] first did for KI.

The method involves a pulse sequence $\frac{\pi}{2} - \tau - \phi$ where τ is the time between the $\frac{\pi}{2}$ and ϕ pulses and ϕ is optimised. The echoes generated are of two types: 'allowed echoes', bell-shaped curves obtained because the magnitude of the rotating component of the radiofrequency field is much greater than the quadrupole interaction and 'forbidden echoes', derivatives of bell-shaped echoes obtained because the inequality just mentioned is not strictly kept. The details of the echo formation are given in Solomon's paper but we merely mention that the number of echoes is large in Ge since the spin is so great and thus the intensities of the signals would be small. We searched for such echoes in our samples without success though the diligence with which this was done was not as great as we should have liked. Our lack of sedulity was the result of the excessive nuclear relaxation times in Ge:As. Now, clearly the quadrupole broadening in our specimens cannot be zero so that we conclude that the quadrupole broadening present is evidently not large. Additional support for this inference is gained when it is recalled that a first order quadrupole broadening is independent of the applied magnetic field and a second order broadening inversely dependent on field. Our linewidths have a positive field dependence which signifies that the main contributor to ΔB is of magnetic origin. The fact that for $N_D < N_C$, the measured linewidths $\sim$ 0.2 - 0.4 mT or roughly ten times the nuclear dipolar width and our conclusions above lead us to tentatively ascribe some of the linewidth to the interaction between Ge^{73} nuclei and local moments or Kondo centres.

For $N_D > N_C$, the linewidths increase and scale approximately linearly with the Knight shift. Such behaviour was also observed by Brown and Holcomb in Si:P and the implication is that their model of the existence of a Knight shift distribution in these heavily doped semiconductors (cf. chapters 2, 3, 4) seems appropriate.

Regarding lineshapes, asymmetry is apparent in the computer plots of the lines obtained from the Fourier transform computer program. The low-field tailing is present in all specimens as shown in figure (5.9) for three specimens. It should be noted that the traces in figure (5.9) are examples of the better data obtained from the computer program. Often, noise masked any low field tailing of the resonance lines, especially in the low doping density samples. The peak of the line, of course, remained as well defined as the program and/or the resonance linewidth allowed which was our only interest as far as the determination of the Knight shifts was concerned. Time did not permit a more thorough investigation of the lineshapes and widths of the resonance lines.

The lineshape asymmetry observed is similar to that seen in the Si:P system and is explicable in terms of the models described in chapter 4. If we take an impurity wave function falling off exponentially with distance, then the low field tailing that we observed is consistent with the idea that the Ge^{73} nuclei are in contact with the impurity electrons via the Fermi interaction, i.e. the number of Ge^{73} nuclei with a given contact field will be smaller than that number of nuclei with a smaller given contact field.

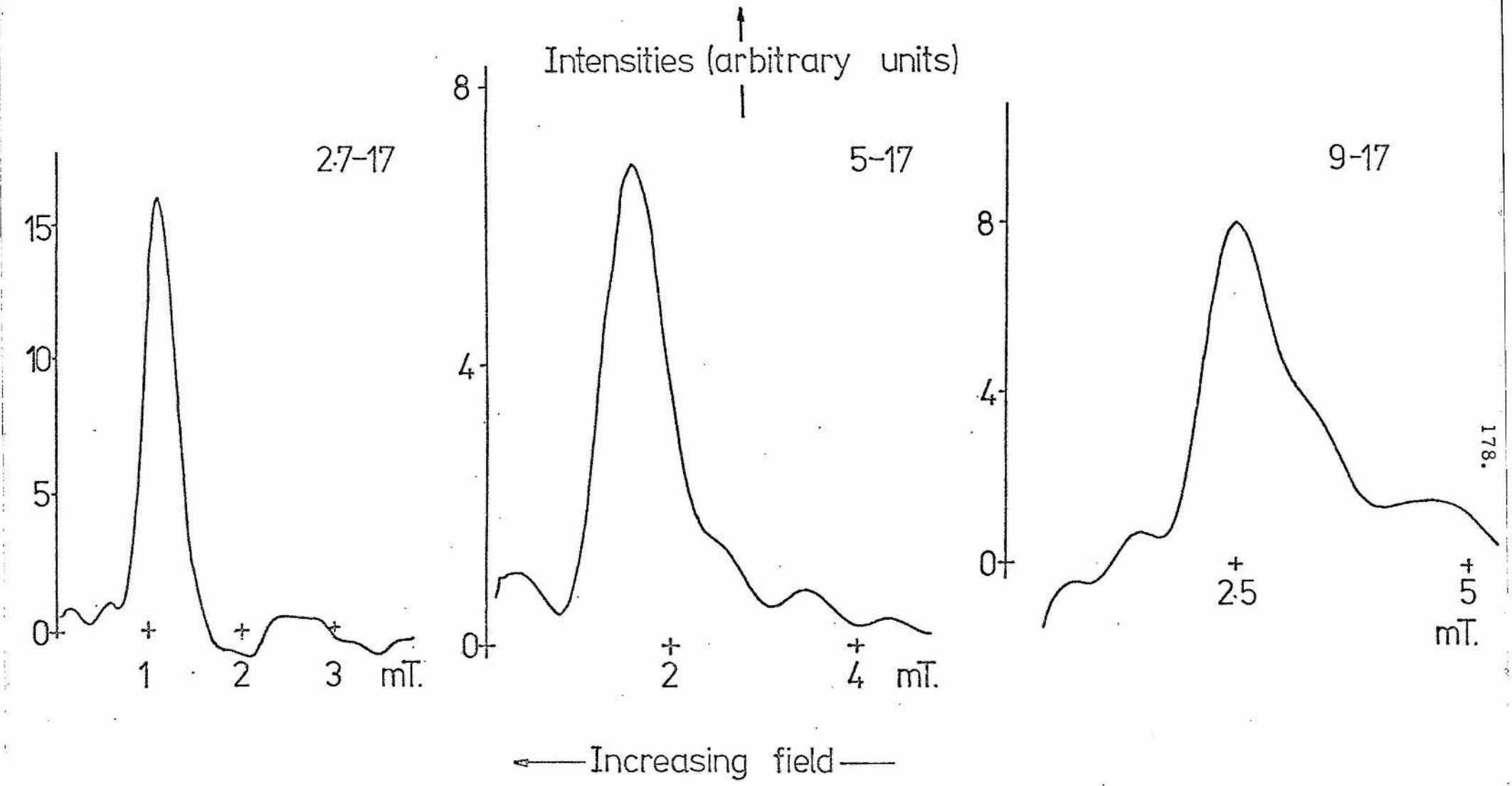

FIG. 5. 9 Resonance lineshapes obtained by computer.

Finally, no special measurement was taken of the line intensities save to note that the intensity for sample 1.75 - 19 was roughly a factor of two less than that of sample 2.7 - 17. This might be construed as evidence for the presence of quadrupole effects since, with a spin $\frac{9}{2}$ nucleus, it is possible to lose as much as 85% of the available resonance intensity in satellite lines. However an alternative or complementary explanation is that appropriate numbers of nuclei are Knight-shifted so far from resonance as to be unobservable and thus the line intensity will fall as the doping density increases.

In conclusion, whilst we do not have detailed information on the linewidths and shapes for our samples, the data which has been obtained is in accord with the assumptions of local moments/Kondo centres being present in our samples.

The ideas that we have advanced in this section are open to some criticism and, in order to present a balanced argument, we must consider such difficulties as may be present. Firstly, Kondo systems are at present poorly understood in spite of the vast experimental and theoretical effort that has been devoted to their comprehension. Results of NMR studies of classic Kondo alloys such as Cu:Mn are not readily extrapolated to doped semiconductors when consideration is taken of, for example, the number of impurity spins, the radius of the electron orbit and the impurity-conduction electron interaction. Our explanation of the lack of a discontinuity in our low field data was based on the assumption that, if Kondo states are present, then their character is unchanged in traversing the metal-nonmetal transition. While this may be plausible we have

no method of justifying such a claim physically. Mott[144] has stated that if Kondo centres exist in the metallic concentration regime then they must necessarily exist in the region where $N(E_F)$ is finite but the states at E_F are Anderson localised. It is also interesting to recall that the Alloul-Bernier experiments in Cu:Mn showed that spin diffusion theory which is more familiarly applied to paramagnetically doped insulating materials can also be successfully used for metal systems. In this sense, the moments would appear to behave in a similar fashion whether embedded in insulating or metallic matrix though the respective fluctuation frequencies must be quite different. It is worth repeating though that a number of experiments (cf. chapter 4) have been understood as evincing the presence of local moments on both sides of the transition. However, as we have stated in chapter 4, most of the experiments are also interpretable in other ways.

The idea of the suppression of spin fluctuations in a magnetic field as an explanation of a field dependent T_1 has also been advocated by Ikehata et al.[3,4] for the Si:P system. They find that the relaxation rates for both the host and impurity nuclei increase at low temperatures (0.6K) and are describable by the equation

$$(T_1T)^{-1} = C_1 + C_2(T - T_a)^{-\frac{1}{2}} \qquad (5.45)$$

where T_a is a constant and the coefficients C_1, C_2 are only adjusted with respect to the differences in Knight shift and magnetogyric ratio for the Si^{29} and P^{31} nuclei. At the same low temperatures, $T_1(P^{31})$ and $T_1(Si^{29})$ show an increase with magnetic field. Now the treatment of Moriya and Ueda[145,146] of relaxation in weakly

antiferromagnetic metals gives

$$(T_1T)^{-1} \propto (T - T_N)^{-\frac{1}{2}} \qquad (5.46)$$

so Ikehata et al.[3] have propounded that Si:P is an example of like kind. The value of T_a is then to be identified with a Neel temperature T_N and is, as determined experimentally, of order 0.1K.

Equation (5.46) is derived in a so-called renormalised spin-fluctuation theory (RSF) which is claimed to be slightly more sophisticated than the random phase approximation (RPA). In the latter case, Moriya-Ueda give

$$(T_1T)^{-1} \propto (T^2 - T_N^2)^{\frac{1}{2}} \qquad (5.47)$$

Recently, Borza and Lecander[185] have examined the B^{11} relaxation time in CrB_2. This material is metallic and undergoes an antiferromagnetic ordering at $\sim$ 85K. The B^{11} relaxation rate increases and the signal intensity reduces at a temperature of this order (see figure (5.10)). The data can only be fitted to equation (5.47) over the whole temperature range with T_N = 76K. Close to T_N, the measurements may also be fitted to equation (5.46) with T_N = 78K but the implied dependence of T_1^{-1} on $T^{\frac{1}{2}}$ at $T \gg T_N$ from equation (5.46) is not observed experimentally. A further marked difference between CrB_2 and Si:P is the lack of field dependence of $T_1(B^{11})$ in contrast with the strong enhancement of $T_1(Si^{29})$ and $T_1(P^{31})$ in the latter materials. Such a comparison of materials may not be meaningful if CrB_2 is essentially individualistic; e.g. VB_2 shows a simple Korringa behaviour of the B^{11} relaxation rate (figure (5.10)).

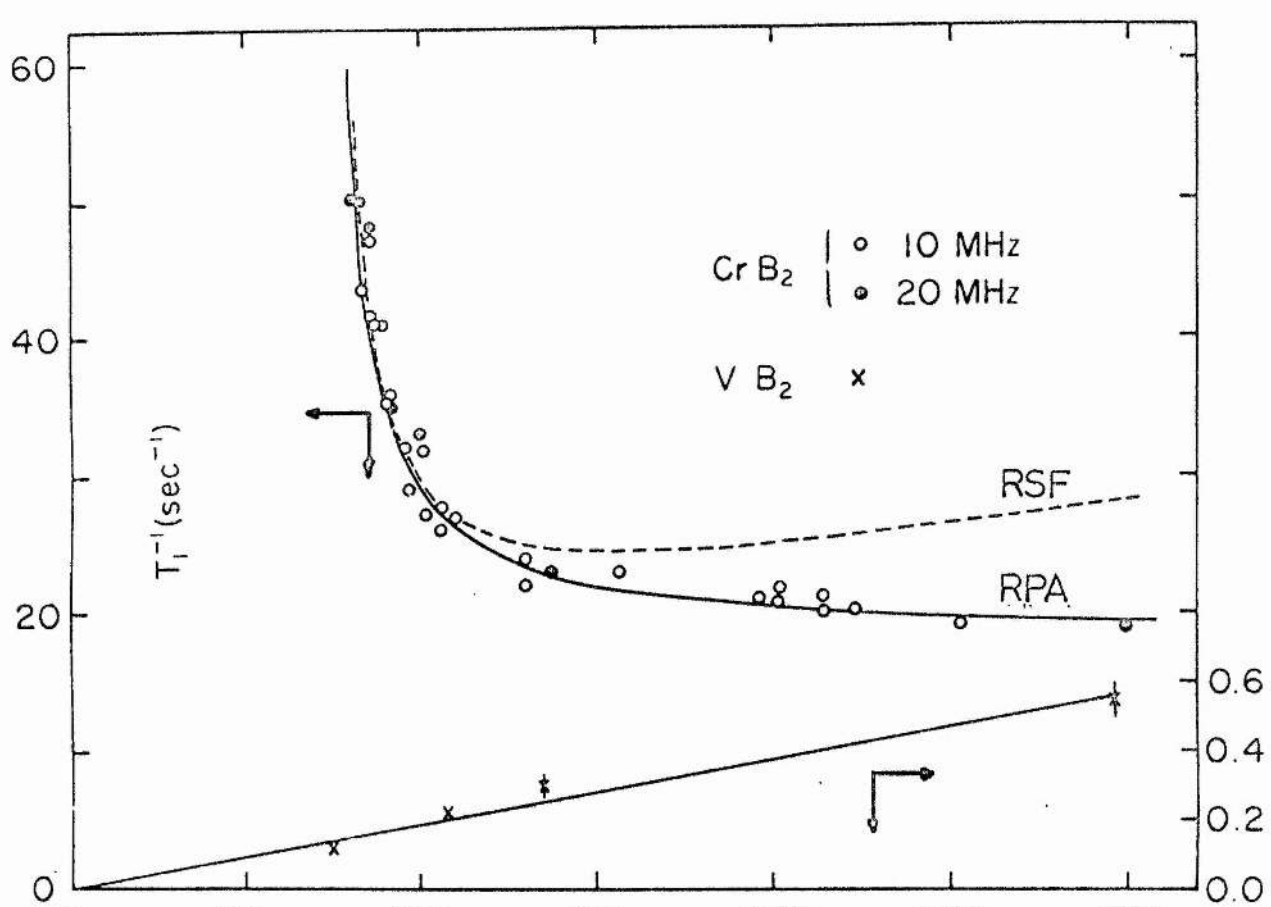

FIG. 5.10 B^{11} relaxation rates in CrB_2 and VB_2. After Borsa and Lecander.[185]

Mott[59] has shown that in a crystalline antiferromagnet that the impurity moment is reduced from the free ion value by the amount

$$1 - \frac{z I^2}{U^2} \qquad (5.48)$$

For a random antiferromagnet this reduction factor is increased by virtue of the fact that neighbouring moments will tend to couple to form an analogue of a hydrogen molecule having no resultant moment. Thus the random antiferromagnet should consist of smaller, strongly coupled moments than in the crystal with a small number of free moments. Mott argues that when the Hubbard bands overlap, moments may persist into the metallic region though of reduced magnitude in comparison to the crystalline case. The moments' size should also lead to enhancement of the Pauli paramagnetism expected for a highly correlated gas not being fully realised. The existence of moments in metallic Si:P should, as we have noted above, be manifested as a broadening of NMR linewidth unless the moments are very small. Neither Sundfors and Holcomb nor Sasaki et al. find evidence for such broadening. Mott has commented on the absence of line broadening in semiconducting Si:P at 1.3K since a calculated value of the Neel temperature (Berggren; quoted by Mott[59] as a private communication) is $T_N \sim 5K$. A much lower value of T_N, as Ikehata et al.[3] quote, would remove this discrepancy.

The reduction of the Pauli paramagnetism due to the spatial randomness of the donors has to be taken as less of an effect than the Brinkman-Rice enhancement expected of the highly correlated gas.

We should mention that Benedict and Look[130] have argued that their NMR work on CdO:Cl shows that moments are present in the metallic region. This deduction is based on the fact that the recovery of the nuclear magnetisation following saturation of the Cd^{113} resonance may be fitted to two exponential functions of time. This implied the existence of two relaxation times characteristic of their samples which they take to be due to those nuclei close to an impurity which relax quickly through the strong moment-nucleus interaction and those nuclei in the bulk which have a slower approach to thermal equilibrium. No such behaviour of the nuclear magnetisation was observed in Si:P or in our samples.

Compensation may play a role in determining the behaviour of an amorphous antiferromagnet. The time rate of change of the spin of the moment will change in the presence of hopping so that such a rate increase will be greatest in those materials which are compensated.

In conclusion, we may say that the existence of local moments/ Kondo centres or the electron dynamics in an amorphous antiferromagnet may be used in an attempt to explain the NMR data. Our lack of low temperature measurements (which would be extremely difficult to perform) precludes us from judging the applicability of the Moriya-Ueda theory of relaxation in weakly antiferromagnetic metals but, to explain the linewidths, we would clearly require a higher T_N than has been found experimentally by Ikehata et al.. The latter workers have not given a quantitative explanation of the field dependence of the relaxation times at low temperatures. As we have pointed out above, the ideas expressed in this section

do not as yet have a sound theoretical basis and it is apparent that existing theories often contain parameters which are unavailable from experiment.

In the following section, we describe the magnetic behaviour expected of a material undergoing an Anderson form of the metal-nonmetal transition and compare this with our data. Again, the difficulty of quantitative comparison is evident and we are thus restricted to general remarks.

5.7 Magnetic Properties at an Anderson Transition

Our first consideration is of the properties of a material on the nonmetallic side but close to an Anderson transition. If moments are to exist then we must have some singly occupied sites at the Fermi level and so our first question is to determine the type of occupancy of the Anderson localised states. This problem was first discussed by Ball[186] and later refinements added by Mott[1]. Ball has argued that every localised state may contain two electrons of opposite spin. If localisation is strong, then the intraatomic correlation may be large enough for a second electron to prefer to occupy a different localised state from that of the first electron even though the energy of the second state may be slightly higher (ΔE) than the first occupied state. Since the density of states at the Fermi level is continuous, ΔE can be infinitesimal and the implication is that all states at the Fermi level will be singly occupied. The range of energy below E_F where states contain a single carrier is dependent on the degree of localisation.

Mott's[1] conclusions are similar and he draws the density of states as shown in figure (5.11): the barrier between singly and doubly occupied sites at energy E_M is not sharply defined. Close to the transition, Mott gives the fraction of singly occupied to the total number of sites as

$$\frac{n_1}{N_D} \sim (a\alpha)^3 \qquad (5.49)$$

where α^{-1} is approximately the radius of the localised state and a the interatomic distance. The distance between the n_1 sites is of order α^{-1} so that the states overlap strongly leading to the moments being strongly antiferromagnetically coupled. The presence of moments should lead to a broadening of the nuclear resonance line. The effect of a large magnetic field on the nuclear relaxation time is difficult to ascertain. The application of a large field to an Anderson-localised system clearly leads to an increase in the number of singly-occupied sites since α^{-1} decreases with field and $n_1 \sim \alpha^3$. If the nuclear relaxation is dominated by fluctuation of moments, then the increased number of moments generated by the applied field might be thought to lead to an increase in the nuclear relaxation rate. However, even with an increase of the number of singly-occupied states, the nuclear relaxation time will increase if the frequency component of the moment fluctuation at the Larmor frequency is decreased. Such an effect can readily be envisaged to occur if a large external field is applied to our system thereby suppressing the spin flip rate of the moments. Our results for Ge:As show T_1 to increase strongly for $N_D < N_C$ suggesting that the latter

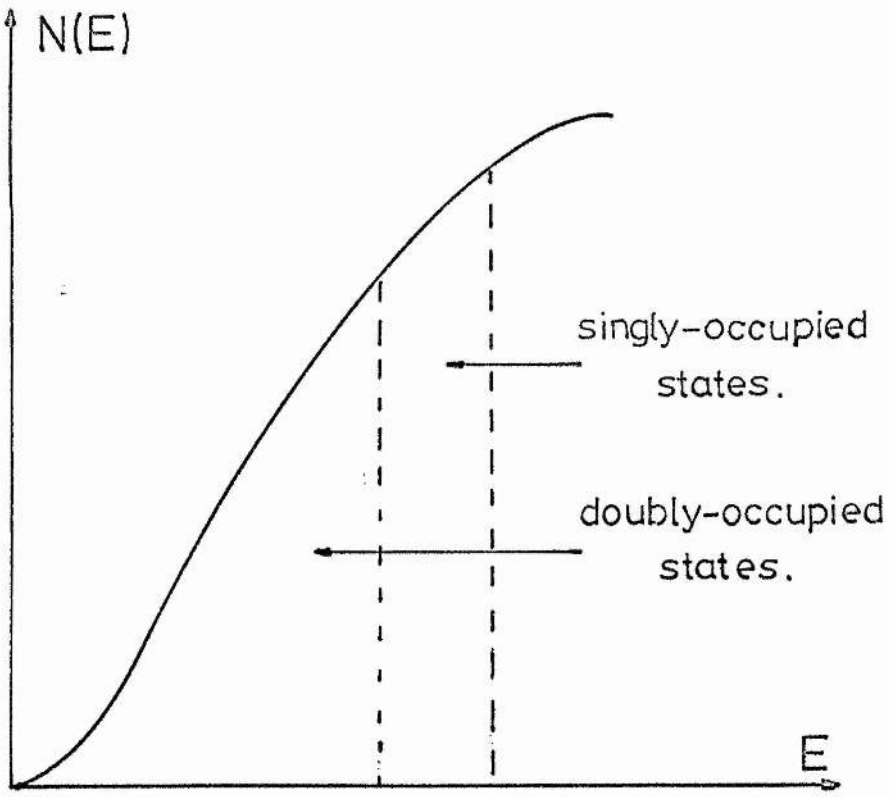

FIG. 5.11 Density of states for a Fermi glass.

mechanism predominates. Indeed the number of singly occupied states may be rather small in our samples since their number is a function of the size of the intraatomic correlation U which we have given reason to believe is not of major importance in determining the characteristics of our samples.

The region of concentration where there is overlap but states are localised is quite narrow: the measurements of conductivity of Ge:As in the presence of microwave radiation indicates the range to be 10^{17} - $3.10^{17} cm^{-3}$. Above $3.10^{17} cm^{-3}$, the electrons become extended which is in agreement with our observation of a non-zero Knight shift at and above an impurity concentration of $3.1.10^{17} cm^{-3}$. Other pertinent experimental evidence for the existence of the amorphous antiferromagnetic region is that of the spin susceptibility measurements by Ue and Maekawa[83] on Si:P and the ESR spectrum observed by Morigaki and Maekawa[108] on Si:P that we have described in chapter 2. The results of χ_S show a rapid decrease with increasing temperature above 1.5K indicating that the Neel temperature is probably of this order. Lower temperature measurements would be valuable here since χ_S should decrease with decreasing temperature below T_N.

5.8 Correlation and Exchange in an Electron Gas

Our discussion of electron interaction is divided into two parts: firstly with respect to the corrections to the Hartree-Fock approximation and secondly in consideration of the features of the Brinkman-Rice highly correlated gas.

The early work of Hartree was the first to include the Coulomb force between electrons but only in the sense that an electron was taken to experience an interaction with an average field of the other electrons assumed to be a uniform smeared-out charge distribution. The total wave function of the system was taken to be a product of one-electron functions. A refinement by Fock (the Hartree-Fock theory) was to write the total wave function as a determinant of one-electron functions - the wave function then being antisymmetric as stipulated by the Pauli exclusion principle. Thus whilst the Hartree-Fock theory included the correlation between electrons of parallel spin, via the Pauli principle, Coulomb repulsion was not explicitly included and the correlated motion of electrons of antiparallel spin completely ignored. The Hartree-Fock theory overemphasises the effect of exchange between electrons and it was the later work of Bohm and Pines, summarised by Pines[25] and by Raimes[187] that treated electron exchange and correlation in a more realistic fashion. Our main interest is in the spin susceptibility χ_S^{int} which Pines shows to be enhanced over the non-interacting Pauli value χ_S such that

$$\chi_S^{int} = \frac{4}{3} \frac{\chi_S}{\alpha} E_F \qquad (5.50)$$

with

$$\alpha = \frac{20}{9} E_F + \frac{8}{9} E_X + \alpha_{lr} + \alpha_{sr} \qquad (5.51)$$

where the exchange term is written

$$E_X = - \frac{12.5}{r_s} \text{ eV} \qquad (5.52)$$

and the long and short range Coulomb correlation corrections between electrons of parallel spin are represented by $\propto_{lr}$ and $\propto_{sr}$ respectively. The symbol r_s is the radius of a sphere representing the mean volume per atom and is related to the electron density n_e by the expression

$$\frac{4}{3}\pi r_s^3 a_{HO}^3 = n_e^{-1} \tag{5.53}$$

in which a_{HO} is the Bohr radius $(0.53.10^{-11}\text{m})$ and thus r_s is expressed in atomic units. For metals, r_s lies between 3 and 6 atomic units and the susceptibility enhancements are of the order of several tens of per cent.

An alternative theoretical approach based on the Hubbard approximation and applied to narrow band materials leads to an expression for the susceptibility enhancement

$$\chi_S^{int} = \frac{\chi_S}{1 - N(E_F)\,U} \tag{5.54}$$

where U is the Hubbard intraatomic interaction term

$$U = \frac{1}{4\pi\epsilon_o}\iint \frac{e^2}{r_{12}} |\psi(r_1)|^2 \cdot |\psi(r_2)|^2 d^3x_1 d^3x_2 \tag{5.55}$$

and the denominator of (5.54) is called the Stoner factor. Strictly speaking we should replace U in equation (5.54) by U_{eff} where U_{eff} is an exchange term which Herring[188] writes as

$$U_{eff} \propto \langle f(\underline{k}+, \underline{k}'-)\rangle - \langle f(\underline{k}+, \underline{k}'+)\rangle \tag{5.56}$$

The right hand side is the difference between averaged interaction terms which are defined for quasiparticle states $\underline{k}$, $\underline{k}'$ spins +, - at the Fermi surface. Similarly

$$U \propto f(\underline{k} + \underline{k}') \tag{5.57}$$

In the Hartree-Fock scheme

$$f(\underline{k}+, \underline{k}'+) = 0 \tag{5.58}$$

so that

$$U_{eff} = U \tag{5.59}$$

Whilst recognising that this equality does not hold in a precise theoretical treatment, we assume equation (5.54) to be true to simplify the ensuing discussion on the relative values of χ_S^{int}(Ge) and χ_S^{int}(Si).

Since the Knight shift is directly proportional to the spin susceptibility, we may expect an enhancement in K if electron-electron effects are present in the electron system. Such effects may also lead to an augmented relaxation rate as discussed by Narath[27] and Moriya[26], though experiment shows T_1^{-1} enhancements in simple metals to be smaller than given by theory. If we now consider doped semiconductors, then to compute r_s we make the substitutions $n_e \rightarrow N_D$, $a_{HO} \rightarrow a_H$ and if, in particular we assume $N_D = N_C$ then

$$\begin{aligned} r_s(\text{Si},\ N_C &= 3.10^{18}\text{cm}^{-3},\ a_H = 1.5\text{ nm}) = 2.8 \\ r_s(\text{Ge},\ N_C &= 3.10^{17}\text{cm}^{-3},\ a_H = 3\text{ nm}) = 3.1 \\ r_s(\text{Ge},\ N_C &= 3.10^{17}\text{cm}^{-3},\ a_H = 2\text{ nm}) = 4.6 \end{aligned} \tag{5.60}$$

Inspection of the results for the alkali metals tabulated by Pines shows that although $\propto$ decreases as r_s increases, the percentage difference of χ_S^{int} and χ_S is smaller at the higher r_s values. Thus enhancements of χ_S and K could be less in Ge:As than in Si:P.

If we consider the alternative approach involving, finally, the Stoner factor, then recalling that in doped semiconductors, we substitute

$$\frac{e^2}{r_{12}} \rightarrow \frac{e^2}{\varkappa\, r_{12}} \tag{5.61}$$

in the formula for U then it follows that

$$U(\text{Ge}) < U(\text{Si}) \tag{5.62}$$

since

$$(a_H, \varkappa)(\text{Ge}) > (a_H, \varkappa)(\text{Si}) \tag{5.63}$$

In particular, we expect

$$U(\text{Ge}) \sim 0.1\, U(\text{Si}) \tag{5.64}$$

Now Kamimura and Kanehisa[141] have determined $U(\text{Si}) = 12.5$ meV for Si:P at the metallic transition. The implied value for $U(\text{Ge}) \sim 1$ meV may be compared to the previously calculated bandwidth $B_w \sim 10\text{K} \sim 1$ meV for Ge:As at the critical concentration N_C, where we expect B_w/U to be of order unity. Since specific heat measurements in Ge:As and Si:P give

$$N(E_F)_{\text{Ge:As at } N_C} \simeq N(E_F)_{\text{Si:P at } N_C} \tag{5.65}$$

then it follows that the susceptibility enhancement in Ge:As is less than that in Si:P.

We refer now to the work of Brinkman and Rice[56]. They used a variational method for the Hubbard model and found a metal-nonmetal transition to occur when the intraatomic Coulomb term reached a critical value U_{crit}. Brinkman and Rice give an expression for the spin susceptibility as

$$\chi_S^{-1} = \frac{1 - \left(\frac{U}{U_{crit}}\right)^2}{N(E_F)} \left[1 - N(E_F)U \left\{ \frac{1 + \frac{U}{2U_{crit}}}{\left(1 + \frac{U}{U_{crit}}\right)^2} \right\} \right] \qquad (5.66)$$

The term in square brackets is a Stoner-type factor but the important term with respect to an enhancement in χ_S is the pre-parenthetical interaction term. Brinkman and Rice show that

$$1 - \left(\frac{U}{U_{crit}}\right)^2 = \frac{m_{enh}}{m} \qquad (5.67)$$

where m_{enh} is the enhanced mass due to correlation. Enhancements in χ_S, $d\chi_S/dT$ and the specific heat γ are predicted to arise from the enhanced effective mass. The Brinkman-Rice treatment, applicable to a nearly-antiferromagnetic electron gas is quite different from the Stoner enhancement in nearly-ferromagnetic metals where χ_S but not $d\chi_S/dT$ nor γ are enhanced. We can now only avoid an increase of χ_S at N_C by assuming that U is small and also that U never reaches its critical value: i.e. the metal-nonmetal transition occurs due to some mechanism other than correlation. The prime candidate for this alternative mechanism is Anderson localisation. We are then led to make the bold suggestion that the metal-nonmetal transition in n-Ge occurs because of electron localisation in the Anderson sense and that electron-electron effects play no essential role. This statement is in agreement with our experimental results which we have stated as showing itinerant electron interaction to be absent in our system. The origin of the Anderson potential is considered in chapter 6.

5.9 Summary

We have seen that our data does not lend itself to easy interpretation but does show characteristics predicted by modern ideas on the metal-nonmetal transition. The increase of T_1 with magnetic field is a startling result which we have seen may be explained on the assumption of a narrow impurity band. On the other hand such a model cannot be extended to explain, for example, the linewidth measurement. The more sophisticated approaches in terms of the suppression with field of spin fluctuations of, perhaps, Kondo centres or local moments or the relaxation expected in an antiferromagnetic metal have been described though a quantitative treatment has not proved possible. The fact that, as we have pointed out, these theories are found to be sometimes at variance with experimental observations in other materials apart from Ge is some measure of the gap extant between theory and experiment. A more formal appraisal of our results and their implication as well as a comparison of the behaviour of Si and Ge is given in the following chapter.

Chapter 6

CONCLUSION

6.1 Comparison of Ge:As and Si:P and General Conclusions

We stated in chapter 1 that the purpose of this investigation was threefold. Firstly we wished to determine whether the electron gas in a metallic semiconductor is describable as a single-phase system or if the gas contains coexisting electrons of localised and mobile type. A second aim was to ascertain whether the electrons in an impurity-banded semiconductor were of the non-interacting or interacting kind. Finally we wished to compare our NMR data with that taken in Si:P and specifically to resolve the discrepancy existing in the literature on the sharpness of the appearance of the Knight shift in Si:P at the metal-nonmetal transition.

With regard to the Knight shift, we have found that K(Ge) appears abruptly at the critical concentration N_c in agreement with the recent studies of Si:P made by Sasaki et al.[2] and in conflict with the earlier measurements of Sundfors and Holcomb[7]. Prior to our work, there was no obvious way of selecting which set of data in Si:P was correct though the fact that

$$T_1 (Si^{29}, \text{Sasaki}) > T_1 (Si^{29}, \text{Sundfors-Holcomb}) \qquad (6.1)$$

implied that the Si:P samples used by Sasaki et al. were purer than those of the earlier workers. Whilst we again caution that Ge:As and Si:P may behave differently under the same experimental conditions, our findings are in good agreement with the Japanese data in Si:P both in terms of the magnitude and appearance of the Knight shift. With regard to the gentle increase in $K(Cd^{113})$ observed[130, 131] in n-CdO and CdS:Cl our argument here is that these Cd compounds

are of somewhat unknown purity and character. For example, the donors[130] in n-CdO are thought to be either Cd interstitials or oxygen vacancies and compensation is a completely unknown quantity. Samples are clearly difficult to fabricate and the minimum doping density that can be achieved is 3.10^{18} donors cm^{-3}. Again, in CdS:Cl, it is admitted[131] that the purity is rather difficult to control. We feel that detailed comparison between materials exhibiting a metal-nonmetal transition is only meaningful if the characters of such materials are well known. Here, workers in Si and Ge have a clear advantage stemming from the large amount of experience that has been gained in the growth of high purity group IV semiconductors.

Despite the extensive studies that have been made in doped Ge and Si, there exists the surprising anomaly that the determination of the number of carriers in a doped semiconductor from transport property measurements is not straightforward. We discuss the matter in some detail in Appendix 2 but it is worth emphasising here that we are confident in our N_D assignments, the concentration gradient in every sample and the background impurity content of the specimens.

We consider now the second aim of our work, namely the investigation of electron-electron interaction in heavily-doped Ge:As. Studies of Si:P have revealed enhancements of the host Knight shift and nuclear relaxation rate close to the metallic side of the transition and a concomitant increase of the Korringa product above unity. We have not witnessed any enhancements of T_1^{-1}

and K in the Ge:As system and have noted that $T_1(2)$ and K show concentration dependences of free-electron type. The hybrid Korringa product $K^2T_1(2)T$ falls below the Korringa value for $N_D \lesssim 10^{18}cm^{-3}$ with the discrepancy being largest at N_C. This effect has been shown not to be due to additional relaxation paths for the nuclei due to dipolar, orbital and dynamic quadrupolar electron-nuclear interactions. The Warren[29] dwell-time hypothesis is also untenable since we have observed higher T_1 values at higher magnetic field which is in opposition to our expectation if the Warren mechanism were operating in our system. The lack of exchange enhancements in T_1^{-1} and K have been conjectured to be the result of smaller intraatomic Coulomb forces being present in n-Ge than in n-Si. A further inference from our data is that the electron gas in Ge:As close to the metal-nonmetal transition is not highly correlated in the Brinkman-Rice[56] sense. (We did not consider the added complication of finite temperatures in our description of the highly correlated gas. Chao and Berggren[86] have calculated the spin susceptibility of Si:P under these conditions but since no direct experimental data exists for χ_S(Ge), further speculation on the effect of temperature seems unwarranted.) If the Brinkman-Rice theory did apply then the electronic specific heat and spin susceptibility would be enhanced close to the transition and also the thermopower would change sign at N_C. The specific heat measurements in Ge:Sb of Bryant and Keeson[95] showed no enhancement and Allen's results for the thermopower in compensated Ge:As (quoted by Mott[70]) did not show a change in sign at the

critical concentration. Clearly our NMR data is consistent with these other experiments and we therefore conclude that the metal-nonmetal transition in n-Ge is not driven by correlation. The transition must then be due to disorder and thus of Anderson type. It is worth noting that for Si:P, both NMR and ESR experiments show the spin susceptibility to be enhanced and the electronic specific heat is also enhanced, though less than theory predicts, as shown by Marko et al.[84].

If the metal-nonmetal transition in doped Ge is an Anderson transition then we should enquire as to the origin of the Anderson potential. In compensated material, it is evident that vertical disorder will obtain due to the random potential fluctuations created by the majority and minority centres and crystal imperfections. Lateral disorder will also be present owing to the random spatial siting of the dopant atoms. Our experiments were conducted with uncompensated, single crystal specimens so that we must take the lateral disorder in our samples to be sufficient to provide a localising Anderson potential. It follows that, for ~~an~~ this Anderson transition, vertical disorder is less important than lateral disorder and hence the effect of compensation on the critical dopant concentration should be small. This is in accord with the experimental observations of Davis and Compton[210] on single crystal Ge:Sb specimens. Mott and Davis[72] have replotted the Davis-Compton data and show that N_C is little changed by compensation ratios as high as 80%.

In chapter 3, it was stated that the Knight shift should appear abruptly at an Anderson transition, in agreement with our data in

Ge:As and with results in Si:P of Sasaki et al. We conclude that the metallic transitions in both materials may be taken to be of Anderson type but with the Hubbard U playing a more prominent role in the behaviour of the electron gas in Si:P close to the transition than in Ge:As. This idea is in accord with Hall measurements in both materials as we describe in Appendix 2.

In consideration of our high field relaxation data, we showed firstly that the assumption of a narrow impurity band could lead to a positive field dependence of T_1. A rough calculation gave order of magnitude agreement with experimental $T_1(7)$ to $T_1(2)$ ratios and it was shown that $K^2T_1(2)T$ could fall below the Korringa value as we have observed.

A second model to account for the inequality of $T_1(7)$ and $T_1(2)$ was based on the assumption of Kondo centres being present in a doped semiconductor. The origin of the local moments is taken to be the result of statistical fluctuation in the donor density leading to some sites being relatively isolated rather than a large U favouring singly-occupied sites. Mott has shown that a spread of Kondo frequencies can lead to a negative magnetoresistance linear in field in agreement with experiment. If Kondo moments exist then they should furnish a nuclear relaxation mechanism in addition to that due to nuclear contact with the band electrons in Ge:As. We have postulated that this could explain the fall in $K^2T_1(2)T$ below the Korringa value and the fact that $T_1(2)$ is continuous across the metal-nonmetal transition. At high fields, the local moment fluctuation is suppressed and the nuclear relaxation

rate decreases. We have observed that $T_1(7) > T_1(2)$ in the impurity band region in agreement with the moment fluctuation theory. Moreover if the high field nuclear relaxation is predominantly due to conduction electron contact then we would expect a dramatic change in $T_1(7)$ at N_C where the Knight shift alters sharply. This is again in accord with our observations. For very heavily-doped material, we expect nuclear relaxation to be due solely to Fermi contact with conduction band electrons and thus T_1 should be independent of field. Our data shows $T_1(2) = T_1(7)$ for $N_D \gtrsim 10^{18} cm^{-3}$ in good agreement with the estimates of the dopant concentration at which the Fermi level enters the conduction band. The presence of local moments leads to broadening of NMR resonance lines, as we noted in chapter 5, with the broadening being proportional to field. We also mentioned that the somewhat similar idea of a Knight shift distribution model could lead to broadened resonances with a similar field dependence. It was, moreover, argued that a major contribution to the linewidth was not of quadrupolar origin. The local moment model clearly fits our data in the qualitative sense and is also in agreement with negative magneto resistance observations and the Raman study of Ge:As by Doehler[96]. The model however seems not to be applicable to Si:P. Specifically, Brown and Holcomb[6], whilst not ruling out the existence of local moments in Si:P, found no evidence for their presence in their NMR experiments. Further, the Raman spectra of Jain et al.[97], the ESR data of Pifer[87] and the magnetic specific heat measurements of Hedgcock et al.[93] and Marko and Harrison[94] show no sign of localised states existing above N_C.

Parenthetically, it is interesting to speculate that, if as we have argued above, $U(Si) > U(Ge)$ then we should expect the probability of existence of moments to be greater in Si:P than Ge:As. The discrepancy could be removed by assuming that intraatomic correlation is not as important for Si:P as we have believed and thus the presence of local moments is determined primarily by fluctuations in doping density. (This point of view has recently been advanced by Mott[70, 71].) Although $N_c(Si) \sim 10 N_c(Ge)$ it is not clear whether the probability of finding a centre with low Kondo temperature is greater for n-Ge than n-Si since although there may be a greater chance of finding isolated sites in n-Ge we have noted in chapter 3 that impurity clusters can also behave as low-T_K sites. If the highly correlated gas does not exist in Si:P then alternative explanations of the enhancement of χ_s, K, etc. must be sought. Hedgcock et al.[93] pointed out that the moment-lifetime might be such as to make their presence detectable by ESR since ω_K, for a T_K of a few Kelvin, is of the order of the electron Larmor frequency. In an equilibrium property, such as specific heat, the moment-lifetime might be too short to have a noticeable effect. The nuclear Larmor frequency is however much less than that of the electrons so that enhancements in K and T_1^{-1} remain unexplained on the Hedgcock proposal. An alternative viewpoint is that the electron gas in Si:P should be considered in terms of an amorphous antiferromagnet as we now discuss.

Ikehata et al.[4] have advocated that the suppression of spin fluctuations with increasing magnetic field can explain their field

dependent T_1 data in Si:P. They obtain good agreement between their observed T_1T enhancements at low temperature and the theory of Ueda and Moriya[145, 146] of nuclear relaxation in weakly antiferromagnetic metals. As we have not made any very low temperature measurements of T_1 in Ge:As, we cannot comment on the applicability of the Ueda-Moriya theory to our system. A criterion for determining whether, say, Si:P is antiferromagnetic is the ratio of $\hbar\omega_K$ and the interaction between the moments whether of damped RKKY or other type. For weak interaction, the moments behave as the Kondo sites described above but for strong moment-interaction the material is better described as an amorphous antiferromagnet. Sasaki et al. have deduced that the Neel temperature is 0.1 K for Si:P so that no broadening of nuclear resonance lines is expected at the temperatures at which the experiments were performed ($\geqslant$ 0.6 K), i.e. the moments are not static in comparison with the nuclear Larmor frequency. It is interesting to note that for an amorphous antiferromagnet the χ^{-1} against T curves are similar in form to those due to a highly correlated gas. Finally, it should be mentioned that Benedict and Look[130] have argued the existence of moments in heavily doped CdO on the basis of their observation of two-valued nuclear relaxation times. This phenomenon has not however been observed in Si:P or Ge:As.

6.2 Summary

The overall conclusion from this work is that the metal-nonmetal transition in Ge:As appears to be of Anderson type. We believe an Anderson transition also occurs in Si:P but the Hubbard intraatomic correlation term would seem to play a more important role in determining the behaviour of the electron system in Si:P than in Ge:As. We have shown that the field dependence of $T_1(Ge^{73})$ may be explained on the basis of a single-phase electron system in a narrow impurity band. Alternatively, some two-phase character leads to agreement with our data and those of other experiments but the lack of a quantitative theory to test our results is a severe, if as yet necessary, omission. Conversely a two-phase electron system seems seriously at variance with the Si:P experimental data. Whether these materials are describable as amorphous antiferromagnets remains speculative.

The attitude of workers in this field of physics is perhaps best indicated by noting that firstly Mott, who for so long has considered Si:P to be the archetype for a transition due to correlation, now advocates an opposite view and introduces elements of a two-phase system into his new approach[70,71]. To the contrary, Marko, who interpreted his ESR and specific heat data in Si:P on the basis of a two-phase electron gas[81,82,84] has, on the evidence of magnetic specific heat data and the calculations of $\chi_S^{int}(T)$ by Chao and Berggren[86], rejected the two-phase model completely for a theory based on correlation[94].

From a practical standpoint, Ge:As is a far less attractive material than Si:P with which to perform NMR (and ESR) experiments. The high spin, low magnetogyric ratio and most importantly the long relaxation times of Ge^{73} all conspire to make experimentation difficult. Moreover, the lower doping density required to study the metal-nonmetal transition in n-Ge means that impurity NMR is below the normal detection limits. To its credit, however, high quality Ge samples of known impurity concentration are available and we regard this feature as a prerequisite for any study of the metal-nonmetal transition.

Appendix 1

APPARATUS AND EXPERIMENTAL TECHNIQUES

A1.1 Introduction

The requirements of a pulsed NMR system have been listed by Clark[189] and we may summarise them as follows. Firstly the transmitter must be capable of delivering intense radiofrequency pulses to the sample coil which forms part of a tuned circuit. The pulses must be capable of being varied in phase, width and repetition rate. The receiver must be sensitive to both the phase and amplitude of the nuclear signal and should be able to amplify without distortion of the signal. The stability of the gain of the receiver is required to be good since measurements of the amplitude of the signal are used in determining T_1 values. As regard the magnetic field in which the experiment is performed, good stability is required especially when small Knight shift measurements are attempted. Furthermore the inhomogeneity of the static field over the sample volume should be low to permit Knight shift and linewidth data to be taken. The Ge^{73} nucleus is a severe test of some of the requirements noted above and we describe our approach for attempting to observe the Ge^{73} resonance in the following section. Later paragraphs are devoted to descriptions of the NMR spectrometer, magnet systems, cryogenic practice and the methods of measurement employed.

A1.2 Observability of the Ge^{73} Resonance

For equal numbers of nuclei at constant field, the Ge^{73} nucleus is $\sim 10^{-3}$ times the sensitivity of the proton and $< 20\%$ of the sensitivity of the Si^{29} nucleus. In order to determine the optimum

experimental conditions for observing the Ge^{73} nuclear resonance, a simple expression for the signal-to-noise ratio in a pulsed NMR experiment is derived. Following Abragam[8], the peak amplitude of the induced nuclear signal in a coil following a $\pi/2$ pulse is

$$v \sim \eta \mu_o M_o \omega_o Q A_n \qquad (A1.1)$$

where η is the filling factor of the coil, i.e. the ratio of the sample to coil volumes V_s/V_c, M_o is the nuclear magnetisation per unit volume, Q is the quality factor of the coil, A is the cross-sectional area and n the number of turns in the coil. For a solenoid of length l, the inductance L is given by

$$L = \mu_o \frac{n^2 A}{l} \qquad (A1.2)$$

An expression for the signal-to-noise ratio becomes[190]

$$\frac{S}{N} \sim \frac{Q M_o \omega_o (\mu_o L \eta V_c)^{\frac{1}{2}}}{(4kT \Delta v \cdot Q L \omega_o)^{\frac{1}{2}}} \qquad (A1.3)$$

where Δv is the bandwidth and T the temperature of the tuned circuit.

The formula for S/N is only of order of magnitude significance and it is not possible to determine exactly how S/N changes if any one quantity is changed since the components of the formula are not independent of each other. The interaction between the various terms has recently been treated by Hoult and Richards[191].

However, faute de mieux, our expression implies that we should work with a large volume, high Q coil at high frequency ω_o and using the smallest receiver bandwidth possible. The magnetisation may be optimised by using large static magnetic fields and low temperatures.

The easiest factor to increase is the working frequency ω_o but we immediately face the problem of the low magnetogyric ratio γ of Ge^{73}. The first electromagnet that we used had a maximum field of 1.6 T but we were restricted to a field of 1.44 T as the homogeneity was poor at the higher value. Since

$$\omega_o = \gamma B_o \qquad \text{(A1.4)}$$

the implied working frequency is 2.14 MHz which is low by normal NMR standards. The arrival of a superconducting magnet system in our laboratory allowed later measurements to be performed at 5 T and 7.4 MHz.

The samples were of volume $\sim 2\ cm^3$ which was coextensive with the volume over which the field inhomogeneity and the concentration gradient of the dopant along the sample were acceptable. Low temperatures were used because of the physics of our samples and $\Delta\nu$ was kept to a few kHz but not so low as to distort the nuclear free induction decay (f.i.d.).

As regards coil design, the sample volume fixed A and l. The inductance L and Q are related to the impedance R of the circuit by

$$R = Q \omega_o L \qquad \text{(A1.5)}$$

and the tuning capacitance in the sample tank circuit is given by the usual formula

$$C = \frac{1}{\omega_o^2 L} \qquad \text{(A1.6)}$$

If R is chosen as 50Ω, then a high value of Q requires L to be small and this may make C inconveniently large. A further problem of high Q coils is that the natural time constant of the tuned circuit is proportional to Q. Following a large r.f. pulse, the tank must ring down to a level at which it is able to accept the small nuclear signal. The natural time constant of the circuit τ is given by

$$\omega_o \tau = 2Q \qquad \text{(A1.7)}$$

and the ring down time of the pulse is

$$\tau_{rd} \sim 6\tau \qquad \text{(A1.8)}$$

Finally, in a pulsed NMR experiment, a large rotating magnetic field B_1 is required. If the energy stored in a coil when a current i flows is

$$\tfrac{1}{2} L i^2 \quad \text{and} \quad i = \frac{V}{L\omega_o} \qquad \text{(A1.9)}$$

where V is the voltage developed across the coil, then

$$B_1 = \left(\frac{\omega_o L}{4A1}\right)^{\frac{1}{2}} i \qquad \text{(A1.10)}$$

A low inductance coil can thus generate large values of B_1 and has the further advantage that breakdown problems associated with high impedance coils are suppressed.

In practice it is impossible to ensure simultaneous optimisation of all aspects of coil design and indeed further problems arise when the coil forms part of a spectrometer system rather than the isolated unit that we have considered here. We defer discussion of these effects until the spectrometer has been described.

A1.3 The NMR Spectrometer

The equipment is of the wide band type based on the design of Lowe and Tarr[192]. A schematic is shown in figure (A1.1) and a photograph of the 7.4 MHz apparatus is given in plate 1. In the Lowe-Tarr design, a single coil is used both to deliver a high power pulse and pick up the induced nuclear signal. The series-crossed diodes and the diode short enable the coil to switch between the transmitting and receiving modes. On pulse, both sets of diodes conduct heavily so that a large voltage is developed across the coil but the receiver is protected from severe overload by the high power pulse. Off pulse, the series-crossed diodes stop conducting thus isolating the transmitter from the receiver and the diode short goes open circuit so that the receiver can accept the nuclear signal. In Lowe and Tarr's original design, half-wavelength cables were used between transmitter-coil and coil-receiver to obtain maximum power transfer whilst a quarter-wavelength line between the two sets of diodes ensured that the diode short did not shunt the tuned circuit. These authors also used 180 Ω cable to match the ouput impedance of the power tubes in the output of the power amplifier and thus the tank circuit was required to have an impedance of 180 Ω also. In our case, the electrical lengths of $\lambda/4$ and $\lambda/2$ coaxial lines were excessive at 2.14 MHz and would have introduced large losses and possibly prevented tuning of the sample coil. In the following we describe our design for 2.14 MHz and indicate later the modifications made for operation at 7.4 MHz.

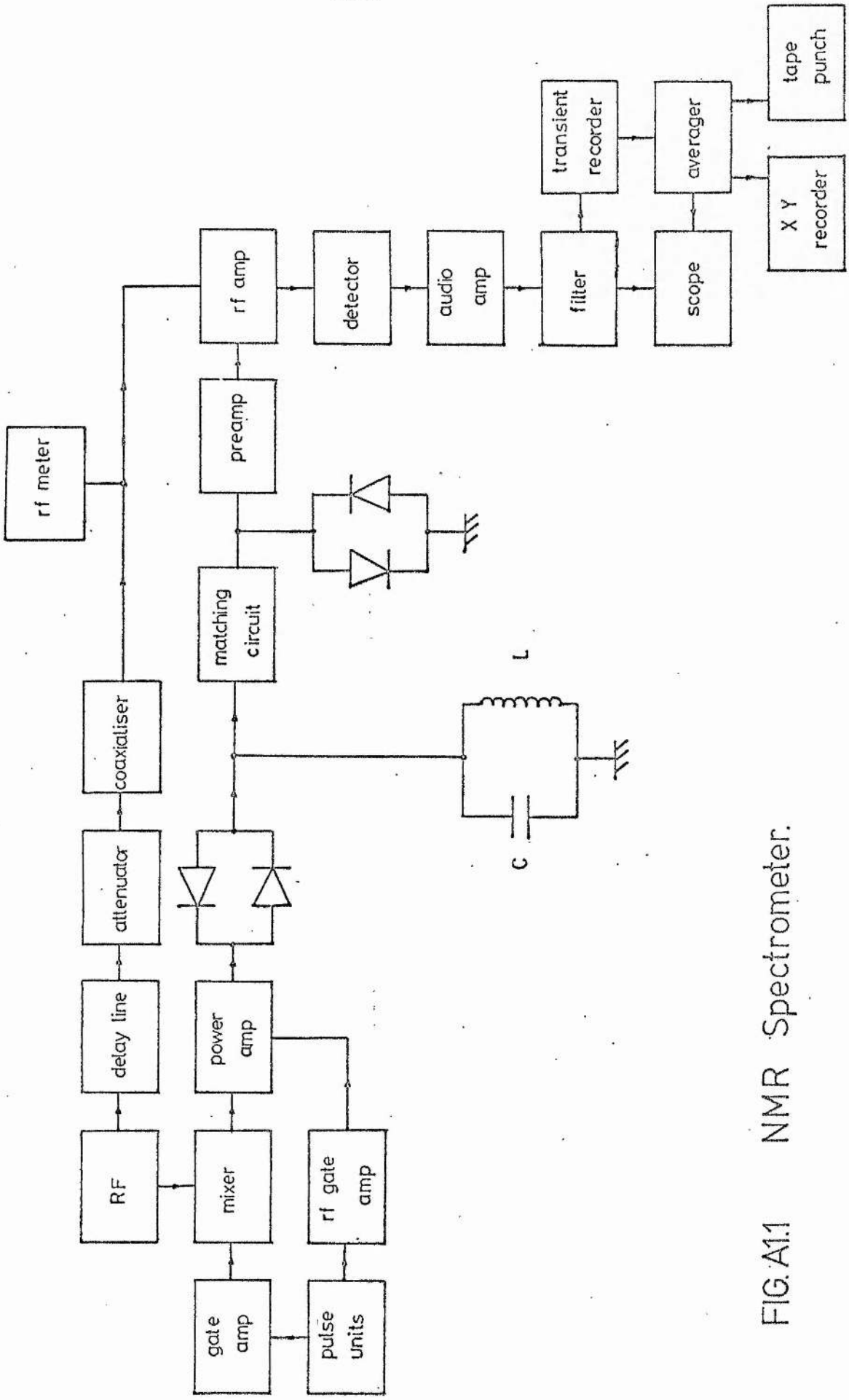

FIG. A1.1 NMR Spectrometer.

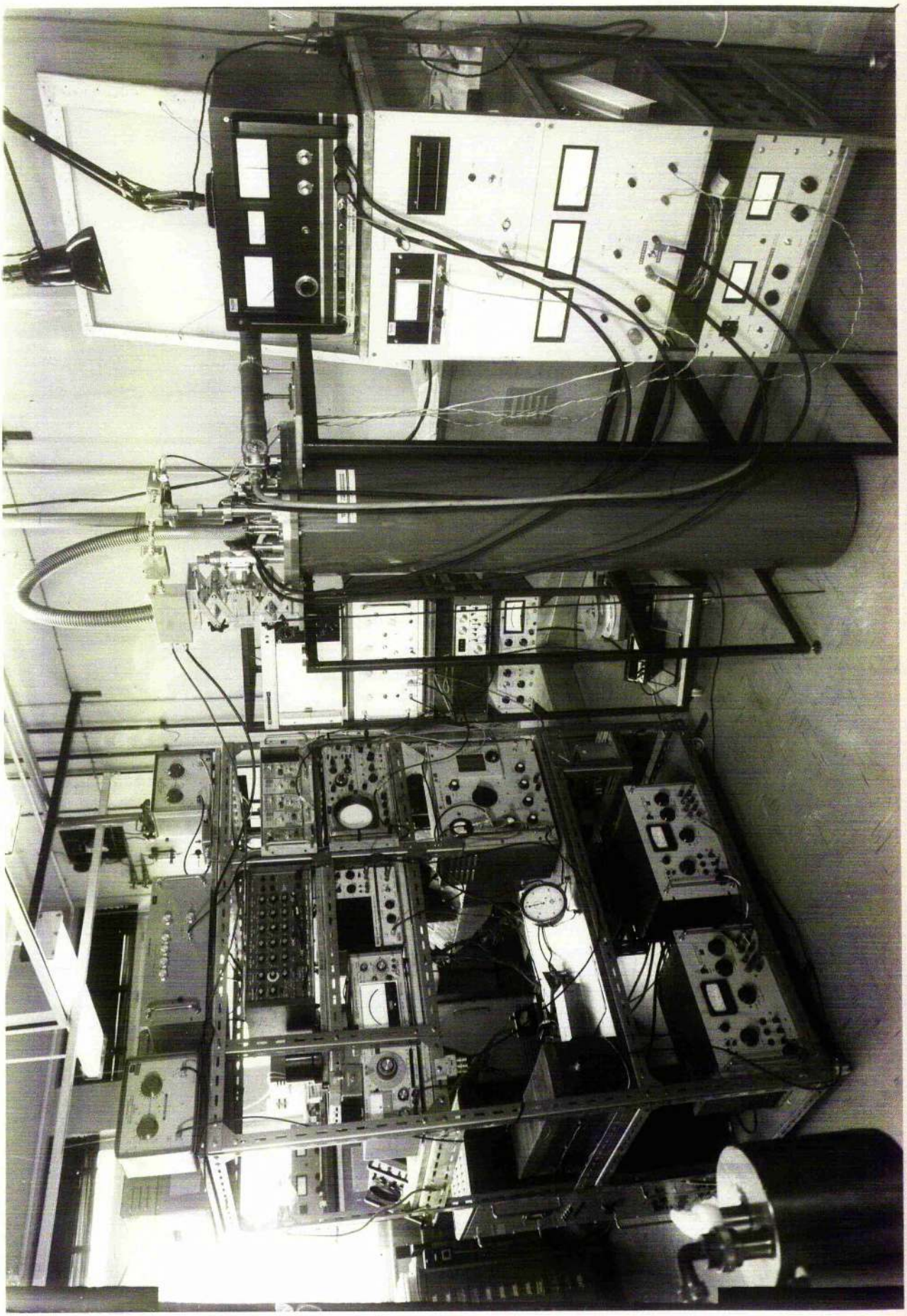

Our procedure was to choose an impedance of 50 Ω for the sample tank and to then match the output impedance of the final stage of the amplifier to 50 Ω by winding a suitable output transformer to replace the torroidal transformer of Lowe and Tarr. The sample coil consisted of ten turns of copper strip about 1 mm wide and separated by about 0.5 mm glued with 'Araldite' to a thin 'Mylar' cylinder which was a snug fit to the Ge:As samples. The inductance was ~ 1 μH and the Q ~ 40 at room temperature. The Q was measured on a Marconi circuit magnification meter and also by injecting a radiofrequency input to the tuned circuit in place on the NMR probe and noting the half-power points with a Hewlett-Packard 5246L frequency meter. The Q increased to ~ 60 at 4.2K, presumably due to a change in resistivity of the copper winding. The tuning capacitors used were of the dipped silver mica type (Sangamo). These capacitors have a tough, phenolic coating enabling them to withstand many thermal cycles from room to helium temperatures without degradation. In addition, they have a low temperature coefficient of capacitance so that the entire probe could be tuned at room temperature with the confidence that it would remain tuned at 4.2K. No other capacitors were found to have such convenient properties from an NMR viewpoint. The single disadvantage is that some are fitted with magnetic leads and must therefore be discarded. The capacitors were mounted as close to the coil as possible and with very short leads to avoid introducing any stray inductance from the leads. The tuning capacitance at 2.14 MHz is ~ 5000 pF and the rotating B_1 fields for the coil were ~ 5 mT for a pulse of 300 V peak across the circuit.

Initial attempts to find a nuclear signal at low temperatures were thwarted by an oscillation or ringing of the coil lasting for $\sim$ 2 msec after the pulse had terminated. The observed ringing was dependent on the magnitude of B_o and B_1 as Speight et al.[193] have noticed. These authors cured the ringing by surrounding the coil by a closely wound coil of enamelled copper wire. The insulation was removed at one point on each turn and a thick copper grounding strip soldered in place. Their reason for using a 'discrete' shield was on account of their observation that the ringing was caused by eddy currents being produced in a solid shield by the r.f. pulse and being reflected back to the coil by the static field. In contrast we found that the ringing could be reduced by surrounding the coil in a brass can and rigidly tying the coil down with an earthing strip to the shield. Undoubtedly, the prevention of physical movement of the coil is important in pulsed NMR work. This modification permitted the easily-seen Al^{27} resonance to be observed but the ring down time of the tuned circuit was rather long ($\sim 100\,\mu s$) due to the high Q coil. In normal circumstances, with a nucleus of reasonable sensitivity, this could be circumvented by lowering the Q by inserting a small length ($\sim$5 mm) of manganin wire of resistance $\sim 20\ \Omega\ m^{-1}$ in series with the coil. For Ge^{73}, which had not to our knowledge been observed before by pulse techniques, we wished to keep Q high to effect the greatest S/N ratio. Accordingly, we inserted a 200 Ω resistor between the r.f. line and ground on the transmitter side of the series diodes. On pulse, the transmitter sees a low Q circuit formed by the

200 Ω resistor in parallel with the tuned circuit. The tank rings down quickly to the threshold of the diodes (0.5 V) at which point the 200 Ω quench resistor is switched out of the circuit. The sample tank then rings down with its natural Q to the sub-millivolt range in order to accept the nuclear signal. The advantage of having a high Q coil in the receiving mode and a low Q circuit in the transmitting mode has to be balanced with the inevitable loss in B_1 due to the shunting effect of the quench resistor. Observation of a nuclear resonance indicated that the receiver dead time was reduced to ~ 25 μsec at 2.14 MHz using the quencher.

The equipment used for the transmitting side of the spectrometer in addition to the gates and power amplifier of Lowe and Tarr were a radiofrequency generator and a set of pulse units. The r.f. was supplied by an Airmec 201 signal generator with its internal power supply replaced by a Farnell 6.5 A stable d.c. power supply for the tube heaters and a stable, Farnell 300 V, 70 mA unit for the high tension. This was necessary to remove 50 and 100 Hz ripple otherwise present on the output. The low level output of the Airmec (1 v rms) was fed to the mixer and the high level (4 v rms) used in the reference line to the receiver. Since the signal generator was not crystal controlled, the output frequency was continuously monitored by a Hewlett-Packard 5246 L frequency counter or Racal SA 535 counter-timer with a Racal SA 548 decade divider. Since the time scale of our experiments was so long, we merely had to ensure the frequency was at ω_o to better than 10 Hz every time we performed a measurement and no inconvenience was experienced.

The d.c. pulses for the gates were provided by a bank of Tektronix 2600-series pulse units and/or a set of AIM pulse units. These provided square pulses in widths from less than 1 μsec to 100 sec, with our usual working range being ~ 20 μ sec for a 90° pulse.

We consider now the receiver side of the spectrometer. The protection circuit consists of a tuned LC circuit which presents a high impedance to the pulse and thus ensures that the pulse is developed across the sample tuned circuit. The diode short limits the receiver saturation to 0.5 V.

The amplification system consisted originally of an Arenberg WA-600E wideband amplifier and an Arenberg PA-620-B preamplifier. The WA-600E contains a multi-tube r.f. amplification stage, mixer, detector and video amplifier allowing observation of the nuclear signal directly on the oscilloscope. The pass band was stated to be 2 - 60 MHz and this was checked to ensure the gain was not falling rapidly at our working frequency. The preamplifier was a three-tube unit with tuned input and output stages and was stated to have a pass band of 5 - 60 MHz. Although the cathode leg and interstage capacitances were increased and new tuning inductances wound for both input and output, the performance was very poor at 2.14 MHz. We therefore replaced the PA-620-B with a solid-state Polaron preamplifier which had a frequency response of 4 - 60 MHz. Satisfactory performance at 2.14 MHz was achieved by increasing the capacitance of the input stage of the preamplifier. Although a nuclear signal was now observable, the signal was distorted by the

video section of the WA-600E. To alleviate this problem we picked off the signal at a point after it had been amplified and mixed with the reference and passed the whole to a homemade half-wave detector. The detected wave form was then amplified by a Hewlett-Packard HP 465 audio amplifier before final filtering in a low pass filter to improve the S/N. The undistorted nuclear signal could then be viewed on an oscilloscope and passed on to the averaging system.

The averaging system consisted of a Datalabs DL905 transient recorder interfaced to a Datalabs DL101 100-point signal averager enabling short nuclear f.i.d's to be recorded over the full 100 points of the averager. The output could be observed on an oscilloscope, plotted on an X-Y recorder or fed to a Data Dynamics 1133 tape punch to produce output for subsequent processing by computer. The oscilloscopes used were of the storage type, Hewlett-Packard models 141A or 181A with appropriate plug-in units. These instruments considerably facilitated the 'setting-up' of the spectrometer in the early work of searching for the Ge^{73} resonance.

The reference signal supplied by the Airmec signal generator was first fed into an Ad-Yu delay line which was 'ended' to keep the VSWR low and then passed to a Marconi TF 1073A/1 r.f. attenuator before entering the reference (mixer) input of the WA-600E. An earth loop problem was solved by inserting a coaxialiser between the attenuator and the main amplifier.

The conversion of the spectrometer to operate at 7.4 MHz required replacement sample tank and protection circuits and the removal of the low frequency modification of the input to the preamplifier. Although operation at the higher frequency would have allowed the use of a very low inductance coil permitting large B_1 fields to be generated, we discovered that our samples severely loaded such a coil and we reverted to the use of a coil of $\sim 0.8\ \mu H$ tuning at 7.4 MHz with 570 pF. The purchase of a Polaron receiver allowed us to dispense with our hybrid receiver consisting of the Arenberg WA-600E, detector, audio amplifier and filter. Earth loop problems occurred, however, that were not then curable by the insertion of a coaxialiser in the reference line. The pick-up was reduced to tolerable levels in two ways. Firstly, double-screened coax was used for the reference and signal inputs to the receiver with the outer screens grounded at the receiver end only. Secondly the mains earths of the tube heater and high tension supplies for the signal generator were removed.

A1.4 Gain Monitoring Circuit

Since the relaxation times that we measured were very long, we required to be confident that the gain of our receiver system was constant over the experimental period. In order to check the gain, we built a simple circuit to monitor the gain of the system continuously : a block diagram is shown in figure (A1.2). The r.f. levels in the transmitter and reference lines were measured using Advance valve voltmeters or a Levell r.f. meter for operation

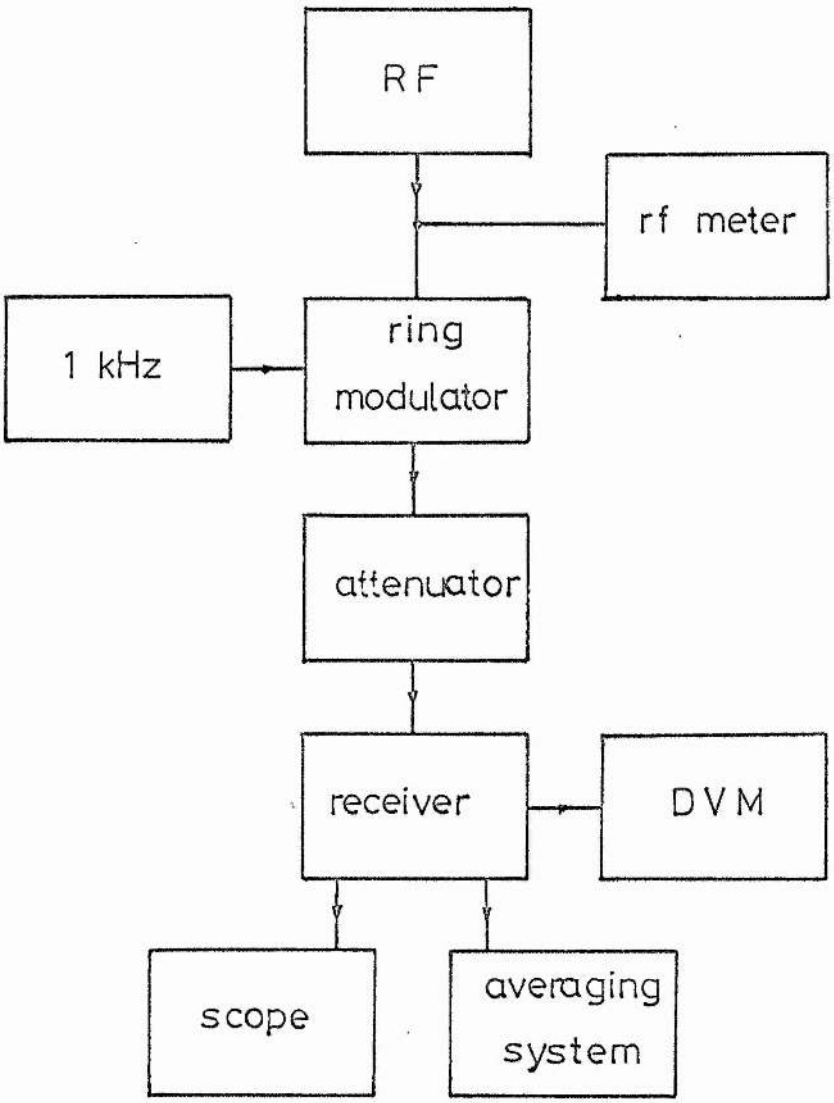

FIG. A1.2 Gain monitoring circuitry.

at 7.4 MHz. The r.f. output from the signal generator was disconnected from the gates and connected instead to one port of a Hatfield double-balanced or ring modulator. The second input to the ring modulator was a 1 kHz sinusoid provided by a stable Farnell LFM2 signal generator. The output of the ring modulator was then a modulated r.f. signal with a modulation depth of 100%. This signal was then attenuated to below the saturation level of the preamplifier. Finally, the signal was applied to the probe side of the protection circuit, the probe being disconnected and shielded to prevent r.f. leakage to the coil and sample. The rms value of the detected wave could then be read directly on an Advance DMM2 digital voltmeter and displayed on an oscilloscope.

We found that the gain of the Arenberg WA-600E varied by as much as 20% over a full day's experimentation but this could easily be allowed for using our gain monitoring circuit and the fact that the gain was a linear function of signal amplitude. (This linearity was checked for both the Arenberg and Polaron in our region of operation.) The gain of the Polaron receiver was very stable with time even though, at 7.4 MHz, the spectrometer was operated continuously for several weeks.

The monitoring circuit also had a second advantage in that the whole receiver including the averaging system could be very easily and quickly checked for correct operation.

The transmitter was checked before attempting a measurement by connecting a 50 Ω , non-inductive load to the output of the power amplifier and observing the pulse on the oscilloscope.

A1.5 Mechanical Design of the Probes

The low frequency probe consisted essentially of a long, thin-walled, stainless-steel tube sleeved internally with PVC. The r.f. lead in the centre of the tube was a length of 50 Ω coax from which the outer shield had been removed to minimise the heat leak to the liquid helium from the top of the cryostat: the stainless-steel down-tube furnished the earth return. Small lengths of copper braid were soldered between the ends of the coax cable and the top bnc connector and the lower probe assembly comprising the sample coil rigidly mounted inside a brass shielding can. These braids allowed for the contraction of the cable at low temperatures which could otherwise lead to ruptured solder joints at either end of the cable. In practice, multistrand coax proved less susceptible to lead to broken joints than cable of the single-central-conductor type.

The high frequency probe consisted of a length of thin-walled stainless-steel tubing with a central, stainless-steel conductor inside. The radii of the tubes was chosen so that the entire probe formed a solid coaxial line of 50 Ω impedance, assuming a vacuum dielectric, and separation of the conductors was effected by Teflon spacers that were perforated longitudinally to allow the entire probe to be evacuated. The lower part of both conductors were fabricated in brass as some stainless-steels can exhibit magnetism in the strong fields that we wished to use. The bottom end of the probe was sealed with 'Stycast', an epoxy resin which withstands low temperatures and thermal cycling. The head of the probe was fitted with a bnc connector, a miniature valve through which the

probe could be pumped and a pressure relief valve. The latter ensured that an internal overpressure would not occur if liquid helium did enter the probe and subsequently vapourise as the cryostat warmed up after experimentation. The sample coil was again shielded by a brass can and an internal Teflon yoke afforded mechanical rigidity of the coil.

A1.6 Cryogenics

All the low frequency measurements were performed in an Oxford Instruments Dewar with a capacity of about 3 litres of liquid helium. Temperatures below 4.2 K were obtained by pumping on the liquid. The liquid level was monitored by observing the change in resistance of a Nb-Sn superconducting wire which was superconducting below the liquid and normal above. The wire was driven by a simple constant current power supply giving a voltage swing between full and empty of 4 V. This level indicator was a great improvement on an earlier method by which the resistance changes of strategically placed, Allen-Bradley carbon resistors were monitored by Avometer, since the resistances in cold helium gas and liquid helium were hardly distinguishable. The T_1 measurements were generally so long that they were unmeasurable with one fill of the dewar. Top-up transfers were then necessary and whilst not inherently difficult, great care had to be taken when inserting the transfer tube to prevent a sudden boil-off of the liquid which could leave the sample uncovered: the liquid level was constantly monitored to ensure this did not occur. A further precaution made was to create

a small overpressure in the storage dewar to prevail over the propensity of the liquid to 'self-transfer' from the cryostat to the storage vessel. An important practical point was that the transfer tube would invariably block during a top-up transfer unless, following the initial transfer, the siphon was thoroughly baked-out, flushed with dry nitrogen or helium gas and had both ends sealed off to prevent absorption of water vapour onto the inner walls of the tube.

The high frequency measurements were performed using a superconducting magnet system which was supplied with its own cryostat by Thor Cryogenics. The cryostat of overall height ~ 1.5 m and ~ 0.5 m diameter consisted of a superinsulated helium space of 25 l capacity surrounded by a superinsulated nitrogen chamber of 30 l capacity and finally a vacuum jacket fitted with a pumping port and a pressure relief valve. The superinsulation, consisting of thin, multilayer wrappings of aluminium-clad mylar, made the fitting of a nitrogen cold trap and solenoid baffle valves mandatory for external pumping units. Contamination of the sheeting by diffusion pump oil would have had an extremely deleterious effect on its insulating properties. Preparation of the cryostat for an experiment was performed as follows.

Firstly, the vacuum jacket was well pumped, usually four days at 10^{-5} torr, as the superinsulated helium space does not act as a powerful cryopump for air. Precooling was achieved by filling the nitrogen and helium chambers with liquid nitrogen and allowing the dewar to stand overnight. The following morning, the liquid nitrogen in the helium space was blown out through a stainless-

steel tube that reached the bottom of the cryostat using dry nitrogen gas of about 1 p.s.i.g. pressure. The liquid nitrogen remaining after this process was removed by successive pumping and back-filling with helium gas. Care was taken not to pump below 100 torr to prevent the possibility of the nitrogen solidifying. The blow-out, pumping and back-filling procedure took about 2.5 hours to complete. Liquid helium could then be transferred; the gas flow rate was kept at several cubic feet per minute, as measured on a domestic gas meter, until a liquid level was obtained. A full transfer usually took 3 to 4 hours. Since the precooling was so time consuming, we kept the cryostat cold for as long as possible: experimental periods of three weeks duration were usually performed. The liquid helium evaporation rate was found to be $\sim$ 0.4 l hr^{-1} even with careful baffling of the upper part of the cryostat. This is twice the manufacturer's stated boil-off rate but still gave us useful experimentation time. The liquid level was monitored using a superconducting wire and power supply manufactured by Thor Cryogenics. At the finish of an experimental run, the dewar was allowed to warm up to room temperature (one week) but was kept sealed from the atmosphere even after the helium had completely evaporated. This was to ensure that no moisture condensed out onto the cold cryostat surfaces. Even with this precaution, the helium and nitrogen spaces were well pumped out periodically to remove water vapour. This was necessary since small water droplets could lead to local hotspots on the superconducting solenoid or even a dewar wall failure.

A1.7 Magnetic Field Production

The low frequency measurements were performed in a field of 1.44 T. This field was supplied by a Mullard EE1035 electromagnet driven by a Mullard EE4038 100 A power supply. The maximum field available with tapered pole pieces fitted was 1.7 T but here the inhomogeneity becomes greater than 0.1 mT so the lower field of 1.44 T was chosen. In order to investigate the homogeneity of the field, a Newport magnetometer type P, mark II, was used. This instrument allows the proton or lithium nuclear resonance to be observed in a sample of a saturated solution of lithium acetate doped with cupric nitrate using a so-called marginal oscillator method of observation. Initially the observed proton signal was poor and Li^7 signal unobservable which implied, according to the magnetometer manuual that the field inhomogeneity over the sample volume was worse than 2 parts in 10^4 ($\sim$300 μT). Various shim coil arrangements have been described in the literature and we wound three orthogonal sets corresponding to the axial etc. directions of the main field. Two of the sets were of the saddle-coil configuration and followed the geometry described by, for example, Abel et al.[194] and the remaining set was cylindrically symmetric. By suitable adjustment of the magnitude and direction of the shim currents, the inhomogeneity was reduced to 5 μT over the sample volume of length 13 mm, diameter 5 mm. However, it was also found that alteration of the parallelism of the pole pieces could also reduce the inhomogeneity so that eventually the pole pieces were optimally

adjusted and the shim coils discarded resulting in a net inhomogeneity of 10 μT over a cylindrical volume of 13 mm by 10 mm diameter. Although the shim coils were not finally used they were indispensable for the ease of adjustment of the pole pieces. The figures of field inhomogeneity quoted here are values of the field difference between the maxima of the derivative of the Li^7 resonance as obtained directly from a PAR lock-in detector. When the measured linewidths of the Ge^{73} resonance in semiconducting Ge:As turned out to be rather larger than the anticipated dipolar width, some doubt was cast on the inhomogeneity figures quoted above. We therefore checked our figures by observing a proton resonance at 50 MHz (1.2 T) using a Clark-type spectrometer[189] and found agreement with our previously ascertained values. The proton signal also afforded a measure of the stability of the electromagnet and it was found that field drift was negligible over a typical experimental period.

The high frequency measurements were performed using the superconducting solenoid referred to earlier (plate 2). This had a maximum field of 5 T and we operated at near maximum field corresponding to a Ge^{73} resonance frequency of 7.4 MHz. The magnet was driven by a three-phase supply manufactured by Thor Cryogenics. A field of 5 T corresponded to a driving current of 37.79 A but the ammeter supplied was far too crude to allow the setting of the field to within, say, a nuclear linewidth. We therefore picked off the voltage on the ammeter's current shunt and displayed this on a five-figure Exel XL 2000 digital voltmeter enabling us to set the field to within 5 mT.

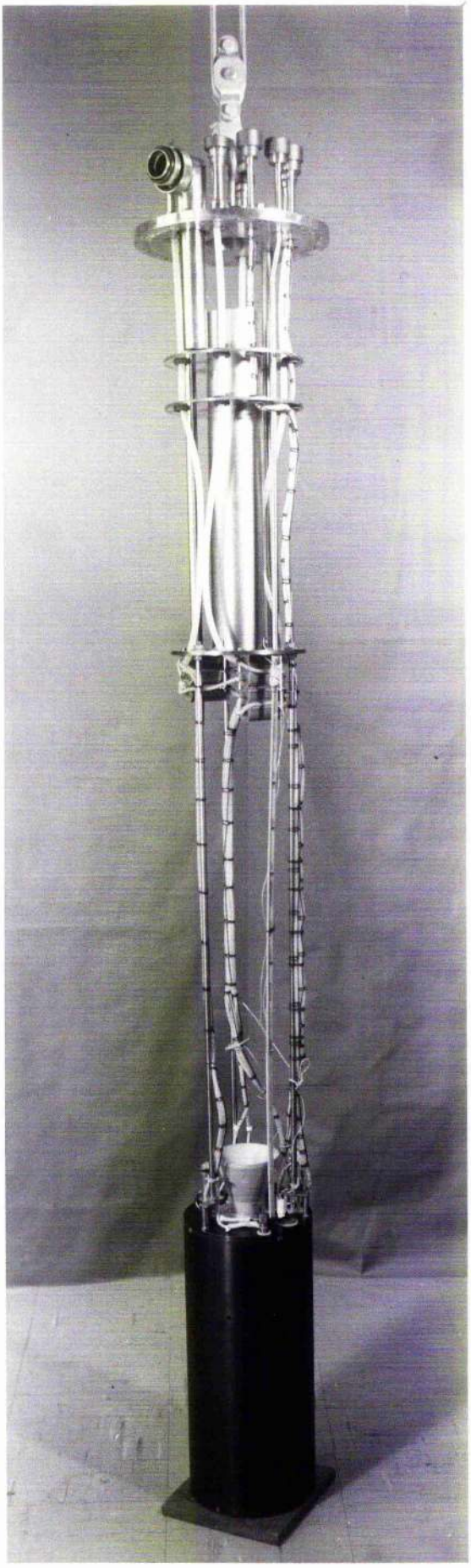

The solenoid was energised in the following manner. The power supply is connected to the solenoid by a superconducting switch. This switch may be closed by applying a current to a heater coil surrounding the switch thus driving it into the normal state. With the switch heater on, the supply was programmed to charge up to the desired current over a period of about 1.5 hours. (A faster charging rate could cause the magnet to quench.) When the desired field was attained, the superconducting switch was opened and the power supply turned to zero. The solenoid was then in the persistent mode and had the completely negligible field decay rate of 1 in 10^8 per day. All Knight shift measurements were performed with the solenoid in persistent mode to be certain that the applied field was the same for all samples.

The homogeneity of the field over a cylinder 10 mm long and 10 mm diameter was quoted by the makers as better than 50 μT. This could have been improved upon by using the supplied set of shim coils but time did not permit a determination of the optimum shim currents and we thus worked with the 'bare' homogeneity value. Later experimentation using a room temperature insert in the cryostat and an aqueous NaCl sample confirmed that the unshimmed inhomogeneity was less than 50 μT.

A1.8 Measurement Techniques

A1.8.1 Spin-Lattice Relaxation Time Measurements

With a multipulse spectrometer such as ours, a convenient method of measurement of T_1 is the use of the pulse train technique.

A series of ten or more 90^{o} pulses, separated by about $5\ T_2$ is applied to saturate the nuclear spin system, i.e. the net nuclear magnetisation is reduced to zero. At any time t after saturation, a single 90^{o} observation pulse is applied to sample the size of the nuclear magnetisation M_z which has regrown along the static field direction in time t. Then

$$M_z = M_o\left(1 - \exp\left[-\frac{t}{T_1}\right]\right) \qquad \text{(A1.11)}$$

and T_1 may be found. Here M_o is the equilibrium value of the magnetisation which is usually found by waiting a time t_o of at least $5\ T_1$ after saturation when more than 99% of the magnetisation has regrown. In our low field measurements, the length of the relaxation time for low-doped samples restricted t_o to $\sim 3T_1 \sim$ 5 hours so that we have an error in M_o of order 5%. At high field, the samples could be conveniently left to polarize overnight in the superconducting solenoid set in persistent mode. However, the increase in T_1 with field meant that the semiconducting samples had to be polarised for many hours before M_o could be determined. Whilst the T_1 measurements were not inherently difficult it must be said that the initial setting up of the spectrometer to find the Ge^{73} resonance was immensely tedious.

As the equilibrium value of the magnetisation proved so difficult to determine the prospect suggested itself of being able to determine T_1 without finding M_o. Mangelsdorf[195] has published a method of determining rate constants when asymptotic values of a parameter are unknown. If we write the magnetisations at

time t and $t + t'$ as

$$M(t) = M_o \left(1 - \exp\left[-\frac{t}{T_1}\right]\right) \qquad (A1.12)$$

$$M(t + t') = M_o \left(1 - \exp\left[-\frac{t + t'}{T_1}\right]\right) \qquad (A1.13)$$

then

$$M(t + t') = M(t) \exp\left[-\frac{t'}{T_1}\right] + M_o \left(1 - \exp\left[-\frac{t'}{T_1}\right]\right) \qquad (A1.14)$$

If we plot successive values of the magnetisation against each other, i.e. $M(t + t')$ against $M(t)$ for equal intervals of t', we can obtain T_1. In practice we found that such a plot must be taken to at least $t = T_1$, otherwise the accuracy was very poor. In fact with our S/N ratio, a Mangelsdorf plot was more difficult to interpret than a $\ln M_z$ versus t plot and the experimental times were approximately the same for both methods. We therefore used a pulse train technique for finding T_1 and only drew a Mangelsdorf plot as a check on our result.

An alternative method of measurement of long T_1 values is to use the artifice described by Bridges and Clark[196] in their study of In^{115}, Sb^{121} and Sb^{123} resonances in InSb. Briefly, their method was to include a short-T_1 calibrator sample ($Na^{23}Cl{:}Fe^{2+}$) with the InSb specimen inside the NMR coil. At temperatures at which the In,Sb nuclei had short relaxation times, the relative amplitudes of the In, Sb and Na nuclear signals were measured. At low temperatures where the T_1's for the In, Sb nuclei were long but that for Na was still short, Bridges and Clark[196] inferred M_o (In^{115}, Sb^{121} or Sb^{123}) from the measured value of $M_o(Na^{23})$ and the previously determined

calibration ratios. The values of T_1(In, Sb) were then obtained from M_z(In, Sb) for short times following saturation of the respective nuclear magnetisations. The method relies on the fact that all nuclei obey Curie's Law as far as their magnetisation is concerned and also that all nuclei relax with a single exponential in time. We could not use such a scheme for two reasons. Firstly, working at constant frequency we should have had to change the static field value from that corresponsing to the Ge^{73} resonance to the calibrator resonance and back again. This would have been extremely difficult to do successfully as we have noted above that the Ge^{73} resonance was rather elusive. Secondly, S/N considerations did not allow us to lower the filling factor of the coil by including a calibration sample or by constructing some sample changing device. Clearly Bridges and Clark had the advantage that the nuclei that they studied were 30 to 250 times more sensitive than the Ge^{73} nucleus.

We could however use a variation on the Bridges-Clark idea which was useful for sub-helium temperature measurements of long T_1 values at low field. Here the small liquid helium capacity of the dewar prevented M_o measurement from being made for the majority of the samples. Our method was to measure M_o at 4.2K and then infer the equilibrium magnetisation at lower temperatures by using Curie's Law. We could then measure M_z for various times after saturation at the appropriate temperature. Whilst Curie's Law for nuclear magnetisation is perfectly general and applicable to our system, equilibrium magnetisations inferred in this way could not be expected to be very accurate. For those samples for which M_o

could be directly measured at low temperatures, we obtained reasonable agreement between the measured values and that calculated from M_o (4.2K). Moreover a Mangelsdorf plot could always be made to provide an additional check on our computed values of T_1. Finally, all low field T_1 measurements were repeated to determine the reproducibility of the results and they were found to be consistent to within $\sim$ 15%. Time did not permit the high field T_1 measurements to be repeated.

A1.8.2 Knight Shift Measurements

Values of the Knight shift were measured using the superconducting solenoid in persistent mode, by sequentially inserting the samples and observing the nuclear resonance. A check was made to determine whether repeated insertions of the probe might abstract energy from the solenoid and cause the field to change: no such effects were observable. To determine the Knight shift, we recorded successive f.i.d.'s of the samples and stored the results on paper tape. Since the f.i.d. is the Fourier transform of the lineshape, the f.i.d.'s were suitably processed by computer. The differences between the line peak positions and the zero reference yielded the Knight shift. The zero datum was the (insulating) germanium sample containing 7.10^{16} carriers cm^{-3} at room temperature. The advantage of using reference and metallic samples of the same material is that any chemical shift should be the same for both and hence cancel in a determination of the Knight shift. The magnitude of the shifts were positive and of the same order as observed in, for example, Si:P being a few parts in 10^5 and thus much less than those observed in

normal metals. The long T_1 values precluded us from using signal averaging techniques to increase the S/N ratio and thus narrow the uncertainty in the determination of the peak positions of the resonance lines. We did however measure the shifts several times and obtained good reproducibility between results. Each quoted result is the arithmetic mean of at least six and generally more measurements.

The Fourier transform program that we used was checked by observing the Na^{23} resonance firstly in an aqueous solution of NaCl doped with paramagnetic ions to reduce the relaxation time and then the Na^{23} signal in sodium metal. The latter consisted of metal particles, with dimensions smaller than the skin depth at 7.4 MHz, dispersed in a light oil. This sample was produced by simultaneous gentle heating and ultrasonic stirring of a test tube containing a small amount of Na metal under a light oil to which a few drops of oleic acid had been added to lower the surface tension of the sodium. The measured shift was $0.72(6) \pm 0.01$ mT which compares favourably with the accepted value of $0.113\% \equiv 0.729$ mT at our working resonance field of 0.645 T.

A1.8.3 Linewidth Measurements

Linewidths were calculated by assuming

$$\Delta B \sim \frac{2}{\gamma T_2^*} \qquad \text{(A1.15)}$$

Values of T_2^* were taken from the f.i.d.'s at both low and high field. At high field, the computed linewidths agreed well with those measured from the computer plots of the lineshapes. Again, Ge is not an ideal

material from an NMR point of view in that the f.i.d.'s were short (~ few hundred μsec) and this made T_2^* difficult to determine accurately. The fact that the linewidths were broad led to the further difficulty of determining the centre of the resonance line for the Knight shift results.

Appendix 2

SAMPLES

An important part of our data has been the determination of the concentration dependence of those quantities that we have measured. A prerequisite is a knowledge of the doping densities of our samples and we shall consider this and other aspects in some detail below.

Our original requirement was for a set of perhaps six samples of Ge:P spanning the metallic transition with which to perform experiments to compare with those undertaken in Si:P. Since the metal-nonmetal transition in n-Ge occurs at a doping density which is an order of magnitude lower than in Si:P we have less carriers and thus a higher resistivity. The skin depth δ which is given by the convenient formula

$$\delta = 5.03.10^{-4} \left(\frac{\rho}{\nu}\right)^{\frac{1}{2}} \text{ m} \qquad \text{(A2.1)}$$

where the resistivity ρ is in $\mu\Omega$m and ν the resonant frequency in MHz, is thus a less intrusive effect in n-Ge than in n-Si. We are thus able to use single crystal samples whereas workers in Si have had to use powdered specimens. The doping density required for Ge:P was $\sim 10^{17} - 10^{20}$ cm^{-3} and the samples were to be grown by the Royal Radar Establishment (RRE)[197] by doping Ge with $CaHPO_4$. After protracted trials, large single crystals of high doping density ($> 10^{17}$ cm^{-3}) proved impossible to prepare even though the literature showed that small samples with the desired characteristics could be made. We therefore changed our requirement to As-doped Ge which RRE produced using the liquid encapsulated Czochralski technique. The samples were fabricated

in the form of cylinders ~ 13 mm diameter and ~ 15 mm long and are listed together with their electrical properties in table A2.1. We identify each sample by the notation A-B and this indicates the room temperature concentration $A.10^{B}$ cm^{-3}. The generating axes of the sample cylinders were perpendicular to the growth axis $\langle 100 \rangle$ of the boule except for sample 1.75-19 which was cut parallel to $\langle 100 \rangle$. The two most heavily doped samples were cut into slices of the order of the skin depth at 7.4 MHz and reassembled with thin, insulating Mylar sheets interleaving the Ge slices. Samples 5.9-17 and 5.3-17 were composites formed from three short cylinders (~ 5 mm long) trepanned out of the boule. The component parts of the sample were crystallographically marked so that the monocrystalline nature of the total specimens was preserved. Finally sample 4.4-17 was an irregularly-shaped composite formed from pieces left after mechanical rupture during fabrication.

The room temperature carrier concentrations were originally determined by RRE using four-point probe resistivity measurements and a graph of resistivity ρ_{RT} versus carrier density N_D similar to that of Sze[198]. At our insistence, Hall effect and resistivity measurements were also made on clover-leaf van der Pauw discs[199] to determine N_D. It was found that

$$N_D(\text{4 pt. probe}) > N_D(\text{vdP})$$

with the discrepancy being of order 30%. Since we required to investigate the concentration dependence of various NMR measurements a precise value of N_D was necessary and the dependence of N_D on the method of measurement was clearly unacceptable. An investigation

TABLE A2.1

Sample Carrier Densities and Resistivities

Sample Designation	Carrier Density at 300K (10^{17} cm^{-3})	Resistivity at 300 K ρ_{300} (10^{-2} Ω cm)	Resistivity at 4.2 K $\rho_{4.2}$ (Ω cm)	Carrier Density at 4.2K (10^{17} cm^{-3})
7-16	0.7 ± 0.1	4.35		
2.1-17	2.1 ± 0.2	1.95	1.1	0.72
2.7-17	2.7 ± 0.4	1.62		
2.7-17	2.7 ± 0.3	1.62		
3.1-17	3.1 ± 0.6	1.48	0.12	2.1
3.5-17	3.5 ± 0.5	1.36	0.015	3.5
4.4-17	4.4 ± 0.7	1.16		
5.0-17	5.0 ± 0.25	1.06		
5.3-17	5.3 ± 0.3	1.03		
5.9-17	5.9 ± 0.4	0.96		
9-17	9.0 ± 1.5	0.72		
1.75-19	175 ± 55	0.118	0.00118	175
K1062B*	2.0	1.5	1.2	0.6
Z184*	3.1	1.0	0.062	2.0

* From Le Hir[43]

by RRE showed that the four-point resistivity values were difficult to reproduce and this was adjudged to be due to 'end effects' of an unknown origin in one of the measurement potentiometers. In fairness, our required samples were of much lower resistivity than those normally produced by RRE so that a potentiometer was being used at an extreme of its working range. The Hall measurements were, in contrast, entirely reproducible. RRE used two different operators utilising two completely different sets of apparatus and obtained identical values of N_D[200]. Moreover our own check measurements yielded similar values. The van der Pauw data were also in very good accord with the theoretically predicted mass fraction of solute (As) dissolved in the boule as a function of distance from seed to tail[200]. Again, the four-point probe data did not agree with the anticipated mass fraction dissolved and RRE concluded that the four-point probe method was thus very unsatisfactory. The van der Pauw discs were cut from slices adjacent to the extremities of every sample cylinder and contacts were made by alloying tin dots into the surface. Indium dots were also tried but yielded unreliable results and low N_D values[200].

It is also noteworthy that all crystals were pulled with the growth axis a few degrees away from a normal crystal axis to avoid a facet effect. This occurs in the crystal pulling process if a crystal plane finds itself parallel to the melt surface. In this case the boundary between the grown crystal and the melt changes from its normal convex downwards shape to a flat facet, i.e. the aforementioned crystal plane. The result is that the incorporation of dopant atoms

in the faceted interface between solid and liquid increases. The effect varies with material and crystal plane, being predominant for a $\{111\}$ plane. As regards materials, faceting is most prevalent in InSb:Te where the ratio of doping densities on and off the facet is seven to one. For Ge, the ratio is about 20%. RRE were able to assure us that X-ray examination of the crystals and van der Pauw slices showed the facet effect to be negligible for our specimens[200].

We turn now to our own Hall data which was performed at 300 and 4.2 K. We found as has Cuttriss[201] that our measured N_D values agreed with those derived from the ρ_{RT} versus N_D curve if we assumed $A(300\,K)$ is unity in the expression[202]

$$N_D = \frac{A}{R_H e} \quad \text{where} \quad A = r\left\{\frac{3K(K+2)}{(2K+1)^2}\right\} \qquad (A2.2)$$

K is the ratio of longitudinal to transverse mass and for conduction band electrons in germanium the term in braces is 0.8. The Hall scattering factor r has been shown by Walton and Moss[203] and Hartmann and Kleman[204] to be greater than unity in our doping density region so that the assumption of $A(300\,K) = 1$ should not be greatly in error. Detailed Hall effect and resistivity data for Ge:As at carrier levels up to $3.10^{17}\,cm^{-3}$ over a wide temperature range have been given by Le Hir[43]. Our Hall measurements at 4.2 K indicate that the carrier concentration is sensibly independent of temperature for $N_D \gtrsim 3.5.10^{17}\,cm^{-3}$ in agreement with the results of Le Hir[43], Fritzche[42] and Fistul[205]. The low temperature carrier levels were determined from Hall measurements again

assuming A equal to unity. We feel that the concentration gradients in our samples, which were an inevitable consequence of our requirement of single crystal samples of the stated dimensions, are large enough for us to neglect a small change in A with temperature. Our need for large specimens was governed by the dictates of signal to noise in an NMR experiment as we have described in Appendix 1. It is interesting to note that we had already begun measurements of the nuclear spin lattice relaxation time at 2.14 MHz, $T_1(2)$ when RRE communicated the results of their investigation on four-point probe and van der Pauw determinations of N_D. We had found equal values of $T_1(2)$ within experimental error for two samples originally quoted at 3.5 and $4.10^{17} cm^{-3}$ and also T_1^{-1} was not directly proportional to T which we would expect for samples with $N_D > N_C$. The reassessment of doping levels by RRE led to both samples being credited with the same number of donors, $2.7.10^{17} cm^{-3}$ and thus below the metallic transition. Our NMR data clearly supported the revised carrier concentrations.

The characterisation of our samples is clearly not a trivial problem and the analogous arguments for Si:P on the value of A and the relative merits of Hall effect data or the use of experimentally determined curves of ρ_{RT} versus N_D (the so-called Irvin curve[206]) have been given in detail by Quirt and Marko[82]. These authors show that A is of order 1.3 but that putting A = 1 in the Hall formula yields N_D values lower than those obtained by the Irvin curve whilst measurements of N_D by the neutron activation analysis of Backenstoss[207] yield values greater than Irvin curve

values. Thus Quirt and Marko[82] conclude that the Irvin curve represents a compromise approach to the problem of determining N_D. Sasaki et al.[2] have claimed that the difference between their Si^{29} Knight shifts and those reported by Sundfors and Holcomb[7] is due in part to Sasaki's use of a Hall formula with $A = 1$ and Sundfors and Holcomb's use of the resistivity plus Irvin chart to determine N_D. Sasaki et al. criticize Sundfors and Holcomb for using an 'indirect' method of estimating N_D. Brown and Holcomb[6], in their study which postdates the publications by Sasaki et al. and Quirt and Marko, have continued to use the Irvin curve method on the strength of the arguments presented by Quirt and Marko. The result is that the American and Japanese workers differ by a factor of roughly two in their appraisal of the critical donor concentration, etc. occurring in Si:P.

A thorough analysis of Si:P from 10^{14} to 10^{20} carriers cm^{-3} has subsequently been carried out using neutron activation and Hall measurements by Mousty et al.[208]. For 10^{18} to 10^{19} cm^{-3}, the Hall data are lower than Irvin values but there is good agreement between the latter and neutron activation measurements. From 10^{19} to 10^{20} cm^{-3}, Hall and neutron data are in good accord but the Irvin curve overestimates the N_D values with the discrepancy becoming $\sim$ 30% at $10^{20} cm^{-3}$. These conclusions differ from the early study by Backenstoss[207] cited by Quirt and Marko as evidence for taking the Irvin curve as a convenient compromise to the problem of determining N_D. It is worth noting that the Hall data can be made to agree with the neutron activation measurements

if A is allowed to vary smoothly from unity at $10^{17}cm^{-3}$ to 1.3 at $10^{18}cm^{-3}$ and then unity again at $10^{19}cm^{-3}$. This leads to an interesting speculation on the Hall effect in Si:P.

We have seen in chapter 4 that recently Mott[70], on the basis of the Yamanouchi et al.[76] Hall data and the redefined N_C of $3.10^{18}cm^{-3}$ (see figure A2.1) has argued that a Friedman anomaly in the Hall coefficient does occur with $g = 0.7$. This value of g is consistent with but a small decrease in the density of states at E_F and Mott has argued that this suggests that the Hubbard U is not of importance in splitting the Hubbard bands. If, however, we replot the Yamanouchi et al. data using the determination of the concentration dependence of A plotted by Mousty et al., we obtain the dotted line shown in figure A2.1. (Yamanouchi et al. used a value of unity for A for all data points.) Then, applying a similar reasoning to that of Mott, we obtain $g \sim 0.3$, in good agreement with the estimated value (cf. chapter 2) of g at which Anderson localisation commences in the pseudogap between the Hubbard bands. Application of this analysis to Ge:As using our data and those of other workers[42,43] and assuming A(Ge) = 1 for all temperatures leads to a value of $g \sim 0.6 - 0.7$. Whilst our ideas are speculative they are clearly not in disagreement with the conclusions reached earlier in this report on the relative magnitudes of the Hubbard U in Ge:As and Si:P.

Returning to our Ge:As specimens, no such detailed analyses of donor content similar to Mousty et al.'s study have been performed. We are thus forced to use the Sze[198] curve and van der Pauw[199]

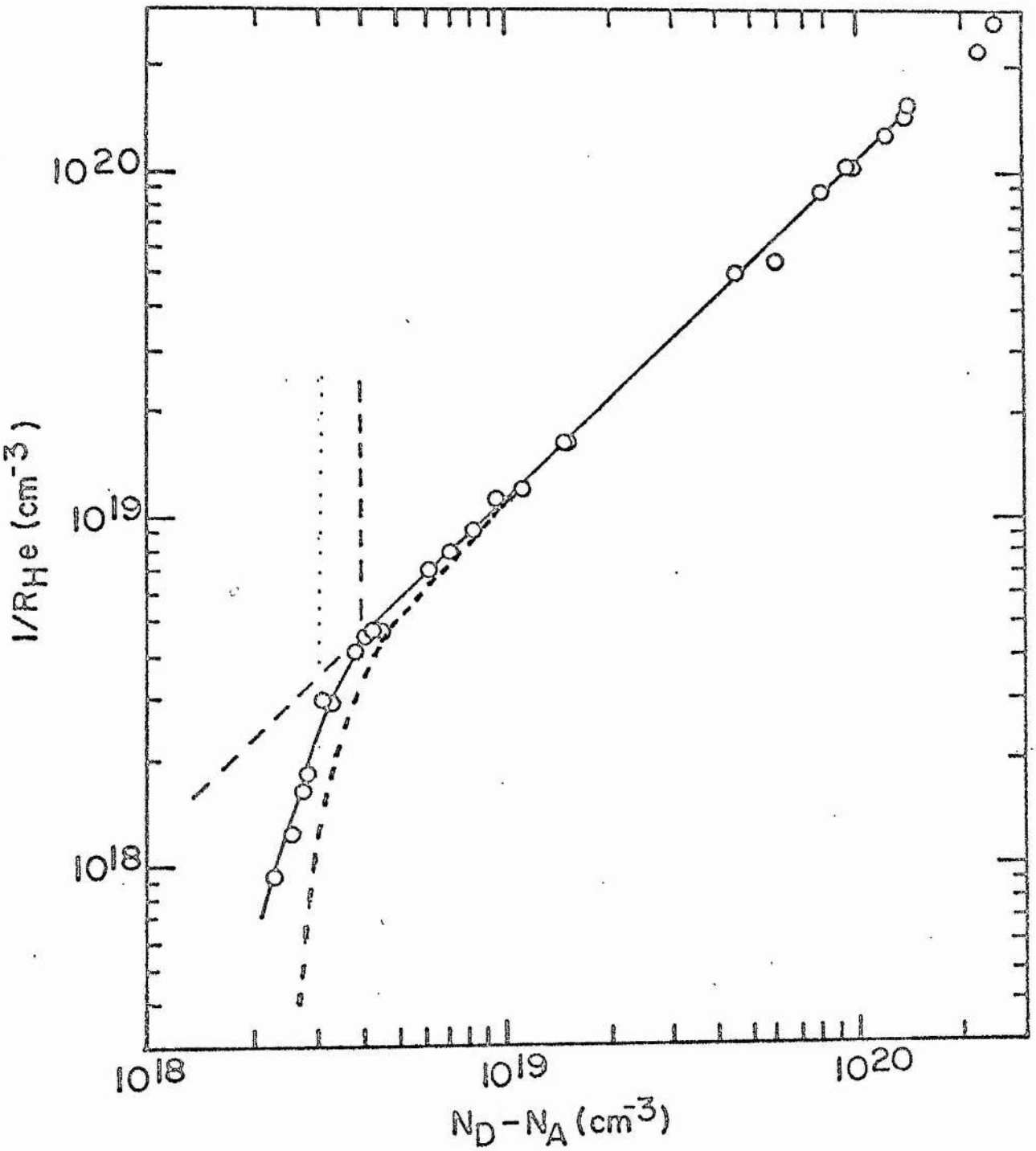

FIG. A2.1 Hall data for Si:P.

After Yamanouchi, Mizuguchi and Sasaki.[7]

measurements but it is worth re-emphasing that the combined data of several workers plotted by Cuttriss[201] show good agreement between the two methods of determining N_D.

Finally, we consider the purity of our specimens. The manufacturer[200] quotes background impurity concentrations of 10^{13} - 10^{14} atoms cm^{-3} as deduced from electrical measurements on nominally undoped and low-level doped crystals. Hence the compensation ratio $\lesssim$ 0.1%. Mass spectrographic data show slightly higher contamination but comparison is difficult since nearly all elements searched for are subject to interference from permutations of the five germanium isotopes, multiple charges and singly-charged polyatomic species. The deduced compensation ratio is only however $\sim$ 1% and we can safely assume that compensation plays no significant role in our samples.

REFERENCES

1) Mott, N. F., (1974), 'Metal-Insulator Transitions', Taylor and Francis, London

2) Sasaki, W., Ikehata, S. and Kobayashi, S-I, (1974) J. Phys. Soc. Japan 36, 1377

3) Ikehata, S., Sasaki, W. and Kobayashi, S-I, (1975) J. Phys. Soc. Japan 39, 1492

4) Ikehata, S., Sasaki, W. and Kobayashi, S-I, (1976) Solid State Commun. 19, 655

5) Sasaki, W., (1976) J. de Phys., Colloq C-4, 307

6) Brown, G. C. and Holcomb, D. F., (1974) Phys. Rev. B10, 3394

7) Sundfors, R. K. and Holcomb, D. F., (1964) Phys. Rev. 136, A810

8) Abragam, A., (1961) 'The Principles of Nuclear Magnetism', O.U.P., London

9) Slichter, C. P., (1963) 'Principles of Magnetic Resonance', Harper and Row, New York

10) Winter, J., (1971) 'Magnetic Resonance in Metals', O.U.P., London

11) Rushworth, F. A. and Tunstall, D. P., (1973) 'Nuclear Magnetic Resonance', Gordon and Breach, London

12) Cohen, M. H. and Reif, F., (1957) Solid State Phys. 5, 321

13) Knight, W. D., (1956) Solid State Phys. 2, 93

14) Bennett, L. H., Watson, R. E. and Carter, G. C., (1970) J. Nat. Bur. Standards 74A, 569

15) Bloembergen, N. and Rowland, T. J., (1955) Phys. Rev. 97, 1679

16) Ruderman, M. A. and Kittel, C., (1954) Phys. Rev. 96, 99

17) Shulman, R. G., Wyluda, B. J. and Hrostowski, H. J., (1958) Phys. Rev. 109, 808

18) Korringa, J., (1950) Physica 16, 601

19) Obata, Y., (1963) J. Phys. Soc. Japan 18, 1020

20) Mitchell, A. H., (1957) J. Chem. Phys. 26, 1714

21) Kessel A. R., (1967) Fiz. Metal Metalloved 23, 837

22) Haga, E. and Maeda, S., (1972) J. Phys. Soc. Japan 32, 324

23) Obata, Y., (1964) J. Phys. Soc. Japan 19, 2348

24) Narath, A. and Alderman, D. W., (1966) Phys. Rev. 143, 328

25) Pines, D., (1955) Solid State Phys. 1, 367

26) Moriya, T., (1963) J. Phys. Soc. Japan 18, 516

27) Narath, A., (1967) in 'Hyperfine Interactions', ed. Freeman, A.J. and Frankel, R. B., Academic Press (p.287)

28) Narath, A. and Weaver, H. T., (1968) Phys. Rev. 175, 373

29) Warren, W. W. (1971) Phys. Rev. B 3, 3708

30) Bloembergen, N., (1949) Physica 15, 386

31) Khutsishvili, G. R., (1970) Prog. Low. Temp. Phys. 6, 375

32) Blumberg, W. E., (1960) Phys. Rev. 119, 79

33) Tse, D. and Lowe, I. J., (1968) Phys. Rev. 166, 292

34) Tse, D. and Hartmann, S. R., (1968) Phys. Rev. Lett. 21, 511

35) Rogerson, A. and Tunstall, D. P. (1975) Proc. 18th. Amp. Congress, II, 367

36) Jerome, D., Ryter, C. and Winter, J. M., (1965) Physics 2, 81

37) Solomon, I., (1958) Phys. Rev. 110, 61

38) A review of Mott's early work is contained in Mott, N. F., (1958) Supp. Nuovo Cimento 7, 312

39) Kohn, W., (1957) Solid State Physics 5, 256

40) Morgan, T. N., (1965) Phys. Rev. 139, A453

41) Mott, N. F. and Twose, W. D. (1961) Adv. Phys. 10, 107

42) Fritzche, H., (1962) Phys. Rev. 125, 1552

43) Le Hir, M. J. F., (1967) J. de Phys. 28, 563

44) Alexander, M. N. and Holcomb, D. F., (1968) Rev. Mod. Phys. 40, 815

45) Martino, F., Lindell, G. and Berggren, K-F., (1973) Phys. Rev. B 8, 6030

46) Berggren, K-F., (1973) Phil. Mag. 27, 1027

47) Berggren, K-F. and Sernelius, B., (1976) Solid State Commun. 19, 487

48) Sinha, O. P. and Puri, O. P., (1975) Phys. Rev. B 12, 1395

49) Kreiger, J. B. and Nightingale, M., (1971) Phys. Rev. B 4, 1266

50) Kohn, W., (1967) Phys. Rev. Lett. 19, 439

51) Mott, N. F. and Davis, E. A., (1971) 'Electronic Processes in Non-Crystalline Materials', O.U.P., London

52) Hubbard, J., (1964) Proc. Roy. Soc. A 277, 237

53) Epstein, A. J., Etemad, S., Garito, A. F. and Heeger, A. J., (1972) Phys. Rev. B 5, 952

54) Mott, N. F., (1973) Contemp. Phys. 14, 401

55) Mott, N. F., (1972) Adv. Phys. 21, 785

56) Brinkman, W. F. and Rice, T. M. (1970) Phys. Rev. B 2, 4302

57) Luttinger, J. M., (1960) Phys. Rev. 119, 1153

58) Mott, N. F., (1973) in 'Electronic and Structural Properties of Amorphous Semiconductors', ed. Le Comber, P. G. and Mort, J., Academic Press, New York (p.1)

59) Mott, N. F., (1971) Phil. Mag. 24, 935

60) Johansson, B., (1973) J. Phys. C 6, L71

61) Anderson, P. W., (1958) Phys. Rev. 109, 1492

62) Mott, N. F., (1970) Phil. Mag. 23, 7

63) Anderson, P. W., (1968) Comments Solid State Phys. 2, 193

64) Cohen, M. H., Fritzche, H. and Ovshinsky, S. R., (1969) Phys. Rev. Lett. 22, 1065

65) Mott, N. F., (1972) Phil. Mag. 26, 1015

66) Mott, N. F., Pepper, M., Pollitt, S., Wallis, R. H. and Adkins, C. J., (1975) Proc. Roy. Soc. A 345, 169

67) Tunstall, D. P., (1975) Proc. 18th Amp. Congress II, 333

68) Miller, A. and Abrahams, E., (1960) Phys. Rev. 120, 745

69) Mott, N. F., (1969) Phil. Mag. 19, 835

70) Mott, N. F., preprint

71) Mott, N. F., (1976) J. de Phys., Colloq. C-4, 301

72) Mott, N. F. and Davis, E. A., (1968) Phil. Mag. 17, 1269

73) Allen, F. R. and Adkins, C. J., (1972) Phil. Mag. 26, 1027

74) Allen, F. R., Wallis, R. H. and Adkins, C. J., (1974) Proc. 5th Int. Conf. on Amorphous and Liquid Semiconductors, Taylor and Francis, London (p. 865)

75) Wallis, R. H., Results quoted by Mott et al., ref. (65)

76) Yamanouchi, C., Mizuguchi, K. and Sasaki, W., (1967) J. Phys. Soc. Japan 22, 859

77) Holcomb, D. F. and Rehr, J. J., (1969) Phys. Rev. 183, 773

78) Friedman, L., (1971) J. Non-Crystalline Solids 6, 329

79) Acrivos, J. V., (1972) Phil. Mag. 25, 757

80) El-Hanany, U. and Warren, W. W., (1975) Phys. Rev. Lett. 34, 1276

81) Quirt, J. D. and Marko, J. R., (1972) Phys. Rev. B 5, 1716

82) Quirt, J. D. and Marko, J. R., (1973) Phys. Rev. B 7, 3842

83) Ue, H. and Maekawa, S., (1971) Phys. Rev. B 3, 4232

84) Marko, J. R., Harrison, J. P. and Quirt, J. D., (1974) Phys. Rev. B 10, 2448

85) Berggren, K-F., (1974) Phil. Mag. 30, 1

86) Chao, K. A. and Berggren, K-F., (1975) Phys. Rev. Lett. 34, 880

87) Pifer, J. H., (1975) Phys. Rev. B 12, 4391

88) Sasaki, W. and Kinoshita, J., (1968) J. Phys. Soc. Japan 25, 1622

89) Kjeldaas, T. and Kohn, W., (1957) Phys. Rev. 105, 806

90) Bowers, R., (1957) Phys. Rev. 108, 683

91) Saitoh, M. Fukuyama, H., Uemara, Y. and Shiba, H., (1969) J. Phys. Soc. Japan 27, 26

92) See, e.g., Gopal, E.S.R., (1966) 'Specific Heats at Low Temperatures', Heywood, London

93) Hedgcock, F. T., Heiniger, F. and Paoli, A., (1974) Physics Can. 30, 33

94) Harrison, J. P. and Marko, J. R. (1976) Phil. Mag. 34, 789

95) Bryant, C. A. and Keesom, P. H., (1961) Phys. Rev. 124, 698

96) Doehler, J., (1975) Phys. Rev. B 12, 2917

97) Jain, K., Lai, S. and Klein, M. V. (1976) Phys. Rev. B 13, 5448

98) Romestain, R., Geschwind, S. and Devlin, G. E., (1976) J. de Phys., Colloq C-4, 313

99) Khosla, R. P. and Fischer, J. R., (1972) Phys. Rev. B 6, 4073

100) Khosla, R. P. and Fischer, J. R., (1970) Phys. Rev. B 2, 4084 and references therein

101) Toyozawa, Y., (1962) J. Phys. Soc. Japan 17, 986

102) Hedgcock, F. T. and Raudorf, T. W., (1970) Solid State Commun. 8, 1819

103) Giovannini, B. and Hedgcock, F. T., (1972) Solid State Commun. 11, 367

104) Lass, J. S., (1972) Can.J. Phys. 50, 165

105) Balkanski, M. and Geismar, A., (1966) J. Phys. Soc. Japan Suppl. 21, 554

106) Fletcher, R. C., Yager, W. A., Pearson, G. L., Holden, A. N., Read, W. T. and Merritt, F. R., (1954) Phys. Rev. 94, 1392

107) Lancaster, G., (1966) 'ESR in Semiconductors', Hilger and Watts, London

108) Morigaki, K. and Maekawa, S., (1972) J. Phys. Soc. Japan 32, 462

109) Slichter, C. P., (1955) Phys. Rev. 99, 479

110) Rosso, M.,(1975) J. Phys. Soc. Japan 38, 780

111) Rosso, M. and Maekawa, S., (1975) J. de Phys. 36, 1131

112) Wilson, D. K., (1964) Phys. Rev. 134, A 265

113) Chazalviel, J-N., (1975) J. Phys. Chem. Solids 36, 387

114) Toyotomi, S., (1974) J. Phys. Soc. Japan 37, 130

115) Morigaki, K. and Onda, M., (1972) J. Phys. Soc. Japan 33, 1031

116) Kamimura, H. and Mott, N. F., (1976) J. Phys. Soc. Japan 40, 1351

117) Bethin, J., Castner, T. G. and Lee, N. K., (1974) Solid State Commun. 14, 1321

118) Castner, T. G., Lee, N. K., Cieloszyk, G. S. and Salinger, G. L., (1975) Phys. Rev. Lett. 34, 1627

119) Castner, T. G. and Lee, N. K., (1976) Solid State Commun. 19, 323

120) D'Altroy, F. A. and Fan, H. Y., (1956) Phys. Rev. 103, 1671

121) Yoshihiro,K. and Yamanouchi, C., (1975) Solid State Commun. 17, 1749

122) Yoshihiro,K., Tokumoto, M. and Yamanouchi, C., (1974) Proc. 12th Int. Conf. on Phys. Semicond., Teubner, Stuttgart (p.1128)

123) Norton, P., (1976) Phys. Rev. Lett. 37, 164

124) Nagasaka, K. and Narita, S., (1973) J. Phys. Soc. Japan 35, 797

125) Taniguchi, M. and Narita, S., (1976) Solid State Commun. 20, 131

126) Taniguchi, M., Hirano, M. and Narita, S., (1975) Phys. Rev. Lett. 35, 1095

127) Narita, S. and Taniguchi, M. (1976) Phys. Rev. Lett. 36, 913

128) Shulman, R. G. and Wyluda, B. J., (1956) Phys. Rev. 103, 1127

129) Alexander, M. N., (1968) Phys. Rev. 172, 331

130) Benedict, R. P. and Look, D. C., (1970) Phys. Rev. B2, 4949

131) Adams, F. D., Look, D. C., Brown, L. C. and Locker, D. R., (1971) Phys. Rev. B 4, 2115

132) Carver, G. P., Holcomb, D. F. and Kaeck, J. A., (1971) Phys. Rev. B 3, 4285

133) Brown, G. C. (1974) Thesis, University of Cornell, U.S.A.(unpublished)

134) Bloembergen, N. (1949) Physica 15, 588

135) Behringer, R. E., (1957) J. Phys. Chem. Solids 2, 209

136) Owen, J., Browne, M., Knight, W. D. and Kittel, C., (1956) Phys. Rev. 102, 1501

137) Walstedt, R. E. and Walker, L. R., (1974) Phys. Rev. B 9, 4857

138) Walstedt, R. E. and Walker, L. R., (1975) Phys. Rev. B 11, 3280

139) Heeger, A. J., Klein, A. P. and Tu. P., (1966) Phys. Rev. Lett. 17, 803

140) Kamimura, H., (1974) Phil. Mag. 29, 65

141) Kamimura, H. and Kanehisa, M. A., (1972) Proc. 11th Int. Conf. on Phys. Semicond., P.W.N., Poland (p.231)

142) Cullis, P. R. and Marko, J. R., (1970) Phys. Rev. B 1, 632

143) Kohn, W. and Luttinger, J. M. (1955) Phys. Rev. 97, 883

144) Mott, N. F. (1974) Phil. Mag. 29, 59

145) Moriya, T. and Ueda, K., (1974) Solid State Commun. 15, 169

146) Ueda, K. and Moriya, T., (1975) J. Phys. Soc. Japan 38, 32

147) Yafet, Y., Keyes, R. W. and Adams, E. N., (1956) J. Phys. Chem. Solids 1, 137

148) Von Ortenberg, M., (1973) J. Phys. Chem. Solids 34, 397

149) Fenton, E. W. and Haering, R. R., (1967) Phys. Rev. 159, 593

150) Keyes, R. W. and Sladek, R. J., (1956) J. Phys. Chem. Solids 1, 143

151) Dyakonov, M. I., Efros, A. L. and Mitchell, D. L., (1969) Phys. Rev. 180, 813

152) Serre, J., Ghazali, A. and Leroux Hugon, P., (1976) J. de Phys., Colloq. C-4, 359

153) Straub, W. D., Roth, H., Bernard, W., Goldstein, S. and Mulhern, J. E., (1968) Phys. Rev. Lett. 21, 752

154) Matveev, G. A., Sokolov, V. I. and Tsidil'kovskii, I.M., (1974) Sov. Phys. Semicond. 8, 727

155) Sadasiv, G., (1962) Phys. Rev. 128, 1131

156) Yamanouchi, C., (1963) J. Phys. Soc. Japan 18, 1775

157) Friedman, L. and Mott, N. F., (1972) J. Non-Crystalline Solids 7, 103

158) Deshmukh, V. G. I. and Tunstall, D. P., (1976) J. de Phys., Colloq. C-4, 329

159) Jeffries, C. D., (1953) Phys. Rev. 92, 1262

160) Bloembergen, N., (1954) Physica 20, 1130

161) Wyluda, B. J., (1962) J. Phys. Chem. Solids 23, 63

162) Kopfermann, H., (1958) 'Nuclear Moments', Academic Press, London

163) Childs, W. J. and Goodman, L. S., (1966) Phys. Rev. 141, 15

164) Barnes, R. G. and Smith, W. V., (1954) Phys. Rev. 93, 95

165) Bacher, R. F. and Goudsmit, S., (1932) 'Atomic Energy States', McGraw-Hill, New York

166) Bessis, N., Picart, J. and Desclaux, J. P., (1969) Phys. Rev. 187, 88

167) Matsubara, T. and Toyozawa, Y., (1961) Prog. Theor. Phys. 26, 739

168) Berggren, K-F., (1973) Phil. Mag. 27, 1027

169) Reuszer, J. H. and Fisher, P., (1964) Phys. Rev. 135, A1125

170) Czavinsky, P., (1960) Phys. Rev. 119, 1605

171) Larsen, D. M., (1968) J. Phys. Chem. Solids 29, 271

172) Halbo, L., (1973) Phys. Stat. Sol. B 59, 387

173) Bassani, F., Iadonisi, G. and Preziosi, B., (1974) Rep. Prog. Phys. 37, 1099

174) Aoki, H. and Kamimura, H., (1975) J. Phys. Soc. Japan 39, 1169

175) Aoki, H. and Kamimura, H., (1976) J. Phys. Soc. Japan 40, 6

176) Toyozawa, Y., (1954) Prog. Theor. Phys. 12, 421

177) Heeger, A. J., (1969) Solid State Phys. 23, 283

178) Van Den Berg, G. J., (1964) Prog. Low Temp. Phys. IV, 194

179) Sasaki, W., (1965) J. Phys. Soc. Japan 20, 825

180) Saint-Paul, M., Souletie, J., Thoulouze, D. and Tissier, B., (1972) J. Low Temp. Phys. 7, 129

181) Gershenzon, E. M., Pevin, N. M. and Fogelson, M. S., (1970) Phys. Stat. Sol. 38, 865

182) Gershenzon, E. M., Pevin, N. M. and Fogelson, M. S., (1972) Phys. Stat. Sol. B 49, 411

183) Alloul, H. and Bernier, P., (1973) J. Phys. F 3, 869

184) Alloul, H. and Bernier, P., (1974) J. Phys. F 4, 870

185) Borsa, F. and Lecander, R. G., (1976) Solid State Commun. 20, 389

186) Ball, M. A., (1971) J. Phys. C 4, L 107

187) Raimes, S., (1957) Rep. Prog. Phys. 20, 1

188) Herring, C., (1966) in 'Magnetism', IV ed. Rado, G. T. and Suhl, H., Academic Press, London

189) Clark, W. G., (1964) Rev. Sci. Inst. 35, 316

190) Tunstall, D. P., (1973) Unpublished Report on NMR Probe Design

191) Hoult, D. I. and Richards, R. E., (1976) J. Mag. Res. 24, 71

192) Lowe, I. J., and Tarr, C. E., (1968) J. Phys. E 1, 320 and 604

193) Speight, P. A., Jeffrey, K. R. and Courteney, J. A., (1974) J. Phys. E 7, 801

194) Abel, W. R., Anderson, A. C., Black, W. C. and Wheatley, J.C., (1965) Physics 1, 337

195) Mangelsdorf, P. C., (1959) J. Appl. Phys. 30, 442

196) Bridges, F. and Clark, W. G., (1967) Phys. Rev. 164, 288

197) Electronic Materials Unit, RRE, Great Malvern, Worcestershire

198) Sze, M. S., (1969) 'Physics of Semiconductor Devices', Wiley, New York

199) van der Pauw, L. J., (1958) Philips Res. Repts. 13, 1

200) Jones, O., RRE, Private Communication

201) Cuttriss, D. B., (1961) Bell Syst. Tech. J. 40, 509

202) Brooks, H., (1955) Adv. Electron Electron. Phys. VII, 85

203) Walton, A. K. and Moss, T. S., (1961) Proc. Phys. Soc. 78, 1398

204) Hartmann, B. and Kleman, B., (1960) Arkiv For Fysik 18, 75

205) Fistul, V. I., (1969) 'Heavily Doped Semiconductors', Plenum Press, New York

206) Irvin, J. C., (1962) Bell Syst. Tech. J. 41, 387

207) Backenstoss, G., (1957) Phys. Rev. 108, 1416

208) Mousty, F., Ostoja, P. and Passari, L., (1974) J. Appl. Phys. 45, 4576

209) Kikuchi, M., (1977) J. Phys. Soc. Japan 41, 1459

210) Davis, E. A. and Compton, W. D., (1965) Phys. Rev. 140, A 2183